

This document was produced
by scanning the original publication.

Ce document est le produit d'une
numérisation par balayage
de la publication originale.



GEOLOGICAL SURVEY OF CANADA
BULLETIN 405

PRECAMBRIAN GEOLOGY OF THE ATIKOKAN AREA, NORTHWESTERN ONTARIO

D. Stone, D.C. Kamineni, and M.C. Jackson

1992



Energy, Mines and
Resources Canada

Energie, Mines et
Ressources Canada

Canada

THE ENERGY OF OUR RESOURCES

THE POWER OF OUR IDEAS

GEOLOGICAL SURVEY OF CANADA
BULLETIN 405

**PRECAMBRIAN GEOLOGY OF
THE ATIKOKAN AREA,
NORTHWESTERN ONTARIO**

D. Stone, D.C. Kamineni,
and M.C. Jackson

1992

© Minister of Supply and Services Canada 1992

Available in Canada through authorized
bookstore agents and other bookstores

or by mail from

Canada Communication Group — Publishing
Ottawa, Canada K1A 0S9

and from

Geological Survey of Canada offices:

601 Booth Street
Ottawa, Canada K1A 0E8

3303-33rd Street N.W.,
Calgary, Alberta T2L 2A7

A deposit copy of this publication is also available for reference
in public libraries across Canada

Cat. No. M42-405E
ISBN 0-660-14421-2

Price subject to change without notice

Critical readers

K.D. Card
S. Tella

Authors' addresses

D. Stone
Ontario Geological Survey
Sudbury Ontario P3B 5W2

D.C. Kamineni
AECL Research, Whiteshell Laboratories
Pinawa, Manitoba R0E 1L0

M.C. Jackson
Department of Geology
University of the Witwatersrand
Johannesburg, 2050
South Africa

Preface

The Eye-Dashwa pluton is among the youngest major intrusions in the Atikokan area and is compositionally zoned from a quartz monzodiorite rim to a granite core.

This report and accompanying map provide the regional geological setting of the Eye-Dashwa pluton by defining geological boundaries as well as mineralogical, petrological, and geochemical characteristics of the pluton and neighbouring lithological units.

Major structural fractures and metamorphic conditions are discussed, and using isotopic age data, the geological events affecting the Archean crust in this area are examined. Certain unresolved problems in Archean geology of the area are identified.

This study was undertaken by Atomic Energy of Canada Limited as part of the Canadian Nuclear Fuel Waste Management Program to develop and demonstrate technology for the safe disposal of nuclear fuel waste in plutonic rocks of the Canadian Shield.

*Elkanah A. Babcock
Assistant Deputy Minister
Geological Survey of Canada*

Préface

Le pluton d'Eye-Dashwa est l'une des intrusions majeures les plus jeunes de la région d'Atikokan et présente une zonation de composition; ainsi, de la bordure au centre, on passe de la monzodiorite au granite.

Le présent rapport et la carte qui l'accompagne illustrent le contexte géologique régional du pluton d'Eye-Dashwa; y sont présentées les limites géologiques ainsi que les caractéristiques minéralogiques, pétrologiques et géochimiques du pluton et des lithologies environnantes.

Les principales fractures structurales et les conditions de métamorphisme sont décrites, sans oublier les événements géologiques ayant eu lieu au niveau de la croûte archéenne de cette région qui sont analysés à l'aide des données de datation isotopique. Sont également identifiés certains problèmes sur la géologie archéenne de la région.

Les travaux ont été effectués par l'Énergie atomique du Canada Limitée dans le cadre du Programme canadien de gestion des déchets de combustible nucléaire; ils visaient à concevoir et à mettre à l'essai une technique d'entreposage des déchets de combustible nucléaire dans les roches plutoniques du Bouclier canadien.

*Elkanah A. Babcock
Sous-ministre adjoint
Commission géologique du Canada*

CONTENTS

1	Abstract/Résumé
3	Summary/Sommaire
7	Introduction
7	Topography and forest cover
7	Scope of this study
7	Previous work
12	Iron mining in the Atikokan area
13	Geological setting
13	Nomenclature
14	Lithological description
14	Pre- to synvolcanic intrusions
14	Mafic tonalite
15	"Old" tonalite
16	Tonalite gneiss
17	Mafic tonalite gneiss
17	Supracrustal rocks
17	Wagita Formation
18	Mosher Carbonate Formation
19	Jolliffe Ore Zone Formation
20	Dismal Ashrock Formation
21	Mafic metavolcanic rocks
22	Intermediate to felsic metavolcanic rocks
23	Metagreywacke, argillite
24	Meta-agglomerate, metasandstone
24	Metaconglomerate
25	Syn- to postvolcanic intrusions
25	Metagabbro
26	"Young" tonalite
26	Diorite, hornblendite
27	Quartz monzodiorite, quartz monzonite
27	Granodiorite
28	Granite
29	Gabbro dykes
29	Surficial deposits
29	Stratigraphy
35	Geochemistry
35	Analytical techniques and presentation of results
36	Pre- to synvolcanic intrusions
36	Mafic tonalite
36	"Old" tonalite
37	Tonalite gneiss
37	Mafic tonalite gneiss
37	Supracrustal rocks
37	Wagita Formation
38	Mosher Carbonate Formation
38	Dismal Ashrock Formation
39	Mafic metavolcanic rocks
41	Intermediate to felsic metavolcanic rocks
42	Metagreywacke, argillite
42	Syn- to postvolcanic intrusions
42	Metagabbro

43	"Young" tonalite
43	Diorite, hornblendite
44	Quartz monzodiorite, quartz monzonite
44	Granodiorite
45	Granite
45	Gabbro dykes
46	Alteration
46	Supracrustal rocks
47	Intrusive rocks
47	Petrogenesis
47	Pre- to synvolcanic tonalites
48	Metavolcanic rocks
50	Granitic rocks
51	Structure
51	The subprovinces and accretionary tectonism
52	Oval structures and structural trends
53	Folds
53	Gneisses
53	Metavolcanic rocks
54	Quetico metasediments
55	Lineaments
55	Faults
56	Ear fault zone
56	Marmion fault system
57	Samuel and Atikokan faults
57	Rawn fault
58	Faults in Quetico metasediments
58	Quetico fault
58	Fractures in the Eye-Dashwa pluton
61	Metamorphism
62	Metavolcanic rocks
63	Tonalites and gneisses
64	Quetico metasediments
67	Metamorphic pattern
69	Conclusions
69	Supracrustal rocks
69	Felsic intrusive rocks
69	Stratigraphy
69	Structure
70	Metamorphism
70	Acknowledgments
70	References
	Tables
9	1. Chronostratigraphic subdivision of Archean rocks in the Rainy Lake area
11	2. Chronostratigraphic subdivision of Archean rocks in the Atikokan-Lake Superior area
19	3. Partial analyses of material from the Jolliffe Ore Zone Formation
20	4. Mineralogy of pit-run ore in the Steep Rock Lake iron area
32	5. Comparison of Steep Rock Group stratigraphic subdivisions and their relations to other rocks
35	6. Method of determination and reliability of chemical analyses
38	7. Magnesium numbers of metavolcanic rocks of the Atikokan area
63	8. Fracture groups in the Eye-Dashwa pluton
64	9. Microprobe analyses of feldspars

- 65 10. Microprobe analyses of calcic amphiboles
- 66 11. Recalculated formulae for garnet and biotite
- 67 12. Temperature estimates from garnet-biotite geothermometers
- 68 13. Geobarometer data for section 40-115-1

Illustrations

in pocket Map 1666A – Geology, Atikokan area, Ontario

- 8 1. Generalized geological map of the Atikokan area
- 9 2. Geological map of the Rainy Lake-Atikokan area
- 10 3. Geological map of the Steep Rock Lake area
- 11 4. Geology of the Steep Rock Lake area
- 12 5. Geological map of the Steep Rock Lake area
- 13 6. Geology of the Atikokan area
- 14 7. Geological map of the Steep Rock Lake area
- 15 8. Geological map of the Steep Rock Lake area
- 16 9. Lithotectonic domains and abandoned open-pit iron mines of the Atikokan area
- 16 10. Quartz-alkali feldspar-plagioclase (QAP) plot for crystalline rocks of the Atikokan area
- 16 11. Tonalite gneiss cut by granodiorite dyke northeast of the Eye-Dashwa pluton
- 17 12. Mafic tonalite gneiss containing amphibole xenoliths and cut by granodiorite dykes northeast of the Eye-Dashwa pluton
- 17 13. Mainly tonalite clasts in metaconglomerate of the Wagita Formation at the northern end of Steep Rock Lake
- 18 14. Mosher Carbonate Formation from the Fairweather reservoir, eastern margin of the Steep Rock belt
- 18 15. Hemispherical and pseudocolumnar stromatolites from the northeastern end of the Hogarth pit
- 20 16. Dismal Ashrock Formation lapilli tuff from the western side of the Roberts pit
- 21 17. Pillows in mafic metavolcanic rocks at the western side of Steep Rock Lake
- 23 18. Amphibolitized, gneissic mafic metavolcanic rocks cut by a granodiorite dyke from the Highland Lake area
- 23 19. Intermediate volcanic fragmental rocks from north of Atikokan
- 24 20. Well-bedded greywacke-argillite metasediments from east of Lerome Lake
- 24 21. Metaconglomerate bed in metagreywacke south of Atikokan
- 24 22. Deformed metaconglomerate of the Seine Group (?) southwest of Atikokan
- 25 23. Detailed geological map of the northeastern contact of the Steep Rock belt and Marmion batholith
- 27 24. Hornblende of the Little Eye stock cut by granodiorite dykes
- 27 25. Quartz-alkali feldspar-plagioclase plot showing samples from the Eye-Dashwa pluton
- 30 26. Surficial geology of the Atikokan area
- 31 27. Stratified sand and gravel in the Eagle-Finlayson end moraine at Forsberg Lake
- 31 28. Grain-size distribution of varved clay in Steep Rock Lake
- 31 29. Water content of clay varves
- 33 30. Geology and structure of the western side of the Errington, Roberts, and Hogarth mines
- 34 31. Sketch of contact relations between the Dismal Ashrock Formation and metavolcanic flows northwest of Strawhat Lake
- 36 32. K₂O-Na₂O-CaO plot for crystalline rocks of the Atikokan area
- 36 33. REE plot of mafic tonalite and "old" tonalite from the Atikokan area
- 36 34. REE plot of tonalite gneiss and mafic tonalite gneiss
- 37 35. AFM plot for Wagita Formation (labelled star) and greywacke-argillite metasediments of the Quetico Subprovince
- 37 36. REE plot of Wagita Formation and Mosher Carbonate Formation
- 38 37. AFM plot for volcanic rocks of the Atikokan area
- 39 38. REE plot of mafic and felsic rocks of the Steep Rock, Finlayson, and Perch belts
- 40 39. Variation in selected major oxides with distance from west to east across the Steep Rock belt
- 40 40. Comparison of the distributions of selected major oxides in lower mafic units of the Steep Rock belt, Finlayson belt, parts of the Finlayson belt at amphibolite grade, and the Perch belt

- 41 41. Comparison of selected incompatible, compatible, and chalcophile elements in lower mafic units of the metavolcanic belts
- 42 42. Comparison of incompatible, Ti-group, immobile, compatible, and chalcophile trace elements in selected rocks of the Atikokan area
- 42 43. Comparison of average REE patterns for "old" tonalite, Steep Rock upper felsic unit, and Quetico metasediments
- 43 44. REE plot of metagabbro
- 43 45. REE plot of "young" tonalite and "young" tonalite-granodiorite of the Righteye pluton
- 44 46. REE patterns for diorite and hornblende of the Little Eye stock
- 44 47. Larsen Index (Larsen 1938) plot for samples from the Eye-Dashwa pluton
- 45 48. AFM plot for samples from the Eye-Dashwa pluton
- 45 49. Variation in selected incompatible, immobile, compatible, and chalcophile elements in felsic plutonic rocks
- 45 50. REE plots for felsic intrusive rocks
- 46 51. REE plot for 20 samples of the Eye-Dashwa granite pluton
- 46 52. REE plot for 30 samples of the White Otter granite batholith
- 46 53. Average REE plot for three gabbro dykes
- 48 54. Yttrium versus Mg# ($100 \times \text{Mg}^{2+} / (\text{Mg}^{2+} + \text{Fe}^{2+})$; $\text{Fe}^{3+} / \text{Fe}^{2+} = 0.15$) for "least-altered" metavolcanic rocks
- 49 55. Immobile trace elements versus yttrium for "least-altered" metavolcanic rocks. Symbols as in Figure 54.
- 50 56. Oval structures and structural trends of the Atikokan area
- 51 57. Poles to foliation measurements in the Marmion batholith
- 52 58. Linear elements including axes of crenulations, drag folds, rodding structures, grooves, slickensides, and stretched minerals in the eastern Steep Rock belt
- 53 59. Axes of minor folds in western, middle, and eastern parts of the Quetico Subprovince
- 54 60. Rose diagram showing strike of bedding in Quetico metasediments of the Kemuel Lake area.
- 55 61. Airphoto lineament map of the Atikokan area
- 56 62. Lineations defined by elongate mineral grains in the Ear fault zone
- 56 63. Fault rocks of the Marmion fault system, Moose Lake
- 56 64. Slickenlines from the Marmion fault system
- 57 65. Lineations defined by elongate mineral grains in the Rawn fault
- 58 66. Length and spacing distributions of fractures at the grid area as shown by "box whisker" symbols
- 59 67. Location of boreholes ATK-1 to ATK-5 at the grid area (see Fig. 1) showing contoured diagrams of poles to fractures
- 60 68. Location of boreholes ATK-6 to ATK-8 showing contoured diagrams of poles to fractures
- 61 69. Total fractures, open and possibly open fractures, lithology, and fracture orientations in borehole ATK-6
- 62 70. Surface traces of dextral faults with curved and splayed ends at the grid area (see Fig. 1)
- 62 71. The average aperture of open fractures per 20 m interval as a function of depth below surface in boreholes ATK-1 to ATK-5
- 62 72. Variation in composition of groundwater with depth in the Eye-Dashwa pluton

Appendices

- 76 A1. Modal analyses of crystalline rocks
- 77 A2. Major element geochemistry
- 86 A3. Trace element geochemistry
- 98 A4. Rare earth element geochemistry
- 104 A5. Selected, least-altered analyses of metavolcanic rocks

PRECAMBRIAN GEOLOGY OF THE ATIKOKAN AREA, NORTHWESTERN ONTARIO

Abstract

This bulletin reviews Precambrian geology, including lithology, geochemistry, petrogenesis, structure, and metamorphism, in the vicinity of Atikokan, northwestern Ontario. The area spans approximately 1100 km² of the volcano-plutonic Wabigoon Subprovince and the metasedimentary Quetico Subprovince – two large linear lithostructural elements of the Superior craton. Nineteen major rock units are classified into pre- to synvolcanic intrusions, supracrustal rocks, and syn- to postvolcanic intrusions. The early intrusive suite comprises four varieties of tonalite and tonalite gneiss, the oldest of which is dated at 3001 Ma (U/Pb zircon). Tonalite is concentrated mainly in the Marmion batholith whereas gneisses occupy belts and a large complex in the north. These rocks probably originated by melting of a pyroxene granulite of tholeiitic composition.

The Marmion batholith is unconformably overlain by supracrustal rocks of the Steep Rock Group consisting of discontinuous metaconglomerate and metasandstone (Wagita Formation), limestone beds (Mosher Carbonate Formation), ironstones (Jolliffe Ore Zone Formation), and an ultramafic pyroclastic rock (Dismal Ashrock Formation). The unconformity typically comprises a 2 to 10 m transition zone from tonalite through altered, friable tonalite and quartz-sericite "grit" to bedded metasediments. The Jolliffe Ore Zone Formation was mined from 1944 to 1979 and yielded 100 million tonnes of mainly goethite ore.

The upper contact of the Dismal Ashrock Formation is tectonized and poorly exposed and precludes clear definition of stratigraphic relations of the Steep Rock Group to contiguous metavolcanic rocks. In addition to the ashrock, metavolcanic rocks include mafic pillow flows and intermediate to felsic flows, tuffs, and breccias. The ashrock is unusual among Archean komatiites in its dominantly pyroclastic mode of occurrence and enriched incompatible trace element composition. The ultramafic magma may have formed by melting of anomalously enriched mantle or by interaction with sialic crust. The mafic lavas are typical Archean tholeiites. They probably evolved by fractionation of more primitive high-magnesium basalt. The intermediate to felsic metavolcanic rocks have relatively high contents of compatible trace elements and other geochemical characteristics, which are inconsistent with an origin by fractionation of the mafic lavas. Processes of magma mixing or assimilation are required to explain the petrogenesis of these rocks.

Units of clastic metasediments in the metavolcanic belts are made up of agglomerate, sandstone, conglomerate, and greywacke/argillite. Voluminous turbidites were derived mainly from an intermediate to felsic volcanic source with a lesser component of tonalite and mafic volcanic detritus and were deposited in the Quetico basin about 2695 Ma ago.

Although some metagabbro dykes predate deposition of the Steep Rock Group, the majority are grouped with syn- to postvolcanic intrusions. Metagabbro dykes and sills are particularly common in the Steep Rock belt and compose up to 30 per cent of some felsic intrusions such as the Marmion batholith. Diorite/hornblendite occupies a stock central in the area and thin units marginal to metavolcanic and gneiss belts. The syn- to postvolcanic felsic intrusions range in size and form from small dykes in gneisses to plutons. U/Pb zircon dates range from 2936 Ma for tonalite to 2665 Ma for granite of the Eye-Dashwa pluton. The monzodiorite rim of this youngest pluton could have been derived by partial melting of a lithophile-element-enriched mantle source.

The regional linear disposition of Quetico metasediments adjacent to Wabigoon metavolcanic rocks has been attributed to subduction-driven accretion of trench-fill turbidites (Quetico) against the Wabigoon volcanic arc about 2695 Ma ago. Accretion was followed by strong dextral transpression and imposed a pervasive east-west strike to foliations, bedding, and isoclinal folds in Quetico metasediments. Metamorphic grade increases south toward late granites at the central axis of the Quetico Subprovince.

The Wabigoon Subprovince is dominated by large felsic oval structures that typically have a felsic plutonic core, an outer gneissic envelope, and concentric foliations. Belts of folded supracrustal rocks and mafic gneisses separate oval structures and can be metamorphically zoned with greenschist cores and amphibolite rims. This structural and metamorphic pattern may result from emplacement and spreading of hot, low-density felsic plutons and gneisses in oval structures that shortened and contact metamorphosed supracrustal rocks in adjacent belts.

Dip-slip faults occur at the southwestern margin of the Dashwa oval structure and within the Steep Rock belt; the Marmion batholith is cut by a complex, northeast-trending network of faults. The Eye-Dashwa pluton was pervasively faulted and fractured during a brittle deformation event at about 2300 Ma. Mild fracturing occurred at about 1100 Ma. Fractures are open and transmit groundwater mainly within 200 m of surface.

Résumé

Dans le présent bulletin, est examinée la géologie précambrienne, en particulier la lithologie, la géochimie, la pétrogenèse, la structure et le métamorphisme des régions aux alentours d'Atikokan dans le nord-ouest de l'Ontario. Cette région couvre approximativement 1 100 km² de la sous-province de Wabigoon et de la province métasédimentaire de Quetico - qui sont deux grands éléments lithostratigraphiques linéaires du craton du lac Supérieur. On a classé dix-neuf grandes unités lithostratigraphiques en intrusions prévolcaniques à synvolcaniques, roches supracrustales et intrusions synvolcaniques à post-volcaniques. La suite intrusive initiale comprend quatre variétés de tonalite et de gneiss tonalitique, dont le plus ancien est daté de 3 001 Ma (datation par la méthode U/Pb sur le zircon). La tonalite se concentre principalement dans le batholite de Marmion, tandis que les gneiss occupent diverses zones et un vaste complexe au nord. Ces roches se sont probablement formées par fusion d'une granulite pyroxénique de composition tholéiitique.

Le batholite de Marmion est recouvert en discordance par les roches supracrustales du groupe de Steep Rock composé de métaconglomérat et de métagrès discontinus (formation de Wagita), de lits calcaires (formation du carbonate de Mosher), de roches sédimentaires ferrugineuses (formation de la zone minéralisée de Joliffe) et de roches pyroclastiques de caractère ultramafique (formation du sable volcanique de Dismal). Typiquement, la discordance comprend une zone de transition de 2 à 10 m allant d'une tonalite, en passant par une tonalite altérée et friable et par un «grès grossier» quartzeux-sériciteux, à des métasédiments lités. La formation de la zone minéralisée de Joliffe a été exploitée de 1944 à 1979 et a produit 100 millions de tonnes de minerai principalement constitué de goéthite.

Le contact supérieur de la formation du sable volcanique de Dismal est tectonisé et affleure assez rarement; pour cette raison, il est difficile de préciser clairement les relations stratigraphiques entre le groupe de Steep Rock et les roches métavolcaniques contiguës. Outre le sable volcanique, les roches métavolcaniques comprennent des coulées de laves mafiques en coussins et des coulées de laves, des tufs et des brèches de composition felsique à intermédiaire. Le sable volcanique est inhabituel parmi les komatiites archéennes en ce qu'il est principalement de type pyroclastique et que sa composition montre un enrichissement en éléments traces incompatibles. Il est possible que le magma ultramafique se soit formé par fusion d'un manteau anormalement enrichi ou par interaction avec la croûte sialique. Les laves mafiques sont des tholéiites archéennes typiques. Elles se sont probablement formées graduellement par fractionnement d'un basalte plus primitif riche en magnésium. Les roches métavolcaniques de composition intermédiaire à felsique se caractérisent par des teneurs relativement élevées en éléments traces compatibles et par d'autres propriétés géochimiques qui ne s'accordent pas avec une origine liée au fractionnement de laves mafiques. Il faut invoquer les processus de brassage des magmas ou d'assimilation par des magmas pour expliquer la pétrogenèse de ces roches.

Les unités métasédimentaires clastiques contenues dans les zones métavolcaniques sont constituées de brèches volcaniques, de grès, de conglomérats, et de grauwacke/argilite. Les volumineuses turbidites proviennent principalement d'une source intermédiaire à felsique de produits volcaniques, avec composante mineure de tonalite et de débris volcaniques mafiques, et se sont déposées dans le bassin de Quetico il y a environ 2 695 Ma.

Bien que certains dykes de métagabbro soient plus anciens que le dépôt du groupe de Steep Rock, la majorité d'entre eux sont regroupés avec des intrusions synvolcaniques à post-volcaniques. Les dykes et filons-couches de métagabbro sont particulièrement fréquents dans la zone de Steep Rock et représentent jusqu'à 30 % de certaines intrusions felsiques telles que le batholite de Marmion. La diorite/hornblendite occupe un stock volcanique central dans la région, et de minces unités en marge des zones métavolcaniques et gneissiques. Les intrusions felsiques synvolcaniques à post-volcaniques ont des dimensions et configurations allant de celles de petits dykes contenus dans des gneiss à celles de plutons. Les valeurs des datations U/Pb sur le zircon se situent entre 2 936 Ma dans le cas de la tonalite à 2 665 Ma dans le cas du granite du pluton d'Eye-Dashwa. L'auréole de monzodiorite de ce pluton qui est le plus récent est peut-être le produit de la fusion partielle d'une source mantellique enrichie en éléments lithophiles.

La disposition linéaire des métasédiments de Quetico qui jouxtent les roches métavolcaniques de Wabigoon a été attribuée à l'accrétion, générée par la subduction, des turbidites comblant les fosses océaniques (Quetico) avec l'arc volcanique de Wabigoon, il y a environ 2 695 Ma. L'accrétion a été suivie d'une forte transpression dextre et a imposé aux foliations, au litage et aux plis isoclinaux une direction est-ouest pénétrante. Le degré de métamorphisme augmente au sud en direction des granites tardifs dans l'axe central de la sous-province de Quetico.

La sous-province de Wabigoon contient principalement de grandes structures ovales de composition felsique qui typiquement ont un noyau plutonique également felsique, une enveloppe externe gneissique, et des foliations concentriques. Des zones de roches supracrustales plissées et de gneiss mafiques séparent les structures ovales et peuvent présenter une zonation métamorphique à noyaux composés de schistes verts et à auréoles composées d'amphibolite. Ce schéma structural et métamorphique est peut-être le résultat de la mise en place et de l'étalement de plutons felsiques chauds de faible densité et de gneiss dans des structures ovales qui se sont contractées et dans des roches supracrustales qui ont subi un métamorphisme de contact dans les zones adjacentes.

Des failles transversales apparaissent sur la marge sud-ouest de la structure ovale de Dashwa et à l'intérieur de la zone de Steep Rock; le batholite de Marmion est traversé par un réseau complexe de failles de direction générale nord-est. Le pluton d'Eye-Dashwa a été traversé de façon pénétrante par des failles et des fractures durant un épisode de déformation fragile il y a environ 2 300 Ma. Un épisode de fracturation légère du terrain s'est également produit il y a environ 1 100 Ma. Les fractures sont ouvertes et permettent surtout le passage des eaux souterraines sur 200 m à partir de la surface.

SUMMARY

The Atikokan area is situated 210 km west of Thunder Bay, Ontario and encompasses 1100 km² of the southwestern Superior Province. The area hosts a diverse assortment of Archean rocks that have been extensively studied over the past century. The most notable features include a rare Archean unconformity and rich iron ores that were mined from 1944 to 1979.

The southwestern Superior Province shows a conspicuous alternating pattern of megascopic linear volcano-plutonic and metasedimentary domains (subprovinces) two of which, the Wabigoon and Quetico, are present in the Atikokan area. The Wabigoon segment comprises metavolcanic belts (Steep Rock, Finlayson, Perch, and Nevison), the Dashwa gneiss complex, and parts of 12 separate intrusions that are composed mainly of tonalite, granodiorite, and granite. Well-bedded, greywacke-argillite metasediments are widespread in the Quetico segment. All major lithological units are Archean in age.

Intrusive rocks are subdivided into pre- to synvolcanic and syn- to postvolcanic varieties on the basis of stratigraphic and crosscutting relations. Pre- to synvolcanic intrusions include mafic tonalite and "old" tonalite which are the dominant lithologies in the Marmion batholith and occur at scattered localities in the Dashwa gneiss complex. These approximately 3000 Ma, mainly quartz-plagioclase-biotite-hornblende rocks are well foliated and transected by metagabbro dykes and shear zones. They are distinguished from other felsic intrusions by a low K₂O content and evidence for alteration including the presence of about 18%

SOMMAIRE

La région d'Atikokan se situe à 210 km à l'ouest de Thunder Bay en Ontario et englobe 1 100 km² du sud-ouest de la province du lac Supérieur. La région contient tout un assortiment de roches archéennes qui ont été étudiées en détail au siècle dernier. Les détails les plus remarquables sont la présence d'une rare discordance d'âge archéen et de minerais riches en fer qui ont été exploités entre 1944 et 1979.

Le sud-ouest de la province du lac Supérieur présente un schéma bien visible d'alternance de domaines linéaires mégascopiques, volcano-plutoniques et métasédimentaires (sous-provinces), dont deux, le domaine de Wabigoon et le domaine de Quetico, se trouvent dans la région d'Atikokan. Le segment de Wabigoon englobe des zones métavolcaniques (Steep Rock, Finlayson, Perch et Nevison), le complexe gneissique de Dashwa, et des portions de 12 intrusions distinctes qui se composent principalement de tonalite, de granodiorite et de granite. Des métasédiments bien lités composés de grauwaque et d'argillite occupent de vastes étendues dans le segment de Quetico. Toutes les grandes unités lithologiques sont d'âge archéen.

Les roches intrusives sont subdivisées en variétés prévolcaniques à synvolcaniques en fonction des relations stratigraphiques et des recoupements avec les travers-bancs. Les intrusions prévolcaniques à synvolcaniques comprennent une tonalite mafique et une tonalite «ancienne» qui sont les lithologies dominantes du batholite de Marmion et existent dans des localités dispersées du complexe gneissique de Dashwa. Ces roches âgées d'environ 3 000 Ma, principalement composées de quartz-plagioclase-biotite ± hornblende, sont clairement foliées et recoupées par des dykes de gabbro et par des zones de cisaillement. Elles se distinguent des autres intrusions felsiques par une plus faible teneur en K₂O et par des signes d'altération, en particulier la présence dans une proportion approximative de 18 % de minéraux secondaires

secondary minerals (muscovite, chlorite, and epidote). "Old" tonalite has a low rare earth element (REE) content and a lanthanum/ytterbium (La/Yb) ratio of 24.9.

Tonalite gneiss and mafic tonalite gneiss are included with pre- to synvolcanic intrusions. Tonalite gneiss is leucocratic (<20% biotite) and has short, discontinuous gneissic layering. It is structurally and geochemically gradational to both prevolcanic and postvolcanic tonalite. Mafic tonalite gneiss (>20% biotite + hornblende) has prominent dioritic and amphibolitic components and occurs mainly in belts where it shows gradational relations to amphibolitized mafic metavolcanic rocks.

The Marmion batholith is unconformably overlain by the Steep Rock Group, the formations of which are described here in ascending stratigraphic order. The Wagita Formation consists of metaconglomerate and metasandstone, which occur discontinuously at the unconformity. The presence of tonalite clasts and geochemical evidence suggest that this formation was derived by erosion of the Marmion batholith.

The Mosher Carbonate Formation comprises variably massive, bedded or brecciated limestone to dolostone and contains several species of stromatolites. It is overlain by the Jolliffe Ore Zone Formation, which is subdivided into the Manganiferous Paint Member (a possible regolith), and the Goethite Member. Nearly 100 million tonnes of goethite-hematite ore were mined from the Goethite Member between 1944 and 1979. Secondary alteration of a pre-existing iron formation is the most likely origin for the iron ores among the various models that have been put forward.

The Dismal Ashrock Formation probably marks the earliest volcanism in the Steep Rock belt. This unusual komatiitic unit is dominantly lapilli tuff with rare lava flows. It has a mean composition of 44% SiO₂ and 22% MgO, and is enriched in As, Be, and Li, as well as chalcophile and compatible group elements, compared to other volcanic rocks of the area. It has high FeO* (FeO* = FeO + Fe₂O₃) and TiO₂ and a fractionated, light-enriched, heavy-depleted, chondrite-normalized REE pattern, features unusual among Archean komatiites elsewhere.

The Dismal Ashrock Formation is in poorly exposed and tectonized contact with voluminous massive to pillowed, mainly tholeiitic basalts of the Steep Rock lower mafic unit. These mafic metavolcanic rocks and associated metagabbro intrusions are widespread and of similar chemical composition in the Steep Rock, Finlayson, Perch, and Nevison belts. They typically contain 49 to 50% SiO₂ and show iron-enrichment fractionation trends. Ubiquitous alteration of these units has caused addition of volatiles (up to 6 wt.%) and considerable scatter on geochemical variation diagrams. However, mafic metavolcanic samples from all belts show unfractionated REE patterns typical of Archean tholeiites elsewhere.

(muscovite, chlorite et épidote). La tonalite «ancienne» a une faible teneur en terres rares (REE) et se caractérise par un rapport lanthane/ytterbium (La/Yb) de 24,9.

Le gneiss tonalitique et le gneiss tonalitique mafique sont regroupés avec les intrusions prévolcaniques à synvolcaniques. Le gneiss tonalitique est leucocrate (20 % biotite), et sur une faible épaisseur montre une stratification gneissique discontinue. Il représente une gradation structurale et géochimique vers la tonalite prévolcanique et aussi avec la tonalite post-volcanique. Le gneiss tonalitique mafique (20 % biotite + hornblende) a des composantes dioritiques et amphibolitiques bien visibles et apparaît principalement dans des zones où il présente des relations transitionnelles avec les roches métavolcaniques amphibolitisées de caractère mafique.

Le batholite de Marmion est recouvert en discordance par le groupe de Steep Rock, dont les formations sont décrites ici dans un ordre stratigraphique ascendant. La formation de Wagita se compose de métaconglomérat et de métagrès, qui apparaissent de façon discontinue au niveau de la discordance. La présence de clastes de tonalite et les indices géochimiques suggèrent que cette formation est le résultat de l'érosion du batholite de Marmion.

La formation du carbonate de Mosher comprend un calcaire et une dolomie plus ou moins massifs, lités ou bréchiformes, et contient plusieurs espèces de stromatolites. Elle est recouverte par la formation de la zone minéralisée de Jolliffe, qui est subdivisée en deux membres, le membre manganifère bariolé et le membre à goethite. Presque 100 millions de tonnes métriques de minerai de goethite et d'hématite ont été extraites du membre à goethite entre 1944 et 1979. L'altération secondaire d'une formation ferrière préexistante représente l'origine la plus probable des minerais de fer dans les divers modèles présentés.

La formation du sable volcanique de Dismal marque probablement le volcanisme le plus ancien de la zone de Steep Rock. Cette unité komatiitique inhabituelle se compose principalement de conglomérat volcanique à lapilli, et de quelques rares coulées de laves. Elle a une composition moyenne de 44 % de SiO₂ et de 22 % de MgO, et est enrichie en As, Be et Li, et aussi en éléments des groupes chalcophiles et de groupes compatibles, comparativement aux autres roches volcaniques de la région. Elle a une teneur élevée en FeO* (FeO* = FeO + Fe₂O₃) et TiO₂ et présente un schéma REE (concentrations de terres rares) normalisé par rapport aux chondrites, de fractionnement, d'enrichissement en minéraux légers et d'appauvrissement en minéraux lourds, ce qui est inhabituel pour les komatiites archéennes dans les autres régions du monde.

La formation du sable volcanique de Dismal se trouve en contact tectonisé et peu exposé, avec les volumineux basaltes massifs ou en coussins, surtout tholéiitiques, de l'unité mafique inférieure de Steep Rock. Ces roches métavolcaniques et les intrusions de métagabbro associées occupent de grandes étendues et ont une composition chimique similaire dans les zones de Steep Rock, de Finlayson, de Perch et de Nevison. Elles contiennent typiquement 49 à 50 % de SiO₂ et montrent des tendances à la cristallisation fractionnée avec enrichissement en fer. L'altération pénétrante de ces unités a ajouté des produits volatils (jusqu'à 6 % en poids) et explique la dispersion considérable observée dans les diagrammes de variations géochimiques. Cependant, les échantillons de roches

Limited structural data suggest that the youngest metavolcanic units are intermediate to felsic and consist of lava flows, tuffs, and breccias of mainly andesitic to dacitic composition. Breccias vary from poorly-sorted, monolithic varieties to lahars that are transitional to meta-agglomerates and metasediments. The Steep Rock upper felsic unit is dominantly calc-alkaline. It has a relatively high content of the compatible group trace elements for rocks of intermediate Si content. This is inconsistent with an origin by crystal fractionation from the lower mafic unit. It also has light REE (LREE) enriched patterns. These geochemical characteristics are suggestive of an origin by magma mixing of mafic and felsic magmas or assimilation of continental crustal material. Thin units of felsic metavolcanic rocks occur in the Finlayson belt interbedded with pillowed mafic units. These rocks are calc-alkaline, more felsic (dominantly rhyolitic), and more alkali-enriched than the Steep Rock upper felsic unit. Their REE patterns are more fractionated and exhibit heavy REE depletion similar to the tonalites.

Detrital zircons within monotonous sequences of metagreywacke and argillite in the Quetico Subprovince are dated mainly at 2720 to 2700 Ma. Sediment deposition is bracketed in a 10 Ma interval between 2698 Ma (the youngest detrital zircon) and 2688 Ma (age of a pluton that intrudes Quetico metasediments). Typical beds are sharply defined (20 to 300 mm thick) and are commonly graded, characteristic of turbidity deposits. Detrital clasts and compositional similarities suggest a source of mainly intermediate volcanic rocks and tonalite for Quetico sediments. Small units of metaconglomerate containing assorted volcanic, chert, and tonalite clasts in a coarse, sandy matrix occur at the Quetico-Wabigoon boundary. They are tentatively correlated with the Seine Group on the basis of similar clast lithologies and structural position at the subprovince boundary.

Supracrustal sequences and gneisses are intruded successively by "young" tonalite (2936 Ma), granodiorite (2800 Ma), and granite (2665 Ma) that occur in a variety of forms ranging from dykes to plutons. These intrusions show a trend of potash enrichment and strong LREE-enriched patterns. The Eye-Dashwa pluton is compositionally zoned from a quartz monzodiorite rim to a granite core and, except for rare gabbro dykes (1138 Ma; K-Ar whole rock) is among the youngest major intrusions in the area.

The Quetico-Wabigoon boundary is a major lithostructural feature of regional extent that passes through the Atikokan area and separates mainly metavolcanic rocks on the north from metasediments to the south. The Quetico turbidites have been interpreted as trench-fill deposits adjacent to an active volcanic arc (Wabigoon). Subduction-related accretion of the sedimentary prism against the volcanic arc took place about 2695 Ma ago and was followed by strong dextral transpression.

métavolcaniques mafiques prélevés dans chacune des zones montrent des schémas de teneurs en terres rares dépourvus de fractionnement, donc typiques des tholéiites trouvées ailleurs.

Les quelques données structurales disponibles semblent indiquer que les plus jeunes unités métavolcaniques sont de composition intermédiaire à felsique et constituées de coulées de laves, de tufs et de brèches surtout andésitiques à dacitiques. Les brèches sont de caractère variable, allant de variétés monolithiques à des lahars qui marquent la transition avec des méta-agglomérats et des mégagrès. L'unité felsique supérieure de Steep Rock est principalement calco-alkaline. Elle montre une teneur relativement élevée en éléments traces des groupes compatibles dans les roches de teneur intermédiaire en Si. Ceci ne concorde pas avec l'hypothèse d'une cristallisation fractionnée à partir de l'unité mafique inférieure. Elle montre également des schémas d'enrichissement en terres rares légères. Ces caractéristiques géochimiques suggèrent que la roche a pour origine un brassage des magmas mafiques et felsiques ou l'assimilation de matériaux de la croûte. Il existe dans la zone de Finlayson de minces unités de roches métavolcaniques felsiques interstratifiées avec des unités de laves mafiques en coussins. Ces roches sont calco-alkalines, plus felsiques (surtout rhyolitiques) et davantage enrichies en produits alcalins que l'unité felsique supérieure de Steep Rock. Leurs schémas de teneurs en terres rares montrent un fractionnement plus poussé et un fort appauvrissement en terres rares comme dans les tonalites.

Des zircons détritiques trouvés dans des séquences monotones de métagrauwacke et d'argilite de la sous-province de Quetico ont été principalement datés de 2 720 à 2 700 Ma (dans le cas du zircon détritique le plus récent) et de 2 688 Ma (âge d'un pluton intrusif dans des métasédiments de Quetico). Les lits typiques sont très nettement définis (20 à 300 mm d'épaisseur) et montrent souvent un granoclassement de leurs éléments, ce qui caractérise les dépôts de courants de turbidité. Les clastes détritiques et les similarités de composition semblent indiquer que les sédiments de Quetico ont pour origine des roches volcaniques et une tonalite de composition surtout intermédiaire. De petites unités de métaconglomérat contenant des clastes de roche volcanique, de chert et de tonalite assortis, présents dans une matrice sableuse grossière, apparaissent à la limite entre les sous-provinces de Quetico et de Wabigoon. Elles sont provisoirement corrélées avec le groupe de Seine en raison de la similarité lithologique de leurs clastes et en raison de leur situation à la limite des sous-provinces.

Les séquences supracrustales et les gneiss sont successivement traversés par des intrusions de «jeune» tonalite (2 936 Ma), de granodiorite (2 800 Ma) et de granite (2 665 Ma), qui se présentent sous diverses formes allant des dykes aux plutons. Ces intrusions montrent une tendance à un enrichissement en potasse et des schémas de fort enrichissement en terres rares légères. Le pluton d'Eye-Dashwa présente une zonation compositionnelle, allant de l'auréole de monzodiorite quartzique au noyau granitique, et excepté de rares dykes de gabbro (1 138 Ma; datation par la méthode K/Ar de la roche entière) constitue l'une des plus récentes intrusions majeures de la région.

La limite entre les sous-provinces de Quetico et de Wabigoon est un important détail lithostructural d'envergure régionale qui traverse la région d'Atikokan et sépare les roches principalement métavolcaniques au nord des métasédiments au sud. Les turbidites de Quetico sont considérées comme des dépôts de remplissage de

Accretion and subsequent transpression have significantly affected structure of the Quetico metasediments. Bedding, foliations, and axes of large-scale isoclinal folds are aligned east-west and mesoscopic Z-style folds are widespread. Transpression became localized in a dextral transcurrent boundary fault (Quetico fault) elsewhere along the Wabigoon margin; however, mapping suggests that this structure is not well developed at Atikokan.

Although syn- to postvolcanic intrusions have variable sizes and shapes, the larger examples in the Wabigoon Subprovince are approximately oval. Gneisses and belts of supracrustal rocks partially or completely envelope most felsic plutons giving rise to concentrically zoned patterns of foliation, gneissosity and lithology. These oval structures, which are of regional extent in the northern Atikokan area, contrast with straight east-west trends in the south (Wabigoon-Quetico Subprovince boundary area). The oval lithostructural patterns may be generated by intrusion are spreading of the felsic core plutons.

A mylonite zone with subvertical mineral lineations (Ear fault) separates the Dashwa oval structure from the Nevison belt. Metagabbro dykes and complex branched fault zones composed of schistose, altered, and fractured tonalite strike northeasterly in the Marmion batholith. Dip-slip, probably reverse displacement faults are mapped in the Steep Rock belt. The Samuel fault appears to have thrust a segment of the Marmion batholith up into the central Steep Rock belt. The Atikokan fault is conformable with the upper contact of the Dismal Ashrock Formation in the Steep Rock Mine area and prevents stratigraphic correlations between the Steep Rock Group and contiguous metavolcanic rocks.

Age determinations of fracture filling materials show that the Eye-Dashwa pluton was cut by a pervasive network of fractures and mesoscopic transcurrent faults at about 2300 Ma, probably contemporaneous with the formation of many airphoto lineaments in the area. A subsequent mild fracturing event occurred at about 1100 Ma. Rejuvenation of ancient sealed fractures that are within about 200 m of surface is the youngest recognized deformation. The rejuvenated fractures lack fillings or contain soft materials (carbonate, clay, goethite) and significantly affect strength and permeability of the near-surface zone.

Metamorphic grade varies from greenschist facies in the cores of metavolcanic belts to amphibolite facies at their margins and in the gneisses. Metamorphic grade does not change at the Quetico-Wabigoon boundary but increases steadily southward as indicated by the first appearance of biotite, amphibole, and garnet. Pressure-temperature conditions of 230 to 430 MPa and 419 to 577°C are estimated for the garnet zone using published geothermometers and geobarometers. Thermal energy transferred from the lower crust by felsic intrusions and gneisses in oval structures and late plutons

fosses jouxtant un arc volcanique actif (Wabigoon). L'accrétion, liée aux processus de subduction, du prisme sédimentaire avec l'arc volcanique s'est produite il y a environ 2 695 Ma et a été suivie d'une forte transpression dextre.

L'accrétion puis la transpression ultérieure ont fortement influencé la structure des métasédiments de Quetico. Le litage, les foliations et les axes des plis isoclinaux de grande envergure montrent un alignement est-ouest et les plis mésoscopiques de style Z sont répandus. La transpression s'est concentrée dans une faille limitrophe de décrochement dextre (faille de Quetico) ailleurs sur la marge de Wabigoon; cependant, la cartographie suggère que cette structure n'est pas nettement développée à Atikokan.

Bien que les intrusions synvolcaniques à post-volcaniques aient diverses dimensions et configurations, les intrusions de plus grande envergure citées comme exemples dans la sous-province de Wabigoon sont approximativement de forme ovale. Les gneiss et zones de roches supracrustales enveloppent partiellement ou complètement la plupart des plutons felsiques et génèrent des schémas de zonation concentrique à la fois pour la foliation, la gneissosité et la lithologie. Ces structures ovales, d'étendue régionale dans la région nord d'Atikokan, contrastent avec les directions linéaires est-ouest observées au sud (région limitrophe des sous-provinces de Wabigoon et Quetico). Les schémas lithostructuraux à configuration ovale, peut-être générés par des intrusions, indiquent l'étalement des plutons à noyau felsique.

Une zone mylonitique caractérisée par des linéations minérales subverticales (faille d'Ear) sépare la structure ovale de Dashwa de la zone de Nevison. Les dykes de metagabbro et les zones de failles à ramifications complexes composées de tonalite schisteuse, altérée et fracturée, ont une direction nord-est dans le batholite de Marmion. Des failles normales, et probablement des failles inverses, sont cartographiées dans la zone de Steep Rock. La faille de Samuel semble avoir charrié un segment du batholite de Marmion jusque dans la zone centrale de Steep Rock. La faille d'Atikokan est concordante avec le contact supérieur de la formation du sable volcanique de Dismal dans la région de la mine de Steep Rock et empêche toute corrélation stratigraphique entre le groupe de Steep Rock et les roches métavolcaniques contiguës.

Les datations des matériaux de remplissage des fractures montrent que le pluton d'Eye-Dashwa a été recoupé par un réseau pénétrant de fractures et de failles transversales mésoscopiques il y a environ 2 300 Ma, probablement à l'époque de la formation de nombreux linéaments repérés sur les photographies aériennes de la région. Il y a environ 1 100 Ma, a eu lieu un modeste épisode de fracturation du terrain. Le rajeunissement des anciennes fractures scellées qui vont de la surface jusqu'à approximativement 200 m de profondeur, constitue la déformation la plus récente identifiée. Les fractures rajeunies ne contiennent pas de remplissage ou contiennent des matériaux tendres (carbonates, argile, goethite) et influencent de façon significative la résistance mécanique et la perméabilité de la zone de subsurface.

Le degré de métamorphisme varie du faciès des schistes verts dans les noyaux des zones métavolcaniques au faciès des amphibolites sur leurs marges et dans les gneiss. Le degré de métamorphisme ne change pas à la limite entre les sous-provinces de Quetico et de Wabigoon, mais augmente régulièrement vers le sud comme l'indiquent la première apparition de la biotite, celle de l'amphibole et celle du grenat. Les conditions de pression et de

at the central axis of the Quetico Subprovince may be responsible for the higher metamorphic grade of supracrustal rocks at margins of belts.

température, 230 à 430 MPa et 419 à 577° C, ont été estimées pour la zone des grenats, au moyen des géothermomètres et géobaromètres. L'énergie thermique transmise par la croûte inférieure par le biais des intrusions felsiques et des gneiss aux structures ovales et aux plutons tardifs, suivant l'axe central de la sous-province de Quetico, explique peut-être le plus fort degré de métamorphisme des roches supracrustales sur les marges des zones.

INTRODUCTION

The present study area of approximately 1100 km² is located near the town of Atikokan about 210 km west of Thunder Bay in northwestern Ontario (Fig. 1). Atikokan is accessible by Trans-Canada Highway 11 between Thunder Bay and Fort Frances, and by scheduled air service to other towns in northwestern Ontario. The Canadian National Railway also passes through the town but does not offer public transportation. Highway 622 extends north from Atikokan and connects with Highway 17 between Dryden and Ignace. Atikokan was originally founded as a railway station and flourished as an iron mining town between 1944 and 1979. At present, forest resource and service industries and tourist outfitting are the main sources of employment for the resident population of about 5000 people.

Geological mapping was carried out between 1979 and 1985 at a scale of 1:15 840. Structural measurements and lithological descriptions were recorded on aerial photographs and code sheets in the field and transferred to computer storage devices. Field data were compiled on 1:15 840 scale basemaps, reduced, and transferred to 1:50 000 scale National Topographic Series maps.

Topography and forest cover

Relief is subdued but the land surface is rugged, varying in elevation from 385 m above sea level (Perch Lake) to about 500 m in northeastern parts of the area. Rolling, wooded hills are separated by lakes and low-lying, commonly swampy valleys. Areas underlain by metavolcanic rocks, such as around Steep Rock Lake, are characterized by steep, elongated ridges. Drainage is westward through the Little Turtle River and Seine River to the Rainy River and northward through the Winnipeg River and Nelson River to Hudson Bay.

In 1943 the Seine River was diverted around Steep Rock Lake by way of Finlayson, Little Falls, and Modred lakes. The middle and east arms of Steep Rock Lake were subsequently drained to permit mining of iron from the former lakebed. Following the cessation of mining in 1979, open pits in the former lakebed have flooded from natural runoff.

Most of the area is covered by a thick forest of black spruce, jack pine, balsam fir, poplar, and white birch with scattered red maple in the south. Red pine and white pine are

the largest species of tree, particularly in the vicinity of Miranda Lake. Hazel and alder shrubs comprise a thick ground cover beneath large trees and in logged areas.

Scope of this study

The regional geological study of the Atikokan area was undertaken by Atomic Energy of Canada Limited (AECL) as part of the Canadian Nuclear Fuel Waste Management Program. The focus of the program is to develop and demonstrate the technology for safely disposing of nuclear fuel waste in plutonic rocks of the Canadian Precambrian Shield (Dormuth and Nuttall, 1987). This includes development of equipment and methods for evaluating structural, mechanical, hydrogeological, and geochemical characteristics of plutonic rocks. Accordingly, mapping, geophysical surveys, diamond drilling, and hydrogeological testing were initiated on several plutons in the Superior Province including sites within the Eye-Dashwa pluton about 15 km north of Atikokan (Fig. 1).

A partial summary of AECL's geoscience research in the Eye-Dashwa pluton is given by Stone (1984); fracture characteristics are included here. The main objective of the present study, however, is to characterize the regional setting of the pluton. This includes defining geological boundaries as well as mineralogical, petrological, and geochemical characteristics of the Eye-Dashwa pluton and neighbouring lithological units.

Major structural features (foliation patterns, folds, lineaments, faults, and fractures) and metamorphic conditions are described. With the help of isotopic age determinations, we examine the sequence of plutonic, volcanic, sedimentary, structural, and metamorphic events which affected the Archean crust. Certain unresolved problems in Archean geology of the area are identified.

Previous work

The southwestern Superior Province, which includes the Atikokan area, has a long history of geological research that began in the nineteenth century. In this area early workers made key advances in subdividing Precambrian rocks into chronostratigraphic units or series. Atikokan became the type locality for the Steep Rock Series; however, the task of identifying various series, correlating them from place to place, and establishing their relative ages proved both

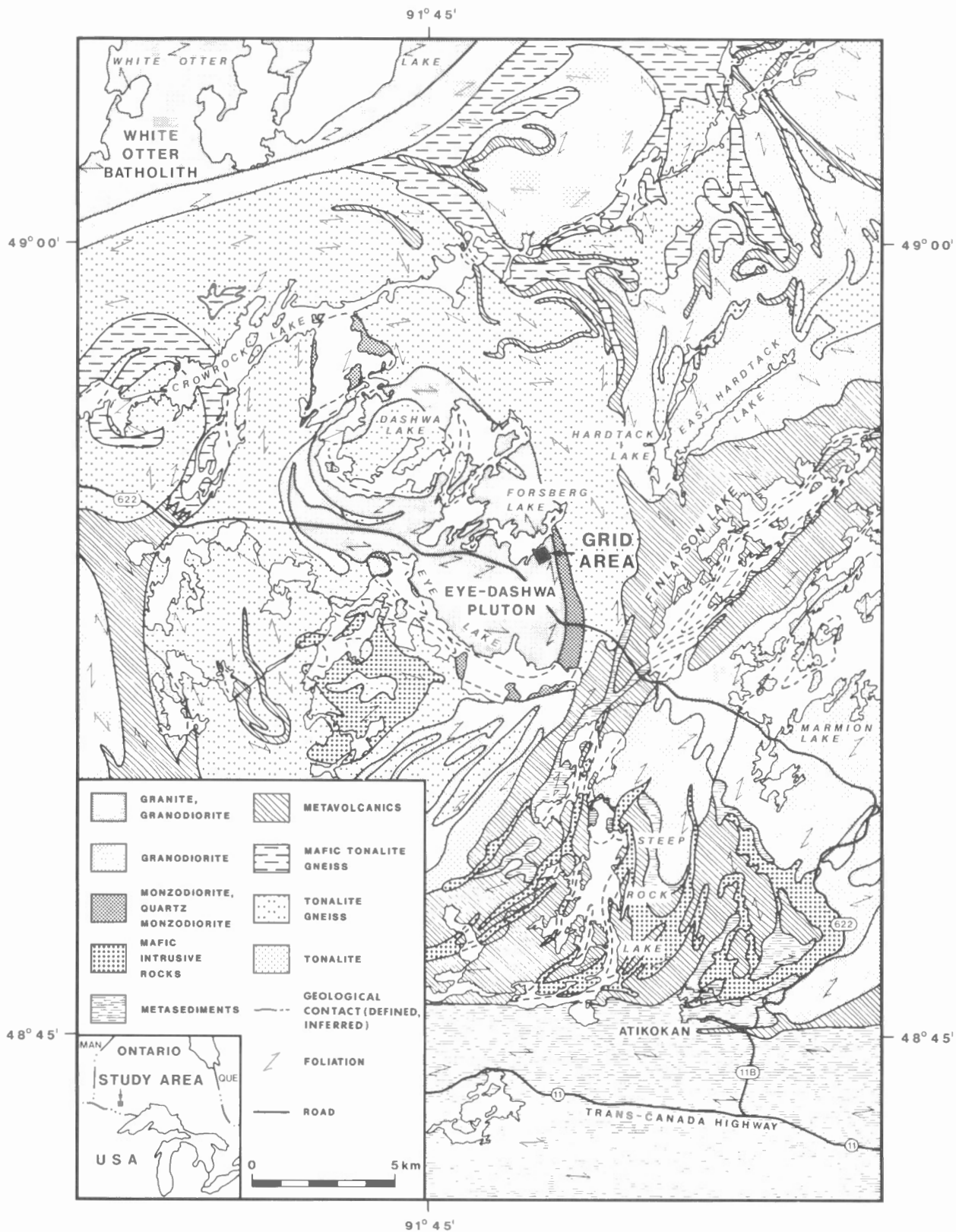


Figure 1. Generalized geological map of the Atikokan area.

difficult and controversial. Debate about nearly all aspects of the Steep Rock and other series is recorded in literature dating well into the twentieth century. The following review of this subject provides not only a historical perspective of previous work in this area but also traces several important steps in the understanding of complex Precambrian geology.

Subdivision of the Precambrian was initiated by Logan et al. (1863) who applied the term "Huronian" to a succession of sediments at Lake Timiskaming and on the northern shore of Lake Huron where they unconformably overlie a basement complex of "Laurentian" gneisses. The term "Huronian" was subsequently applied to a wide range of Precambrian rocks at various localities, including the region west of Lake Superior (e.g. Bell, 1873, 1882), and it remained for Lawson (1885) to add further refinements. Lawson (1885) constructed a detailed geological map of Lake of the Woods and applied the term "Keewatin Series" to severely folded, predominantly metavolcanic schists, and proposed on the basis of crosscutting relations that they must be older than Logan et al.'s (1863) type Laurentian. Subsequently, Lawson (1888) mapped extensive metasedimentary schists at Rainy Lake, which he named "Coutchiching Series", and based on the observation that the metasedimentary schists dip beneath the metavolcanic schists, he concluded that the Coutchiching Series was older than the Keewatin Series.

Coleman (1898) compiled a geological map (Fig. 2) showing the distribution of the major Precambrian series and the general structure of the region, in particular, how the supracrustal Keewatin and Coutchiching series occur in narrow belts between the oval masses of the intrusive Laurentian Series.

An international committee of geologists, set up to standardize geological nomenclature, toured the region and drew exception to the relative ages of the Keewatin and Coutchiching series as proposed by Lawson (1888). The committee (Adams et al., 1905) noted pebbles of Keewatin schists in basal conglomerate units of the Coutchiching Series and interpreted that the Coutchiching must be the younger series; this initiated a debate that was to continue for decades. Lawson (1913) restudied the Rainy Lake area and reaffirmed his earlier interpretation that the Coutchiching was oldest based on the overlying position of the Keewatin. He identified a late "Algoman" series of granites and proposed that the extensive conglomerate units, which contained both metavolcanic and metasedimentary clasts, were not the base of the Coutchiching but rather another series which he termed

Table 1. Chronostratigraphic subdivision of Archean rocks in the Rainy Lake area after Lawson (1913)

Algoman Series	(granitic intrusions)
Seine Series	(metasediments)
Laurentian Series	(granitic intrusions)
Keewatin Series	(metavolcanic rocks)
Coutchiching Series	(metasediments)

"Seine". Lawson (1913) considered the Seine Series to be younger than both the Keewatin and Coutchiching series (Table 1).

The stratigraphic position of the metasedimentary schists became known as the "Seine-Coutchiching problem" depending upon whether the sediments were thought to be younger than the Keewatin (Seine) or older (Coutchiching). Grout (1925) used sedimentary younging directions derived from graded beds to interpret that the Coutchiching metasediments postdate the metavolcanic rocks at several localities in Minnesota and Ontario. Tanton (1926) noted that sedimentary beds in the Coutchiching young north toward the Keewatin contact in a small area west of Atikokan and, assuming a monoclinical sequence, interpreted that the Keewatin must overlie the Coutchiching. Hawley (1930) and Gill (1931) debated relative ages of the Keewatin and Coutchiching on the basis of models for the spatial relation between the two series that should be expected following dextral shearing at their contact in the Atikokan area. Merritt (1934) examined the contact between the two stratigraphic units from Rainy Lake to Lac des Mille Lacs and favored a postvolcanic age for the metasediments. Final resolution of the Seine-Coutchiching problem did not come until much later when detailed structural analysis by Poulsen et al. (1980) showed that the sequence in Lawson's (1913) type locality at Rainy Lake is overturned and that even though the metasediments are structurally beneath the metavolcanics, they are stratigraphically younger.

Geological mapping initiated by Smyth (1891) in the Atikokan area (generally known as the Steep Rock Lake area) brought to light further complications in stratigraphic subdivisions of Precambrian rocks in the region. The first geological map of Steep Rock Lake (Fig. 3) shows a

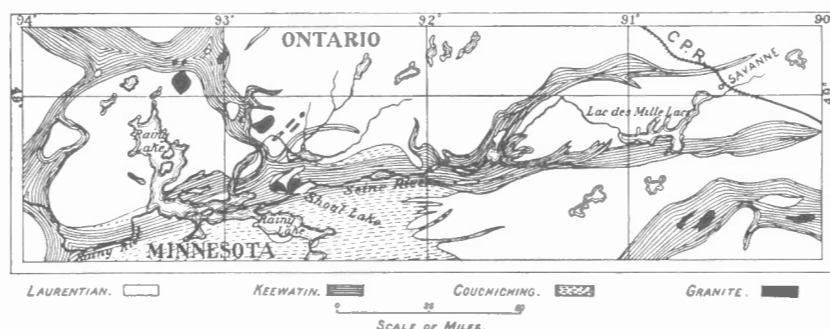


Figure 2. Geological map of the Rainy Lake-Atikokan area (after Coleman, 1898). Reproduced with permission of the Geological Society of America.

monoclinal sequence of nine formations that unconformably overlie a granitic basement complex. Smyth's (1891) Steep Rock Series consisted of discontinuous basal conglomerate, overlain successively by dolomite, volcanic ash, and an assortment of volcanic and sedimentary rocks, all of which are intruded by granite in the vicinity of Lake Margaret (Fig. 3). Smyth (1891) had identified a rare example of an unconformity in early Precambrian rocks, that led to the "Steep Rock Problem" of determining where to stratigraphically position the Steep Rock Series relative to other supracrustal series, notably the Couthiching and Keewatin. Smith (1893) concluded that the Steep Rock Series was deposited unconformably on the Laurentian, and hence must be distinctly younger than the Couthiching and

Keewatin. This view was endorsed by van Hise and Leith (1911) and later by Lawson (1912) who positioned the Steep Rock Series above the Keewatin and Couthiching but below the Seine (Table 2).

Figure 4, after Smith and McInnes (1897), shows the extent of the major series in the Atikokan area. Although the unconformable contact of the Steep Rock Series with the plutonic basement was easily identified along the eastern shores of Steep Rock Lake, McInnes (1897) noted difficulty in establishing the western limits of the Steep Rock Series where it was expected to unconformably overlie the Keewatin. Indeed, definition of the boundaries between the supracrustal series was a task that occupied geologists for many years in this area.

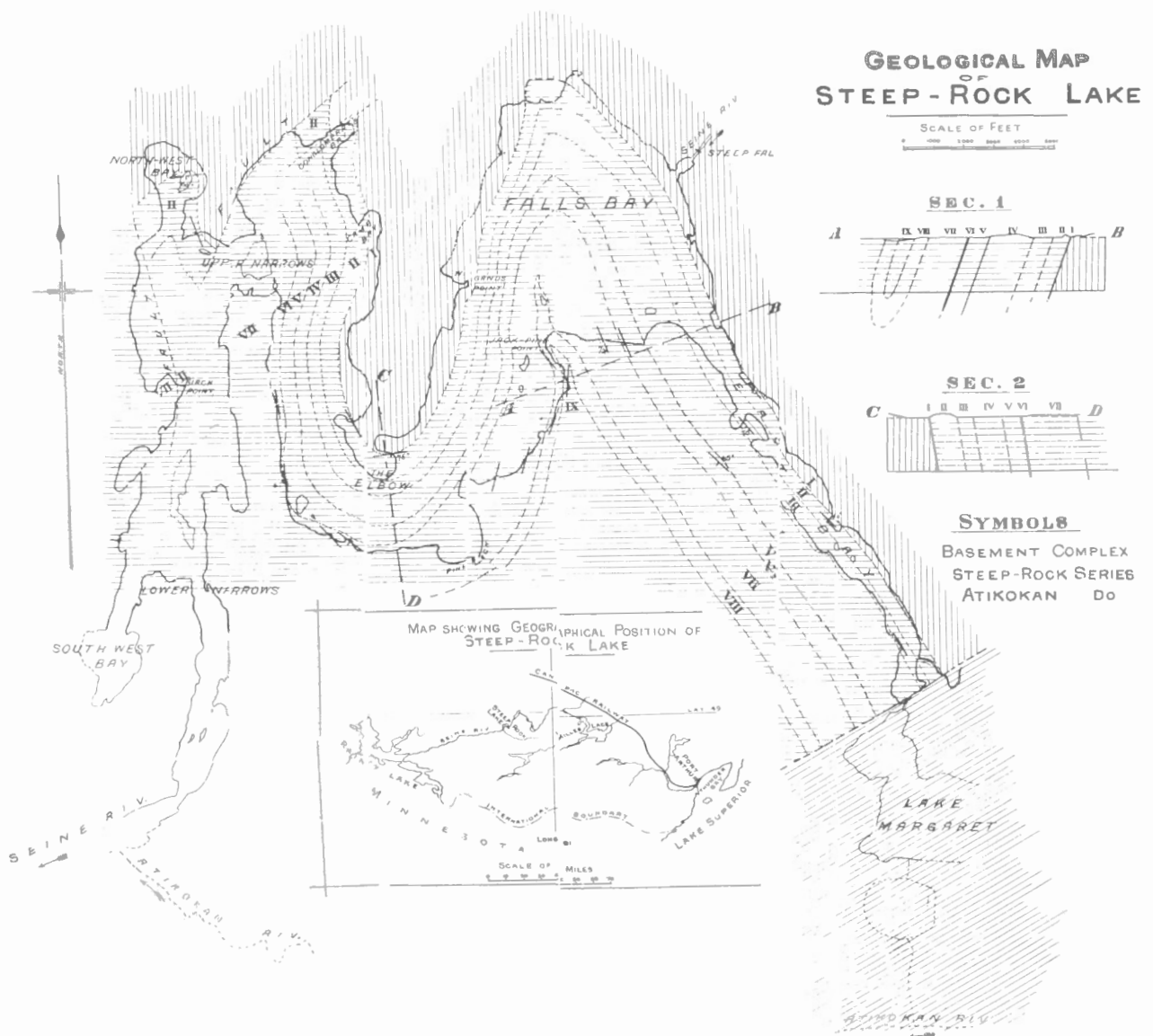


Figure 3. Geological map of the Steep Rock Lake area (after Smyth, 1891). Reproduced with permission of the American Journal of Science.

Table 2. Chronostratigraphic subdivision of Archean rocks in the Atikokan-Lake Superior area after Lawson (1912)

Keweenaw	(metavolcanic rocks and intrusions)
Animikie	(metasediments)
Algoman	(granitic intrusions)
Seine	(metasediments)
Steep Rock	(metasediments and metavolcanic rocks)
Laurentian	(granitic intrusions)
Keewatin	(metavolcanic rocks)
Coutchiching	(metasediments)

Lawson (1912) confirmed the unconformity at the base of the Steep Rock Series but disputed many of the upper formations as proposed by Smyth (1891). The structure of the Steep Rock Series was interpreted as a synclinal trough overlying the Keewatin-Laurentian contact. Based on Lawson's (1912) field work, Uglow (1913) constructed the geological map of the Steep Rock Lake area shown in Figure 5. Most of the area was interpreted to be Keewatin (unit 1 in Fig. 5) overlain by the Seine Series near the southern boundary of the map area.

Smith and McInnes (1897) had extended the Keewatin up to 5 km south of the Atikokan River (see Fig. 4), but Grout (1925), Tanton (1926), and Merritt (1934) showed that the southern limit of the Keewatin schists followed the Seine and Atikokan rivers (Fig. 5). This led to a consensus on the southern limit of the Keewatin; however, several interpretations of the lateral extent of the Steep Rock Series were offered. For instance, Tanton (1937) extended the Steep Rock Series to include metasediments mapped as Keewatin north of Atikokan and at Finlayson Lake (Fig. 6). Moore (1939) considered the Seine Series and Steep Rock Series to have been deposited contemporaneously and produced a map comparable to that of Tanton (1937; Fig. 6).

During the Second World War, parts of Steep Rock Lake were drained to exploit an iron ore zone at the top of a carbonate unit with the result that new exposures, drilling, and detailed mapping associated with mining shed new light on the geology of the area. Jolliffe (1955, 1966) described four main formations – a basal conglomerate overlain by limestone and dolomite beds, the ore zone, and pillowed flows and volcanic tuff (ashrock) – that face southwest (Fig. 7). The ashrock, which is not distinguished from pillowed flows, tuff, and agglomerate in Figure 7, is approximately 400 m thick and lies west of the ore zone (unit 4 of Figure 7). Jolliffe (1966) noted northeast-facing sedimentary beds in the assemblage of tuffs, flows, and sills southwest of the ashrock in the vicinity of the "B" ore zone of Figure 7. This structural complexity led Jolliffe (1966) to

restrict his Steep Rock Group to "the well-established homoclinal succession from basal conglomerate to uppermost ashrock".

Structural relations between the Steep Rock Group in the mine area and supracrustal assemblages to the southwest were not clearly defined during the mining activity and remain speculative. Indeed, the wealth of new data from mine exposures fostered diverse interpretations of Steep Rock stratigraphy and structure. For example, Hicks (1950) regarded the limestone unit and ore zone as replacement rather than sedimentary in origin. Shklanka (1972) saw no evidence for an unconformity at the base of the Steep Rock Group and considered the contact with adjacent crystalline rocks to be a fault (the Steep Rock Lake Fault, Fig. 8). The Steep Rock Group was interpreted to be the upper stratigraphic section of a volcano-sedimentary sequence transected by numerous faults. Subsequent studies including Schau and Henderson (1983) and Wilks (1986) supported the

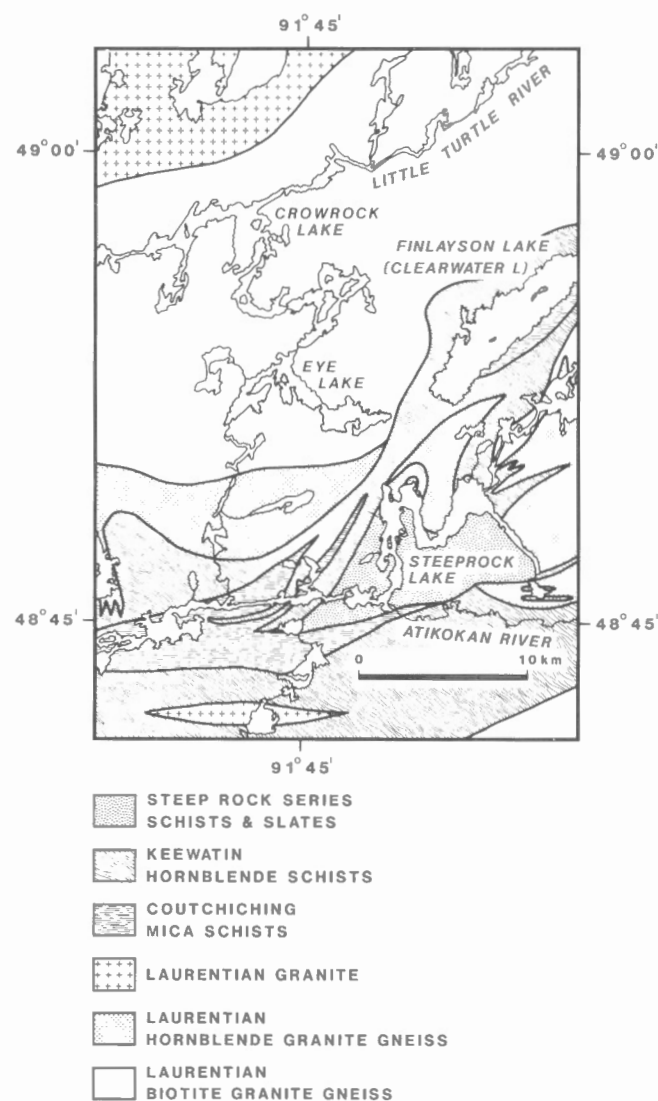


Figure 4. Geology of the Steep Rock Lake area (after Smith and McInnes, 1897).

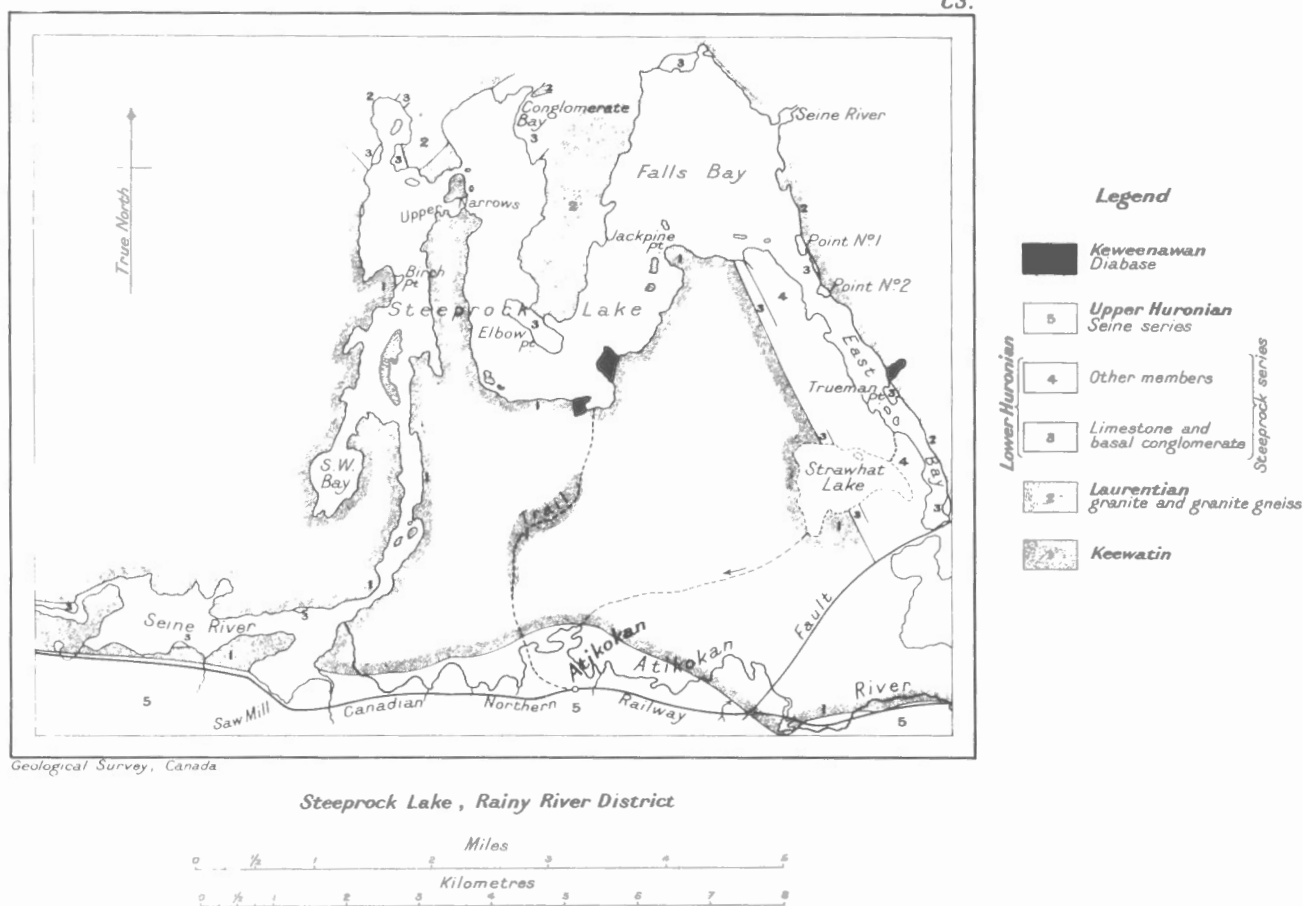


Figure 5. Geological map of the Steep Rock Lake area (after Uglow, 1913).

model of Jolliffe (1966) whereby the Steep Rock Group unconformably overlies a crystalline basement. Burnsall et al. (1988) and Wilks and Nisbet (1988) emphasized the highly deformed nature of the upper ashrock contact in the mine area and consequently, the need for further work to define the stratigraphic relation between the Steep Rock Group and neighbouring metavolcanic rocks.

Northern parts of the present study area (Fig. 1) received much less attention than the Steep Rock Lake area. Moore (1939) and Fenwick (1976) mapped large areas that include Finlayson Lake, Dashwa Lake, and Crowrock Lake with emphasis on the definition of boundaries of the metavolcanic belts.

The initial subdivision of the granite-gneiss complex in northern parts of the present study area (Schwerdtner et al., 1979, 1985) identified the Eye-Dashwa pluton, the White Otter batholith, and general structural trends in the gneisses. Morgan (1987) studied structural relations between the Finlayson Lake metavolcanic belt and the enveloping plutonic rocks. Geotechnical research by Atomic Energy of Canada Limited included fracture studies, geophysical surveys, and diamond drilling in the Eye-Dashwa pluton (Stone, 1984).

Iron mining in the Atikokan area

Iron ore was known to exist in the Atikokan area at least as early as 1893 when W.H.C. Smith noted boulders of hematite along the southern shoreline of Steep Rock Lake. McInnes (1897) succinctly assessed the provenance of the boulders by stating:

"The beds from which the blocks of rich float were derived seem to be largely covered by the waters of the lake,..."

The presence of iron ore beneath Steep Rock Lake was also predicted by Miller (1903) and Tanton (1927) but, despite extensive staking and prospecting, no development work was done until 1937. At that time Steerola Exploration Limited initiated drilling of magnetic anomalies detected by dip needle surveys. Hematitic ore was intersected at the contact between a carbonate formation and a magnetite-bearing ashrock, and a combination of magnetic and electrical surveys (Brant, 1939) were used to trace this horizon beneath the lakebed. Initial attempts at underground mining failed because of flooding; therefore, the main mining method consisted of draining Steep Rock Lake for open pit excavation.

Steep Rock Iron Mines Limited was incorporated in 1939 and, financed in part by loans from the United States Government, began the immense task of diverting the Seine River around Steep Rock Lake using a series of dams, rock cuts, channels, and adjacent lakes. The middle and east arms of Steep Rock Lake were subsequently dewatered at a rate of about 10⁶ L/minute using 14 electric pumps. One of the most difficult tasks, prior to mining, consisted of removing extensive deposits of varved clay, silt, and boulder till from the lakebed. This was done largely by dredging and pumping of slurries to adjacent settling basins and provided excellent exposures for research on the physical properties and origin of varved clays (Antevs, 1951; Legget and Bartley, 1953; Eden, 1955; Hardy and Legget, 1960).

Open pit mining began in 1945 from the "B" ore zone (see Fig. 7) and was eventually extended to the "A" and "G" ore zones which were known as the Errington, Hogarth, and Roberts mines respectively. Limited underground mining was done from shafts at the Errington and Hogarth localities between 1952 and 1961. In 1949, the "C" ore zone was leased to Inland Steel Limited and began production in 1960 as the Caland Mine. Between 1958 and 1965 the Canadian Charleson Mine produced 796 000 tonnes of ore from geothite-hematite-bearing gravel deposits located in the vicinity of the present Atikokan airport. This deposit forms part of an iron ore boulder train extending southwesterly from Steep Rock Lake (Dreimanis, 1956).

The Caland Ore Company Limited and Steep Rock Iron Mines Limited installed pelletizing plants in 1965 and 1967, respectively, and continued production until 1979. A total of 99.7 million tonnes of iron ore was mined from the Atikokan area (Northern Miner Press, 1981).

Geological setting

The Atikokan area is located in the Archean Superior Province of the Canadian Shield (see Map 1666A inset). On a regional scale, the Superior Province is subdivided into lithotectonic subprovinces based on variation in structural style, lithology, metamorphic grade, isotopic ages of rock units, and geophysical and metallogenic characteristics. Boundaries between subprovinces are marked by fault zones, intrusive contacts, and abrupt changes in metamorphic grade or style of deformation. Card and Ciesielski (1986) recognized four types of subprovinces comprising plutonic, volcano-plutonic, metasedimentary, and high-grade gneiss varieties, which form subparallel easterly trending belts. The Atikokan area includes parts of the Wabigoon and Quetico subprovinces where supracrustal rocks are dominantly of volcanic and sedimentary origin, respectively, and occur on opposite sides of a locally faulted contact.

Lithotectonic subdivision of the Superior Province has replaced the chronostratigraphic subdivision that was the subject of intense debate in the early part of this century. Use of the terms "Keewatin", "Coutchiching", "Steep Rock", and "Seine" is restricted to their type localities in the Rainy Lake-Atikokan area (e.g., Blackburn et al., 1985).

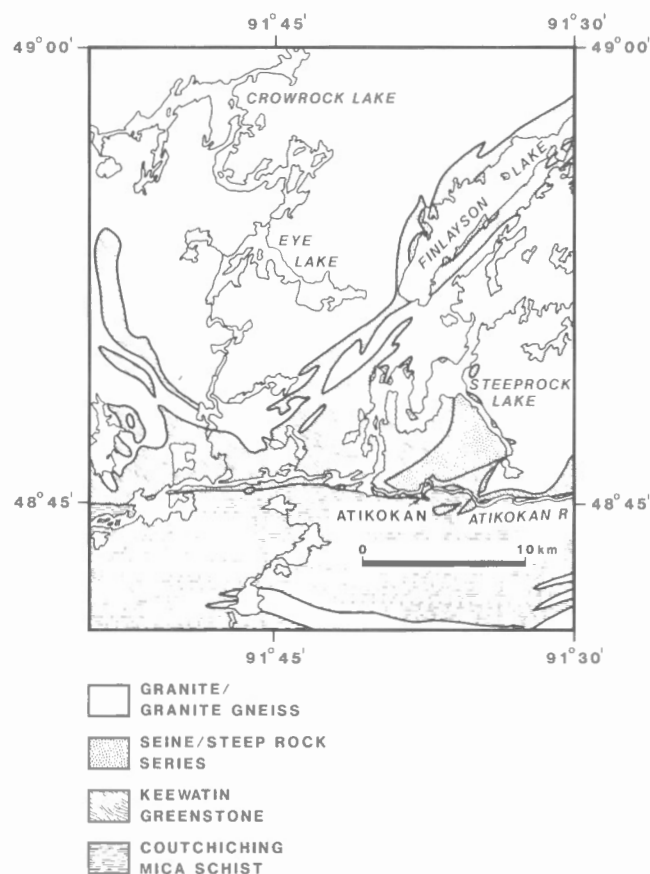


Figure 6. Geology of the Atikokan area (after Tanton, 1937).

The Keewatin is broadly comparable to metavolcanic rocks of the Wabigoon Subprovince and the Coutchiching to clastic metasediments of the Quetico Subprovince.

Nomenclature

The Atikokan area (Fig. 1; Map 1666A, in pocket) straddles an elongate belt of metasediments to the south (Quetico Subprovince) and mixed metavolcanic, gneissic, and felsic plutonic rocks to the north (Wabigoon Subprovince). For descriptive purposes the map area is divided into lithotectonic domains, each of which is characterized by a certain rock type and mode of emplacement (Fig. 9). Supracrustal sequences include dominantly metasediments in the Quetico Subprovince and metavolcanic rocks in the Nevison, Perch, Steep Rock, and Finlayson belts of the Wabigoon Subprovince. Pre- to synvolcanic intrusions include mafic tonalite and "old" tonalite (which predate the Steep Rock Group) in the Marmion batholith and Lefteye stock as well as tonalite and mafic tonalite gneisses of the Dashwa gneiss complex. Syn- to postvolcanic intrusions encompass a broad range of felsic to mafic magmas. "Young" tonalite, which postdates some supracrustal rocks, occupies the Nevison, Righteye, Wasp, Bow, and Hardtack intrusions. The Little Eye stock is composed of hornblende and diorite.

Granodiorite and granite occur in the Diversion, Margaret, Bewag, Eye-Dashwa, and White Otter felsic intrusive centres.

LITHOLOGICAL DESCRIPTION

Pre- to synvolcanic intrusions

The pre- to synvolcanic intrusions are subdivided into mafic tonalite, "old" tonalite, tonalite gneiss, and mafic tonalite gneiss (units 1a-1d; Map 1666A).

Mafic tonalite (unit 1a)

Mafic tonalite occurs as irregular lenses associated with gneisses in the northeastern corner of the map area and as scattered xenoliths in "old" tonalite (unit 1b) of the Marmion batholith. A large body of mafic tonalite straddles the Little Turtle River southwest of Bow Lake and exhibits gradational, interdigitated contacts with adjacent mafic tonalite gneiss and tonalite. Outcrops are generally dark grey, variably rounded,

and transected by dykes of tonalite and granodiorite. Mafic tonalite is medium- to coarse-grained, strongly foliated, and locally gneissic due to the presence of leucocratic schlieren.

The mafic tonalite at the western end of the Marmion batholith is unconformably overlain by supracrustal rocks of the Steep Rock belt and intruded by granodiorite (unit 8b) to the north. At this locality the mafic tonalite is well foliated, intensely fractured, and transected by metagabbro dykes that form up to 30% of the exposed bedrock. The mafic tonalite is pale green and contains rounded, blue quartz aggregates. A sample, collected along the electric transmission line north of Wagita Bay of Steep Rock Lake, yielded a U/Pb date of 3001 Ma (Don Davis, Royal Ontario Museum, pers. comm., 1987). This constitutes one of the oldest known dates in the map area.

The mafic tonalite has more than 20% mafic minerals (hornblende and biotite) at the Little Turtle River locality, and chlorite, epidote, and muscovite adjacent to the Steep Rock belt (compare samples 102 and 112 in Table A1; see Appendix A). Quartz is locally deficient to the extent that mafic tonalite may be gradational to quartz diorite.

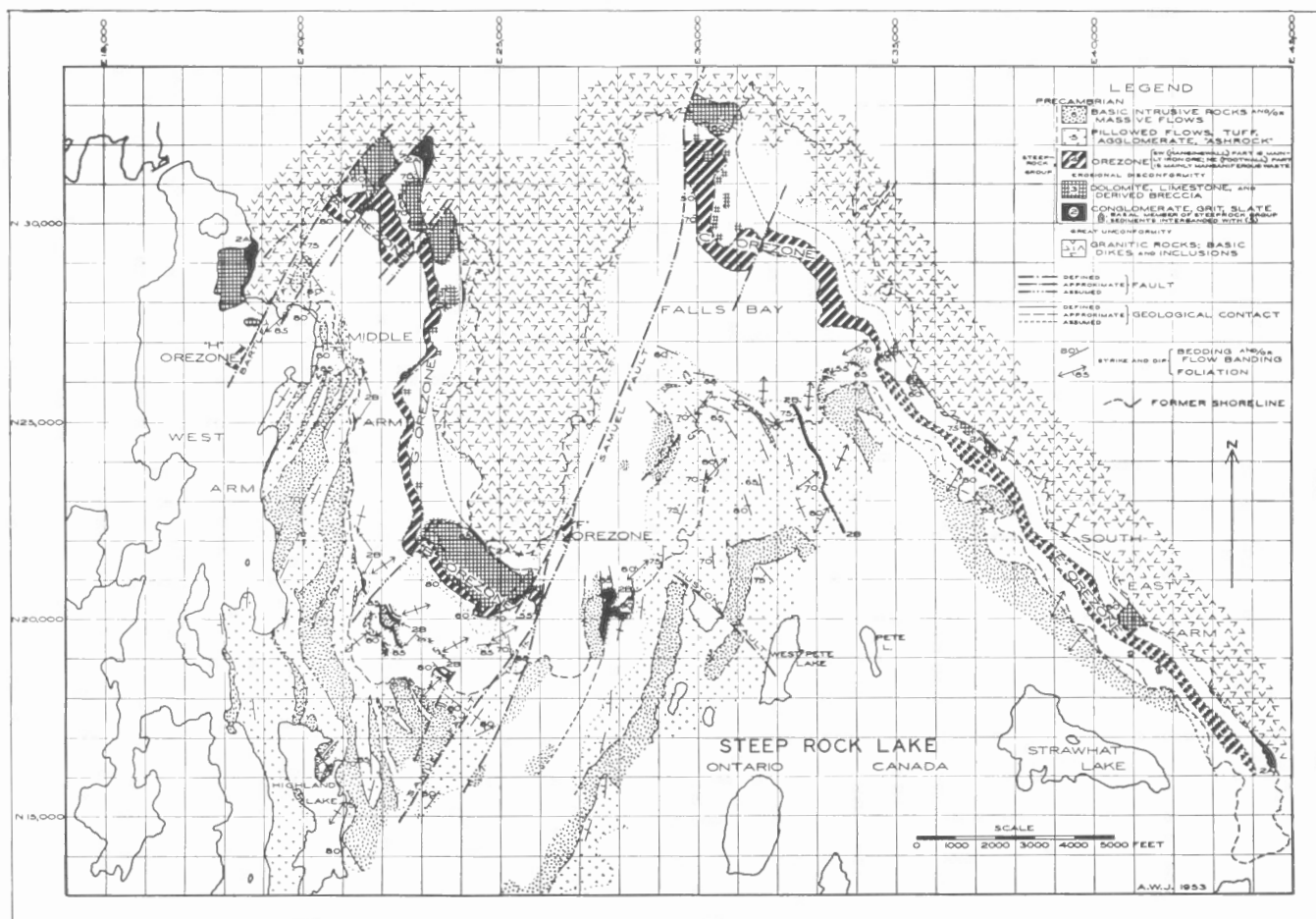


Figure 7. Geological map of the Steep Rock Lake area (after Jolliffe, 1955). Reproduced with permission of Economic Geology.

Microcline varies from 0% in sample 102 to 18% in sample 112 with the result that the latter plots in the granite field of the quartz-alkali feldspar-plagioclase (QAP) diagram (Fig. 10). The abundance of microcline in sample 112 is regarded as anomalous and is probably a result of alteration.

"Old" tonalite (unit 1b)

"Old" tonalite comprises the Marmion batholith, the Lefteye stock, and small bodies located southwest of the Bow pluton and within eastern margins of the Finlayson belt.

"Old" tonalite is so-named because it is the dominant lithology of the basement complex upon which rocks of the Steep Rock Group were deposited. Along northeastern margins of the Steep Rock belt, the "old" tonalite is gradational over distances of several metres to metasandstone and metaconglomerate at the base of the Steep Rock Group. Here the plutonic basement is tan-brown in colour, schistose, highly fractured, and transected by shear zones and abundant metagabbro dykes. The metagabbro dykes are fewer and the "old" tonalite is less intensely foliated in the central Marmion batholith (Marmion Lake area). A sample of this tonalite, collected near the Ontario Hydro generating station, has a

U/Pb titanite date of 2953 Ma (Don Davis, Royal Ontario Museum, pers. comm., 1987). Granodiorite of the Margaret and Diversion stocks (Fig. 9) intrudes the northern and southern margins of the Marmion batholith.

The crescentic Lefteye stock has gradational contacts with tonalite gneiss (unit 1c) and is in fault contact with metavolcanic rocks of the Nevison belt (Fig. 9). It is intruded by hornblende of the Little Eye stock, "young" tonalite of the Righteye stock, and granodiorite dykes. These crosscutting relations and the presence of deformed metagabbro dykes suggest that the age of the Lefteye stock may be similar to that of the Marmion batholith.

West of the Bow pluton a lensoid body of foliated "old" tonalite is mantled by thin gneissic units of amphibolitized mafic metavolcanic rocks, mafic tonalite gneisses, and mafic tonalite (units 3b, 1d, and 1a respectively). A mafic metavolcanic sliver and deformed metagabbro dykes also occur centrally within this body of "old" tonalite.

Two small lenses of "old" tonalite occur within mafic metavolcanic rocks along eastern margins of the Finlayson belt (Map 1666A). Fenwick (1976) traced the northeastern body 3 km beyond the present map boundary. The "old"

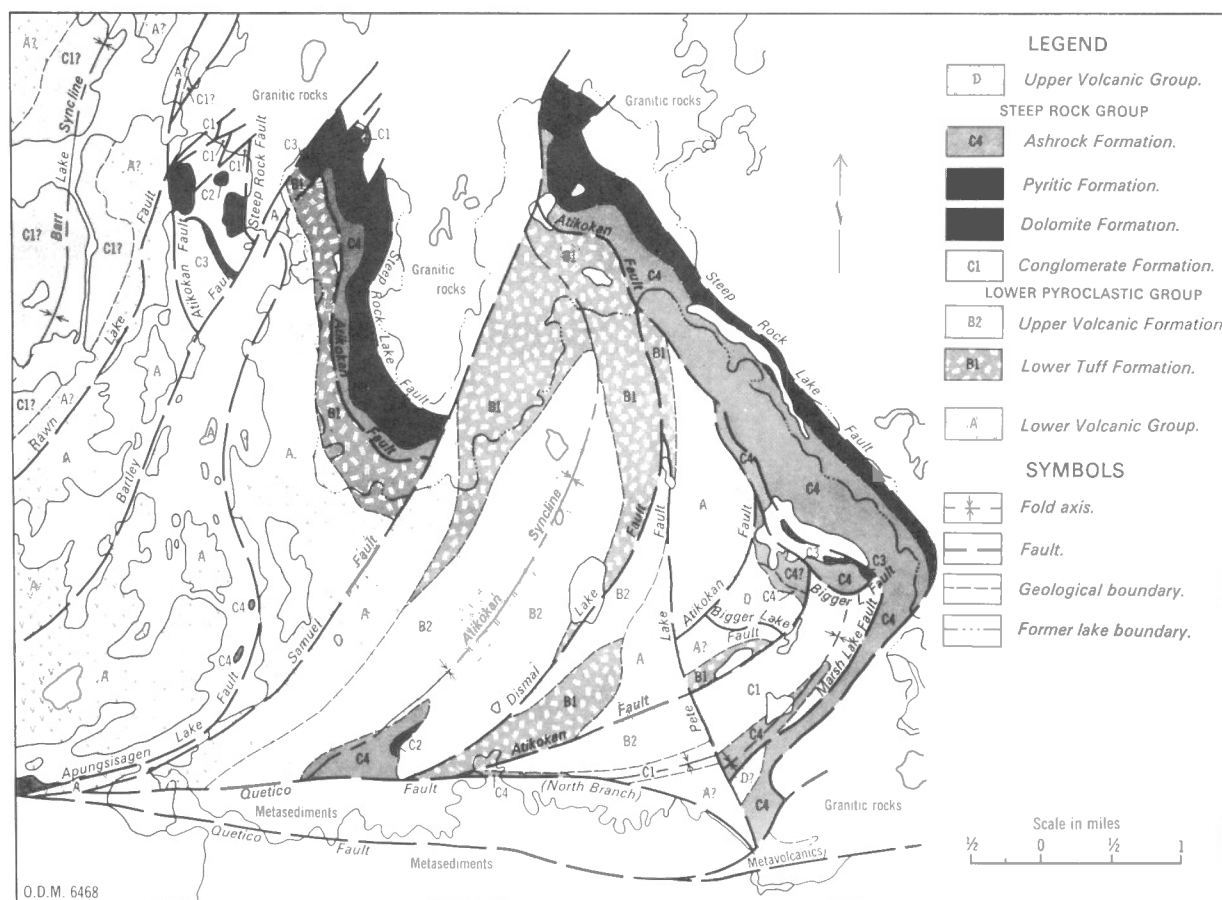


Figure 8. Geological map of the Steep Rock Lake area (after Shklanka, 1972). Reproduced with permission of the Ontario Geological Survey.

tonalite is schistose, exhibits a quartz-eye texture, and contains up to 50% deformed metagabbro dykes and a younger generation of diorite(?) dykes. Contacts with adjacent metavolcanic rocks are poorly defined as a result of high strain. Well-bedded metasandstone and metaconglomerate containing tonalitic and chert clasts occur throughout the northeastern tonalite body and are provisionally correlated with the Wagita Formation (unit 2a). This tonalite unit is interpreted to be a thin, detached slice of the Marmion batholith incorporated in the core of an antiform during folding of the Finlayson belt (see Section B-B'-B'', Map 1666A).

"Old" tonalite is typically medium- to coarse-grained, foliated, and inequigranular to porphyritic. It is composed of plagioclase (40%), quartz (25%), and biotite (20%) (Table A1; Fig. 10). Plagioclase and biotite are extensively altered to epidote, sericite, and chlorite in shear zones and adjacent to the Steep Rock belt.

Tonalite gneiss (unit 1c)

Tonalite gneiss is widespread within the Dashwa gneiss complex in northern parts of the map area (Fig. 9, Map 1666A). Contacts with "old" tonalite, mafic tonalite gneiss, and amphibolitized mafic metavolcanic rocks (units 1b, 1d, and 3b) are gradational and interdigitated.

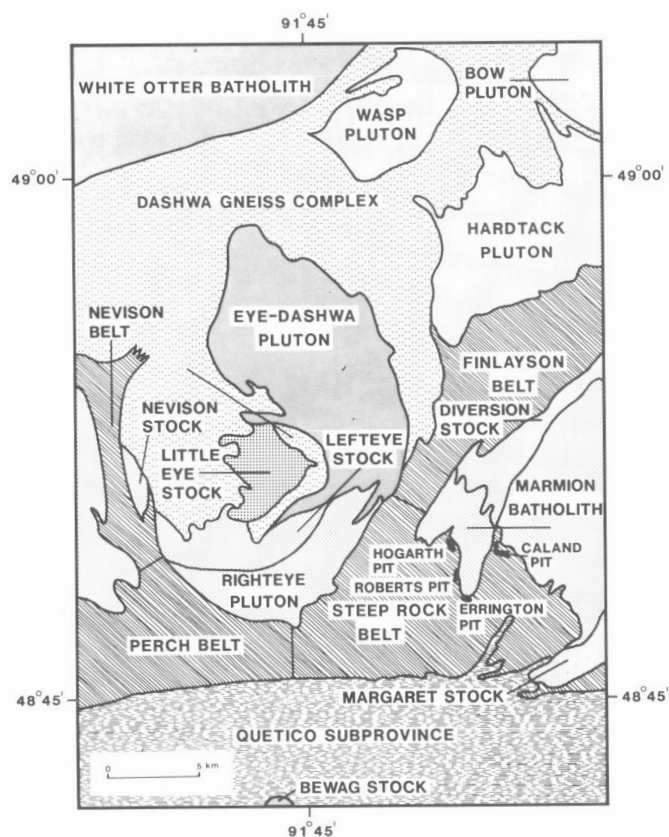


Figure 9. Lithotectonic domains and abandoned open-pit iron mines of the Atikokan area (see legend of Figure 1 for interpretation of map patterns).

Tonalite gneiss is intruded by "young" tonalite, diorite-hornblendite, granodiorite, and granite (units 6, 7, 8b, and 8c). Highly deformed metagabbro dykes, usually in the form of discordant trains of amphibole xenoliths, occur within the gneisses. The white-to-grey tonalite gneiss exhibits a pronounced but discontinuous and wavy mineralogical layering (Fig. 11). The layering, which wraps around amphibole xenoliths, shows local, tight to isoclinal folds and is disrupted by dykes and intrusive masses of "young" tonalite and granodiorite (units 6 and 8b). A sample of tonalite gneiss from northeast of the Eye-Dashwa pluton was dated at 2928 Ma U/Pb zircon (Don Davis, Royal Ontario Museum, pers. comm., 1987).

The mineral constituents of tonalite gneiss are quartz (25%), microcline (15%), plagioclase (35%), biotite (18%), and accessory minerals (Table A1). Microcline in ubiquitous, thin, conformable lenses results in most samples of tonalite gneiss plotting in the granodiorite field of the QAP

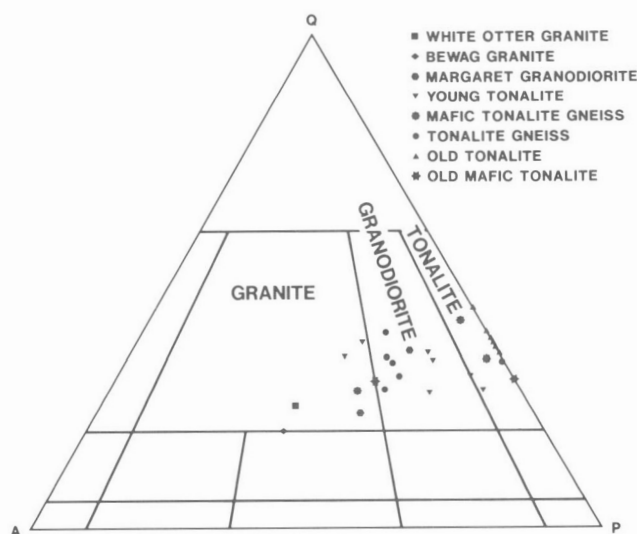


Figure 10. Quartz-alkali feldspar-plagioclase (QAP) plot for crystalline rocks of the Atikokan area.

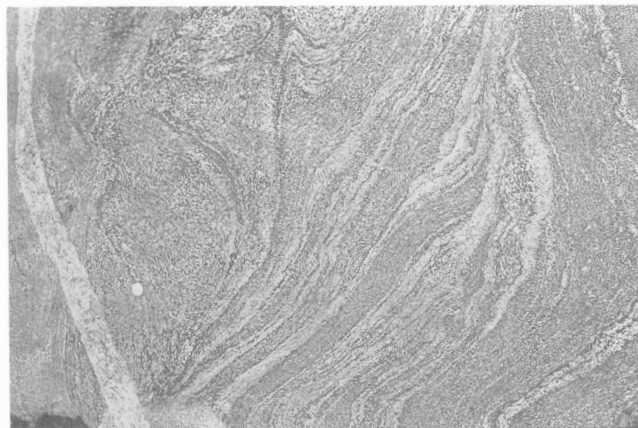


Figure 11. Tonalite gneiss cut by granodiorite dyke northeast of the Eye-Dashwa pluton. Coin is 23 mm in diameter. GSC 204108-M

diagram (Fig. 10). These microcline-bearing lenses have similar mineralogy and texture to granodiorite within crosscutting dykes and, accordingly, may have been introduced at a later stage.

Mafic tonalite gneiss (unit 1d)

Mafic tonalite gneiss mantles the Wasp pluton (Fig. 9) and also occurs as several curved and bifurcated belts throughout northern parts of the map area. A circular belt of mafic tonalite gneiss extends northward from the Nevison metavolcanic belt and envelops a domical enclave of tonalite gneiss (unit 1c). Northeast of the Eye-Dashwa pluton, mafic tonalite gneiss has gradational contacts with tonalite gneiss (unit 1c) and amphibolitized metavolcanic rocks (unit 3b) marked by progressive variation in the proportion of mafic minerals. It is distinguished from tonalite gneiss (unit 1c) by a greater abundance of mafic minerals (>20%) and by a prominent, continuous layering. Mafic tonalite gneiss weathers grey-brown and shows locally folded gneissic layering and rounded amphibole inclusions (Fig. 12). Dykes of "young" tonalite and granodiorite are present in most outcrops.

Mafic tonalite gneiss is composed of quartz (20%), variable proportions of microcline, plagioclase (30%), and mafic minerals (>20%) (Table A1). Most samples plot in the tonalite field of the QAP diagram (Fig. 10), but local concentrations of microcline in some samples shifts the compositions to the granodiorite and granite fields.

Supracrustal rocks

Supracrustal rocks of the Atikokan area include the Steep Rock Group, contiguous metavolcanic rocks in the Steep Rock, Finlayson, Perch, and Nevison belts and metasediments of the Quetico Subprovince. Wilks and Nisbet (1988) defined five formations of the Steep Rock Group, which include the Wagita, Mosher Carbonate, Jolliffe

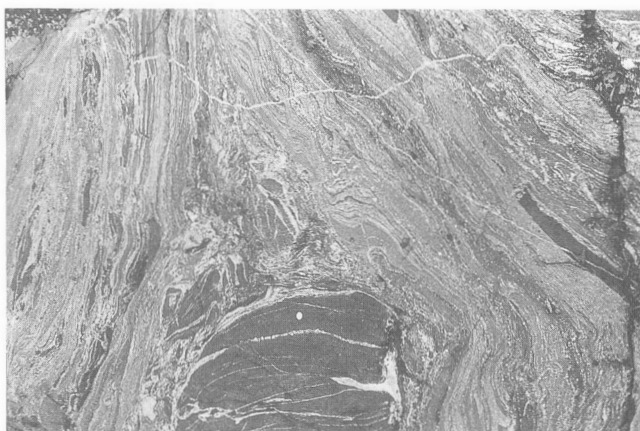


Figure 12. Mafic tonalite gneiss containing amphibole xenoliths and cut by granodiorite dikes northeast of the Eye-Dashwa pluton. Field of view is about 3 m. GSC 204108-Q

Ore Zone, Dismal Ashrock, and provisionally the Witch Bay. These formation names are used here with the exception of the Witch Bay, which is replaced by lithological units including mafic metavolcanic rocks, intermediate to felsic metavolcanic rocks, meta-agglomerate/metasediment, metagreywacke/argillite, and metaconglomerate.

Wagita Formation (unit 2a)

The Wagita Formation consists of metaconglomerate, metasandstone, pebbly metasandstone, and metapelite, which occur discontinuously along the northeastern edge of the Steep Rock belt attaining a thickness of up to 150 m. Localities include the eastern shore of Wagita Bay of Steep Rock Lake, near the former railway tunnel at the northern end of the Hogarth open pit, several sites along the eastern edge of the Hogarth and Roberts pits, the western edge of the Caland pit, the eastern shore of the Fairweather Reservoir, and along the former southeastern arm of Steep Rock Lake (Map 1666A). Clastic metasediments dispersed within the narrow lens of tonalite in the northeastern Finlayson belt are also grouped with the Wagita Formation.

Wilks and Nisbet (1988, p. 371) described the Wagita Formation (Fig. 13) as follows:

"The metaconglomerate varies from an ortho- to paraconglomerate. The clasts are angular to subrounded, 1-15 cm long, and composed of quartz, mafic tonalite, tonalite, and fine-grained, dark grey mafic material. The matrix is extremely variable over distances of 2 m, ranging from a fine, dark, pelitic matrix to a coarse, buff-coloured sand. The metasandstones are buff to light medium grey and consist of angular to subangular clasts of quartz (0.2-1 mm) set in a darker, finer grained matrix of muscovite, chlorite, clays, and calcite. The proportion of matrix in the metasandstones varies considerably (5-20%, visual estimate). The metasandstones are well bedded but poorly sorted. A few graded beds

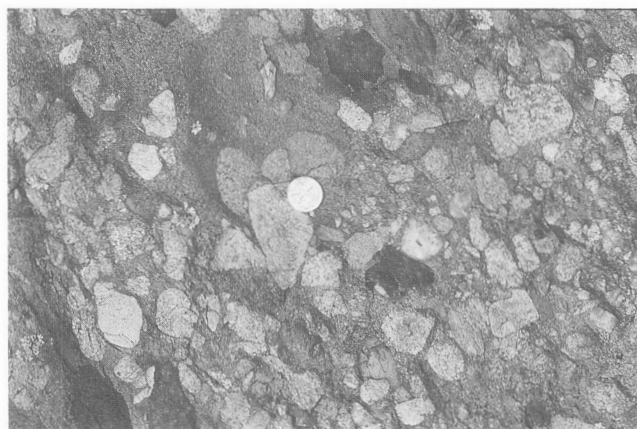


Figure 13. Mainly tonalite clasts in metaconglomerate of the Wagita Formation at the northern end of Steep Rock Lake. Coin is 23 mm in diameter. GSC 204108-P

were observed; these suggest younging to the west away from the Marmion Complex. The pebbly metasandstone is similar to the metasandstone, but scattered throughout it are subrounded clasts of quartz and tonalitic and mafic material up to 6 cm long. The pelite is light grey to dark grey and very fine grained (0.02-0.1 mm), with a well-developed slaty cleavage. The schistosity is well developed in the dark, chlorite-rich layers, throughout which fine grains of opaques are scattered. There are minor amounts of angular, recrystallized quartz and feldspar grains. The banding in the pelite is discontinuous, alternating with carbonate-rich horizons."

A tonalitic clast from the formation north of the Hogarth pit gave a U/Pb zircon date in excess of 2994 Ma (Don Davis, Royal Ontario Museum, pers. comm., 1987) and probably reflects a provenance of nearby mafic tonalite.

The unconformity at the base of the Wagita Formation is marked by a transition from unaltered tonalite to sericitized tonalite and a sericite-carbonate-quartz "grit", which becomes bedded and clast-bearing up section. Thickness of the unconformity and Wagita Formation is about 2 m on the eastern wall of the Roberts pit and about 10 m on the eastern shore of the Fairweather reservoir. Schau and Henderson (1983) regarded the unconformity as a weathered zone containing a mineral assemblage of paragonite-muscovite-chlorite-quartz-opaques.

Mosher Carbonate Formation (unit 2b)

The Mosher Carbonate Formation is distributed along the northeastern margin of the Steep Rock belt and is well exposed in abandoned open pits of the Hogarth, Roberts, Errington, and Caland mines (Map 1666A). Scattered occurrences, west of the Pluswood plant in Atikokan, south of Rawn Street in Atikokan, west of Strawhat Lake and along Highway 622 east of Atikokan, suggest that the Mosher Carbonate Formation underlies most of the eastern Steep Rock belt as shown in Section A-A' (Map 1666A). It occurs

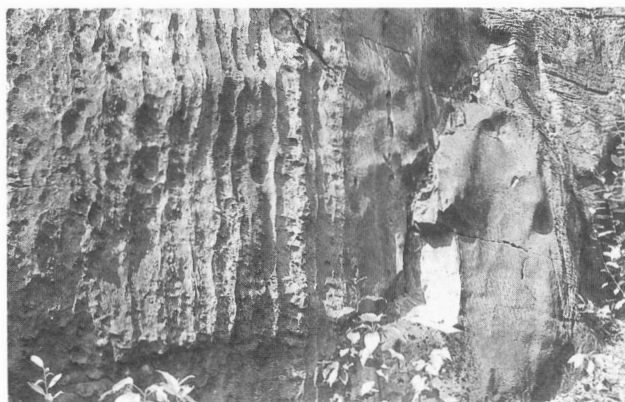


Figure 14. Mosher Carbonate Formation from the Fairweather reservoir, eastern margin of the Steep Rock belt. Carbonate is variably layered (left) to massive (right). Field of view is about 3 m. GSC 1992-074-G

stratigraphically above the Wagita Formation or in direct contact with the tonalitic basement and attains a thickness of up to 500 m.

The Mosher Carbonate Formation has been variously referred to as the Limestone, Dolomite, Carbonate, and, most recently, the Mosher Formation (Smyth, 1891; Lawson, 1912; Moore, 1938; Jolliffe, 1955, 1966; Shklanka, 1972; Wilks and Nisbet, 1988). At most localities, rocks within the formation are massive or layered (Fig. 14) and range in composition from an almost pure calcitic limestone to dolostone.

The Mosher Carbonate Formation contains intraformational metasandstone beds and the lower contact is gradational to underlying clastic metasediments over a distance of less than 1 m. The upper contact is extremely irregular and regarded as a paleokarst surface by Jolliffe (1955).

Wilks and Nisbet (1988, p. 375) described the Mosher Carbonate Formation as follows:

"The weathered surface of the laminated carbonate is light brown or buff. Although fresh surfaces are commonly bluish grey, laminae within the carbonate can vary from white to black. Resistant brownish bands of silica stand several millimetres (1-4 mm) above the general level of weathering and accentuate the banding. The laminated carbonate is composed of varying proportions of calcite, ankerite, and dolomite; minor constituents are quartz, pyrite, and kerogen. The laminae, which are readily seen in outcrop, are distinct in thin section where continuous wispy black layers are present. However, in many cases no organic matter has been preserved and the laminae are diffuse on the microscopic scale. In places the laminated carbonate can be traced upwards into clotty units due to the chaotic pattern of black wispy kerogen-rich stylolites and thin white calcite veins (1-2 mm wide), which have disrupted the original laminae. Extensive zones of breccia occur, notably in the east walls of the

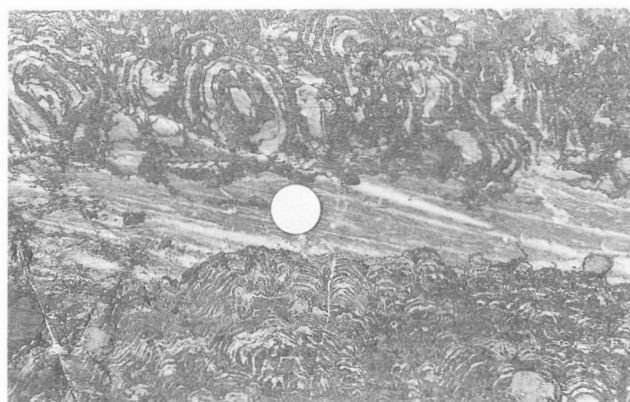


Figure 15. Hemispherical and pseudocolumnar stromatolites from the northeastern end of the Hogarth pit. Coin is 23 mm in diameter. GSC 1992-074-B

Hogarth and Errington pits, where over 500 m (along strike) of breccia outcrops. The breccia consists of angular clasts (1 cm-3 m) of predominantly dark bluish grey carbonate. In some cases brecciation appears to postdate the intrusion of mafic dykes, since mafic clasts also occur in the breccia. The mafic clasts have altered to chlorite. The matrix of the breccia is predominantly white sparry calcite, with minor quartz and clays present."

Several species of stromatolites are described by Lawson (1912), Walcott (1912), and Hofmann (1971). Wilks and Nisbet (1985) identified stratiform, pseudocolumnar, hemispherical, locally branching, conical, and giant columnar varieties. Examples of hemispherical and pseudocolumnar stromatolites are shown in Figure 15.

Jolliffe Ore Zone Formation (unit 2b)

The Jolliffe Ore Zone Formation is grouped with the Mosher Carbonate Formation on Map 1666A but is shown in Figure 7 as defined by Jolliffe (1955). The formation (up to 400 m thick) was extensively mined by open pit and underground operations at the "A", "B", "C" and "G" ore zone localities shown in Figure 7. Drill reports by Steep Rock Iron Mines Limited (Atikokan Museum) show that the Jolliffe Ore Zone Formation becomes thin and discontinuous along the former Southeast Arm of Steep Rock Lake. Drilling by the Quebec Cartier Mining Company intersected siliceous goethite-hematite, which may constitute a small occurrence of the Jolliffe Ore Zone Formation beneath the waters of Strawhat Lake (Shklanka, 1972).

Table 3. Partial analyses of material from the Jolliffe Ore Zone Formation (after Jolliffe, 1966).

	Manganiferous Paint Member		Goethite Member		Pyrite Member	
	1	2	3	4	5	6
Fe	28.9	10-37	59.6	18.	38.6	18.6
Mn	3.8	0.8-5.3	0.23	0.16	0.26	—
SiO ₂	35.5	27.8-60.7	4.63	32.	14.6	24.5
Al ₂ O ₃	1.5	0.4-5.9	1.47	33.	1.4	19.1
P	0.036	0.02-0.06	0.029	0.031	0.025	—
S	0.014	0.004-0.066	0.030	0.025	24.3	18.5
Elemental Carbon	0.02	—	—	—	—	12.9
TiO ₂	—	—	.098	2.2	—	—
Ign. Loss	7.9	5.8-7.9	8.04	14.	—	—
CaO	2.8	0.2-0.6	0.10 est.	0.08	—	0.08
MgO	1.2	0.5-1.1	0.09 est.	0.09	—	—

1. Calculated composition of 8 489 000 tons of Manganiferous Paint in the Errington B-1 zone (Huston, 1956, p. 27, 35).

2. Compositional ranges in 16 weighted averages calculated by A.W. Jolliffe for the Manganiferous Paint from all parts of the Steep Rock Lake area. These represent sludge samples from 6870 feet of drill-hole intersections, 399 chip samples, and a 98.6-foot channel sample (Huston, 1956).

3. Average of ore shipments (962 608 tons) from Steep Rock Iron Mines, Limited, in 1963.

4. "Buckshot" — pisolitic ferruginous bauxite; sample is from No. 7 Stockpile, 1952, Errington Open Pit.

5. Weighted average of drill-hole intersections totalling 1970 feet across pyritic lenses, Hogarth Mine area (Wright, 1959).

6. Carbonaceous pyritic material, Hogarth Mine area (Wright, 1959, p. 72). This sample was analyzed at the Division of Mineral Dressing and Process Metallurgy, Department of Mines and Technical Surveys, Ottawa. This analysis also shows Na₂O : 0.60%, K₂O : 2.43%, and Moisture 0.40%.

All the above represent weight percent, and "Dry Analysis". Most of these were made at the laboratories of Steep Rock Iron Mines, Limited.

Table 4. Mineralogy of pit-run ore in the Steep Rock Lake iron area (after McIntosh, 1972)

Mineral	Percent
Vivianite	0.01
Quartz	5.02
Pyrolusite	0.32
Kaolinite	5.03
Pyrite	0.02
Calcite	0.36
Magnesite	0.61
Goethite	67.3
Hematite	21.0

At present the Jolliffe Ore Zone Formation is exposed at only a few localities on the walls of the abandoned open pits and was not studied by the present authors. Jolliffe (1966) subdivided the formation into three members – a lower Manganiferous Paint, the middle Goethite, and the upper Pyrite. The Manganiferous Paint Member was regarded as a residual soil derived by weathering of the Mosher Carbonate Formation and was described as an incoherent to unctuous, rudely banded to fragmental material containing siliceous bands. The Manganiferous Paint Member is in sharp, but irregular, contact with the underlying Mosher Carbonate Formation and contains carbonate blocks. Huston (1956) identified quartz, chert, goethite, hematite, pyrolusite, illite, kaolinite, cryptomelane, manganite, gibbsite, muscovite, apatite, and carbon in the Manganiferous Paint Member and noted an increase in manganese, alumina, and iron toward the base. Chemical analyses (Table 3) reveal an Mn content ranging from 0.8 to 5.3%.

Jolliffe (1966) regarded the Goethite Member as a chemical and mineralogical variation of the Manganiferous Paint Member distinguished by a marked increase in the iron/magnesium ratio. It is composed dominantly of goethite, hematite, kaolinite, and quartz (Table 4) and shows pisolitic, vuggy, or colloform structures. The Goethite Member is commonly brecciated, with hard dark lumps of goethite and hematite in a lighter-coloured, porous, friable matrix. Local variations within the Goethite Member include conformable bands of sandy material (possibly altered dykes), well-banded cherty iron formation in the Caland pit (McIntosh, 1972), and an irregular body of pisolitic hematite in a matrix of kaolinite and gibbsite at the Errington pit (Fig. 9; Map 1666A). Jolliffe (1966) noted a similarity in appearance and high titanium content of this material (Table 3) with modern ferruginous bauxites. Chemically, the breccia or lump ore is characterized by about 60% iron and an iron/magnesium ratio greater than 200 (Table 3).

Jolliffe's (1966) Pyrite Member occurs as conformable lenses at or near the contact with the overlying Dismal Ashrock Formation (unit 3a). The pyrite grains are up to several centimetres in diameter, show colloform textures, and are interbedded with cherty and aluminous sediments containing small amounts of goethite, hematite, and carbonaceous material. Wright (1959) considered the Pyrite Member to be a syngenetic sedimentary deposit on the basis of texture, close association with other sediments, and trace element content. Wilks and Nisbet (1988), however, noted pyritic lenses characteristic of Jolliffe's (1966) Pyrite Member within the Dismal Ashrock Formation and chose to exclude this member from the stratigraphy of the Steep Rock Group.

The iron ore at Steep Rock Lake was discussed extensively during the mining activity, and various origins including replacement (Tanton, 1941, 1946; Roberts and Bartley, 1943; Hicks, 1950), syngenetic (Jolliffe, 1955, 1966), and secondary alteration of a pre-existing iron formation (Smith, 1942; Shklanka, 1972) were proposed. Kimberley and Sorbara (1976) and Wilks (1986) favoured a secondary alteration model and suggested that the Manganiferous Paint Member may have originated from metasomatic alteration rather than by surface weathering.

Dismal Ashrock Formation (unit 3a)

The Dismal Ashrock Formation is a distinctive lithological unit that occurs stratigraphically above the Jolliffe Ore Zone Formation in the eastern Steep Rock belt. It is continuous and up to 400 m thick along the western side of the Hogarth and Roberts pits to the south of the Errington pit (Fig. 9; Map 1666A). The formation extends southeast from the Caland pit along the former Southeast Arm of Steep Rock Lake where it is extensively disrupted by metagabbro dykes. Small occurrences within the Steep Rock belt are located northwest of the Pluswood plant in Atikokan, south of Rawn Street, north of Mercury Street, and at several localities between West Pete and Strawhat Lakes (Map 1666A). These

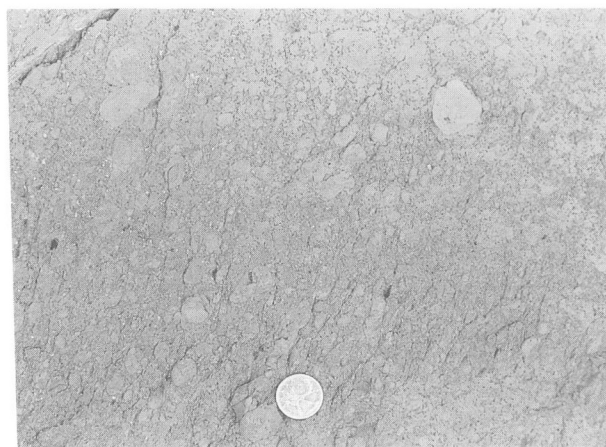


Figure 16. Dismal Ashrock Formation lapilli tuff from the western side of the Roberts pit. Coin is 23 mm in diameter. GSC 1992-074-E

occurrences and a large xenolith(?) in the western end of the Margaret stock suggest that the Dismal Ashrock Formation underlies much of the eastern Steep Rock belt as shown in Section A-A' (Map 1666A).

The Dismal Ashrock Formation is made up of tuff, lapilli tuff, and lapilli-stone (collectively called ashrock) and a lesser component of pillowed lava flows noted by Jolliffe (1955). Lapilli tuffs (Fig. 16) are most abundant. Fragments are poorly sorted as to size, rounded to subrounded, and commonly zoned. Rarely, large blocks are present.

The ashrock is dark grey, greenish, or black with a brownish weathered surface. It is soft, moderately magnetic (attracts a hand magnet), and can have one or more cleavages. The lapilli (chlorite-ferristilpnomelane-magnetite) and white calcitic amygdules are set in a fine grained grey matrix (actinolite-chlorite-talc-iron oxides-calcite). Serpentine, talc, and clay are common within numerous shear zones and faults transecting the ashrock.

A close modern analogue to the unusual fragmental texture of this rock occurs in tuff cones (e.g. Menan Butte) of the Snake River Basin, Idaho (Hamilton and Myers, 1962). At that locality, basaltic magma entered water-saturated river basin sediments and caused explosive subaerial volcanism. Weakly stratified mafic tuffs were deposited in steep-sided cone structures. A similar style of volcanism may have occurred as hot komatiitic magma emerged into the low-lying, variably karsted, and weathered Mosher Carbonate and Jolliffe Ore Zone formations.

Mafic metavolcanic rocks (unit 3b)

Mafic metavolcanic rocks (>35% mafic minerals) are abundant within the Nevison, Perch, Steep Rock, and Finlayson belts and occur as thin gneissic units distributed throughout northern parts of the area (Fig. 9; Map 1666A). Mafic metavolcanic rocks within the belts are generally fine grained (less than 1 mm), foliated, dark green, and massive to pillowed. Individual flow units can be identified in only a few localities such as the Steep Rock Lake area where approximately 80% of the flows are pillowed and the remainder are massive. Flow thicknesses are from 5 to 20 m (uncorrected for strain). Pillows are rarely observed at margins of belts, particularly the Finlayson belt, possibly because rocks in these areas have been highly deformed and metamorphosed.

Mafic metavolcanic rocks are in contact with the Dismal Ashrock Formation on the eastern side of the Steep Rock belt (Strawhat Lake area) and on the western side of the Errington, Roberts, and Hogarth open pit mines. During the authors' initial survey, a narrow unit of intermediate to felsic metavolcanic rocks and associated clastic metasediments was mapped immediately west of the Dismal Ashrock Formation on the western walls of the Errington, Roberts, and Hogarth open pit mines (Map 1666A). The intermediate to felsic metavolcanic rocks within this unit have subsequently been reinterpreted as mainly altered mafic metavolcanic rocks due to their trace element chemistry and the presence of stretched pillows. In this area the contact is the locus of faulting and

folding. Contact relations between mafic metavolcanic rocks and the Dismal Ashrock Formation have an important bearing on the stratigraphy of the Steep Rock belt and have been discussed by Bursnall et al. (1988) and Wilks and Nisbet (1988). Further description is given in the Stratigraphy section.

Mafic metavolcanic units within all belts contain a few thin (<10 m wide) felsic metavolcanic lenses, which are distinguished by a white to pale green colour and fragmental texture. Younging directions derived from pillow shapes suggest that pillowed mafic flows are overlain by intermediate to felsic flows and fragmental units (unit 3c) in the central Steep Rock belt. Mafic metavolcanic rocks are in contact with clastic metasediments (unit 4b) within all metavolcanic belts and along the Quetico-Wabigoon boundary. The supracrustal rocks are disrupted by metagabbro (unit 5) and felsic intrusions (units 6 and 8a, b, c).

Metagabbro can be difficult to distinguish from massive mafic flows where clear intrusive relations are absent. Mafic rocks that show a homogeneous crystalline texture with a grain size in excess of 2 mm are classified as metagabbro. Massive mafic flows tend to be inhomogeneous over



Figure 17. Pillows in mafic metavolcanic rocks at the western side of Steep Rock Lake. Field of view is about 2 m. GSC 204108-O

distances of several metres and crudely stratified, exhibiting a subtle streaky appearance due to changes in colour, grain size, and mineral composition.

Pillows are usually oval and less than 1 m long (Fig. 17) becoming stretched in areas of high strain and metamorphic grade, particularly at the margins of the belts. Large raft-shaped pillows are observed on islands in Steep Rock Lake. Amygdules and internal radial or concentric structures within the pillows are seldom observed although felsic varioles are present in pillows east of Steep Rock Lake. Pillow selvages (1 to 2 cm thick) are fine grained and darker in colour as compared to cores.

The largest accumulation of pillow lavas occurs in the Steep Rock Lake area on the western side of the Steep Rock belt where younging directions, based on pillow shapes, are consistently east over a distance of 5 km. This area may show an oblique section through a tilted volcanic cone. At least seven major folds whose axial traces are spaced less than 1 km apart are identified in the Finlayson belt. Close spacing of the axial traces suggests that the volcanic section may be thin (<1 km) in the Finlayson belt.

Mafic metavolcanic rocks are highly deformed, metamorphosed, and assimilated by "young" tonalite (unit 6) and granodiorite (unit 8b). In the Miranda Lake area, mafic metavolcanic rocks are gradational to diorite (unit 7) over distances of typically a few tens of metres. At the contacts, fine grained metavolcanic rocks are recrystallized into massive medium- to coarse-grained amphibolite occurring as small irregular veinlets. The veinlets become more abundant and leucocratic toward the margins of the unit and give way to medium grained diorite.

The thin units of mafic metavolcanic rocks associated with gneisses (unit 1c) in northern parts of the area are highly deformed and at amphibolite grade of metamorphism. Most units have a gneissic layering (Fig. 18) composed of thin, discontinuous hornblende, epidote, or quartz-feldspar streaks, all of which are cut by granodiorite dykes. The mafic metavolcanic gneisses are gradational to mafic tonalite gneiss (unit 1d) and at some localities, such as within the narrow septum extending northwest from the Finlayson belt, are gradational to mafic metavolcanic flows that contain identifiable pillow structures.

The mineral assemblages in mafic metavolcanic rocks are quartz-tremolite/actinolite-epidote-clinozoisite-carbonate-muscovite, quartz-carbonate-chlorite-muscovite-clinozoisite, and quartz-tremolite/actinolite-epidote-clinozoisite-microcline (Morris, 1986). Within the thin gneissic units, the mineralogy changes to predominantly plagioclase and hornblende with lesser amounts of quartz and epidote.

The age of mafic volcanism is not precisely known and may vary both within individual belts and from one belt to the next. Mafic metavolcanic rocks at the northwestern side of the Finlayson belt are cut by tonalite dykes (unit 6)

correlative with the 2936 Ma Hardtack pluton, which forms a prominent convex embayment into the belt. Accordingly, at least some mafic metavolcanic rocks in the Finlayson belt may be older than 2936 Ma.

Intermediate to felsic metavolcanic rocks (unit 3c)

Intermediate to felsic metavolcanic rocks (colour index <35%) occur in all greenstone belts of the area but in much smaller proportions than mafic metavolcanic rocks. The largest accumulations are north of Atikokan in the Steep Rock belt, along the western side of the Steep Rock belt, and on the northern shore of Perch Lake in the Perch belt. They occur as lenses within mafic metavolcanic rocks of the Nevison and Finlayson belts.

At most localities, intermediate to felsic metavolcanic rocks are medium green to white, fine grained, foliated, and exhibit fragmental structures. Contacts of thin felsic fragmental units that are interbedded with mafic flows are sharp. The thick sequence of pillowed mafic lavas in the western Steep Rock belt faces consistently eastward to the contact with intermediate to felsic metavolcanic rocks (see Map 1666A in general area of the Atikokan airport). This structural evidence suggests that intermediate to felsic metavolcanic rocks overlie mafic metavolcanic rocks in the Steep Rock belt and confirms similar relations that occur locally in the Finlayson belt.

East of the Atikokan airport, intermediate fragmental rocks (Fig. 19) comprise variably sized and shaped monolithic fragments in a fine grained, mottled matrix that is crudely stratified and displays both reverse and normal grading. The ash, lapilli, and a lesser proportion of blocks and bombs are supported both by the matrix and other fragments. Most fragments are fine grained and homogeneous lithic material, but some display a concentric structure (accretionary lapilli?) and others that are crudely stratified are possibly fiamme formed by the collapse of pumice fragments. The monolithic and poorly sorted character of these fragments suggests that they were deposited close to an extrusive volcanic centre. Elsewhere within the large unit of intermediate to felsic metavolcanic rocks extending north from Atikokan toward the Caland pit, the breccias are heterolithic and contain well-rounded lithic fragments in the 10 to 50 mm range. Bedding is seldom visible although the breccias alternate with fine grained, faintly eutaxitic material that may be flow deposited. For the most part, the breccias appear to be lahars and avalanche deposits.

A thin unit of intermediate to felsic metavolcanic rocks was mapped on the west side of the Dismal Ashrock Formation in the western walls of the Errington, Roberts, and Hogarth open pit mines (Map 1666A). This unit has subsequently been reinterpreted as a zone of altered mafic metavolcanic rocks due to the presence of pillows and trace element geochemistry, which shows greater similarity to mafic than felsic rocks.

Intermediate to felsic metavolcanic rocks are interdigitated with and transitional to epiclastic rocks (unit 4b) north of Atikokan and on the western side of the Steep Rock belt. The contact between dominantly fragmental, intermediate to felsic metavolcanic units in the Perch belt and clastic metasediments of the Quetico Subprovince is sharp, occurring over distances of less than 10 m in some places.

The intermediate metavolcanic rocks from the central Steep Rock belt contain a mineral assemblage of plagioclase-quartz-biotite-muscovite-chlorite and minor opaques. Most samples are calc-alkaline andesites with a lesser number of dacites.

Intermediate to felsic metavolcanic rocks in the Atikokan area are undated at present. The ages of similar units located west at Calm Lake, Mine Centre, and Rainy Lake are in the range of 2722.3 ± 1.3 to 2727.4 ± 4.9 Ma (Davis et al., 1989). These dates indicate that volcanic activity occurred within a period of a few Ma at several localities along the Wabigoon-Quetico boundary and imply that the Steep Rock belt, which occupies a similar structural position, may host coeval volcanic rocks.

Metagreywacke, argillite (unit 4a)

Well-bedded metagreywacke and argillite sequences are widespread in the Quetico Subprovince south of Atikokan and extend for hundreds of kilometres to the east and west (see Map 1666A inset). Two synclinal units of metagreywacke and argillite extend northeast from the Quetico Subprovince into the eastern Steep Rock belt and are cut by metagabbro dykes. Small lenses of unit 4a are present in all metavolcanic belts, particularly the Finlayson belt.

Sharply defined vertically dipping beds from 20 to 300 mm thick characterize most outcrops (Fig. 20). Typical beds comprise a fine- to medium-grained (0.05 to 2 mm) poorly sorted base of metagreywacke that grades upward into very fine grained (<0.05 mm), laminated argillite. Massive metagreywacke beds and argillite beds are also common. Metagreywacke is grey, weathers brown, and comprises

subrounded clasts of quartz and feldspar in a very fine grained quartz, feldspar, muscovite, biotite, and/or chlorite matrix. Argillite is dark grey to black and contains a few fine grains of quartz, feldspar, and muscovite in an amorphous matrix.

At several localities south of Atikokan relatively thick beds are noted (200 to 500 mm) containing coarse (up to 5 mm) white lithic material, probably of felsic volcanic origin. Intraformational metaconglomerate beds (Fig. 21) occur in the vicinity of the Ministry of Transportation and Communications base on Highway 11 south of Atikokan. These metaconglomerates contain an assortment of lithic fragments, which include tonalite, chert, greywacke, and felsic volcanic rock, but lack recognizable mafic volcanic clasts.

Reversals in the structural younging direction derived from graded beds indicate that numerous folds are present in the sedimentary sequence. Minor M-shaped folds are well developed at fold closures and bedding is transposed along a penetrative axial plane foliation. Massive metagreywacke beds are thickened at fold closures.

Contacts between clastic metasediments of the Quetico Subprovince and metavolcanic units are exposed west of Perch Lake and on the railway west of Atikokan. At these localities, well-bedded metagreywacke grades through phyllite to fragmental intermediate metavolcanic and massive mafic metavolcanic rocks respectively, over distances of 2 to 10 m. Metaconglomerates (unit 4c) are locally developed at this contact.

Deposition of the Couthiching Group at Rainy Lake (correlative with Quetico metasediments of this area) is constrained in age between 2704 ± 3 Ma detrital zircons and 2692 ± 2 Ma titanite from a crosscutting felsic sill (Davis et al., 1989). Single zircons from Quetico metasediments south of Atikokan are dated mainly at 2700 to 2720 Ma (Davis, 1988); deposition of Quetico metasediments is bracketed between crystallization of the youngest detrital zircon at 2698 ± 3 Ma and crystallization of zircons at 2688 ± 4 Ma in the Blalock pluton, which intrudes the metasediments about 20 km east of Atikokan (Davis et al., 1990). Zircons from the

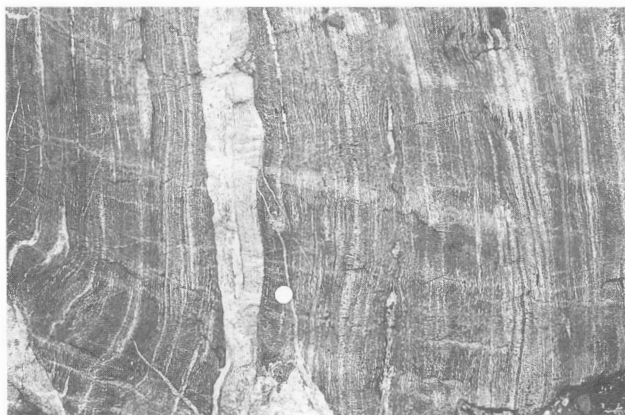


Figure 18. Amphibolitized, gneissic mafic metavolcanic rocks cut by a granodiorite dyke from the Highland Lake area. Coin is 23 mm in diameter. GSC 204108-B

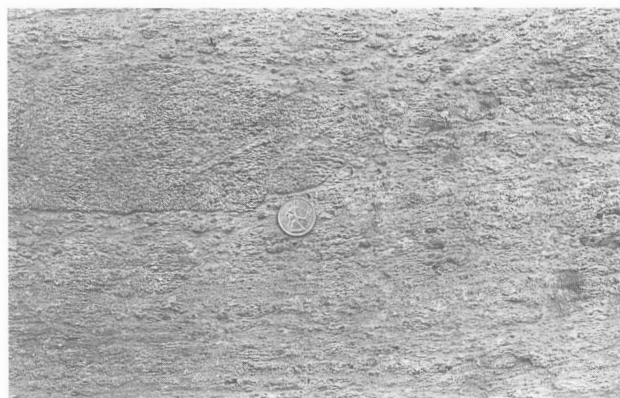


Figure 19. Intermediate volcanic fragmental rocks from north of Atikokan. Coin is 23 mm in diameter. GSC 1992-074-C

intraformational metaconglomerate and a coarse metagreywacke bed give U/Pb dates of 2901 and 3004 Ma respectively, and suggest a component of detritus from the prevolcanic basement complex in Quetico metasediments. A similar source can be postulated for 3001 Ma zircons dated from the small metagreywacke unit west of the Errington pit (Don Davis, Royal Ontario Museum, pers. comm., 1987).

Modal analysis of 45 thin sections by Johnson (1987) showed an average of 30% quartz and 30% feldspar in the Quetico metasediments and variable proportions of muscovite, biotite, chlorite, calcic amphibole, garnet, staurolite, andalusite, epidote, opaques, and carbonate. Metamorphic grade increases southward within the Quetico Subprovince and is discussed further in the Metamorphism section.

Meta-agglomerate, metasandstone (unit 4b)

Meta-agglomerate is used here to imply a metamorphosed, coarse clastic sedimentary rock, which contains abundant lithic fragments of volcanic origin. Meta-agglomerate on the western side of the Steep Rock belt grades northward to metasandstone, which in turn, is transitional to metagreywacke in the Finlayson belt. A small unit of meta-agglomerate is located north of Atikokan in the Steep Rock belt.

Meta-agglomerate comprises a thickly bedded assortment of heterolithic, subrounded, and spherical to elliptical clasts (<10 cm) in a fine- to coarse-grained matrix. Meta-agglomerate on the western side of the Steep Rock belt is transitional to pebbly metasandstone and metasandstone. Pebbly metasandstone is characterized by pebble horizons and isolated, round pebbles composed chiefly of intermediate to felsic metavolcanic material within massive to thickly bedded, coarse grained metasandstone. Metasandstone is tan brown, medium- to coarse-grained, well foliated, and shows faint, discontinuous dark laminations. Many outcrops appear massive and homogeneous lacking recognizable bedding. Rounded quartz and feldspar grains are locally visible, but the penetrative foliation and metamorphic recrystallization have



Figure 20. Well-bedded greywacke-argillite metasediments from east of Lerome Lake. Coin is 23 mm in diameter. GSC 204108-S

largely obliterated the primary granular texture. Quartz, plagioclase, rare lithic fragments, muscovite, biotite, and chlorite are identified in metasandstone.

Meta-agglomerate and metasandstone occurrences, such as on the western side of the Steep Rock belt, are interpreted as a restricted alluvial-fan environment between an elevated volcanic source region and a distant basinal environment characterized by resedimented turbidites (Ojakangas, 1985).

Metaconglomerate (unit 4c)

Metaconglomerate units, possibly correlative with the Seine Group, occur discontinuously along the Quetico-Wabigoon boundary on the northern shore of Perch Lake, northwest of Jackfish Lake, and south and southwest of Atikokan. They are within greywacke/argillite metasediments (unit 4a) of the Quetico Subprovince but adjacent to metavolcanic rocks of the Wabigoon Subprovince.



Figure 21. Metaconglomerate bed in metagreywacke south of Atikokan. This outcrop was partly removed in 1988 to facilitate widening of Highway 11. GSC 1992-074-F



Figure 22. Deformed metaconglomerate of the Seine Group (?) southwest of Atikokan. Coin is 23 mm in diameter. GSC 1992-074-H

The polymictic metaconglomerate contains variably sized pebbles and cobbles of tonalite, quartz, chert, several varieties of intermediate to felsic metavolcanic rock, greywacke, phyllite, and mafic metavolcanic rock (Fig. 22). Tonalite clasts (up to 20 cm long), are well rounded and show transgranular fractures formed during postsedimentary deformation. Quartz and chert clasts are well rounded and spherical, whereas metavolcanic clasts, particularly the more mafic varieties, are highly elongated at least in part owing to deformation. In contrast to the prevolcanic Wagita Formation, these metaconglomerates contain abundant volcanic clasts and a distribution of clast lithologies similar to the Seine Group (Wood, 1980). The matrix is a sericitic metasandstone of variable grain size that comprises more than half of the metaconglomerate. Bedding is vague at most localities except southwest of Atikokan where thick to very thick (up to 3 m) metaconglomerate beds alternate with metasandstone that resembles the metaconglomerate matrix.

Metaconglomerate of the Atikokan area is tentatively correlated with the Seine Group on the basis of similar clast lithologies and structural position of units astride the Quetico-Wabigoon boundary. Davis et al. (1989) constrained deposition of the Seine Group between a 2696 \pm 5/-3 Ma U/Pb zircon date on a clast and the 2686 \pm 2/-1 Ma U/Pb zircon date on the Ottetail Pluton (80 km west of Atikokan), which they believed postdates development of a regional foliation in the Seine Group. Within the limit of errors in the dates, the data show deposition of the Seine Group either contemporaneous with the Couchiching Group or within a few Ma thereafter. Contacts of the metaconglomerate units are not well exposed in the Atikokan area; therefore, their age relation to the Quetico metasediments cannot be verified by field observations.

Syn- to postvolcanic intrusions

Syn- to postvolcanic intrusions include metagabbro, diorite, and hornblende as well as a suite of felsic plutonic rocks ranging in composition from tonalite through granodiorite to granite. Rare gabbro dykes of Middle Proterozoic age transect the granites and gneisses.

Metagabbro (unit 5)

Dykes, sills, and irregular masses of metagabbro transect all rock types in the area except for the late granites and possibly hornblende in the Little Eye stock. Deformed metagabbro dykes are particularly common in metavolcanic rocks (units 3b and 3c) and mafic and "old" tonalite (units 1a and 1b) of the Marmion batholith. A network of anastomosed, northeasterly trending metagabbro dykes transects the Marmion batholith (Fig. 23) and passes through the Steep Rock Group to a metagabbro sill(?) at the contact between the Dismal Ashrock Formation and mafic metavolcanic rocks. The large metagabbro sill extends along the eastern margin of the Steep Rock belt and intrudes clastic metasediments (unit 4a) at Atikokan. The metagabbro complexes form large

rounded bluffs and attain their largest surficial exposure within mafic metavolcanic units of the central and western Steep Rock belt and in the Perch belt.

The thickness and abundance of metagabbro dykes decrease with distance from the metavolcanic belts. Dykes are commonly 100 m wide composing 30% of the Marmion batholith in contact with the Steep Rock belt (Fig. 23) but seldom exceed 10 m width and 10% of the central Marmion batholith. Dykes in the Marmion batholith exhibit an intense foliation, complex curved and bifurcated shapes, and abrupt changes in thickness and terminations that at least partly result from deformation. Metagabbro dykes within tonalite and mafic tonalite gneisses (units 1c and 1d) are ubiquitous, up to 3 m wide, and highly attenuated, boudinaged, and folded. Amphibolite xenoliths within gneisses (Fig. 12) and mafic schlieren may be remnants of similar mafic intrusions.

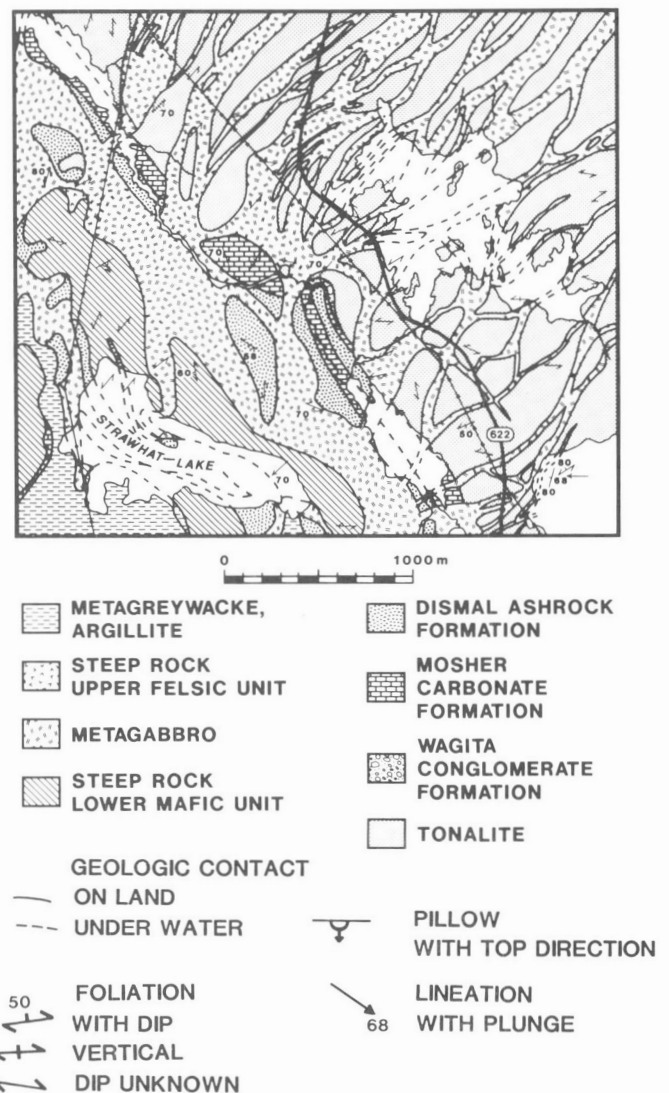


Figure 23. Detailed geological map of the northeastern contact of the Steep Rock belt and Marmion batholith.

Metagabbro dykes transect "young" tonalite (unit 6) but are less abundant than in mafic tonalite, "old" tonalite, tonalite gneiss, and mafic tonalite gneiss (units 1a, 1b, 1c, and 1d). Dykes also transect granodiorite (unit 8b) in the Margaret stock and Diversion stock where they are less deformed than in older rocks.

Metagabbro within volcanic belts is massive and homogeneous but locally foliated, dark green, and crystalline with a grain size exceeding 2 mm. Igneous textures are rarely preserved in metagabbro. Phenocrysts of primary olivine, augite, and plagioclase are present at some localities, but most samples contain actinolite, epidote, chlorite, partly sericitized plagioclase and variable accessory serpentine, carbonate, quartz, and opaques.

Shklanka (1972) identified an early and late suite of mafic intrusive rocks and, on the basis of crosscutting relations, chemical composition, extent of alteration, and mineralogy, Wilks (1986) proposed four generations of dykes. Metagabbro dykes are not subdivided in this study but at least two generations are known to exist. An older set of dykes is unconformably overlain by the Steep Rock Group, particularly along the eastern walls of the Hogarth and Roberts pits, and a younger set transects the Steep Rock Group (Chart A of McIntosh, 1972 and Fig. 23). Most dykes, including those from the Marmion batholith, appear to postdate lower formations of the Steep Rock Group and may represent feeders to the volcanic extrusive centres.

"Young" tonalite (unit 6)

"Young" tonalite occurs as irregular and oval to crescentic intrusions including the Wasp pluton, Bow pluton, Hardtack pluton, Nevison stock, and Righteye pluton (Fig. 9; Map 1666A). Dykes and irregular masses of "young" tonalite have invaded much of the Dashwa gneiss complex (Fig. 9) comprising 10 to 30% of outcrops. Similar intrusions transect mafic and old tonalite of the Marmion batholith and metavolcanic rocks of the Finlayson, western Steep Rock, and Perch belts.

"Young" tonalite is so-named because it intrudes metavolcanic rocks and is thus younger in age than mafic tonalite and "old" tonalite which are unconformably overlain by the Steep Rock Group. A sample collected from the Hardtack pluton gave a U/Pb zircon date of 2936 Ma (Don Davis, Royal Ontario Museum, pers. comm., 1987).

Contacts of "young" tonalite plutons with adjacent tonalite and mafic tonalite gneisses (units 1c and 1d) are gradational over several hundred metres. The "young" tonalite plutons, particularly the Hardtack pluton, are inhomogeneous and contain numerous schlieren, xenoliths, and large enclaves of amphibolitized mafic metavolcanic rocks and "old" tonalite and gneisses. The proportion of inclusions increases toward the contacts with adjacent tonalites and gneisses. Contacts with mafic metavolcanic rocks (unit 3b) are sharp within less than 1 m. The Righteye pluton grades from tonalite to granodiorite and contains large irregular inclusions of diorite and hornblende.

"Young" tonalite is white, weakly foliated, and contains inequigranular megacrysts of quartz and feldspar. It is composed of 20 to 30% quartz, up to 20% microcline, and about 40% plagioclase (An₂₈₋₃₄). Mafic minerals are biotite and chloritized hornblende (Table A1).

"Young" tonalite is distinguished from "old" tonalite by a weaker foliation, lower degree of alteration, and fewer fractures, dykes, and amphibolitic or gneissic xenoliths. "Young" tonalite invariably contains microcline and some samples plot in the granodiorite and granite fields of the QAP diagram (Fig. 10). The Righteye pluton (Tables A2, A3, and A4) is particularly rich in microcline and contains mappable phases of granodiorite (unit 8b).

Diorite, hornblende (unit 7)

A heterogeneous rock unit, compositionally variable from diorite to hornblende, occurs at scattered localities in the map area in association with late felsic intrusions (units 6 and 8b) and tonalite gneisses (unit 1c). Diorite occurs in the Little Eye stock, in crescentic lenses within the large circular enclave of tonalite gneiss in the Eye-Dashwa granite pluton and in small units at margins of the Nevison stock, adjacent to the Nevison and Perch belts, and within the Righteye pluton.

Many diorite bodies form gradational boundaries between mafic metavolcanic rocks (unit 3b) and felsic intrusions (units 6, 8b, and 8c). For example, in the Miranda Lake area the Perch and Nevison belts are successively intruded by tonalite, granodiorite, and granite. Mafic metavolcanic rocks are recrystallized into medium grained, granular amphibolite that becomes leucocratic and gradational to diorite. Mafic schlieren and metavolcanic xenoliths with different degrees of assimilation are common in the diorite. "Young" tonalite, granodiorite, and granite intrude or are gradational to unit 7.

In contrast to the small gradational diorite bodies, the Little Eye stock (Fig. 9, Map 1666A) intrudes tonalitic gneisses (unit 1c) and is not in direct contact with large felsic intrusions (units 6, 8b, and 8c) or mafic metavolcanic rocks (units 3b). Gravity modeling shows that the Little Eye stock dips outward to a depth of 1.6 km (Gibb et al., 1988; Section B-B'-B'', Map 1666A). It is characterized by a high magnetic field similar to that of the Eye-Dashwa pluton (Stone, 1984) and is compositionally variable from diorite at margins to hornblende at the core (Fig. 24).

At most localities, diorite is grey, granular, medium- to coarse-grained, and weakly foliated to gneissic. The proportion of mafic minerals varies markedly such that the composition of unit 7 spans fields of diorite, monzodiorite, quartz monzodiorite, granodiorite, quartz diorite, and tonalite.

Diorite is composed of plagioclase, variable amounts of hornblende, biotite, microcline, quartz, epidote, and titanite. Hornblende, in addition to hornblende, contains biotite and about 10% combined quartz, plagioclase, epidote, calcite, and apatite (Table A1).

Quartz monzodiorite, quartz monzonite (unit 8a)

Quartz monzodiorite mantles the southern part of the Eye-Dashwa pluton and forms a small satellite pluton at Volcano Bay of Crowrock Lake. Contacts with tonalite gneisses (unit 1c) are poorly exposed but appear to be the locus of younger granodiorite intrusions at many locations.

Quartz monzodiorite is pink to red, medium grained, equigranular, and weakly foliated. It is composed of plagioclase and hornblende with lesser amounts of quartz and microcline (Table A1) and contains small rounded hornblende inclusions. Modal estimates vary so that rocks within unit 8a plot in the fields of quartz monzodiorite, monzodiorite, monzonite, and quartz monzonite (Fig. 25). Quartz monzodiorite is gradational through granodiorite to granite (unit 8c) at the core of the Eye-Dashwa pluton.

A sample of quartz monzodiorite from the eastern rim of the Eye-Dashwa pluton gave a K-Ar hornblende date of 2472 ± 20 Ma (Kamineni and Stone, 1983) which may have been reset by extensive fracturing. The field relations and geochemical data suggest that the quartz monzodiorite is an early intrusive phase of the Eye-Dashwa pluton and predates the 2665 Ma granite core (Pb/Pb titanite; Zartman and Kwak, 1990).

Granodiorite (unit 8b)

Granodiorite, locally gradational to tonalite and granite, is widespread throughout felsic plutonic and gneissic domains of the Atikokan area. The Diversion and Margaret stocks (Fig. 9; Map 1666A) are the largest intrusions. Rocks of unit 8b partly rim the White Otter batholith and the Eye-Dashwa pluton and occur as irregular, bifurcated masses between the Eye-Dashwa and Righteye plutons. Dykes and intrusive masses are present in most outcrops of tonalite gneiss, mafic tonalite gneiss, and amphibolitized mafic metavolcanic rocks (units 1c, 1d, and 3b) of the Dashwa gneiss complex.

The Margaret stock intrudes the eastern Steep Rock belt and extends east of the map area. The Margaret stock is of historical interest because Smyth (1891) recognized that it was younger than both the "Marmion basement complex" and "Steep Rock Series" (see Fig. 3). He proposed the term "Atikokan Series" for late felsic intrusions such as the Margaret stock. This prompted many later researchers such as Smith (1893), Lawson (1912), Tanton (1937), and Moore (1939) to visit the locality but all grouped the Margaret stock with the adjacent Marmion batholith and Smyth's "Atikokan Series" never gained acceptance.

The Margaret stock is zoned from an outer mafic granodiorite rim to a coarse grained, porphyritic granite core (Fig. 10). Hornblende is the dominant mafic mineral (Table A1). The stock is cut by metagabbro dykes and has a prominent aeromagnetic expression.



Figure 24. Hornblende of the Little Eye stock cut by granodiorite dykes. Coin is 23 mm in diameter. GSC 204108-N

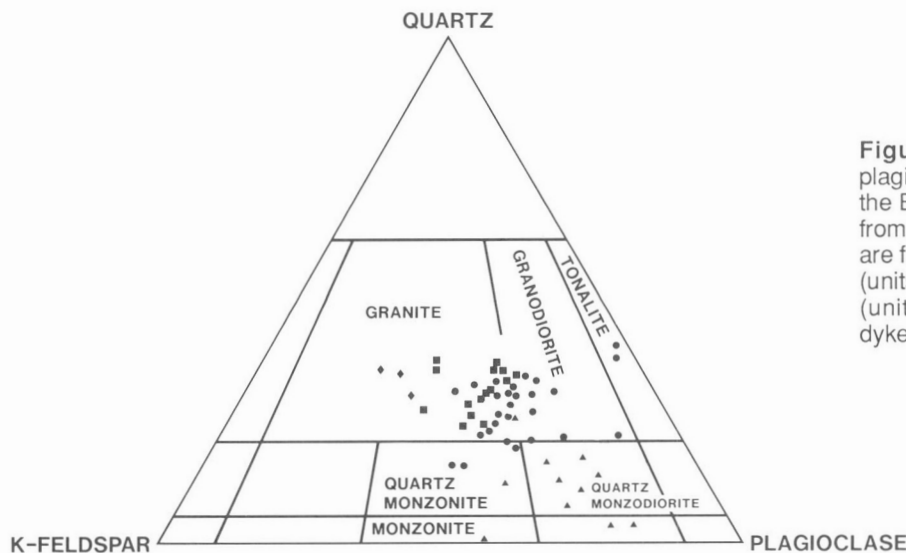


Figure 25. Quartz-alkali feldspar-plagioclase plot showing samples from the Eye-Dashwa pluton. Triangles are from the outermost rim (unit 8a), circles are from the rim gradational to the core (units 8a, c), squares are from the core (unit 8c), and diamonds are aplite dykes.

The Diversion stock has sharp intrusive contacts with the adjacent Finlayson belt and Marmion batholith. It is interdigitated with mafic tonalite, to the southwest and extends northeast beyond the map area. It is composed of coarse grained, weakly foliated, quartz- and microcline-porphyritic granodiorite to granite and contains rare tonalite and metavolcanic inclusions. Metagabbro dykes are common at the southwestern end. The Diversion stock is leucocratic (<15% mafics) and is not compositionally zoned. It has a preliminary U/Pb zircon date of 2800 Ma (Don Davis, Royal Ontario Museum, pers. comm., 1987).

Granodiorite mantles the White Otter batholith in northwestern parts of the map area. Outcrops comprise several crosscutting phases of coarse grained to pegmatitic, leucocratic granodiorite and partially assimilated tonalite gneiss xenoliths. Rocks of the unit appear to have formed by successive injection of dykes and masses of granodiorite at the margins of the White Otter batholith. The granodioritic intrusions diminish southeasterly and tonalitic xenoliths become larger and more abundant at the gradational contact with the Dashwa gneiss complex. Similar intrusions are exposed discontinuously around the Eye-Dashwa pluton and extend southwesterly to the Righteye pluton.

Granodiorite comprises up to 30% of most outcrops in the Dashwa gneiss complex. The form of these intrusions varies from 1 to 2 cm wide, discontinuous and conformable pods to 100 m wide pegmatite dykes. Early intrusions are conformable with gneissic layering and have diffuse contacts whereas the youngest dykes (Fig. 18 and 24), tend to have sharp discordant contacts. Granodiorite is white to pink and made up of quartz, megacrystic microcline, plagioclase, and less than 10% biotite.

Granite (unit 8c)

Granite intrusions record the youngest major igneous activity in the Atikokan area. The White Otter batholith, Eye-Dashwa pluton, Bewag stock, a small stock north of Miranda Lake, and dykes in the eastern Hardtack pluton account for 19% of the area (Fig. 9; Map 1666A). All are homogeneous, coarse grained granodiorite-granite intrusions with a weak foliation defined by the long axes of microcline megacrysts, quartz, or biotite grains.

The White Otter batholith extends approximately 30 km north and west of the present map area. Schwerdtner et al. (1979) outlined a 5 km wide brecciated border zone of angular, unrotated blocks of gneissic tonalite-granodiorite in a massive granodiorite-to-granite matrix, which corresponds to the granodiorite rim (unit 8b) of this study. Tonalitic xenoliths are rare in the White Otter batholith and the grain size coarsens from the rim to the core. Spectacular examples of subhorizontal fractures are exposed in granite cliffs on White Otter Lake.

The elliptical Eye-Dashwa pluton (2665 Ma, Pb/Pb titanite; Zartman and Kwak, 1990) has a surface area of 75 km². It is compositionally zoned from an outer quartz

monzodiorite rim to a granite core and contains 15% xenoliths of tonalite gneiss (unit 1c). The satellite pluton at Volcano Bay of Crowrock Lake is composed entirely of quartz monzodiorite. Foliations in gneissic country rocks are intensely developed adjacent to the granite contact and mantle the pluton. A weak foliation defined by long axes of microcline megacrysts in the granite is concordant with the adjacent gneissic foliation. The foliation defines two circular structures, one within southeastern parts of the pluton and the other that is cored by the large circular gneissic xenolith at the northwestern end (Brown et al., 1980).

Foliations dip inward around margins of the large circular gneissic xenolith and suggest that it may have once been a pendant from the gneissic hood into which the pluton was emplaced. Modeling of gravity data (Gibb et al., 1988) indicates that the pluton dips inward to a depth of less than 5 km at the centre (see Section B-B'-B'', Map 1666a). The large circular gneissic xenolith extends to a depth of 2 km and a sill of granite has intruded easterly beneath adjacent gneisses. The volume of the Eye-Dashwa pluton is estimated to be 122 km³. It is crudely conical in shape and had an undulating, furrowed top (Section B-B'-B'') prior to erosion. The Eye-Dashwa pluton is transected successively by aplite and hornblende-porphyry dykes followed by epidote- and chlorite-filled fractures.

Mineralogical zonation of the Eye-Dashwa pluton is reflected by the plagioclase- and hornblende-rich rim (quartz monzodiorite), which grades into subequal volumes of quartz, plagioclase, and alkali feldspar with generally less than 10% biotite and accessory hornblende, sphene, magnetite, ilmenite, apatite, fluorite, monazite, and zircon at the granite core (Fig. 25). Centres of plagioclase grains are altered to epidote, sericite, and kaolinite. Samples of the White Otter batholith and Bewag stock plot near the bottom of the granite field on the QAP diagram (Fig. 10).

The circular Bewag stock has intruded metasediments of the Quetico Subprovince. It is composed of medium grained, pink, biotite-hornblende leucogranite and is weakly foliated. Similar granite intrusions are present in adjacent areas to the south and east (Percival and Stern, 1984).

The granite stock north of Miranda Lake intrudes the western Nevison belt and "young" tonalite. It contains hornblende-rich phases near the metavolcanic belt but is dominantly a medium grained, quartz-porphyritic, biotite leucogranite.

Two varieties of granite dykes occur in the map area. Pink biotite leucogranite dykes transect "young" tonalite and gneisses at Serpent Lake. They are up to several hundred metres wide with sharp, northwesterly trending contacts. Semidiscordant dykes (up to 10 m wide) of white muscovite-bearing granite occur sporadically throughout metasediments in the southeastern corner of the map area and become more abundant to the south. Percival and Stern (1984) documented voluminous intrusions of white muscovite-bearing granite in the central Quetico Subprovince.

Gabbro dykes (unit 9)

Rare gabbro dykes occur within a west-northwest-trending band across the Eye-Dashwa pluton and at scattered localities in the White Otter batholith. The dykes are vertically dipping, up to 5 m wide, and have sharp chilled contacts. In places they have a stepped trace and contain angular inclusions of country rocks.

The dyke rock is an inequigranular, poikilitic to ophitic assemblage of clinopyroxene, plagioclase, and ilmenite. A sample from Volcano Bay of Crowrock Lake gave a K-Ar whole rock date of 1138 ± 27 Ma (Kaminen and Stone, 1983).

Surficial deposits

Surficial materials of the Atikokan area consist of glacial moraine, outwash, aeolian, and glaciolacustrine deposits on the Precambrian peneplane. Ground morainic till overlies bedrock to a depth of 1 m but is locally thicker within topographic depressions. Till is unsorted, poorly stratified, and composed of pebbles and larger clasts (20%) of the underlying bedrock. Variably-sized sand, silt and clay constitute the matrix.

Two prominent terminal moraines mark the southern limit of stationary, late Wisconsin ice sheets. The Steep Rock moraine is a well-developed, narrow-crested ridge southeast of the area, becoming an irregular, interrupted belt of elongate hills, hummocks, and gravel flats passing northwesterly through Steep Rock Lake (Fig. 26). Iron-bearing sand and gravel were mined from the segment of the moraine immediately east of Steep Rock Lake (Shklanka, 1972).

The Eagle-Finlayson moraine forms an elongate, rounded hill, which passes the southern end of Finlayson Lake and is followed by Highway 622. The surface of the moraine is strewn with large boulders but the moraine is mainly composed of stratified sand and gravel (Fig. 27). Cowan and Sharpe (1988) suggested that the moraine represents a rapid, subaqueous discharge event during deglaciation at the ice margin.

Varved clay overlies till within a broad belt along the Seine and Atikokan river systems generally within topographic depressions and lake basins. Zoltai (1961) noted a "1 foot to 2 foot thick" band of red clay in the uppermost, grey glaciolacustrine clays of the Seine River basin.

Outwash plains composed of well-bedded, flat-lying sand and gravel occur in western and northwestern parts of the area. Small eskers occur within the outwash plain south of White Otter Lake, and Zoltai (1965a) noted sand dunes immediately west of the present area.

Wind-blown, stone-free silt and sand form a thin (<1 m) veneer over till in central and northeastern parts of the area. The loess is prominent north of the Eagle-Finlayson moraine but sporadic in the Steep Rock Lake area to the south.

Recent peat deposits overlie Pleistocene sand, gravel, and clay in low-lying swampy ground and lake basins. Up to 2 m thick, black, fibrous woody peat, which contains poorly

decomposed tree trunks, is present in muskeg swamps along Highway 11. Modern, black gelatinous gyttja blankets most lake basins of the area.

Zoltai (1965a) attributed local glacial features to three successive phases of retreat by the Patricia ice mass during the late Wisconsin glaciation. The earliest Rainy phase extended south of the present area (i.e. Fig. 26) after which the ice mass retreated and remained stationary at the Steep Rock moraine (Steep Rock phase). A brief readvance, which locally overrode the Steep Rock moraine, was followed by retreat to the Eagle-Finlayson moraine (Eagle-Finlayson phase). Varved clays were deposited in glacial lakes marginal to the ice sheets. Glacial transport direction varied from 190 to 230°, as indicated by the iron ore boulder train that extends southwesterly from Steep Rock Lake (Dreimanis, 1956; Fig. 26).

Sonar profiling (Holloway, 1985) confirms the Pleistocene stratigraphic succession of till overlain by varved clay and gyttja in lake basins of the area. An opportunity to examine lakebed sediments arose after 1944 when parts of Steep Rock lake were drained to permit open-pit mining of iron ore from the Jolliffe Ore Zone Formation. Thick Pleistocene lakebed deposits covered most of the ore body and were removed by dredging and pumping. Stratigraphy of the lakebed sediments consisted of "a few feet" of compact glacial till, "over 100 feet" of varved clay, locally "a few feet" of sand and a "thin" layer of black, gelatinous "ooze" (Legget and Bartley, 1953).

The glacial till was widespread over the lakebed, red in colour, and composed of silt, sand, and gravel clasts (0.01 to 100 mm). Varved clay is the most extensive deposit and exhibits an extremely regular laminated texture. Laminations are about 1 cm thick, alternating dark grey and light grey, becoming reddish with depth. Legget and Bartley (1953) noted folded varves and abundant calcareous concretions at lower levels of the clay deposits. Antevs (1951) noted more than 1250 varves in the Steep Rock Lake section and attributed them to annual sedimentary cycles with the dark layers deposited in winter. Grain sizes were less than 0.1 mm with a high proportion less than 0.002 mm (Fig. 28).

The varved clay was stiff and hard to excavate but once disturbed it "liquefied" and flowed and impeded mining. Legget and Bartley (1953) attributed this condition to abnormally high water content in the clays varying from 30% in light grey layers to 80% in dark grey layers (Fig. 29).

STRATIGRAPHY

Stratigraphy of the Atikokan area has been the subject of numerous studies over the past century. Much attention was focused on the Steep Rock Series (later known as the Steep Rock Group) perhaps because of the rare unconformity at its base, the presence of major iron ore deposits, and its lithological diversity. Smyth (1891) divided supracrustal rocks of the eastern Steep Rock belt into nine formations (Fig. 3 and Table 5). Smyth's (1891) Steep Rock Series rested unconformably on a "Basement Complex" of granites and gneisses, all of which were intruded by late granites of

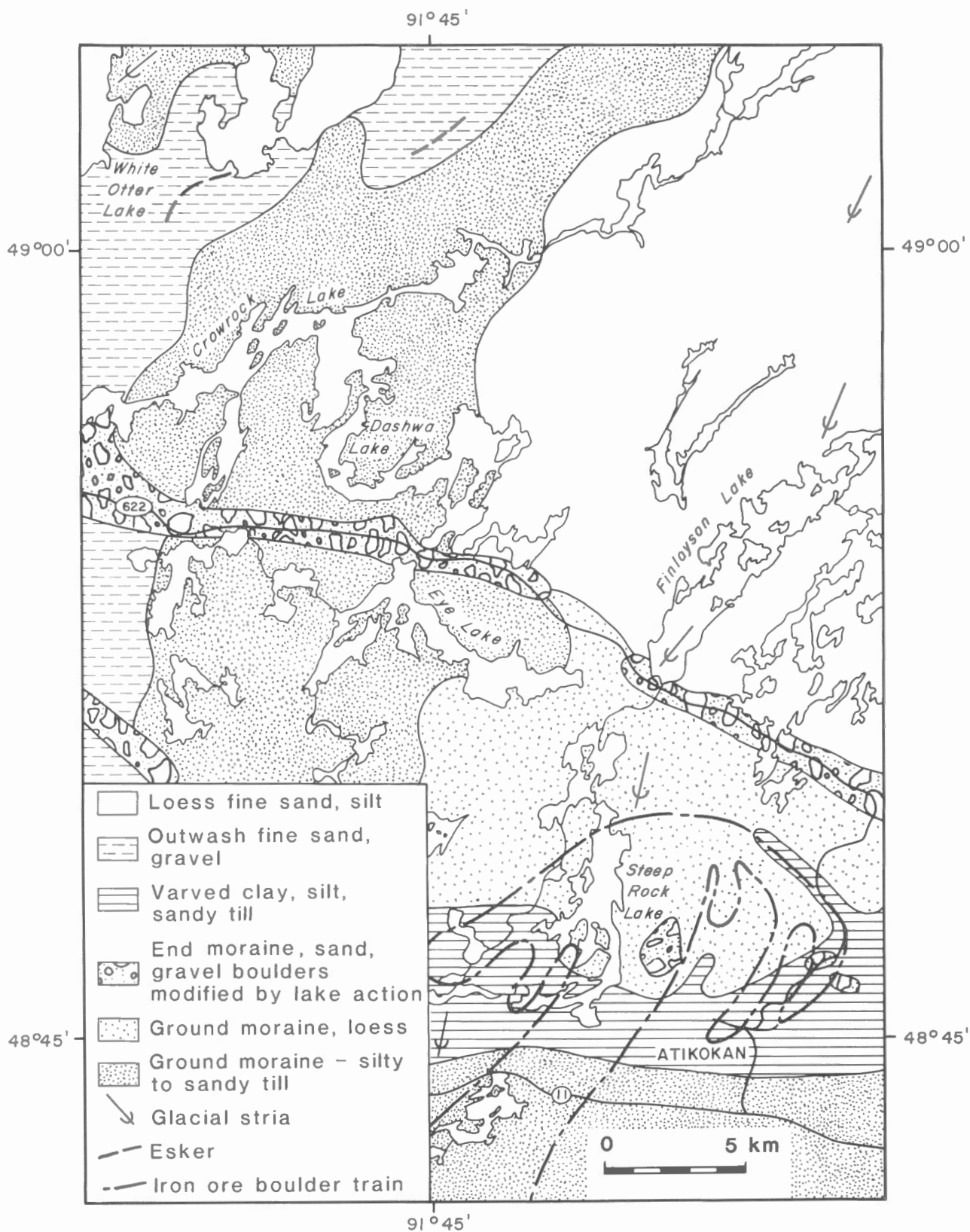


Figure 26. Surficial geology of the Atikokan area (after Zoltai, 1965b and Dreimanis, 1956).

the "Atikokan Series". Lawson (1912) identified four formations and confined the Steep Rock Series to a synclinal trough along the eastern margin of the Steep Rock belt (Fig. 5). The Steep Rock Series was interpreted to unconformably overlie Keewatin to the west and Laurentian to the east and to predate the Seine Series.

Steep Rock stratigraphy was discussed by Tanton (1926), Hawley (1930), Roberts and Bartley (1943), Hicks (1950), and particularly Moore (1938), but the most significant advances followed iron mining. Jolliffe (1966) defined the Conglomerate, Dolomite, Orezone, and Ashrock formations of the Steeprock Group. Jolliffe's (1966) Steeprock Group unconformably overlies a granitic basement complex and contains a second unconformity within the Dolomite Formation. Shklanka (1972) offered an alternative interpretation. His fault-bounded Steep Rock Group was situated between upper and lower volcanic groups. A fault zone defined the base of the Steep Rock Group in place of an unconformity. Subsequently, Wilks and Nisbet (1988) reiterated the stratigraphic succession of Jolliffe (1966) with the exception of the Pyrite Member of the Jolliffe Ore Zone Formation and added formal names to the formations of the Steep Rock Group.

The basal unconformity and four lower formations of the Steep Rock Group (Wagita, Mosher Carbonate, Jolliffe Ore Zone, and Dismal Ashrock) compose a typical example of a quartz arenite and carbonate-bearing sequence of Thurston and Chivers (1990). Such sequences represent sedimentation with minor associated volcanism in shallow water overlying felsic plutonic rocks that are typically greater than 2850 Ma. In the Errington pit – Hogarth pit area the formations young west and are juxtaposed with east-younging metavolcanic rocks. Because of this structural complexity, Jolliffe (1955, 1966) did not define the stratigraphic relation of his Steeprock Group to adjacent metavolcanics. Shklanka (1972) recognized the Atikokan fault at this contact. Wilks and Nisbet (1988) and Bursnall et al. (1988) described the contact as a "major structural break" which Hoffman (1989) considered to be a thrust fault separating the ashrock from allochthonous metavolcanic rocks to the west.



Figure 27. Stratified sand and gravel in the Eagle-Finlayson end moraine at Forsberg Lake. GSC 1992-074-A

Geochronological studies (e.g. Nunes and Thurston, 1980; Corfu and Andrews, 1987) showed multiple ages of volcanic rocks in some large belts of the western Superior Province. Davis et al. (1989) urged caution in applying principles of stratigraphic superposition to such areas due to the possible presence of concordant thrust faults, which have interleaved supracrustal rocks of different ages. Stratigraphic interpretation of the Atikokan area is clearly dependent upon the nature of the ashrock-metavolcanic contact which may represent a thrust fault.

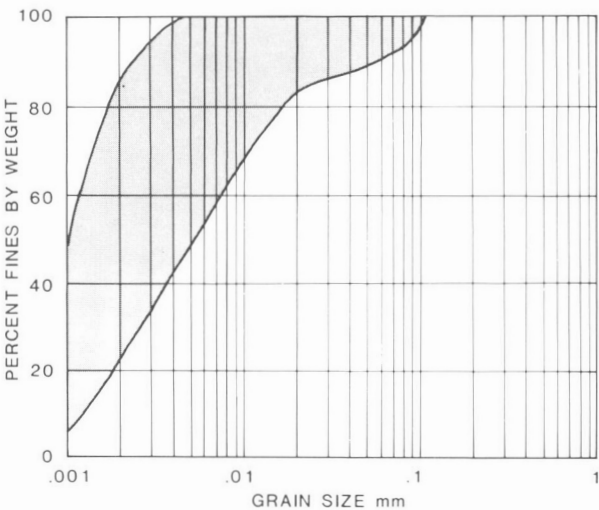


Figure 28. Grain-size distribution of varved clay in Steep Rock Lake (after Legget and Bartley, 1953). Solid lines are envelope of mechanical analyses.

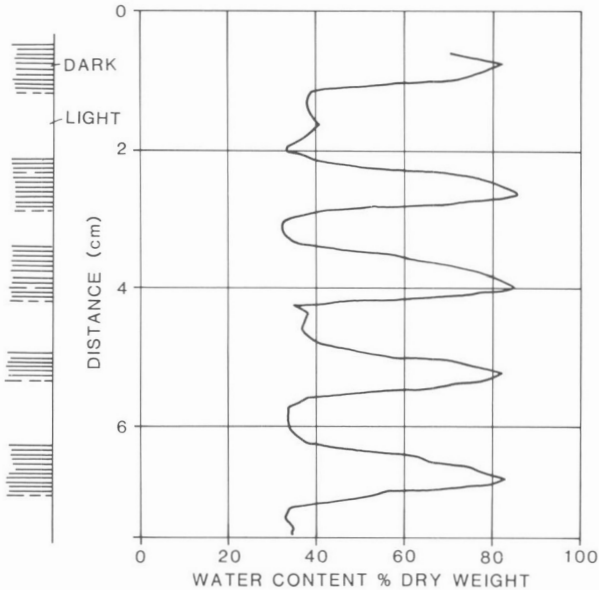


Figure 29. Water content of clay varves (after Legget and Bartley, 1953).

Subsequent to the present authors' initial survey, the western side of the Errington pit-Hogarth pit area was remapped (Fig. 30). The narrow unit of intermediate to felsic metavolcanic rocks originally shown west of the Dismal Ashrock Formation was reinterpreted as altered mafic metavolcanic rocks (compare Map 1666A with Fig. 30). Ashrock and metavolcanic rocks at or near the western contact of the Dismal Ashrock Formation show effects of strong carbonate alteration and are intensely foliated and crenulated. Prominent mineral lineations plunge steeply to the west and southwest. This evidence suggests that the western contact of the Dismal Ashrock Formation is the locus of dip-slip faulting (Atikokan fault zone of Fig. 30). In addition, a series of narrow, discordant, mainly dip-slip faults transect lower formations of the Steep Rock Group in a north-northeasterly direction. Most appear to merge with the Atikokan Fault whereas others such as the Bartley fault clearly crosscut the larger structure.

Younging directions of graded sedimentary beds show that the axis of a syncline is situated within the narrow unit of metagreywacke west of the Errington pit. The fold axis curves and probably merges with the Atikokan fault north of the Roberts pit. West-younging and east-younging strata, which are separated by the synclinal axis in the south (Errington pit area), are brought into juxtaposition across the Atikokan fault in the north (Hogarth pit area). The syncline and fault appear to account for the structural reversal, which has puzzled geologists for decades in the mine area.

The eastern Steep Rock belt provides additional examples of ashrock adjacent to mafic metavolcanic rocks although, in most cases, the contacts are intruded by metagabbro or else not exposed. An exception is found about 200 m north of Strawhat Lake, close to the electric transmission line, where the Dismal Ashrock Formation occurs in curved contact with a variably massive and pillowed flow (Fig. 31). A flow-bottom breccia in one outcrop indicates that the flow

Table 5. Comparison of Steep Rock Group stratigraphic subdivisions and their relations to other rocks

Smyth (1891)	Lawson (1912)		Jolliffe (1966)	Shklanka (1972)	Modified after Wilks and Nisbet (1988)
Atikokan Series (late granites)	Seine Series		Flows, tuffs and sediments	Upper Volcanic Group	Clastic metasediments, Intermediate to Felsic Metavolcanic Rocks
					Mafic metavolcanic rocks
intrusive contact	deformation and erosion		structural relation unclear		fault?
Dark grey clay slate					
Agglomerate			Ashrock Formation	Ashrock Formation	Dismal Ashrock Formation
Greenstones	Crystalline traps (metasediments)		Orezone Formation	Pyritic Formation	Jolliffe Ore Zone Formation
Upper conglomerate			unconformity		unconformity?
Upper calcareous greenschist	Ferruginous formation (volcanic ash)		Dolomite/Limestone Formation	Dolomite Formation	Mosher Carbonate Formation
Interbedded crystalline traps					
Ferruginous formation	Lower limestone				
Lower Limestone	Conglomerate		Conglomerate Formation	Conglomerate Formation	Wagita Formation
unconformity	unconformity		unconformity	fault	unconformity
Basement Complex (granites and gneisses)	Keewatin (metavolcanics)	Laurentian (granites and gneisses)	Granitic Basement Complex	Lower Pyroclastic Group	Marmion batholith
	Coutchiching (metasediments)			Lower Volcanic Group	

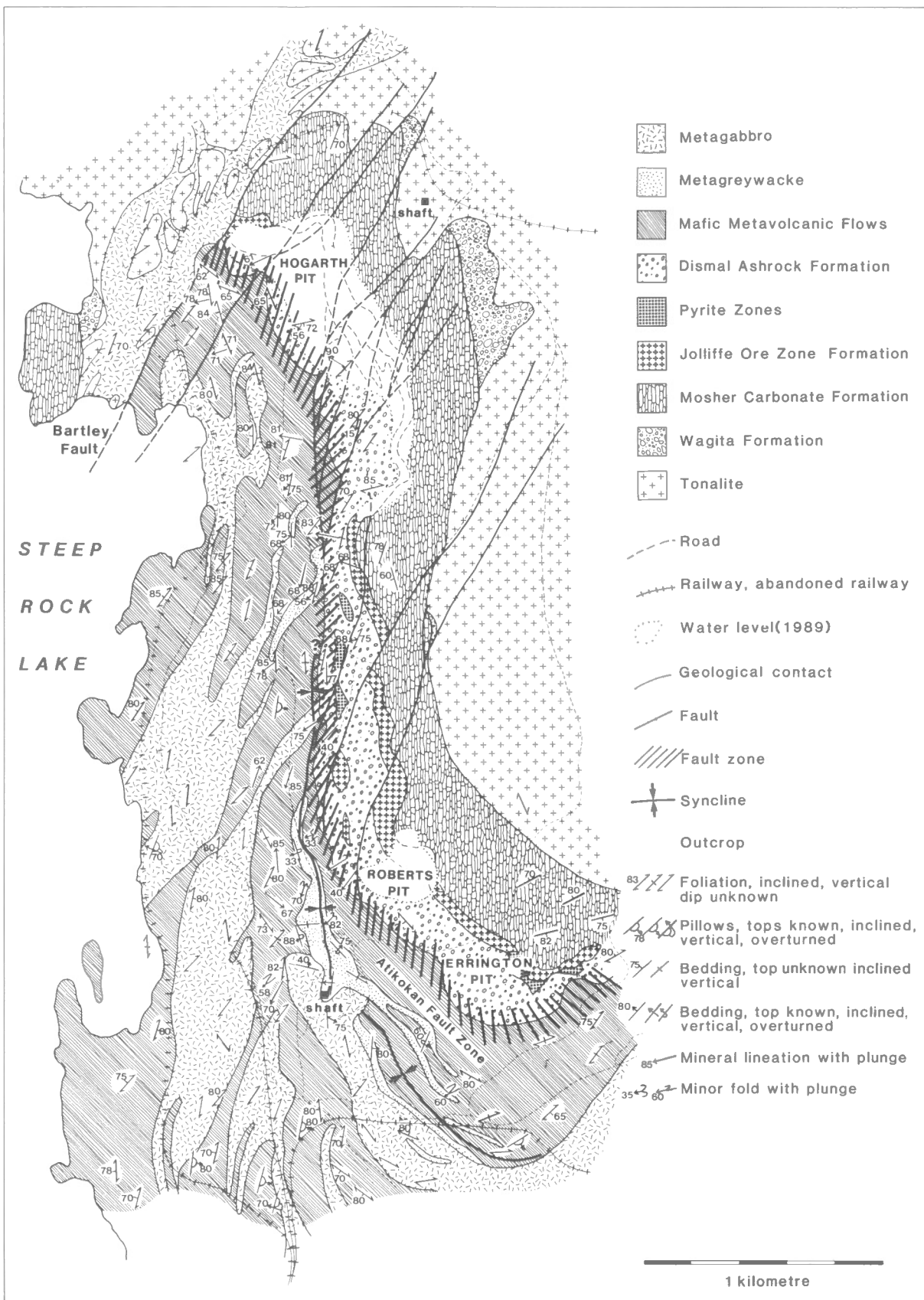


Figure 30. Geology and structure of the western side of the Errington, Roberts, and Hogarth mines. Compiled, in part, from Shklanka (1972).

unit overlies the ashrock. This outcrop may provide sole evidence that the ashrock is overlain by mafic metavolcanic rocks of the central Steep Rock belt. Unfortunately, adjacent areas are not exposed and the flow unit could possibly be contained within the ashrock as has been described by Jolliffe (1955). Additional exposures of contact zones are required to confirm observations in the Strawhat Lake outcrop.

In summary, the stratigraphic relation between the Dismal Ashrock Formation and mafic metavolcanic rocks remains unclear. Mafic metavolcanic rocks could be allochthonous and perhaps different in age with respect to the ashrock and have been shifted into position along the Atikokan fault. This model, which implies that upper contacts of all ashrock units are faulted, can be evaluated by further study of contact zones.

Alternatively, the ashrock may have been overlain, within a poorly constrained time interval ranging up to 300 Ma, by mafic metavolcanic rocks, the mutual contact of which has been locally folded and faulted. This interpretation is shown in Section A-A' (Map 1666A) where the entire supracrustal sequence is deformed by large-scale folds and thrust faults, possibly related to shortening of the belt.

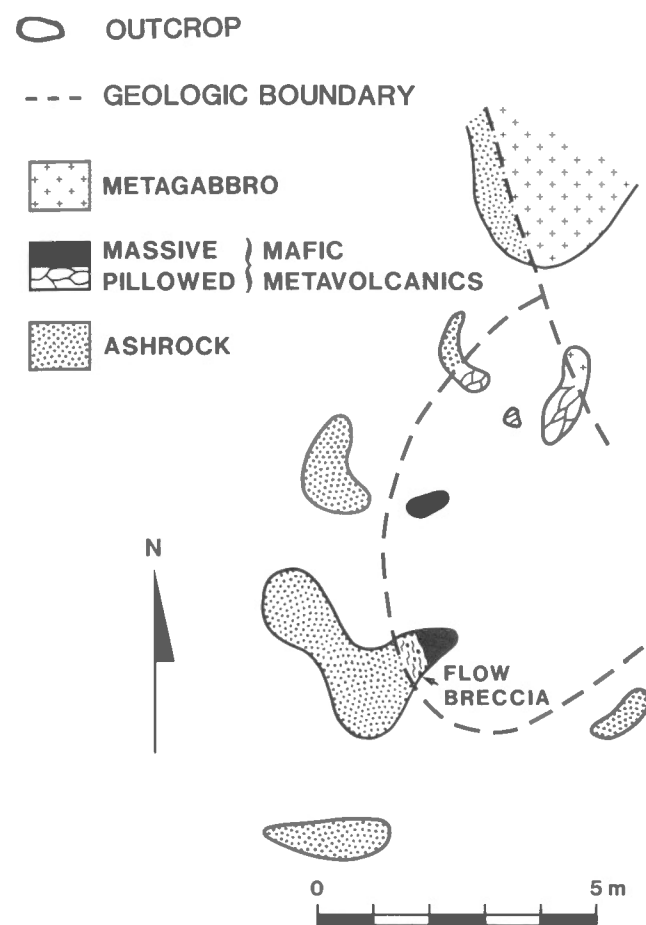


Figure 31. Sketch of contact relations between the Dismal Ashrock Formation and metavolcanic flows northwest of Strawhat Lake.

As a corollary of the latter model, metavolcanic rocks of the central Steep Rock belt can be upper stratigraphic elements of the Steep Rock Group. This interpretation was favoured at an early stage of the present survey (see for example Map 1666A legend) but raises the practical problem of defining boundaries of the group. In view of this difficulty and the uncertain structural character of the upper ashrock contact, the Steep Rock Group is appropriately restricted to the four formations originally specified by Jolliffe (1966). As proposed by Wilks and Nisbet (1988) the Steep Rock Group can be extended to include contiguous metavolcanic rocks if it can be shown that they overlie the Dismal Ashrock Formation.

Contacts between mafic and intermediate to felsic metavolcanic rocks are nowhere clearly exposed in the Steep Rock belt and may possibly be faulted or represent unconformities. For example, mafic metavolcanic rocks of the northwest Finlayson belt appear to predate the intrusive 2936 Ma Hardtack pluton and may be coeval with 2999 Ma felsic tuffs at Lumby Lake (Davis and Jackson, 1985, 1988). Other evidence, including post 2720 Ma detrital zircons in the Quetico Subprovince implies that 2750 to 2710 Ma calc-alkaline volcanic rocks, such as are widespread in the Wabigoon Subprovince (Davis and Edwards, 1986; Davis et al., 1986), may also occur at Atikokan. Unconformities or faults representing up to 300 Ma of time could be present in belts hosting both volcanic sequences and complicate stratigraphic interpretations.

Despite possible age gaps, some felsic units occur with clastic metasediments in synclines of the central Finlayson belt and suggest a position that is stratigraphically superior to mafic metavolcanic rocks. A similar interpretation can be tentatively made in the central Steep Rock belt where a thick homoclinal section of pillowed mafic lavas youngs east toward intermediate to felsic metavolcanic units.

Evidence summarized by Ojakangas (1985) suggests that sedimentation within volcanic areas and in large basins such as the Quetico ought to be concurrent with volcanism even though the sediments contain a component of plutonic detritus. This follows because the bulk of detritus is derived by rapid erosion of nonwelded tuffaceous material from volcanic edifices. Accordingly, metasedimentary units within the belts and adjacent Quetico Subprovince can be stratigraphically equivalent to, i.e. deposited at the same time as, adjacent felsic volcanic units. The available geochronology does not fully support this model however. For example, detrital zircons are dated at 3059 to 2704 Ma in Couthiching metasediments at Rainy Lake (Davis et al., 1989) and 3009 to 2698 Ma in Quetico metasediments at Atikokan (Davis et al., 1990). Oldest zircons probably reflect an early sialic crustal source comparable to the Marmion batholith at Atikokan; other zircons dated at approximately 2723 Ma could be derived from nearby volcanic rocks of the same age, whereas the youngest detrital material postdates known igneous activity by about 20 Ma. This may indicate that sedimentation postdated volcanism, that material was derived from sources other than the adjacent Wabigoon arc, or else that volcanic rocks were actually erupted at margins of the Wabigoon arc about 2700 Ma but have not yet been

dated. Rigorous geochronological work is warranted to constrain the age of metavolcanic rocks in the area and unravel their stratigraphic relation to Quetico metasediments.

GEOCHEMISTRY

Analytical techniques and presentation of results

Nineteen lithological units were identified by field mapping in the Atikokan area, most of which were sampled for petrographic and chemical analysis. The majority of samples submitted for chemical analysis were hand specimens obtained from surface outcrops. Exceptions are drill-core samples of the Eye-Dashwa pluton rim and core, which were obtained from depths as great as 1100 m below surface. Each sample was slabbed and weathered or altered material was removed using a diamond saw. One piece of each sample was crushed to 250 μ m size for chemical analysis.

The major elements were analyzed in 250 samples by X-ray fluorescence (XRF), except for FeO, H₂O, CO₂, and S which were done by wet chemical methods. The analytical method used for each element and the estimated precision of the results is listed in Table 6. The XRF method was used for the trace elements: As, Br, Mo, Nb, Rb, Sr, Th, U, Y, and Zr, as well as Ba, Ni, and Zn in some samples. The elements Pb and Li were analyzed by Atomic Absorption (AA), while the Induced Couple Polarization (ICP) method was used for Ba, Be, Co, Cr, Cu, Ni, V, Yb, Zn, and the rare earth elements (REE) – La, Ce, Nd, Sm, Eu, Gd, Dy, and Yb. The accuracy of each analysis was monitored by replicate analyses of international standard samples BCR-1 (basalt) and G-1 (granite) and comparison of these data to other laboratories.

The 250 samples analyzed for major elements are grouped, for the following discussion, according to rock type, map unit number, or the specific pluton or metavolcanic belt from which they were collected. In Tables A2, A3, and A4, means and other statistical parameters for rock types and units with more than six analyzed samples are shown for major, trace, and rare earth elements, respectively. If the number of analyses is less than six, the data are listed on the right side of the table (Data List) and the mean value only is given for each oxide or element.

In spite of the pervasive alteration of most rock types, each of the 19 lithological units identified by field mapping in the Atikokan area has distinctive chemical characteristics. With the exception of a few severely altered samples, the chemical analyses confirm the field classification of the rocks. The intrusive igneous rocks and gneisses are classified on the basis of modal mineralogy using the IUGS system (Streckeisen, 1976). The felsic intrusions and gneisses are plotted on the modal quartz-alkali feldspar-plagioclase triangle in Figure 10. The metavolcanic rocks are classified by the system of Irvine and Baragar (1971). Rare earth element contents are normalized to the values in chondritic meteorites using the data of Haskin et al. (1968) and Masuda et al. (1973).

Table 6. Method of Determination and Reliability of Chemical Analyses

Element	Method of Determination	Validity of Results
SiO ₂	XRF	±(4% ± 1% of value reported)
TiO ₂	XRF	±(0.02% ± 1% of value reported)
Al ₂ O ₃	XRF	±(2% ± 1% of value reported)
Fe ₂ O ₃	XRF	±(1% ± 1% of value reported)
FeO	rapid chemical	±(2% ± 2% of value reported)
MnO	XRF	±(0.01% ± 1% of value reported)
MgO	XRF	±(1% ± 1% of value reported)
CaO	XRF	±(1% ± 1% of value reported)
Na ₂ O	XRF	±(1% ± 1% of value reported)
K ₂ O	XRF	±(1% ± 1% of value reported)
H ₂ O	rapid chemical	±(1% ± 5% of value reported)
CO ₂	rapid chemical	±(1% ± 3% of value reported)
P ₂ O ₅	XRF	±(0.02% ± 1% of value reported)
S	rapid chemical	±(0.04% ± 5% of value reported)
La	ICP-RE1	±(5 ppm ± 5% of value reported)
Ce	ICP-RE1	±(5 ppm ± 5% of value reported)
Nd	ICP-RE1	±(5 ppm ± 5% of value reported)
Sm	ICP-RE1	±(3 ppm ± 5% of value reported)
Eu	ICP-RE1	±(1 ppm ± 5% of value reported)
Gd	ICP-RE1	±(2 ppm ± 5% of value reported)
Dy	ICP-RE1	±(2 ppm ± 5% of value reported)
Yb	ICP-RE1	±(1 ppm ± 5% of value reported)
Y	ICP-RE1	±(1 ppm ± 5% of value reported)
Ba	XRF or ICP	±(20./20. ppm ± 20./5% of value reported)
Be	ICP-TRI	±(5 ppm ± 5% of value reported)
Co	ICP-TRI	±(5 ppm ± 5% of value reported)
Cr	ICP-TRI	±(10 ppm ± 5% of value reported)
Cu	ICP-TRI	±(10 ppm ± 5% of value reported)
La	ICP-TRI	±(10 ppm ± 5% of value reported)
Ni	XRF or ICP	±(20./10 ppm ± 10./5% of value reported)
Pb	AA	±(20 ppm ± 10% of value reported)
V	ICP-TRI	±(5 ppm ± 5% of value reported)
Yb	ICP-TRI	±(5 ppm ± 5% of value reported)
Zn	XRF or ICP	±(20./5 ppm ± 10./5% of value reported)
Li	AA	±(3 ppm ± 10% of value reported)
As	XRF	±(30 ppm ± 10% of value reported)
Br	XRF	±(10 ppm ± 10% of value reported)
Mo	XRF	±(10 ppm ± 10% of value reported)
Nb	XRF	±(10 ppm ± 10% of value reported)
Rb	XRF	±(10 ppm ± 10% of value reported)
Sr	XRF	±(10 ppm ± 10% of value reported)
Th	XRF	±(30 ppm ± 10% of value reported)
U	XRF	±(30 ppm ± 10% of value reported)
Y	XRF	±(10 ppm ± 10% of value reported)
Zr	XRF	±(10 ppm ± 10% of value reported)

Pre- to synvolcanic intrusions

Mafic tonalite (unit 1a)

Mafic tonalite has relatively low SiO_2 (mean=64%) and higher FeO^* ($= \text{FeO} + \text{Fe}_2\text{O}_3$), MgO , and CaO than other felsic intrusive rocks of the Atikokan area. The K_2O contents range from 0.69 to 2.14 wt.% in mafic tonalite. The highest K_2O content occurs in an altered sample from the western end

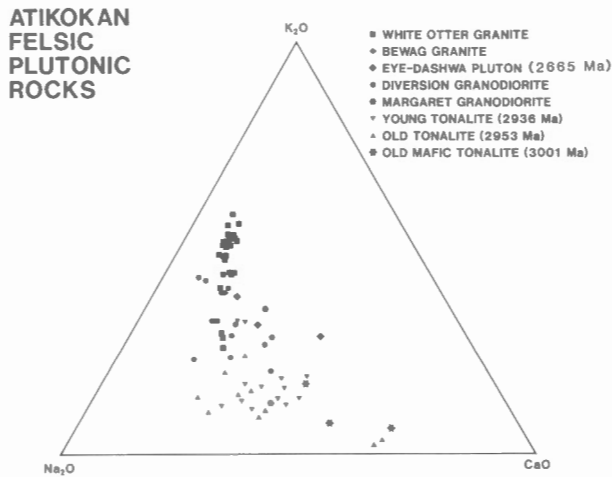


Figure 32. K_2O - Na_2O - CaO plot for crystalline rocks of the Atikokan area. Note that younger rocks plot toward the K_2O corner; a similar trend was reported for Archean rocks of Finland (Martin, 1987).

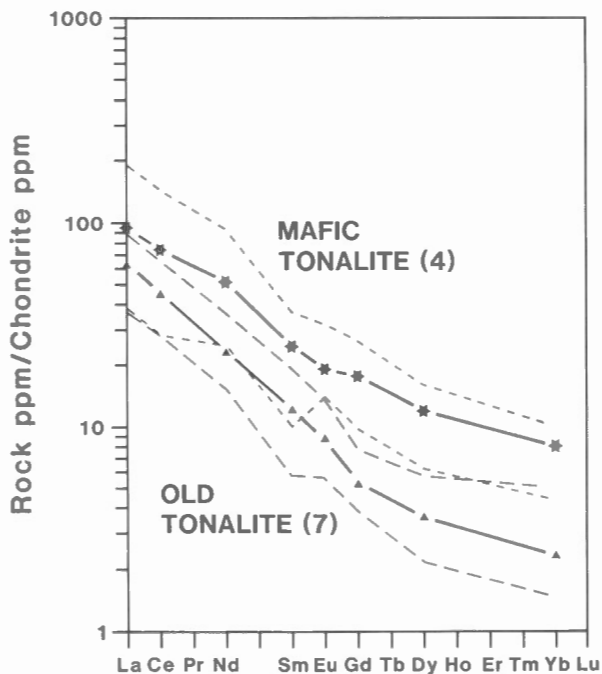


Figure 33. REE plot of mafic tonalite and "old" tonalite from the Atikokan area. Solid lines denote average values and dashed lines denote minimum and maximum values. Number of samples is listed in brackets.

of the Marmion batholith (Table A2). Unaltered samples plot toward the CaO apex of the K_2O - Na_2O - CaO diagram (Fig. 32). The trace elements (Nb, Mo, Y, Yb, V, Zr) are higher in the mafic tonalite than in other felsic intrusive rocks (Table A3). Rare earth elements (REE) were determined in four samples of mafic tonalite from separate localities in the map area (Table A4). The mafic tonalite samples show fractionated chondrite-normalized REE patterns (Fig. 33) and have an average La/Yb_N ratio of 11.1. The altered sample from the western end of the Marmion batholith is enriched in both light and heavy rare earth elements (LREE and HREE) compared to unaltered mafic tonalite.

"Old" tonalite (unit 1b)

"Old" tonalite has higher SiO_2 (mean=68.4%) and lower MgO , FeO^* , and CaO compared to mafic tonalite. Variable Na/K ratios result in "old" tonalite samples plotting in a scattered field at the base of the K_2O - Na_2O - CaO diagram (Fig. 32).

The "old" tonalite has high contents of the compatible and chalcophile trace elements (Co, V, Zn) compared to other felsic intrusive rocks (Table A3). The Th-group, large ion lithophile elements (Th, Pb, Rb, Ba, Be), and REE are depleted in "old" tonalite, especially compared to the younger granodiorite and granite. Chondrite-normalized REE patterns of "old" tonalite are fractionated with an La/Yb_N ratio of 24.9 and a small positive Eu anomaly. Total REE

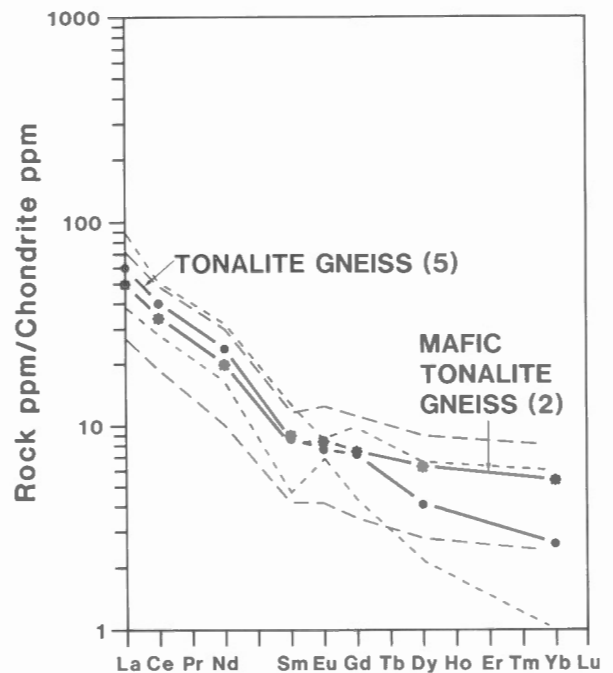


Figure 34. REE plot of tonalite gneiss and mafic tonalite gneiss. Solid lines denote average values and dashed lines denote minimum and maximum values. Number of samples is listed in brackets.

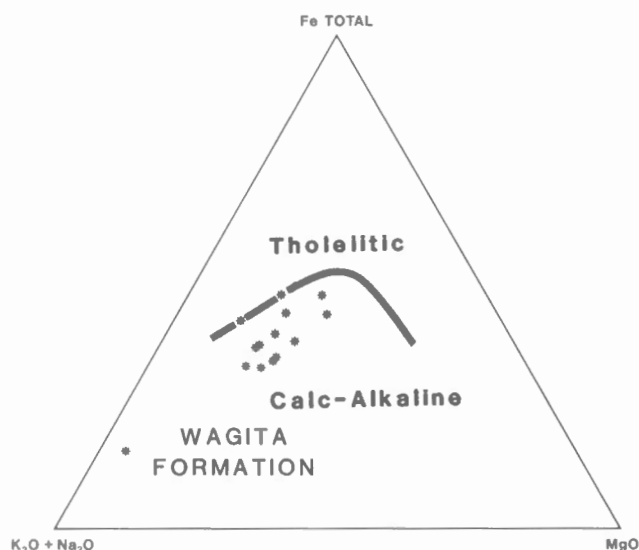


Figure 35. AFM plot for Wagita Formation (labelled star) and greywacke-argillite metasediments of the Quetico Subprovince.

contents in "old" tonalite are lower than mafic tonalite and the chondrite-normalized patterns are more depleted in the HREEs.

Tonalite gneiss (unit 1c)

Tonalite gneiss is generally enriched in Na_2O and deficient in FeO^* , and to a lesser extent TiO_2 and MgO , as compared to other gneisses and felsic intrusive rocks in the area (Table A2). Trace elements, particularly those of the High Field Strength (HFS) and chalcophile groups (Nb, Co, Cr, Cu, Ni, V, Zn), are depleted in tonalite gneiss compared to the other felsic intrusive rocks (Table A3). The chondrite-normalized REE patterns of tonalite gneiss samples are moderately fractionated with an La/Yb_N ratio of 21.5 (Fig. 34). The REE pattern is similar to those of "old" tonalite and "young" tonalite. A slight depression of the middle rare earth elements (MREE), Sm and Eu, is seen in tonalite gneiss samples.

Mafic tonalite gneiss (unit 1d)

Mafic tonalite gneiss has low SiO_2 and Na_2O and is similar to mafic tonalite in composition, but it has slightly lower contents of TiO_2 and P_2O_5 and higher mean K_2O (Table A2). Trace elements Sr, Nb, and La are depleted in mafic tonalite gneiss, whereas Y, Rb, and compatible and chalcophile elements are enriched compared to felsic intrusive rocks. The elements Ni, Cr, and Co are particularly abundant, and in this respect, the mafic tonalite gneiss shows greater geochemical affinity to mafic metavolcanic rocks than to other tonalites and gneisses in the area.

The chondrite-normalized REE patterns of mafic tonalite gneiss show a marked change in slope from rather flat HREE (Sm to Yb) to marked enrichment in the LREE (La to Nd)

(Fig. 34). The La/Yb_N ratio of 8.4 is the lowest of all intrusive rocks and gneisses and is similar to that of the Quetico metasediments. The geochemical characteristics and close field associations with metavolcanic units suggest that the mafic tonalite gneiss may be partly of supracrustal origin.

Supracrustal rocks

Wagita Formation (unit 2a)

One sample of metasandstone from above the unconformity at the northern end of the Hogarth pit was analyzed (Tables A2, A3, and A4). The sample is depleted in MnO , MgO , CaO , Na_2O , and compatible trace elements as compared to "old" tonalite and mafic tonalite. The SiO_2 , TiO_2 and K_2O are enriched in the metasandstone, which plots close to the alkali apex on the $(\text{K}_2\text{O}+\text{Na}_2\text{O})$ - FeO - MgO (AFM) diagram (Fig. 35). The REE (Table A4; Fig. 36) are moderately fractionated ($\text{La/Yb}_N=13.9$).

Geochemical similarity of the Wagita Formation to tonalite of the Marmion batholith supports field evidence that the metasediments are an erosional product of the tonalite. Schau and Henderson (1983) noted a weathered zone in the tonalite immediately beneath the Wagita Formation. The weathered tonalite is characterized by depletion of SiO_2 , CaO , Na_2O , MgO , and FeO ; enrichment of K_2O , Fe_2O_3 , and Li; an increase in LREE; and a decrease in HREE with respect to the unweathered protolith.

The chemical characteristics of the weathered zone and metasandstone are consistent with the interpretation that ferromagnesian minerals and Ca-plagioclase alter

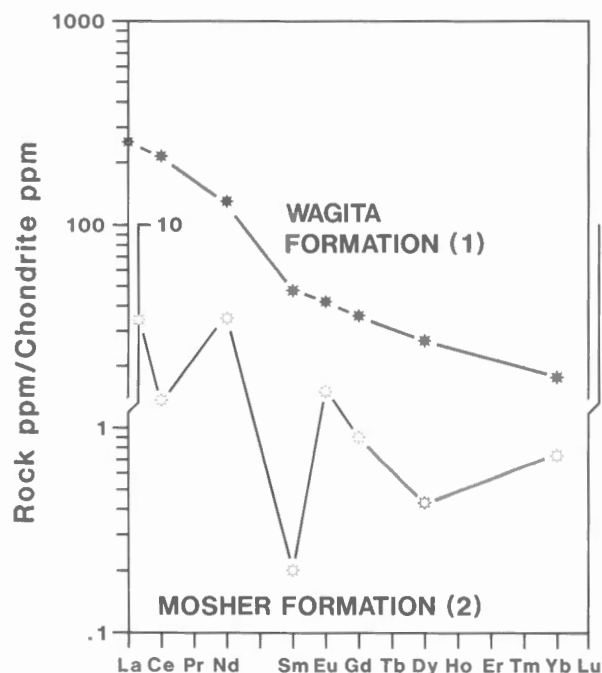


Figure 36. REE plot of Wagita Formation and Mosher Carbonate Formation. Number of samples is listed in brackets.

preferentially during initial stages of chemical weathering (Goldich, 1938). Such conditions would lead to leaching of Mg, Ca, Mn, Co, Ni, and V, while the mobility of Fe was controlled by oxidation potential. The enrichment in LREE can possibly be related to the inert nature and consequent concentration of accessory minerals such as zircon and monazite during chemical weathering.

Mosher Carbonate Formation (unit 2b)

The geochemistry of two samples from the Mosher Carbonate Formation show high CaO and about 2 wt.% combined FeO*, MnO, and MgO (Table A2). Jolliffe (1955, 1966) reported analyses of extensive channel and chip samples across the Mosher Carbonate Formation that yielded up to 20% MgO with seldom more than 2% MnO. The SiO₂, varies from less than 1% to 12%.

The Mosher Carbonate Formation is markedly depleted in almost all trace elements compared to other rock types in the area. A notable exception is Mo, and to a lesser extent, Pb and Cr, which are somewhat enriched compared to other rock types, along with MnO and CaO. The REE chondrite-normalized pattern of the Mosher Carbonate Formation (Fig. 36) is extremely irregular and shows a trend of slight LREE enrichment (La/Yb_N=4.6).

Table 7. Magnesium numbers of metavolcanic rocks of the Atikokan area

Rock Type	Average Magnesium Number	Standard Deviation	Number of Analyses
Steep Rock upper felsic unit	55.12	15.27	12
Finlayson upper felsic unit	53.99	10.30	4
Perch upper felsic unit	33.00	—	2
Steep Rock lower mafic unit	57.21	7.08	32
Finlayson lower mafic unit	56.21	7.02	17
Finlayson amphibolite grade mafic volcanics	54.64	7.62	6
Perch lower mafic unit	53.95	—	2
Dismal Ashrock Formation	71.36	1.00	5
Metagabbro	52.90	16.32	9

Dismal Ashrock Formation (unit 3a)

Samples from the Dismal Ashrock Formation are ultramafic in composition. They contain an average of about 44% SiO₂ and 22% MgO (anhydrous weight percent calculated from Table A2) with an average magnesium number (Mg#) of 71.4 (Table 7; $Mg\# = 100 * \frac{Mg^{2+}}{Mg^{2+} + Fe^{2+}}$, where $Fe^{3+}/Fe^{2+} = 0.15$). On the AFM diagram (Fig. 37) the ashrock samples plot near the FM join owing to their very low alkali (K₂O+Na₂O) contents. They can be classified as ultramafic komatiites after Arndt and Nisbet (1982). Chemically the ashrock is distinguished from other metavolcanics of the area by its low SiO₂, and high MgO, as well as slightly higher TiO₂, FeO*, and MnO, and very high volatile contents (mean CO₂+H₂O=9%) reflected in a modal abundance of carbonate minerals. The ashrock is markedly enriched in As, Be, and Li, as well as the chalcophile and compatible trace elements (Cu, Zn, Ni, Co, and Cr) compared to other metavolcanic rocks in the area (Table A3). Large ion lithophile (LIL) elements (Rb, Sr, and Ba) and the immobile incompatible elements (Y and Zr), as well as Pb, are depleted in the ashrock.

Compared to typical Archean komatiites, such as the average peridotitic komatiite of Munro Township, Ontario (Arndt et al., 1977), the Dismal ashrock has very high TiO₂, FeO*, and MnO and a low Mg#, as well as lower Al₂O₃ and Na₂O and a rather high CaO/Al₂O₃ ratio. In terms of MgO content, Al₂O₃ and alkalies, the analyzed ashrock samples are similar to two samples of spinifex-textured komatiite from the Lumby Lake area (Jackson, 1985). The ashrock differs from these samples in its higher FeO*, TiO₂, and P₂O₅ and higher volatile content. Ni, Cr, and Co are slightly higher in the ashrock than in the Lumby Lake komatiites, while Nb, Y, and Zr contents are similar.

The komatiites of the Dismal Ashrock Formation have fractionated chondrite-normalized REE patterns with a mean La/Yb_N of 6.8 (Fig. 38). Their LREEs are relatively flat at about 30 times chondritic values (mean La/Sm_N = 1.4) and they show progressive depletion of the HREEs from Eu to Yb (mean Sm/Yb_N = 5.0). Their LREE content is thus

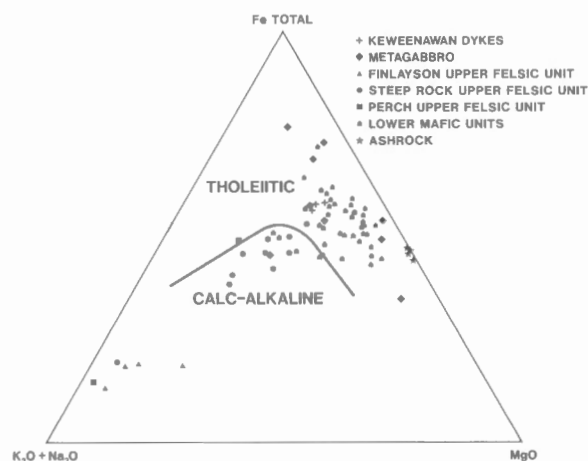


Figure 37. AFM plot for volcanic rocks of the Atikokan area.

intermediate between the lower values of the adjacent Steep Rock lower mafic unit and the highly LREE-enriched upper felsic unit, while their HREEs are more depleted than either metavolcanic unit.

Mafic metavolcanic rocks (unit 3b)

For the purpose of discussion the mafic metavolcanic samples are subdivided according to the belt from which they were obtained. These subdivisions consist of the Steep Rock lower mafic unit, the Finlayson lower mafic unit, and the Perch

lower mafic unit, all of which are at greenschist grade of metamorphism (Tables A2, A3, and A4). Samples from the Finlayson belt are further subdivided according to whether they have the mineral assemblage of greenschist (Finlayson lower mafic unit) or amphibolite metamorphic grade (Finlayson amphibolite grade mafic metavolcanics).

The lower mafic units of the Atikokan area are mainly classified as tholeiitic basalts with a lesser proportion of calc-alkaline basalts, using the classification scheme of Irvine and Baragar (1971). On the AFM diagram (Fig. 37), the lower mafic units plot with considerable scatter but exhibit a

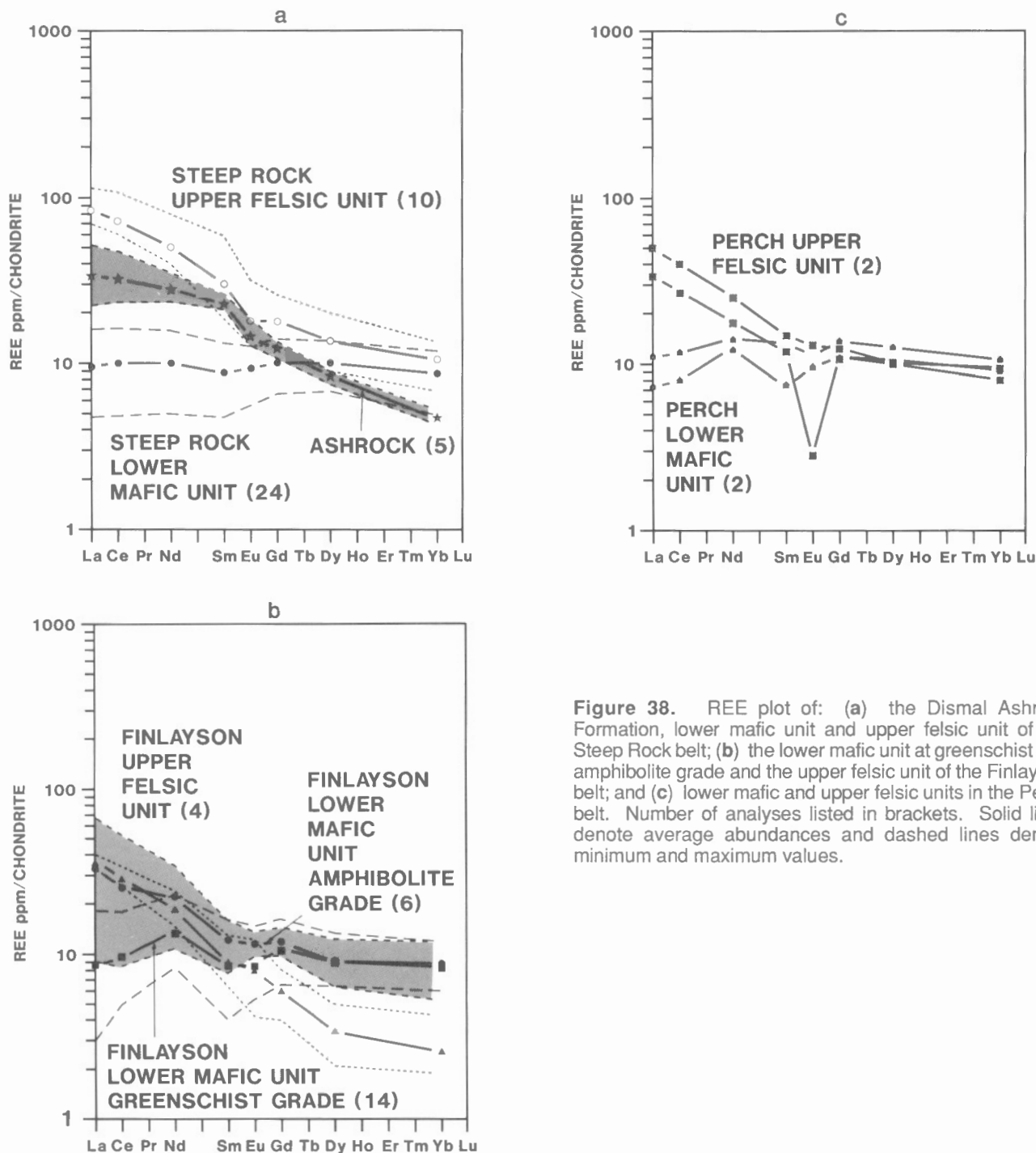


Figure 38. REE plot of: (a) the Dismal Ashrock Formation, lower mafic unit and upper felsic unit of the Steep Rock belt; (b) the lower mafic unit at greenschist and amphibolite grade and the upper felsic unit of the Finlayson belt; and (c) lower mafic and upper felsic units in the Perch belt. Number of analyses listed in brackets. Solid lines denote average abundances and dashed lines denote minimum and maximum values.

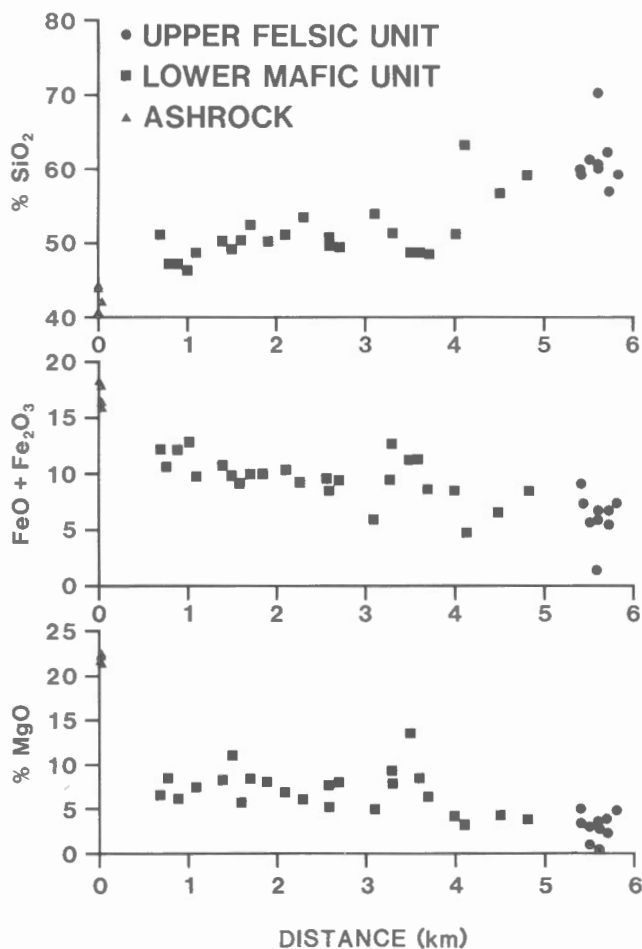


Figure 39. Variation in selected major oxides with distance from west to east across the Steep Rock belt. Ashrock shown for comparison at 0 km.

general trend of iron enrichment and progressively higher Fe/Mg ratios than the Dismal Ashrock Formation. The most primitive mafic metavolcanic rocks are characterized by high Mg#s (about 70) whereas differentiated lavas have Mg#s of about 45; the average Mg# is 54-57 for all belts (Table 7). Systematic variation in major oxides such as decreasing CaO and Al_2O_3 and increasing TiO_2 , Na_2O , K_2O , and P_2O_5 is observed with decreasing Mg#, but is minor.

Some systematic variation in major element chemical composition is observed with distance across the east-younging section of pillow lavas at Steep Rock Lake (Fig. 39). These include generally increasing SiO_2 and decreasing FeO^* and MgO from the Dismal Ashrock Formation (included for comparative purposes) through the lower mafic metavolcanic rocks to the upper felsic metavolcanic unit. Na_2O shows a poor positive correlation with distance, MnO shows a negative correlation, and Al_2O_3 is essentially constant. This variation may be largely due to increasing amounts of alteration (mainly silicification) to the east (see section on Alteration, supracrustal rocks).

The distribution of major oxides in samples from the Steep Rock, Finlayson, and Perch belts can be compared in Figure 40. The Steep Rock belt shows greater range in the abundance of major oxides such as SiO_2 , FeO , MgO , CaO , and Na_2O than does the Finlayson belt at greenschist metamorphic grade, possibly because of the larger number of samples analyzed from the Steep Rock belt. Amphibolite facies metamorphism of the Finlayson lower mafic unit appears to have resulted in an increase in median SiO_2 and Al_2O_3 contents and decreased FeO and MgO . Geometric statistical parameters cannot be shown for the Perch belt owing to the small sample population but, in general,

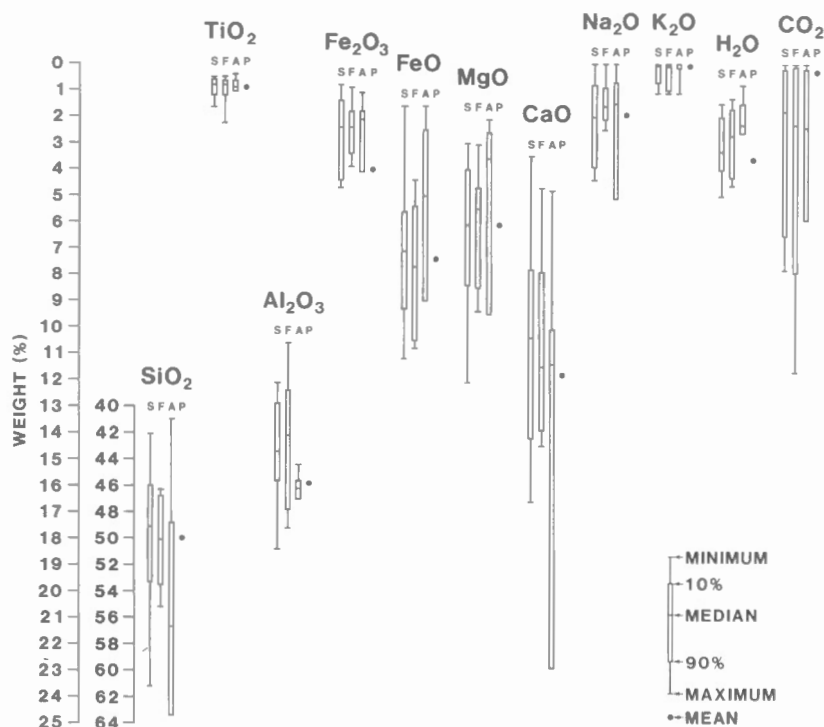


Figure 40. Comparison of the distributions of selected major oxides in lower mafic units of the Steep Rock belt (S), Finlayson belt (F), parts of the Finlayson belt at amphibolite grade (A), and the Perch belt (P). Statistical symbols are shown on the figure. Numbers of samples are respectively 32, 17, 9, and 2.

chemical variations between the belts of greenschist facies of metamorphism are apparently less than those induced by prograde metamorphism in the Finlayson belt.

The immobile trace elements show better correlation with differentiation indices in the Steep Rock metavolcanics than do the major elements. Yttrium (Y) shows an increase with decreasing Mg# (Table A5) whereas Nb and Zr (Table A3) are remarkably constant in the lower mafic unit. Nb and Zr are consistently enriched in the Steep Rock upper felsic unit compared to the Steep Rock lower mafic unit (Nb, 11 ppm versus 6 ppm; Zr, 170 to 260 ppm versus 25 to 230 ppm). In addition, Zr shows a positive correlation with Mg# in the lower mafic unit but has a slight negative correlation with Mg# in the upper felsic unit (Table A5).

The lower mafic metavolcanic units are generally enriched in compatible and chalcophile group trace elements and depleted in incompatible and immobile trace elements compared to upper felsic metavolcanic units. Average abundances of the analyzed trace elements are consistent from one belt to the next (Fig. 41) with the exception of Ba, which is depleted in the Perch lower mafic unit. The range of trace element abundances in each belt is generally comparable to the range of abundances between belts. All three belts contain a lower mafic metavolcanic unit of similar major and trace element composition – tholeiitic basalt.

Rare earth element plots for the lower mafic units at greenschist metamorphic facies in the Steep Rock, Finlayson, and Perch belts are shown in Figures 38a,b, and c

respectively. All three display flat chondrite-normalized REE patterns with average REE content about 7 to 10 times chondritic values. In contrast, the Finlayson amphibolite grade lower mafic unit shows marked LREE enrichment ($\text{La}/\text{Sm}_N = 2.5$), while HREEs are similar to the greenschist grade mafic metavolcanic rocks (Fig. 38b).

Intermediate to felsic metavolcanic rocks (unit 3c)

For geochemical analysis, samples of intermediate to felsic metavolcanic rocks are separated into the Steep Rock upper felsic unit, Finlayson upper felsic unit, and Perch upper felsic unit in Tables A2 to A4. On the AFM diagram (Fig. 37), samples of all three upper felsic units (Table A2) plot in the calc-alkaline field of Irvine and Baragar (1971). Least altered samples of the Steep Rock upper felsic unit have a mean SiO_2 content of 62%, making them siliceous andesites (cf. Irvine and Baragar, 1971). They show varying degrees of alkali enrichment without iron enrichment and a calc-alkaline differentiation trend. The three least altered samples from felsic units in the Finlayson belt are rhyolites with a mean SiO_2 content of 72% and the highest consistent alkali enrichment (mainly Na_2O). Two samples from the Perch felsic metavolcanic unit (Table A2) are dacite and rhyolite with rather low alkali contents. Average magnesium numbers (Mg#) vary from 33 to 55 in all upper felsic units and are highest in the Steep Rock upper felsic unit (Table 7). Mg# generally shows a positive correlation with TiO_2 and a negative correlation with SiO_2 in the felsic metavolcanics (Table A5).

The Steep Rock upper felsic unit is a relatively large volume pyroclastic unit of intermediate, andesitic composition. It is enriched in incompatible elements (Ba, Rb, Sr, Li) and immobile high field strength (HFS) elements Zr and Y, and depleted in compatible and chalcophile elements (Cu, Ni, Mo, Zn) compared to the lower mafic metavolcanic unit (Table A2). Compatible and chalcophile elements are even further depleted in the thin tuffaceous rhyolitic beds of the Finlayson upper felsic unit. The two samples from the Perch belt show varied results.

The REE chondrite-normalized patterns show moderate LREE enrichment with La/Yb_N ratios of 7.5, 12.9, and 4.5 for upper felsic units of the Steep Rock, Finlayson, and Perch belts, respectively (Fig. 37a, b, c). Some samples from the Perch and Steep Rock belts show negative Eu anomalies. The Finlayson upper felsic unit is quite depleted in the HREE compared to the other felsic units, and has slightly lower LREE contents than most Steep Rock upper felsic unit samples.

In general, the upper felsic units from the Atikokan area show textural, mineralogical, and chemical characteristics distinct from the lower mafic units and from the Dismal Ashrock Formation. Unlike the lower mafic units, however, which are remarkably consistent from one belt to the next, the upper felsic units from the Steep Rock and Finlayson belts are chemically distinct. The Steep Rock upper felsic unit is chemically more similar to the lower mafic units than is the Finlayson upper felsic unit.

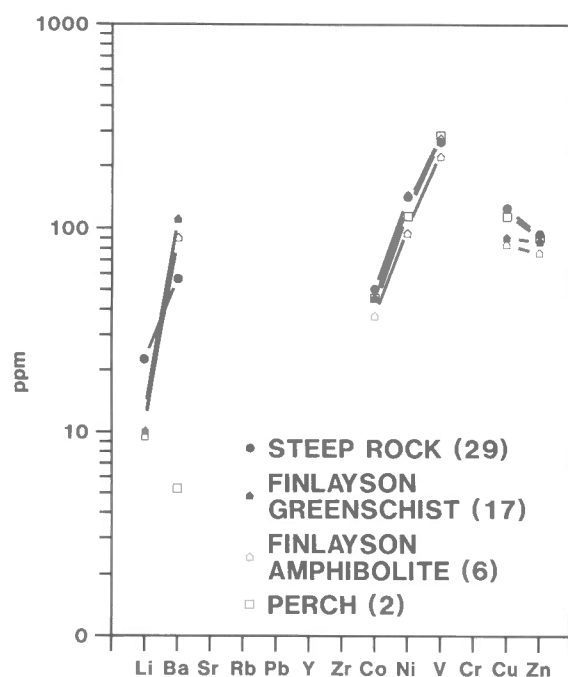


Figure 41. Comparison of selected incompatible (Li, Ba), compatible (Co, Ni, V), and chalcophile (Cu, Zn) elements in lower mafic units of the metavolcanic belts.

Metagreywacke, argillite (unit 4a)

Compared to the average pelite of Shaw (1956), the metagreywacke-argillite sequences of the Quetico Subprovince (Table A2) are slightly higher in SiO_2 and CaO and lower in Al_2O_3 and K_2O . On the AFM diagram (Fig. 35) the Quetico metasediments plot in the calc-alkaline field and, with respect to these major elements, are compositionally similar to the Steep Rock upper felsic unit (compare Fig. 35 and 37).

Quetico metasediments are generally enriched in incompatible trace elements and Pb compared to possible provenance rock units such as the upper felsic and lower mafic units of the Steep Rock belt and "old" tonalite (Fig. 42). Immobile, compatible, and chalcophile trace element values are generally intermediate between the Steep Rock upper felsic unit and "old" tonalite, although high Cr, Ni, and Cu in the Quetico metasediments are comparable to values in the Steep Rock lower mafic unit.

Samples of Quetico metasediments have variable enrichment of REE, but all show a trend of moderate LREE enrichment with an average La/Yb_N ratio of 9.5. The REE chondrite-normalized plot of the Quetico metasediments is intermediate between that of the Steep Rock upper felsic unit and "old" tonalite, all of which show similar LREE enrichment (Fig. 43).

Collectively, the geological and geochemical data suggest that clastic metasediments of the Quetico Subprovince in the Atikokan area could have been derived from intermediate to

felsic metavolcanic rocks (unit 3c) and "old" tonalite (unit 1b) with a lesser component of mafic metavolcanic rocks (unit 3b).

Syn- to postvolcanic intrusions

Metagabbro (unit 5)

Metagabbro samples from the Finlayson belt, Steep Rock belt, and dykes in the Marmion batholith are mostly classified as basalt using the method of Irvine and Baragar (1971); they plot in the tholeiitic field on the AFM diagram (Fig. 37). Most metagabbro samples have major element geochemistry similar to that of mafic metavolcanic rocks, but they show a wider range of Mg#. One sample from the central Steep Rock belt plots in the calc-alkaline field and is compositionally similar to the upper felsic metavolcanic units. Wilks (1986) identified one high-magnesium dyke compositionally similar to the Dismal Ashrock Formation.

Trace element contents in metagabbro samples (Table A3) are comparable to either the Steep Rock lower mafic unit or the upper felsic unit. Incompatible elements Li and Rb are relatively high, close to abundances found in the upper felsic unit. The Ba and Sr abundances are similar to the lower mafic unit, however. Immobile HFS elements (Y, Zr) and compatible elements (Co, Ni, V) in metagabbro samples compare closely with the lower mafic unit, whereas Cr is depleted to values similar to the upper felsic unit. Chalcophile elements, Cu and Zn, have contents in the

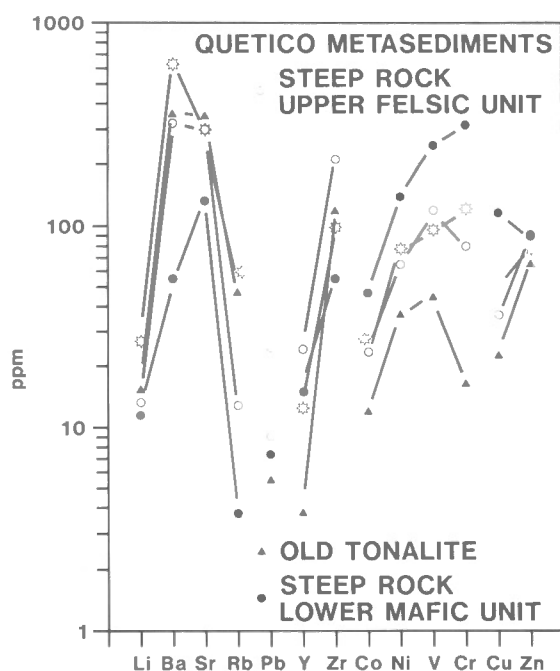


Figure 42. Comparison of incompatible (Li, Ba, Sr, Rb), Ti-group (Pb), immobile (Y, Zr), compatible (Co, Ni, V, Cr), and chalcophile (Cu, Zn) trace elements in selected rocks of the Atikokan area.

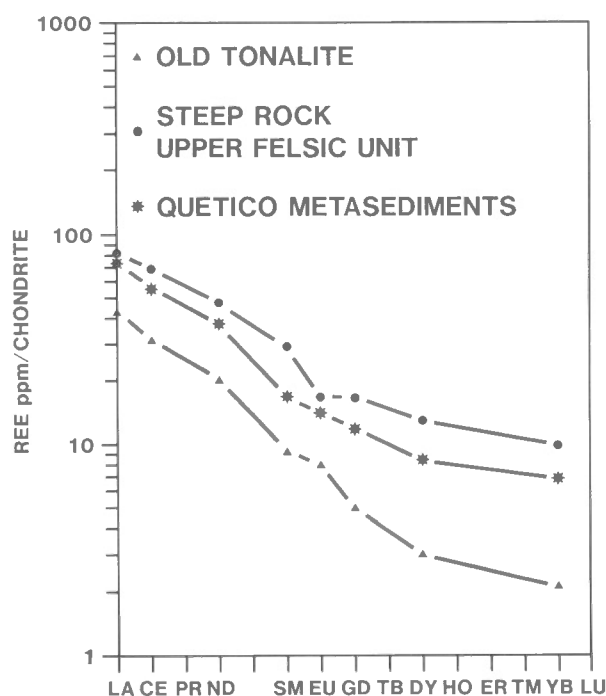


Figure 43. Comparison of average REE patterns for "old" tonalite, Steep Rock upper felsic unit, and Quetico metasediments.

metagabbro that are dissimilar to both metavolcanic units, whereas Mo is at a concentration level similar to the lower mafic unit.

The REE chondrite-normalized plots show two groups of metagabbro samples (Fig. 44): one has a flat pattern comparable to the Steep Rock lower mafic metavolcanic unit; the other group has a LREE-enriched pattern similar to the upper felsic unit.

With minor exceptions the metagabbro samples have geochemical characteristics similar to either mafic metavolcanics or intermediate to felsic metavolcanics.

"Young" tonalite (unit 6)

The chemical composition of "young" tonalite is similar to "old" tonalite except for higher SiO_2 and K_2O accompanied by lower MgO and volatile contents. On the K_2O - Na_2O - CaO diagram (Fig. 32), "young" tonalite overlaps the field of "old" tonalite; however, a few samples, particularly those from the Righteye pluton, are more enriched in K_2O . Trace element geochemistry of "young" tonalite is comparable to that of "old" tonalite except for high Li levels in the Righteye pluton and slightly lower levels of some compatible and chalcophile elements in the "young" tonalite.

The REE chondrite-normalized plots (Fig. 45) show high fractionation in "young" tonalite samples with an average La/Yb_N ratio of 20.1. The REE pattern of "young" tonalite is similar to that of "old" tonalite except for marginally greater enrichment of HREE and a weak positive Eu anomaly implying an amphibolite or garnet granulite source. The

Righteye pluton shows a flat HREE distribution, a weak negative Eu anomaly, and progressive LREE enrichment. This pattern is observed in late granodiorite and granite intrusions in other Archean domains (Taylor and McLennan, 1985) and is attributed to partial melting of crustal material such as tonalite or supracrustal rocks.

Diorite, hornblendite (unit 7)

Major element chemistry reflects the highly zoned nature of the Little Eye stock; the core is enriched in FeO^* , MgO , K_2O , and CaO and depleted in SiO_2 , Al_2O_3 and Na_2O relative to the rim of the intrusion (Table A2). Both rim and core samples plot near the CaO apex of the K_2O - Na_2O - CaO diagram. The core plots in the tholeiitic field of the AFM diagram (not shown) similar to mafic metavolcanic rocks, and the rim is total alkali enriched and plots in the calc-alkaline field.

Incompatible trace elements (Ba, Sr) are enriched in diorite and hornblendite compared to values in "young" tonalite and granite. Zr values are also similar to those in late felsic intrusions. Compatible and chalcophile trace elements are enriched and reflect the high proportion of ferromagnesian minerals in diorite and hornblendite.

The LREE are markedly enriched in both diorite and hornblendite (Fig. 46) with La/Yb_N ratios of 16.2 and 33.3 respectively. Hornblendite exhibits the highest REE content of all rock types in the map area and its REE pattern is comparable to patterns of kimberlites, carbonatites, and

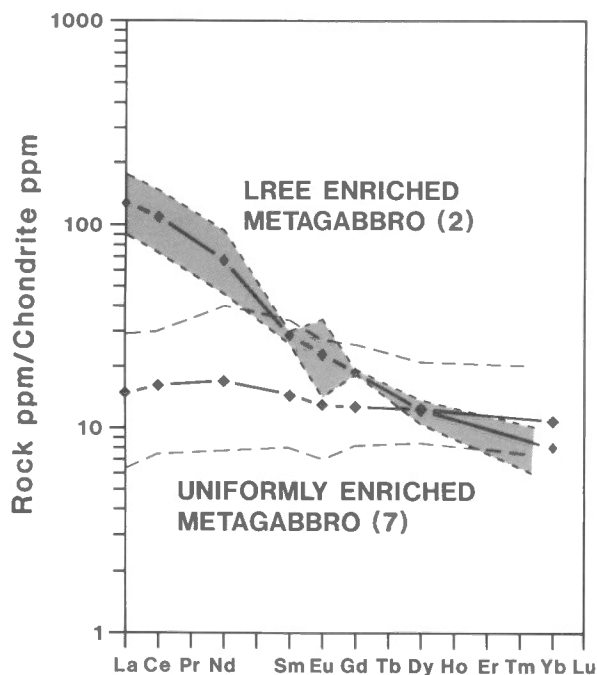


Figure 44. REE plot of metagabbro. Solid lines denote average values and dashed lines are maximum and minimum values. Number of samples is listed in brackets.

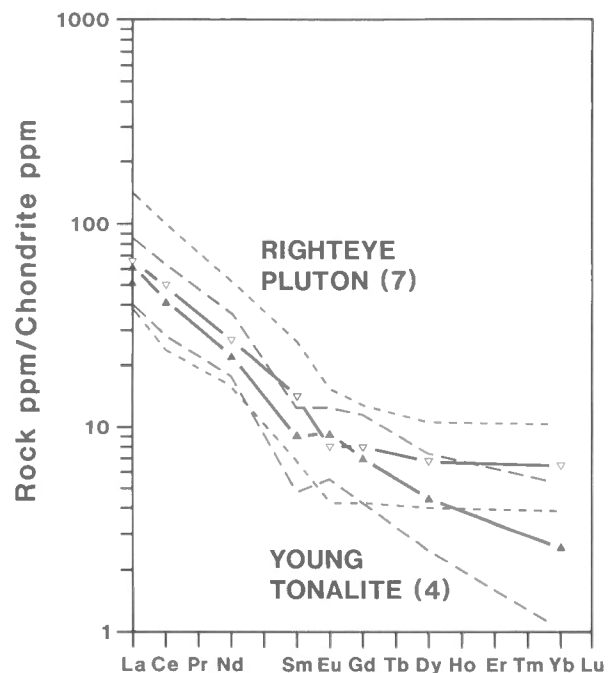


Figure 45. REE plot of "young" tonalite and "young" tonalite-granodiorite of the Righteye pluton. Solid lines denote average values and dashed lines are maximum and minimum values. Number of samples is listed in brackets.

lamprophyres (Cullers and Graf, 1984). Various theories consisting of partial melting of selective mantle materials, zone refining, and fractional crystallization have been proposed to account for such REE patterns.

Quartz monzodiorite, quartz monzonite (unit 8a)

Crosscutting relations show that quartz monzodiorite/quartz monzonite constitutes the earliest intrusive phase succeeded by granite at the core of the Eye-Dashwa pluton.

A trend of decreasing FeO*, MgO, and CaO accompanied by increasing SiO₂ and K₂O occurs from the rim of the Eye-Dashwa intrusion to the core (Fig. 47). Samples from the outermost rim of the Eye-Dashwa pluton plot near the centre of the AFM diagram in the calc-alkaline field and become more alkali enriched toward the core (Fig. 48).

Granodiorite (unit 8b)

Samples from the Diversion and Margaret granodiorite stocks (Tables A2, A3, and A4) plot near the centre of the K₂O-Na₂O-CaO diagram (Fig. 32) and overlap the compositional fields of "young" tonalite and granite.

Incompatible trace elements, particularly Ba and Rb, are enriched in granodiorite compared to most other rock types with the exception of granite (Fig. 49). Compatible and chalcophile elements are enriched in the Margaret and Diversion stocks relative to most other felsic intrusive rocks in the area, probably due to the higher abundance of mafic minerals in these intrusions. The available evidence suggests

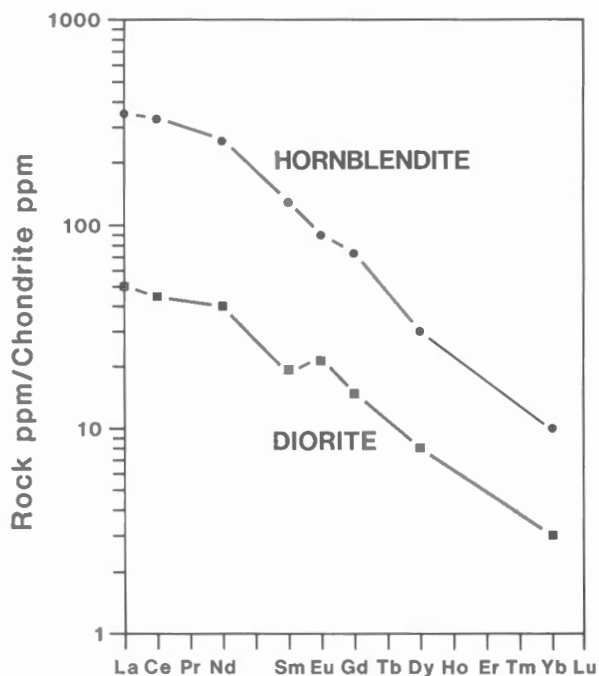


Figure 46. REE patterns for diorite and hornblende of the Little Eye stock.

that contents of Th-group elements (Th, U, Pb) in granodiorite are intermediate between low levels in "old" tonalite and higher values in granite.

Samples from the Diversion and Margaret stocks have LREE-enriched chondrite-normalized REE patterns with La/Yb_N ratios of 17.3 and 30.3, respectively (Fig. 50). The Margaret stock has greater LREE enrichment in the mafic granodiorite rim than in its granite core (Table A4). Excluding the rim of the Margaret stock, La/Yb_N ratios are less than 30 in tonalite and granodiorite but exceed 30 in late granites.

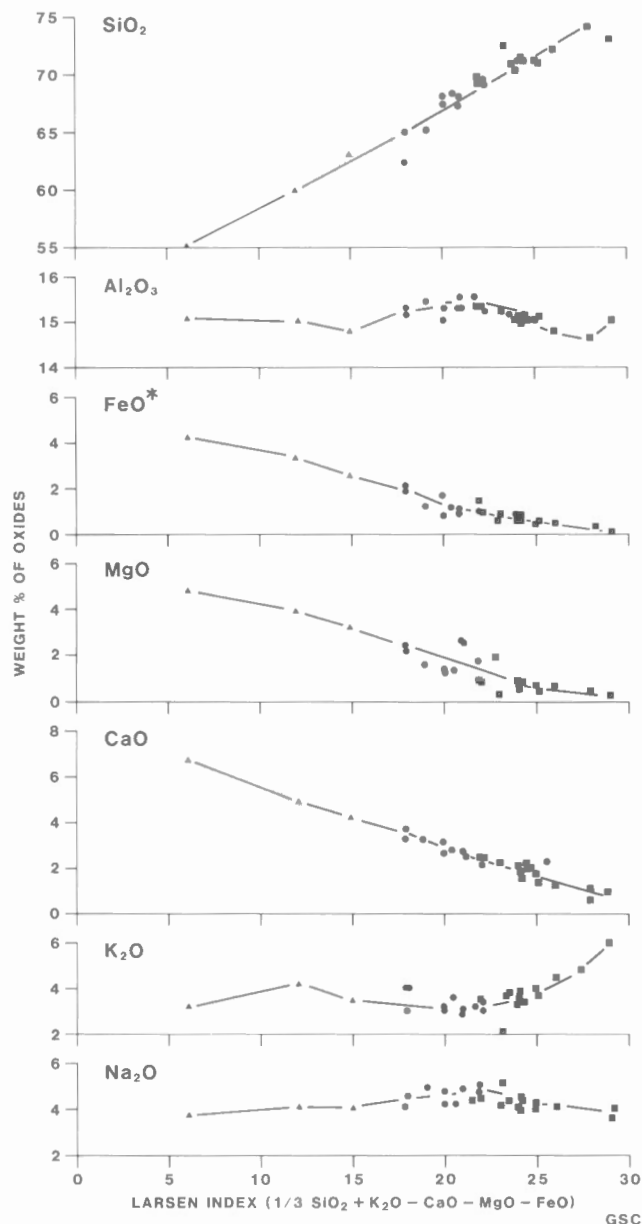


Figure 47. Larsen Index (Larsen 1938) plot for samples from the Eye-Dashwa pluton. Triangles are from the outermost rim (unit 8a), circles are from the rim gradational to the core (unit 8a, c), and squares are from the core (unit 8c).

Granite (unit 8c)

Granites are depleted in MgO and CaO and enriched in SiO₂ and K₂O relative to older felsic intrusive rocks of the Atikokan area. The trend of K₂O enrichment in granites, particularly the White Otter batholith, is apparent in the K₂O-Na₂O-CaO diagram (Fig. 32).

Incompatible trace elements (Ba, Rb, Sr), Th-group elements (Th, U, Pb,) and Be are enriched in granites relative to older felsic intrusive rocks. Compatible and chalcophile elements (Co, Ni, V, Cr, Cu, Zn, Mo), as well as As and Br, are depleted (Fig. 49 and Table A3). The available data suggest that the Bewag stock may have anomalous trace element geochemistry characterized by high Be and Pb and low Zr values.

REE chondrite-normalized plots for the Bewag, Eye-Dashwa, and White Otter granites (Fig. 50, 51, and 52) have pronounced LREE enrichment with La/Yb_N ratios of 31.2, 32.7, and 47.8 respectively. The normalized patterns have increasing slope from HREE to LREE.

Gabbro dykes (unit 9)

Samples from three gabbro dykes have similar major element chemistry and plot in the tholeiitic field in the AFM diagram (Fig. 37). Trace element geochemistry of the gabbro dykes is distinct from metagabbro dykes and is characterized by higher concentrations of incompatible elements (Ba, Rb, Sr), immobile HFS elements (Nb, Y, Zr), Be, and As. Certain compatible elements, notably Cr and Ni, are depleted relative to metagabbro. REE chondrite-normalized patterns of dyke samples are slightly LREE enriched with an average La/Yb_N

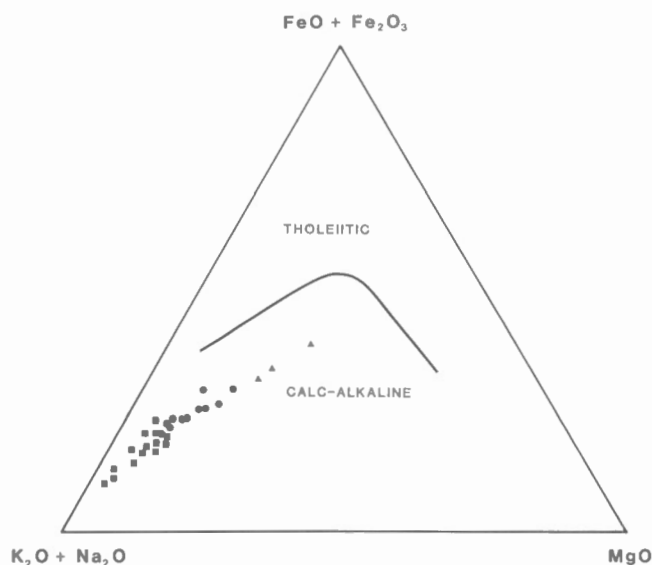


Figure 48. AFM plot for samples from the Eye-Dashwa pluton. Triangles are from the outermost rim (unit 8a), circles are from the rim gradational to the core (units 8a, c), and squares are from the core (unit 8c).

ratio of 4.5 (Fig. 53). The REE pattern of gabbro dykes differs from both the uniformly enriched and LREE-enriched types of metagabbro mainly in their higher contents of HREE.

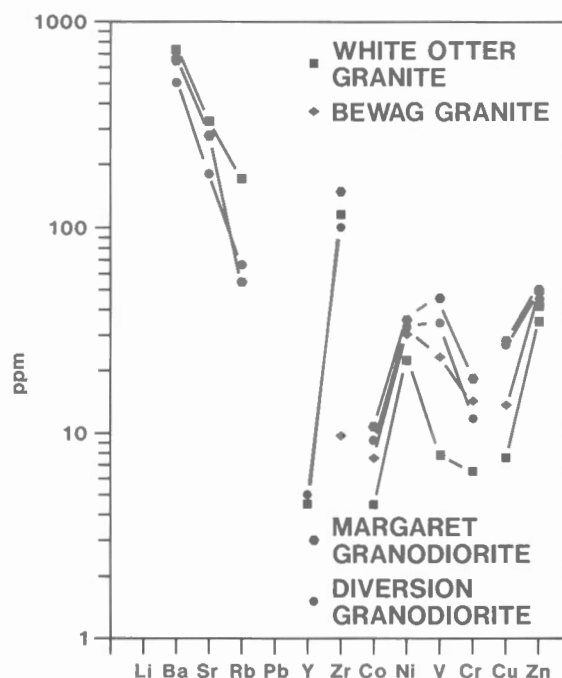


Figure 49. Variation in selected incompatible (Ba, Sr, Rb), immobile (Y, Zr), compatible (Co, Ni, V, Cr), and chalcophile elements (Cu, Zn) in felsic plutonic rocks.

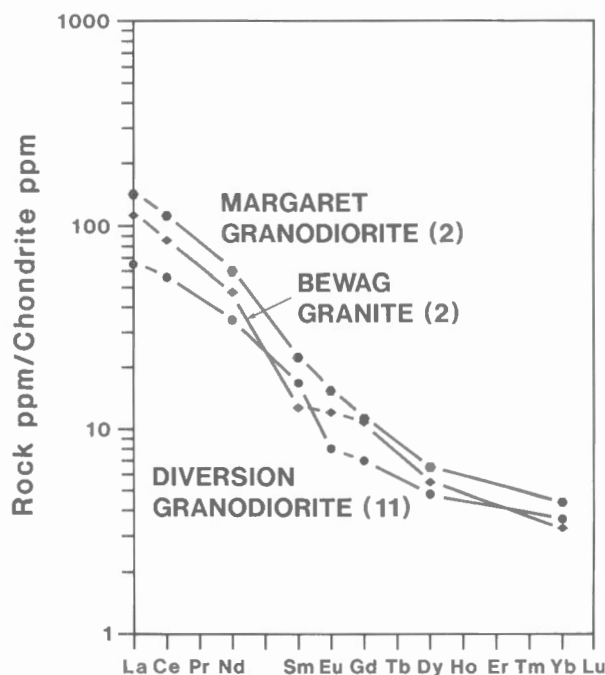


Figure 50. REE plots for felsic intrusive rocks. Curves are averages of the number of samples indicated in brackets.

Alteration

Supracrustal and intrusive rocks of the Atikokan area exhibit varying degrees of alteration, from moderate to intense, affecting their mineralogy and chemical composition. Greenschist facies metavolcanic rocks and metasediments are dominated by hydrous mineralogy: chlorite, sericite, and biotite, as well as carbonate. Biotite, epidote, and amphibole are more abundant in amphibolite facies supracrustal units. This hydrous mineralogy is reflected in the chemistry of rock samples.

Supracrustal rocks

Total volatile content (H_2O+CO_2+S) ranges from an average of 3% in Quetico metasediments and felsic metavolcanic rocks to 6% in mafic metavolcanic rocks and 9% in the Dismal Ashrock Formation. Water generally constitutes about 60% of the total volatile content with CO_2 making up most of the remainder. Sulphur ranges from 0.0 to 0.3 wt.%. Alteration of metavolcanic rocks is reflected in a wide scatter of data points on major oxide variation diagrams, although recalculated volatile-free values are used. The major oxides CaO , Na_2O , K_2O and SiO_2 appear to be most affected by alteration, and elements usually considered to be immobile, such as Ti, Al, Mn, and P, are also apparently affected.

The incompatible trace elements of large ionic radii (e.g. Li, Ba) are highly variable in their abundance in supracrustal rocks, probably as a result of alteration. Thus these elements, which are widely used in some paleotectonic classification schemes (Pearce and Cann, 1973), may not be

reliable for classification here. The immobile elements (Y, Nb, Zr), compatible elements (Co, Cr, Ni, V), chalcophile elements (Cu, Mo, Zn), and HREE (Gd, Dy, Yb) are fairly

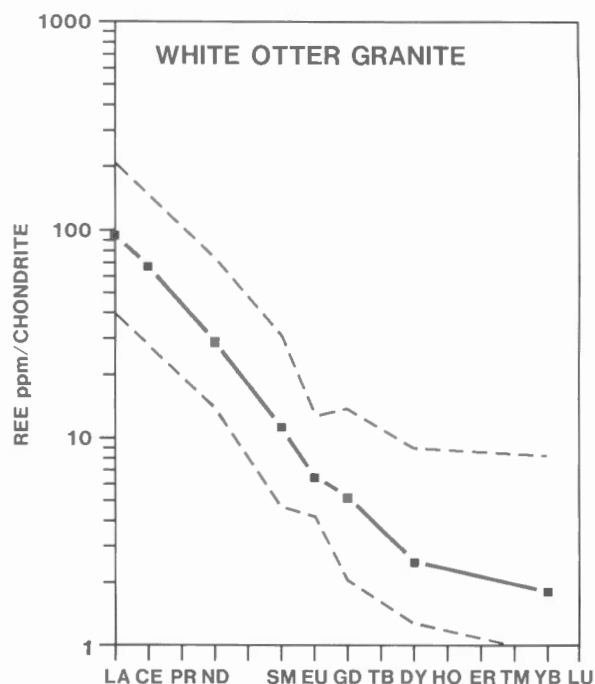


Figure 52. REE plot for 30 samples of the White Otter granite batholith. Solid line is average and dashed lines denote minimum and maximum.

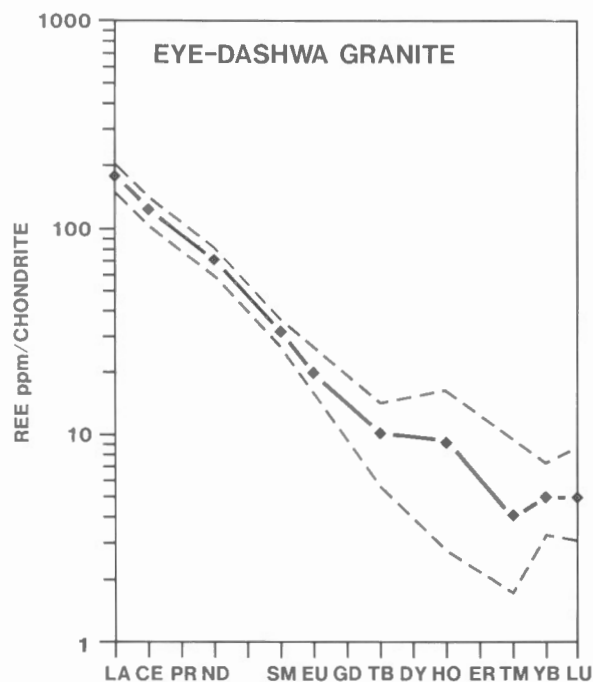


Figure 51. REE plot for 20 samples of the Eye-Dashwa granite pluton. Solid line is average and dashed lines denote minimum and maximum.

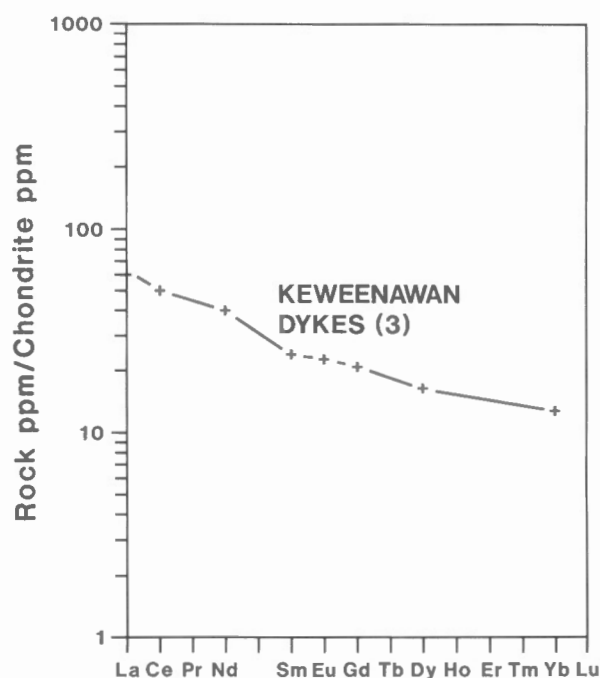


Figure 53. Average REE plot for three gabbro dykes.

consistent in abundance within individual rock types. Thus they may be assumed to be somewhat less affected by alteration than the major elements and incompatible trace elements. LREE and MREE (La, Ce, Nd, Sm, Eu), particularly Nd and Sm, are erratically distributed for some samples on chondrite-normalized plots (e.g. Fig. 38a, b) presumably due to alteration. Amphibolite facies metavolcanic rocks from the Finlayson belt are LREE enriched compared to greenschist facies metavolcanic rocks from the same belt; this may be due to alteration/metasomatism. The range of alteration-induced, within-unit variation is commonly less than the chemical differences between supracrustal units (e.g. mafic metavolcanics versus felsic metavolcanics), however. Thus, the general shape of the REE pattern for each rock type can be discerned, but fine structure of variation between members of the same unit (e.g. Mg-rich mafic metavolcanics versus Fe-rich) are obscured by alteration.

Intrusive rocks

The mineralogy and chemical composition of intrusive rocks are variably altered in much the same way as metavolcanic rocks and metasediments. Normally grey granite (unit 8c) intersected by boreholes in the Eye-Dashwa pluton is pink near surface and adjacent to fractures. Feldspars of pink granite are cloudy, with plagioclase being affected more than potassium feldspar. Plagioclase is coated with hematite and other alteration products such as epidote, chlorite, sericite, and carbonate. The ferromagnesian minerals, hornblende and biotite, are altered to epidote and chlorite (Kamineni and Dugal, 1982). Within tonalites and gneisses (e.g. units 1a, 1b, 1c, and 1d), plagioclase is variably altered to sericite, epidote, and kaolinite. Ferromagnesian minerals consist of epidote and chlorite at low metamorphic grade and biotite and hornblende at high metamorphic grade.

Combined volatiles range from 0.5 wt.% in granite to 2.0 wt.% in "old" tonalite and mafic tonalite, and show a trend of increased volatile content with the age of intrusive rocks. Chemically altered granite is characterized by loss of Ca and Sr, gain of Mg, and by higher $\text{Fe}^{3+}/\text{Fe}^{2+}$ ratios (Kamineni and Dugal, 1982). Tonalites and gneisses exhibit considerable variation in the abundance of K_2O and microcline. For example, one mafic tonalite sample plots in the granitic field and tonalite gneisses straddle the tonalite, granodiorite, and granitic fields (Fig. 10).

Trace elements and REE show a sensitivity to alteration in plutonic rocks that is equivalent to that of supracrustal samples. Only fresh samples of grey granite from the Eye-Dashwa pluton and the gabbro dykes have highly reproducible LREE patterns and appear to be unaltered.

In spite of alteration, supracrustal and plutonic rocks of the Atikokan area exhibit distinct chemical characteristics. With the exception of a few severely altered samples, the chemical analyses confirm field classification of the 19 lithological units identified on the basis of field relations. In addition, the analyses appear sufficiently unaltered so as to permit comparison of genetically similar units such as metavolcanics in various belts, and individual granite

plutons. Comparison of Archean units with modern unaltered equivalents and application of petrotectonic models, such as are developed for modern volcanic rocks, are beyond the scope of the present study.

Petrogenesis

Pre- to synvolcanic tonalites

The pre- to synvolcanic tonalites and gneisses of the Atikokan area (map units 1a to 1d) have geochemical characteristics transitional between the continental- and oceanic-type trondhjemites of Arth (1976) in terms of their Al_2O_3 (~15%) and Yb_N (2 to 8 ppm). The average mafic tonalite gneiss is more like the oceanic-type (ophiolite or island arc) trondhjemites of Arth (1976) because of its relatively low Al_2O_3 (14.3% anhydrous) and higher Yb_N (5.5 ppm) contents. Arth (1976), Taylor and McLennan (1985), and Cullers and Graf (1984) noted that garnet has a high distribution coefficient for HREE. Accordingly, the low HREE content of tonalites and tonalite gneiss imply that these units could have formed by partial melting of the mantle where garnet and the HREE would have remained in the residuum. A petrogenetic model for the generation of the mafic tonalite and "old" tonalite by partial melting of garnet-bearing amphibolite in the upper mantle at depths of greater than 30 km leaving an eclogitic (clinopyroxene + garnet) residuum is consistent with the REE data. Similar models were proposed by Arth and Hanson (1972, 1975) and Hanson and Goldich (1972) for the 2700 Ma Saganaga tonalite of northeastern Minnesota, and Lambert and Holland (1976), Compston (1978), and Drury (1978) for tonalites of other areas.

Tonalite gneiss and mafic tonalite gneiss have a close field relation to amphibolitic mafic metavolcanic units and inclusions. They have positive values of the discriminant function of Shaw (1972), indicating an igneous protolith and may have formed by the partial melting of amphibolite facies metavolcanic rocks. Thus the tonalite gneisses may have been produced by small degrees of melting (10 to 20%) of a typical tholeiitic metavolcanic parent, such as the Steep Rock lower mafic unit or Finlayson greenschist facies lower mafic unit with flat REE patterns and total normalized REE of about 10 times chondritic values. The mafic tonalite, with lower SiO_2 and $\text{La}/\text{Yb}_\text{N}$ values, may have formed by partial melting from approximately the same source as the more felsic tonalite and tonalite gneiss, leaving less garnet in the residuum.

In summary, the pre- to synvolcanic tonalites show evidence of an origin by partial melting of an ancient supracrustal sequence dominated by tholeiitic mafic metavolcanic rocks. The plutonic mafic tonalite and "old" tonalite apparently formed discrete intrusive magmas, whereas the tonalite gneiss and mafic tonalite gneiss were less mobile. Gower et al. (1982) came to a similar conclusion regarding the petrogenesis of tonalite and tonalite gneisses in the Kenora area. They modeled the petrogenesis of tonalite and tonalite gneiss with REE patterns very similar to those of the Atikokan tonalites, by 10% melting of a two-pyroxene garnet granulite with a bulk composition of quartz tholeiite.

Metavolcanic rocks

The Dismal ashrock has an unusual geochemical composition for an ultramafic volcanic rock. It is also unusual among Archean komatiites in its dominantly pyroclastic mode of occurrence. While ultramafic "volcaniclastics" sometimes form a minor portion of komatiitic sections dominated by lava flows (e.g. Gelinis et al., 1977), we know of few other examples of dominantly clastic Archean komatiites (e.g. Schaefer, 1989).

The unusual major element compositional parameters of the Dismal ashrock are its high TiO_2 , FeO total, and MnO , compared to other Archean komatiites. It has a low Al_2O_3 content resulting in a $\text{CaO}/\text{Al}_2\text{O}_3$ ratio of greater than 1.0 (~ 1.6). While this characteristic is typical of the classic komatiite locality of the Barberton area of South Africa and was used as part of the original chemical definition of komatiites (Viljoen and Viljoen, 1969; Brooks and Hart, 1974), it is not common among Canadian komatiites or those of other areas (see discussion of Arndt and Nisbet, 1982).

The Dismal ashrock is unusual in its trace element composition as well. It has high incompatible trace element contents for an ultramafic rock. Although the LIL elements may have been enriched by alteration processes, the elements generally considered "immobile" during alteration (Nb, Y, Zr, REEs, and Ti) are also enriched in the ashrock compared to most komatiites. A similar ultramafic pyroclastic unit occurs about 100 km west of Atikokan (Schaefer, 1989), and there are a few reported occurrences of these unusual incompatible element-enriched komatiites elsewhere in Archean terranes of India (Rajamani et al., 1985), Australia (Sun and Nesbitt, 1978), and Wyoming (Smaglik, 1987, 1988) as well as in younger high-magnesium lavas in California (Ernst, 1987). Several of these other examples of incompatible element-enriched komatiites are also high in Fe and Ti and have $\text{CaO}/\text{Al}_2\text{O}_3$ ratios greater than 1 like the Dismal ashrock (e.g. Rajamani et al., 1985: Table 1; #4). It is intriguing that in several of these other occurrences the enriched komatiites also unconformably overlie continental crust and are thought to have been erupted through the crust in extensional tectonic settings (Nisbet, 1982). This suggests that these unusual geochemical characteristics may be the result of interaction with sialic crust or that the upper mantle beneath the sialic crust was unusually enriched. If the latter was the case the mantle must also have been heterogeneous since in all of these examples the enriched komatiites are contemporaneous with depleted or chondritic lavas, or followed by chondritic lavas in the Steep Rock case.

The mafic to felsic metavolcanic rocks of the Steep Rock area show petrographic and geochemical evidence of extensive alteration. For the purpose of establishing the petrogenetic history of these rocks it is necessary to see through this alteration to their original igneous protolith. Due to the large number of samples analyzed and the variation seen in the degree of alteration it is possible to select a group of "least-altered" samples; this is not possible for the Dismal ashrock. Thus the following discussion will focus on selected "least-altered" metavolcanic samples from the Steep Rock and Finlayson belts listed in Table A5.

In general, the Steep Rock lower mafic metavolcanic samples have geochemical characteristics of the tholeiitic series, i.e. Fe enrichment at nearly constant SiO_2 and concomitant increase in TiO_2 and alkalis with decreasing CaO , MgO , and Al_2O_3 . These trends are obscured by alteration in the data set as a whole but are more readily apparent when only the least altered samples are considered. Least-altered samples were selected as those with less than 4.5% total volatile content and reasonable $\text{Na}_2\text{O}/\text{K}_2\text{O}$ ratios (1.0 to 100). The REE patterns for the least-altered mafic metavolcanic samples are approximately flat with enrichments of about 7 to 20 times chondritic values. These characteristics are similar to other Archean tholeiites and tholeiites from modern ocean floor (MORB) and island arc tectonic environments.

Least-altered metavolcanic samples from the Steep Rock and Finlayson mafic units, the Steep Rock upper felsic unit, and the Finlayson felsic unit plot in distinct fields on some trace element variation diagrams (see below). This argues against a cogenetic or consanguineous relationship between these three rock types. As discussed above, the Dismal ashrock also has a distinctive trace element composition which is inconsistent with a parental role for this ultramafic unit in the petrogenesis of the more evolved volcanic rocks. Figure 54, a plot of the moderately incompatible trace element Y versus Mg\# , shows that the least-altered metavolcanic samples form a fairly coherent trend of increasing Y with decreasing Mg\# . The Finlayson felsic metavolcanic samples have very low Fe contents leading to anomalously high Mg\# . The Dismal ashrock plots at the

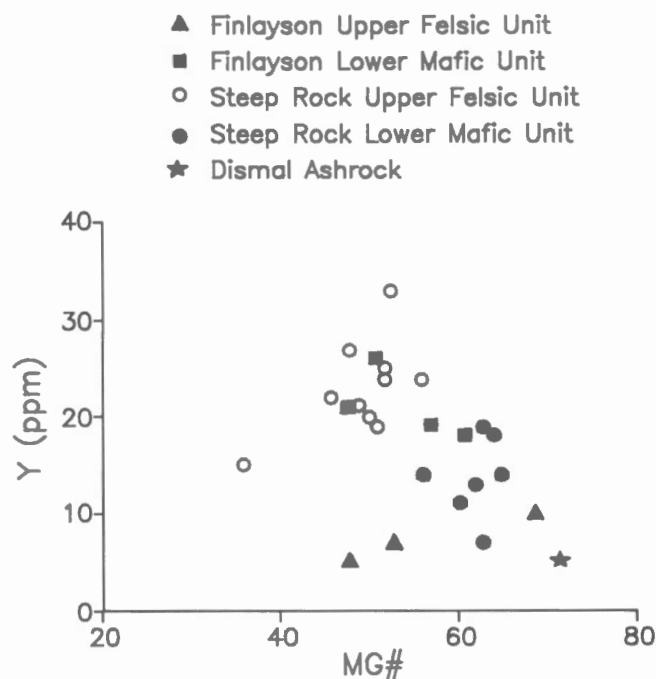


Figure 54. Yttrium versus Mg\# ($100 \cdot \text{Mg}^{2+} / (\text{Mg}^{2+} + \text{Fe}^{2+})$; $\text{Fe}^{3+}/\text{Fe}^{2+}=0.15$) for "least-altered" metavolcanic rocks. See text for selection criteria of "least-altered" samples.

primitive end of the Y-Mg# trend which is consistent with a cogenetic relationship. However, contents of the other incompatible elements preclude such a relationship.

Figure 55 shows variation diagrams of the alteration resistant immobile, compatible, and incompatible (HFS) trace elements with Y as a fractionation index. Yttrium's suitability for this role is demonstrated by Figure 54. On these diagrams the compatible elements, Co, Cr, and Ni,

generally decrease with increasing Y for the Dismal ashrock, mafic, and intermediate metavolcanic units. The ashrock has much higher contents of these compatible elements than the mafic metavolcanic units. This is consistent with a fractionation relationship since these elements partition strongly into olivine and pyroxene. However, the trend from the mafic to the felsic metavolcanic samples is one of a more gentle, linear decrease and the two groups plot in distinct

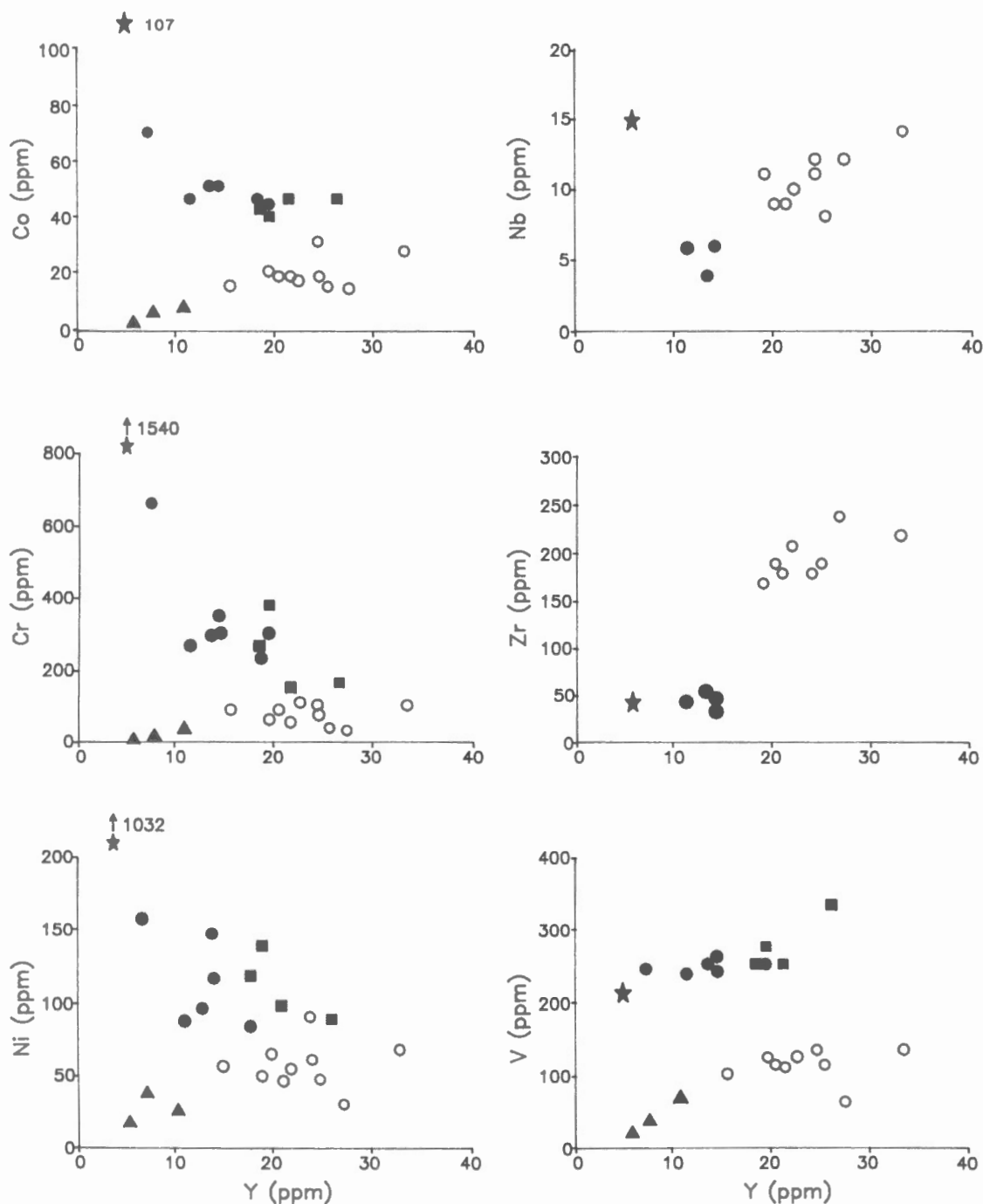


Figure 55. Immobile trace elements versus yttrium for "least-altered" metavolcanic rocks. Symbols as in Figure 54.

fields in terms of the compatible elements (especially Co) with overlapping Y values. The Y-V plot (Fig. 55) shows two distinct trends for the mafic and felsic metavolcanic samples with a substantial gap between the two.

Limited data from the Steep Rock metavolcanic samples for the incompatible elements, Nb and Zr, also show substantial compositional gaps between the mafic and intermediate units. The Dismal ashrock is too enriched in both of these elements (especially Nb) to have been a parental magma for the mafic to felsic metavolcanic rocks.

The Finlayson felsic metavolcanic rocks have low Y contents. They also have low Yb (and other HREE) contents (Table A5). This implies that garnet fractionation was important in their petrogenesis, since garnet has a high distribution coefficient for Y and the HREEs.

The REE patterns of Steep Rock lower mafic unit samples are consistent with fractional crystallization from the more primitive high Mg# basalts with lower total REE contents to the more evolved lower Mg# lower mafic unit samples, with higher total REE contents. This process probably involved the removal of olivine, pyroxene, and plagioclase as indicated by the parallelism of their chondrite-normalized patterns. The REE patterns of upper felsic unit samples are not consistent with an origin by fractional crystallization of these phases from the lower mafic unit, however. The upper felsic unit samples are enriched in LREE but have similar HREE to the lower mafic unit. Since the upper felsic unit is only moderately fractionated compared to the lower mafic unit in terms of its major and compatible trace element chemistry, it could only be related to the lower mafic unit by fractional crystallization if large and unreasonable amounts of clinopyroxene and/or amphibole fractionation are invoked.

As described above for the Steep Rock belt, differences in variation trends and trace element abundance ratios argue against a model for the derivation of the upper felsic unit from the lower mafic unit by a single-stage fractionation process. Magma mixing or assimilation/contamination processes are preferred for modeling the origin of the upper felsic unit. Supporting evidence comes from samples of the Perch belt that show negative Eu anomalies (Fig. 38c). Taylor and Hallberg (1977) interpreted similar patterns in rocks of the Marda complex (western Australia) as evidence of high degrees of partial melting at crustal depths. The relatively high compatible trace element content and Mg# combined with high Zr, Y, and Nb, and intermediate SiO_2 , K_2O , and P_2O_5 , and LREE enrichment are qualitatively consistent with an origin by mixing of a basaltic magma similar to the most primitive "least-altered" lower mafic unit samples with a felsic magma, similar to the Finlayson felsic metavolcanic unit or the "old" tonalite.

The Finlayson felsic metavolcanic samples have REE patterns similar to the tonalites in their relatively low total REE contents and high La/Yb_N values. In this way, as well as their more siliceous major element composition and lower compatible element contents, they differ from the Steep Rock upper felsic unit. They may have formed by a low degree of partial melting of garnet-bearing amphibolite, eclogite, or granulite with the bulk composition of tholeiitic basalt.

Granitic rocks

Several plutons of the Atikokan area, particularly the Margaret, Eye-Dashwa, and the small stock north of Miranda Lake, are compositionally zoned with quartz monzodiorite/quartz monzonite rims and granodiorite/granite cores. This is characteristic of many plutons in the Wabigoon Subprovince, noted by Birk and McNutt (1981) and Shirey and Hanson (1986). These zoned plutons differ from the other late Archean potassic granites by lacking well-developed negative Eu anomalies (see Taylor and McLennan, 1985, p. 220) and by being relatively enriched in Sr. Compared to plutons in the other subprovinces, such as the Lac du Bonnet batholith in the Winnipeg River Subprovince, these plutons characteristically contain high total Sr (500 to 2000 ppm versus 200 to 500 ppm). The Rb/Sr ratios vary from 0.05 to 0.14 (Peterman et al., 1985 and unpublished work) in the rim of the Eye-Dashwa pluton. These ratios are characteristic of the early phases of zoned plutons elsewhere in the Wabigoon Subprovince (Birk and McNutt, 1981). In contrast, the Lac du Bonnet batholith shows a wide range of Rb/Sr ratios, from 0.56 to 5.14 (Cerny et al., 1987), which far exceeds the calculated mean value (0.35) for the exposed rocks of the Canadian Shield (Shaw et al., 1967).

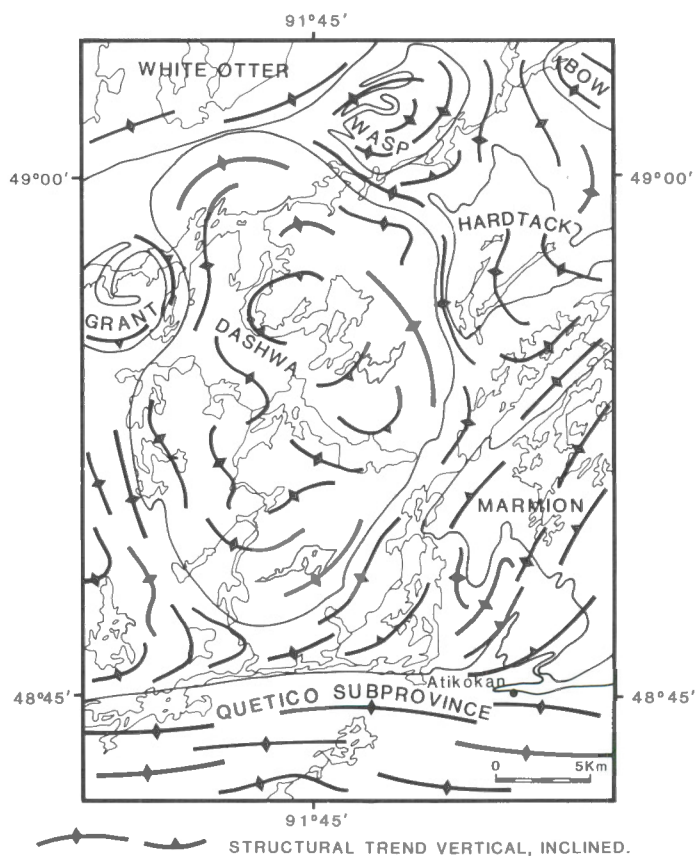


Figure 56. Oval structures and structural trends of the Atikokan area.

The $^{87}\text{Sr}/^{86}\text{Sr}$ ratios are distinctive in granitic plutons of the Atikokan area. For example, Peterman et al. (1985 and unpublished work) noted whole rock $^{87}\text{Sr}/^{86}\text{Sr}$ ratios ranging from 0.70167 to 0.71436 in fresh samples collected from the Eye-Dashwa pluton, and these values compare well with some zoned plutons studied by Birk and McNutt (1981). The Lac du Bonnet batholith has a much higher $^{87}\text{Sr}/^{86}\text{Sr}$ ratio ranging from 0.7639 to 1.3418 (Cerny et al., 1987). These observations suggest that the zoned plutons in the Atikokan area, and perhaps in the Wabigoon Subprovince as a whole, have a distinct petrogenetic history.

The $^{87}\text{Sr}/^{86}\text{Sr}$ ratios of the Eye-Dashwa pluton, discussed above, fall close to the mantle growth curve (Faure and Powell, 1972), suggesting derivation from source rocks with little or no significant crustal prehistory. Moreover, experimental evidence (Brown and Fyfe, 1970) and geochemical evidence (Hanson, 1980) shows that the stable residual phase of granitic magmas formed at crustal depths (<40 km) should be rich in Ca-plagioclase. Retention of plagioclase causes granitic magmas, which form in the crust, to be rich in potassium feldspar and show distinct negative Eu anomalies. Evidently, this is not the case with the Eye-Dashwa pluton.

Shirey and Hanson (1984) suggested a mantle source abnormally enriched in lithophile elements for the Ottetail pluton, which is located 80 km west and shows the same rare earth and incompatible element characteristics of the Eye-Dashwa pluton. Stern et al. (1989) grouped both intrusions with the mantle-derived sanukitoid suite of Archean monzodiorites that underlie about 5% of the southwestern Superior Province. The sanukitoid suite is characterized by 55 to 60 wt % SiO_2 , Mg# greater than 0.6, Ni and Cr greater than 100 ppm, and strong enrichment in LILE and LREE. In general, chemical characteristics of the Eye-Dashwa pluton are typical of sanukitoids except for an Mg# of about 0.5, possibly suggesting variable Mg in the mantle source.

The SiO_2 content in the granodiorite/granite core of the Eye-Dashwa pluton shows a gap of more than 10% with SiO_2 content in the quartz monzodiorite rim (Kamineni and Brown, 1981). This makes fractional crystallization and differentiation of quartz monzodiorite an unrealistic process for producing granodiorite/granite in the core region. Shirey and Hanson (1986) proposed melting of a monzodiorite parent as a source for granodiorite/granite phases. Their model implies recycling of the early monzodiorite phase, leaving a mafic residue. In the Atikokan area, the occurrence of monzodiorite as discrete stocks, such as at Volcano Bay, indicates that these materials were available for recycling to produce granodiorite phases.

STRUCTURE

The subprovinces and accretionary tectonism

The Atikokan area comprises parts of the laterally extensive Wabigoon and Quetico Subprovinces, respectively dominated by mixed metavolcanic-plutonic and metasedimentary rocks. The west-trending boundary

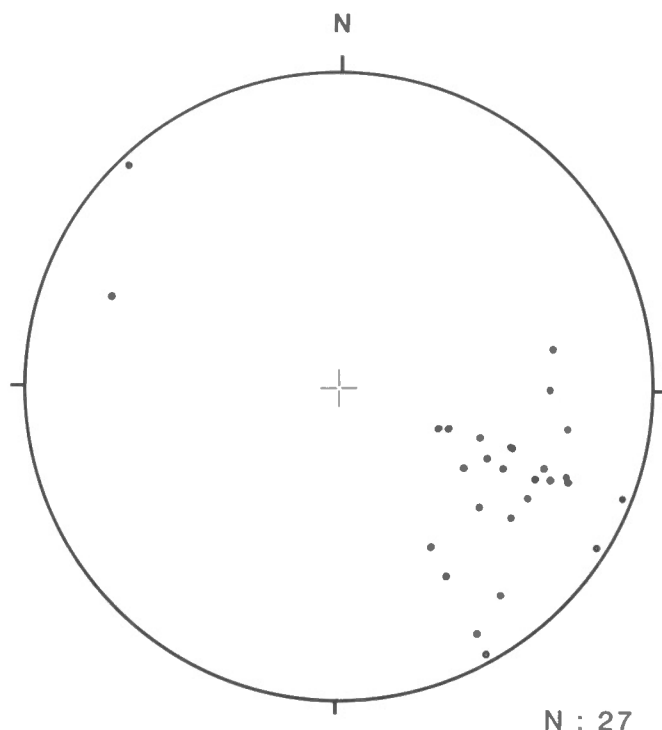


Figure 57. Poles to foliation measurements in the Marmion batholith. Lower hemisphere equal-area projection.

between these subprovinces is the largest and most striking lithostructural feature within the map area. Although regionally straight, the boundary shows local flexures and embayments but nonetheless marks an abrupt lithological transition from metavolcanic rocks of the Perch and Steep Rock belts to Quetico metasediments.

Although the Quetico-Wabigoon boundary has been variously described as a fault, a zone of lithological and metamorphic transition (Blackburn et al., 1985, and references therein), and a wrench zone (Poulsen, 1986), recent tectonic models have favoured accretionary processes for the development of collinear subprovinces such as the Quetico and Wabigoon. Percival and Williams (1989) interpreted Quetico metasediments as a deformed wedge of turbidites deposited in an oceanic trench adjacent to an active calc-alkaline volcanic arc (Wabigoon). Using the constraints of precise age determinations, Percival and Williams (1989) and Percival (1989) defined several developmental stages of the Wabigoon-Quetico boundary.

1. Volcanism was active from 2750 to 2700 Ma at the margin of the Wabigoon arc as a result of oblique, northwestward subduction of oceanic crust. Quetico metasediments were rapidly deposited in the adjacent trench and accreted against the Wabigoon arc. D_1 deformation, which produced a regional planar fabric and steeply plunging mineral lineations (Devaney and Williams, 1989) was initiated.

2. Accretion stopped by about 2695 Ma as the Wawa arc abutted against the Quetico accretionary prism; D_2 deformation ensued with the beginning of metamorphism of Quetico sediments.
3. The Wabigoon was affected by crustal thickening and late plutonism, the Seine Group was deposited, and transpressive deformation (D_3) produced Z-style folds and shear fabrics and transcurrent motion on boundary faults up to 2684 Ma.
4. Major plutonism and static metamorphism continued in the Quetico Subprovince up to about 2650 Ma. Notably, a wide range of geological processes ranging from primary igneous activity to ensuing deformation and metamorphism took place within a few tens of Ma. Regional deformation was attributed mainly to accretion and ensuing transpression as opposed to strain aureoles of granite intrusions.

The accretionary model is strengthened by repetitive volcanic-sedimentary megasequences in the Beardmore-Geraldton area 300 km east of Atikokan, which are interpreted as an imbricate thrust stack produced by the convergent tectonism (Devaney and Williams, 1989). Davis et al. (1989) favour a similar mobilistic model involving collisional plate interactions followed by transpression to account for lithological and age patterns at the Quetico-Wabigoon boundary in the Rainy Lake area. The above models account for the regional juxtaposition of metavolcanic and metasedimentary rocks astride the Quetico-Wabigoon boundary – a prominent feature in the Atikokan area. In addition to the subprovince boundary, however, the Atikokan area hosts other structures including large-scale oval structures, folds, and faults that are described below.

Oval structures and structural trends

Away from the subprovince boundary, the Wabigoon is characterized by large, felsic oval structures (Fig. 56) separated mainly by belts of metavolcanic rocks and mafic gneisses. Typical oval structures are composed of a felsic plutonic core and an outer zone of tonalite gneiss with mafic inclusions. This outer zone (where present) grades into mafic tonalite gneiss or metavolcanic rocks or is cut by felsic plutons.

The Eye-Dashwa pluton is the felsic core of the large oval Dashwa structure (Fig. 56; Map 1666A), the outer tonalite gneiss zone of which is punctured by small intrusions, which include the Nevison and Little Eye stocks and the Righteye pluton. The Dashwa oval structure is bounded by a prominent, U-shaped chain of metavolcanic belts (Nevison, Perch, Steep Rock, and Finlayson) on the south, by curved belts of mafic tonalite gneiss and metavolcanic inclusions on the east and west, and by the White Otter batholith on the north. The Marmion structure includes the Marmion batholith and adjacent Margaret and Diversion stocks, which extend east of the map area (compare Fig. 9 and 56). The Wasp, Bow, and Hardtack plutons form cores of small

imperfect oval structures characterized by interdigitated contacts with mafic tonalite gneiss. The Grant structure has a core of tonalite gneiss enveloped by a curved and bifurcated belt of mafic tonalite gneiss and metavolcanic rocks.

Structural trends defined by gneissosity, foliations, aligned xenoliths, and lithological contacts show mainly concentric zoned patterns within oval structures (Fig. 56). For example, gneissosity in the outer zone of the Dashwa structure wraps almost completely around the central Eye-Dashwa pluton. Foliations within metavolcanic and mafic tonalite gneiss belts that mantle oval structures also form part of the concentrically zoned pattern of structural trends.

Two notable exceptions to concentric zonation of oval structures are found in the eastern part of the map area. First, the felsic plutonic core of the Hardtack structure (Hardtack pluton) is in direct contact with the northwestern Finlayson belt. Foliation trajectories in the Hardtack pluton intersect the contact at a high angle and cross into the metavolcanic belt without deflection. Second, foliation trajectories in the Marmion structure do not curve but maintain a uniform southwesterly trend (Fig. 56 and 57). These trajectories cross into the Steep Rock belt and curve westward into parallelism with the Quetico Subprovince boundary.

Formation of oval structures in the Wabigoon Subprovince has been variously interpreted as due to diapirism (Schwerdtner et al., 1985; Schwerdtner, 1988) or the effects of cross folding (Schwerdtner, 1989). The cross-fold model is supported by the presence of aligned oval

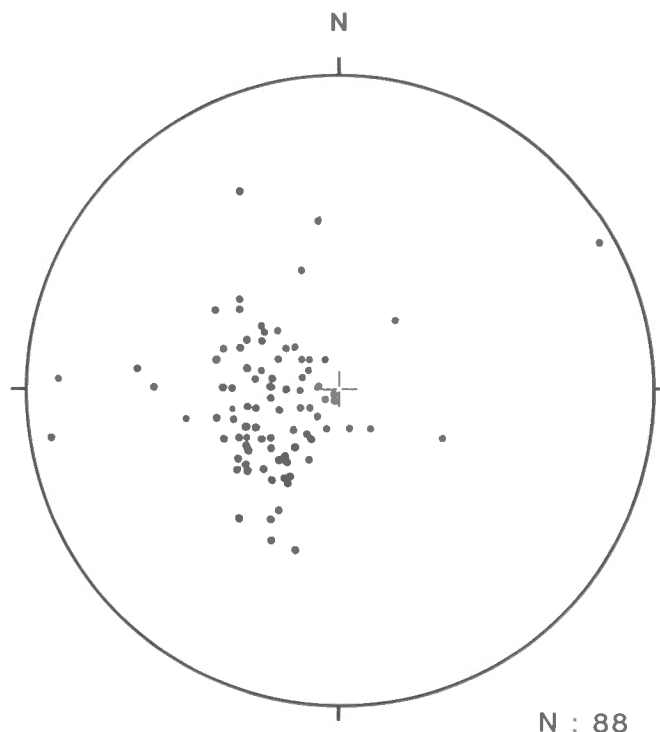


Figure 58. Linear elements including axes of crenulations, drag folds, rodding structures, grooves, slickensides, and stretched minerals in the eastern Steep Rock belt (after Figure 4 of Shklanka, 1972). Lower hemisphere equal-area projection.

structures in parts of the western Wabigoon and Uchi subprovinces and is compatible with a dominantly horizontal strain regime, such as would have existed at the time of accretion of the subprovinces. Core plutons within oval structures are interpreted as minor syntectonic phacoliths (Schwerdtner, 1989) which have evidently not contributed significantly to regional deformation or formation of oval structures.

Diapiric models favour the rise of low-density rocks (here represented by core plutons and tonalite gneisses) accompanied by subsidence of dense, overlying supracrustal sequences into marginal troughs (metavolcanic belts). Physical modeling (e.g. Dixon, 1975) shows that low-density diapirs rise as columns until they reach an obstruction and then spread laterally (mushroom shape) causing radial outward displacement and flattening of the supporting medium.

Although oval structures in the Atikokan area show a slight north-northeast alignment, other evidence supports an origin mainly by vertical displacements. Firstly, core plutons are of variable age (e.g. 2936 Ma for tonalite, 2665 Ma for granite) which implies that oval structures formed at different times that cannot be easily related to known episodes of horizontal shortening such as accretion of the Quetico prism with the Wabigoon arc at about 2695 Ma. Secondly, many oval structures are mantled by mafic rocks that may have formed a dense overlying blanket leading to gravity instability and diapirism. Thirdly, the cross-section of the Dashwa structure (B-B'-B'', Map 1666A), which is based on

gravity modeling of Gibb et al. (1988), shows a broad conical shape to the Eye-Dashwa pluton, which is characteristic of a moderately mature diapir. Spreading of this intrusion may be partly responsible for the strong concentric foliations and oval shape of the Dashwa structure.

The Marmion structure may be unique because the core intrusion (Marmion batholith) predates the Finlayson and Steep Rock belts. Although the metavolcanic belts were affected by the Diversion and Margaret stocks, they were not displaced or shortened by intrusion of the Marmion batholith. This may account for the irregular shape and lack of concentric structural trends at the southwestern end of the Marmion structure (compare Fig. 9 and 56).

In the Quetico Subprovince, structural trends, defined mainly by subparallel bedding and cleavage, are easterly with deflections around the Bewag stock (see Fig. 9) and north into the Steep Rock belt (Fig. 56). The easterly structural trends and isoclinal folds oriented slightly oblique anticlockwise to the Quetico-Wabigoon boundary in this area have been attributed to strong dextral transpression (Borradaile et al., 1988).

Folds

Gneisses

Many outcrops of gneisses show mesoscopic folds. Amphibolite layers were competent members in mafic tonalite gneiss (unit 1d) and formed nearly parallel folds, some of which have boudinaged limbs. Intervening tonalite layers show marked variation in orthogonal layer thickness and are probably Class 3 folds (Ramsay and Huber, 1987, p. 349).

Tonalite gneiss (unit 1c) displays diffuse and discontinuous folds in part due to lack of sharply defined and continuous layering (Fig. 11). These structures are tight to isoclinal, polyharmonic, and commonly parasitic and asymmetrical.

Fold hinges plunge at variable angles, although isoclinal folds tend to be gently plunging or subhorizontal. Large-scale folds are present in gneisses northeast of the Eye-Dashwa pluton and west of the Little Eye stock where trends of foliations and amphibolitized mafic metavolcanic units are curvilinear (Map 1666A).

Metavolcanic rocks

Minor folds are common throughout the metavolcanic units of the Atikokan area. Primary structures (lithological contacts, pillow selvages), volcanic clasts, dykes, quartz veins, and secondary fabrics (gneissosity and foliations) are affected. Folds are particularly common at the junction of the Perch and Steep Rock belts where lithological boundaries, tuffaceous layering, and abundant quartz veins show complex curved geometry. The folds are tight to isoclinal and generally steeply plunging.

Megascopic fold axes are identified in the metavolcanic belts on the basis of stratigraphy, younging directions obtained from pillow tops and graded beds, and lithological

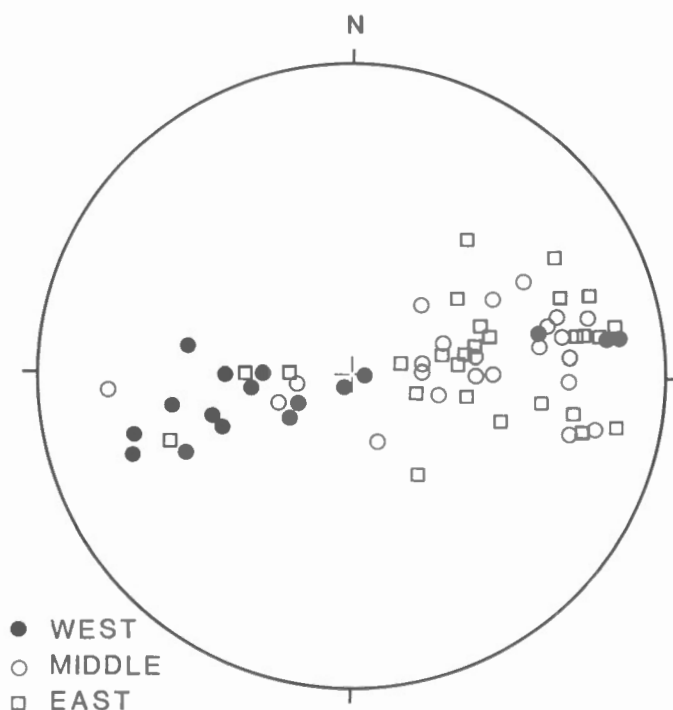


Figure 59. Axes of minor folds in western, middle, and eastern parts of the Quetico Subprovince. Lower hemisphere equal-area projection.

continuity of rock units. For example, pillow structures are abundant in the Finlayson belt and six folds are identified on the basis of younging reversals that occur from east to west such as along Section B'-B" (Map 1666A). Synclines occur mainly in the upper metasedimentary units and anticlines mainly in mafic metavolcanic rocks.

Two synclinal metasedimentary units dip westerly and terminate at depth in the Finlayson belt (Section B'-B", Map 1666A). Reversals in younging directions indicate that the intervening mafic metavolcanic rocks contain an anticline-syncline-anticline structure. The "old" tonalite within the eastern margin of the Finlayson belt is interpreted to be a detached slice of basement that occupies the core of an anticline. Additional folds may occur along the poorly exposed northwestern side of the Finlayson belt.

The two units of metagreywacke-argillite (unit 4a) have minor associated iron formation that can be traced on aeromagnetic maps (Ontario Geological Survey, 1980) through the central Finlayson belt and appear to merge beneath the southern end of Finlayson Lake. The synclines within these metasedimentary units are interpreted to join at this locality, which also marks the southwestern end of the anticline-syncline-anticline structure (see fold axes on Map 1666A). A syncline on the southeastern side of the Finlayson belt passes through metagreywacke to meta-agglomerate and intermediate metavolcanic units along the western side of the Steep Rock belt. This is one of the longest folds (16 km) in the area.

The structure of the Steep Rock belt, such as along Section A-A' (Map 1666A), is marked by a series of north to northeasterly trending fold axes. The syncline on the western side of the belt is juxtaposed with an anticline at the base of a thick sequence of mafic pillow lavas (unit 3b) that underlies Steep Rock Lake. An isoclinal syncline with a steep westerly dipping axial surface is situated within mixed metavolcanic and metasedimentary rocks west of the Errington pit. The narrow intermediate to felsic metavolcanic unit that hosts the fold axis on Map 1666A and Section A-A' has been reinterpreted as altered mafic metavolcanic flows (cf. Fig. 30); however, basic structural interpretation of the area is unaffected. The fold axis curves east at the Errington pit and passes through a small lense of meta-agglomerate (unit 4b) and eventually extends southwest to the Quetico Subprovince. It is a significant fold separating the thick sequence of east-younging pillow lavas at Steep Rock Lake from the remainder of the belt where the younging direction of minor structures is mainly west. North of the Errington shaft the synclinal axis probably merges with the Atikokan fault.

Small amplitude, possibly domical folds occur in the eastern Steep Rock belt. Minor folds and mineral lineations in this area have steep westerly to southwesterly plunge (Fig. 58). Borehole data from the Caland pit area (McIntosh, 1972) indicates that the base of the eastern Steep Rock belt dips to the west ($\sim 40^\circ$).

The eastern Perch belt is characterized by repetitive units of metagabbro and mafic and intermediate to felsic metavolcanic rocks that are crescentic with apices pointing

east. Synclines are interpreted in the intermediate to felsic metavolcanic units on the basis of their inferred stratigraphically superior position. Although highly speculative, these megascopic folds together with numerous minor structures in outcrops suggest that the eastern Perch belt contains some of the most complexly deformed supracrustal sequences in the map area.

Quetico metasediments

Recent studies have documented complex, polyphase, and upright or inverted folds in Quetico metasediments of the Rainy Lake area (Poulsen et al., 1980), northwest of Thunder Bay (Kehlenbeck, 1984), and in the Beardmore-Geraldton area (Kehlenbeck, 1986). West of the present map area at Calm Lake, Borradaile (1982) used bedding-cleavage relations to define four closely spaced folds and an overall easterly facing direction of sedimentary strata. Dutka (1982) identified three northeasterly trending fold axes, which cross Highway 11B south of Atikokan. Borradaile et al. (1988) reconstructed the form surfaces of Quetico metasedimentary strata between Calm Lake and Atikokan and showed a series of mainly east-facing isoclinal sheath folds separated by limb-parallel "slides". The major fold axial planes are oriented slightly oblique to the Quetico-Wabigoon boundary in an anticlockwise sense and were attributed to a kinematic pattern of mainly dextral transpression (Borradaile et al., 1988).

The present mapping shows a dominant easterly trend of subvertical bedding and foliation in the northern Quetico Subprovince. Minor Z-style asymmetrical folds and bedding-cleavage intersection lineations can be recognized in clean outcrops adjacent to Highway 11 and on lakeshores. These features show mainly easterly plunge in the middle and eastern third segments of the map area (Fig. 59).

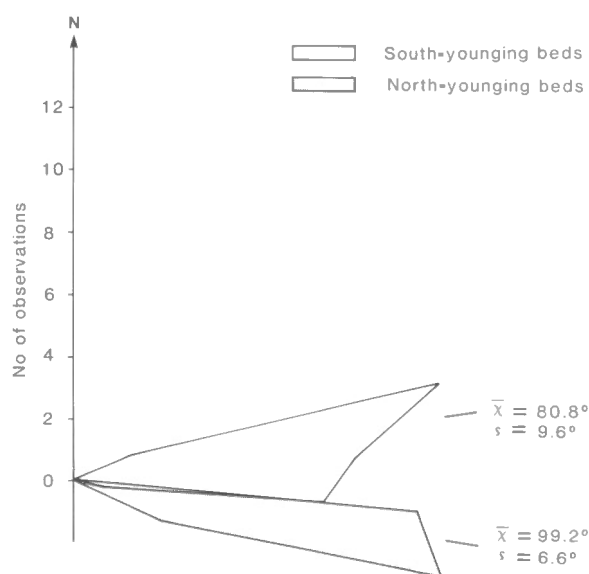


Figure 60. Rose diagram showing strike of bedding in Quetico metasediments of the Kemuel Lake area.

Although sedimentary beds strike approximately east, grain-size gradations within beds show both north- and south-younging directions and confirm the presence of folds in the sequence. South of Highway 11, within an area that extends about 3 km east from Kemuel Lake, subvertical north-younging and south-younging beds strike, on average, 99° and 81° respectively (Fig. 60). The fold or folds affecting these strata have an interlimb angle of about 18°.

In the Perch Lake area, Quetico metasediments young north to the Quetico-Wabigoon boundary. This structural relation changes west of Apungsisagen Lake where Quetico metasediments and adjacent pillow lavas of the Steep Rock belt young south.

Lineaments

Terrain of the Atikokan area is marked by a pervasive network of megascopic, curvilinear structures that are visible in aerial photographs. These airphoto lineaments have prominent topographic expressions such as elongate lakes, linear stream channels, valleys and escarpments, and linear vegetation patterns affecting size and species of trees. Lineaments have also been traced beneath Dashwa, Eye, and Finlayson lakes with the help of boat-mounted sonar equipment (Holloway, 1985).

The Quetico Subprovince is characterized by short (<5 km), isolated northeast- and northwest-trending lineaments (Fig. 61). Curved and braided lineaments extend from the Perch Lake area obliquely across the Quetico-Wabigoon boundary northward through the Steep Rock belt to the Finlayson belt. Granites and gneisses are transected by a braided network of curved northeast-, north-northeast-, and northwest-trending lineaments. Northeast-trending structures can exceed 20 km in length whereas northwest-trending lineaments tend to be less than 5 km long.

The formation of lineaments is commonly attributed to enhanced erosion at the surface trace of structural discontinuities such as lithological contacts, fractures, faults, and dykes in the bedrock (e.g. Nur, 1983). In some instances lithological contacts and faults of the Atikokan area are spatially associated with lineaments. For example, lineaments are concentrated at the Quetico-Wabigoon boundary but are not parallel to the boundary. In the eastern Steep Rock belt, lower formations of the Steep Rock Group are juxtaposed with resistant metagabbro ridges giving rise to highly curved lineaments north of Atikokan. Segments of some lineaments are conformable with margins of the Eye-Dashwa pluton and western Steep Rock belt. Other lineaments are coincident with the Ear fault at the eastern margin of the Nevison belt and certain segments of the Marmion fault system in the Marmion batholith (compare Fig. 61 with Map 1666A).

Despite the above examples, known lithological contacts, dykes, and broad zones of fault rocks account for only a small number of lineaments. At most localities, lack of exposure precludes clear definition of the bedrock structure beneath linear features. This problem was addressed at the grid area

of the Eye-Dashwa pluton (Fig. 1) where surficial material was excavated from a linear valley and a 3 m wide zone of intensely fractured and brecciated rock was revealed. This narrow fault zone shows evidence of 15 m of dextral transcurrent displacement and appears to be coeval with other faults and fractures that have been drilled or mapped in the Eye-Dashwa pluton. Kamineni et al. (1988) noted that these discontinuities contain a common epidote-dominated filling material that gives Early Proterozoic Rb/Sr ages (see section on Fractures in the Eye-Dashwa pluton). They proposed that the Atikokan area was affected by a widespread brittle deformation event at about this time, which gave rise to the majority of structures underlying lineaments shown in Figure 61.

Faults

Mesoscopic faults including ductile shear zones (Ramsay, 1980) and ductile-brittle and brittle structures are present throughout the area and typically have displacements of less than 1 m. They transect all lithostructural elements (e.g. bedding, intrusive contacts, foliation, fold limbs, veins). Brittle transcurrent faults are common in the Eye-Dashwa pluton and their characteristics (size, shape, orientation, and filling materials) are discussed below in the section on Fractures in the Eye-Dashwa pluton.

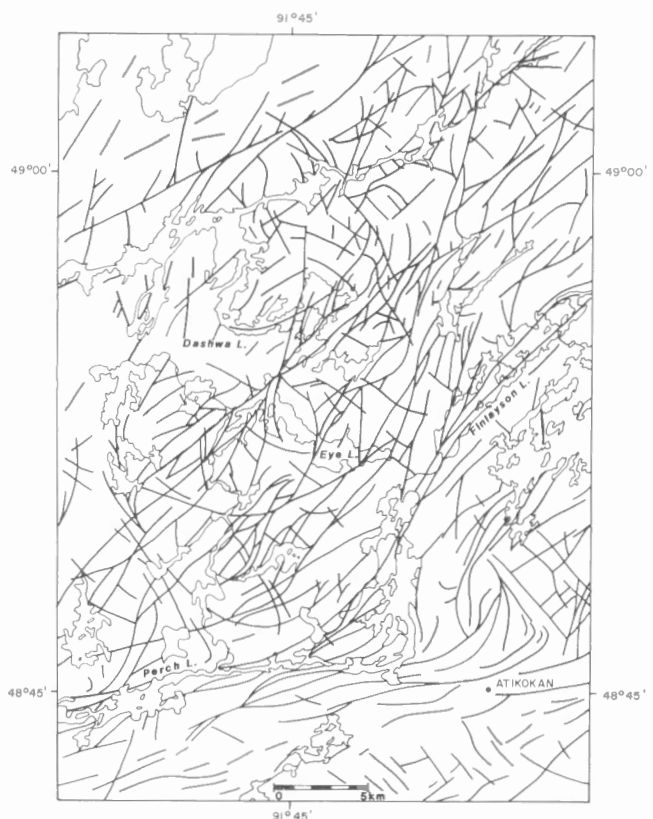


Figure 61. Airphoto lineament map of the Atikokan area.

In addition to the ubiquitous small-scale faults and fractures, several macroscopic fault zones are identified in the Atikokan area. These include the Ear, Marmion, Samuel, Atikokan, and Rawn structures (see Map 1666A).

Ear fault zone

The Ear fault zone (Fumerton, 1986) extends from Dragon Lake to Harold Lake along the eastern boundary of the Nevison and Perch belts. The fault is marked by a diffuse zone of protomylonitic tonalite and granodiorite adjacent to schistose and crenulated metavolcanic rocks. Short splays curve easterly from the Ear fault into the Lefteye stock and Righteye pluton. The southeastern end of the fault zone is marked by curved units of protomylonite that extend into the Perch belt south of Harold Lake. There the fault rocks are extensively fractured and altered and contain gold-bearing quartz veins at the Harold Mine.

The Ear fault zone shows prominent lineations defined by elongate quartz grains and mica aggregates. The lineations plunge steeply (Fig. 62) and imply mainly dip-slip displacement on the fault although the magnitude of displacement is not known. Faulting probably occurred during formation of the Dashwa oval structure in response to shear strain at the interface between rising tonalitic material and subsiding metavolcanic rocks of the Perch belt.

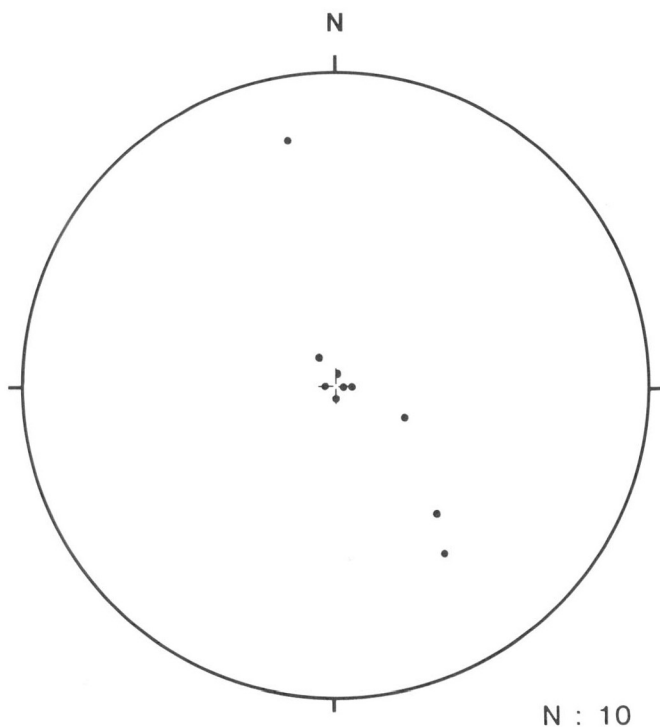


Figure 62. Lineations defined by elongate mineral grains in the Ear fault zone. Lower hemisphere equal-area projection.

Marmion fault system

A complex network of faults extends northeast from the Steep Rock belt through the Marmion batholith. These faults, collectively termed the Marmion fault system, are parallel to the foliation and to dykes in the "old" tonalite but appear to terminate within lower formations of the Steep Rock Group.

Individual segments within the Marmion fault system have gradational boundaries and some are arranged in an en-echelon form. Fault rocks are best exposed between the Caland pit and Moose Lake, particularly below the dam at the southern end of Moose Lake. There, the "old" tonalite is

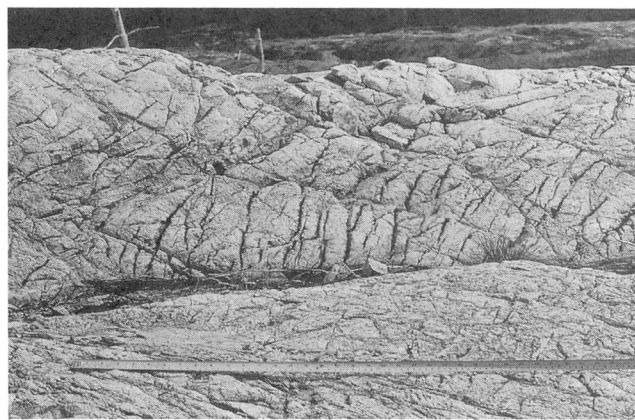


Figure 63. Fault rocks of the Marmion fault system, Moose Lake. GSC 204108-L

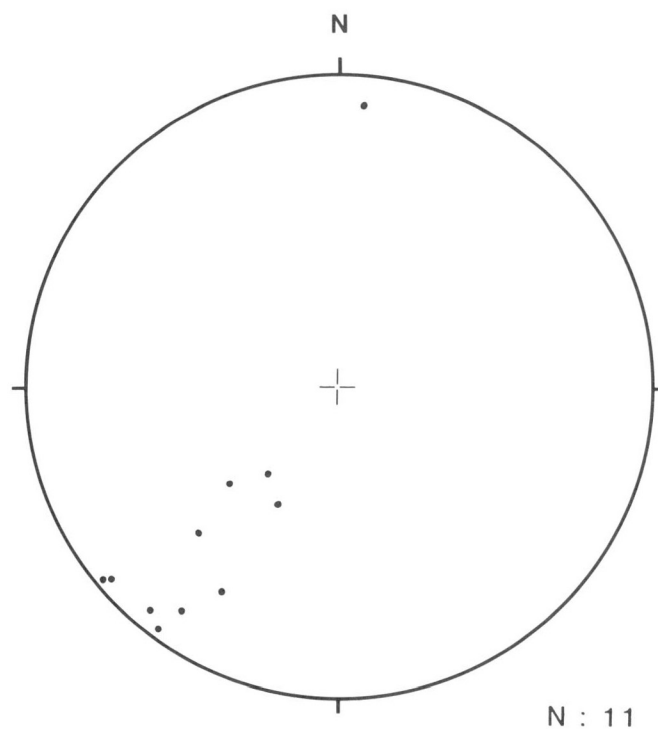


Figure 64. Slickenlines from the Marmion fault system. Lower hemisphere equal-area projection.

altered to a quartz-sericite-carbonate schist and is highly fractured and transected by irregular quartz veins (Fig. 63). Fault rocks are characterized by a braided network of curved, schistose slip surfaces that wrap around lensoid domains of less deformed rock. The absence of augen textures typical of mylonites, and the presence of abundant tensile fractures that transect the lensoid domains suggest faulting at low temperatures.

Displacements appear to be complex and variable. Slip surfaces parallel to the main northeast-trending segment of the Marmion fault cause sinistral strike separation of metagabbro dykes and show slickenlines with variable southwest plunge (Fig. 64). These data indicate oblique south-side-up and sinistral transcurrent displacements. Elsewhere, normal faults are observed. In 1982-83, Moose Lake was drained to permit construction of a water tunnel from the lake basin to the Ontario Hydro generating station and hence to Snow Lake. The tunnel passes through a segment of the Marmion fault system and intersects several slip surfaces, most of which are intermediate-dip normal faults with a few subvertical, mainly strike-slip faults.

Samuel and Atikokan faults

The Samuel fault is marked by a north-northeast-trending diffuse zone of schistose, altered and highly fractured tonalite adjacent to the central Steep Rock belt. The fault separates mafic tonalite (unit 1a) from the Mosher Carbonate Formation (unit 2b) at the northern end of the Caland pit beyond which it is truncated by the Diversion stock. The southern end is poorly exposed and may possibly merge with the Atikokan fault in the vicinity of the Errington pit, extend south-southwesterly, or else die out. Slickenlines plunge 50° westerly in the Caland pit area and imply dip-slip, probably reverse displacement that could be responsible for the uplift of "old" tonalite (unit 1b) into the central Steep Rock belt (Section A-A', Map 1666A). Although the Mosher Carbonate Formation has a strike separation of about 4 km from the Errington pit to the Caland pit, the strike slip of the Samuel fault may be much less because the base of the eastern Steep Rock belt rakes about 30° to the south. Eastward thrusting on the Samuel fault, which cuts up-section through the unconformity, was probably responsible for the southward separation of the Mosher Carbonate Formation in the hangingwall block.

The Atikokan fault is traced north along the western wall of the Roberts pit within the upper part of the Dismal Ashrock Formation and adjacent metavolcanic rocks (Fig. 30). At the Hogarth pit, the Atikokan fault curves westerly and is truncated by the subvertical, dip-slip Bartley fault (Fig. 30) and a thick metagabbro dyke. In the vicinity of the Errington pit, the Atikokan fault follows the upper ashrock contact and curves easterly into a poorly exposed area where it may possibly merge with the Samuel fault. The Steep Rock Group in the Roberts and Hogarth pits is cut by numerous 1 to 2 m wide sinistral transcurrent and dip-slip faults that appear to coalesce with the Atikokan fault. Some minor structures may be splays of the Atikokan fault whereas others, such as the Bartley, are clearly discordant.

Although the Samuel and Atikokan faults are widely recognized, diverse interpretations have been offered for the causes and senses of slip on these structures. Whereas Shklanka (1972) regarded both structures as thrust faults, Wilks (1986) favoured normal displacement on the Samuel fault. Hoffman (1989) suggested that the Atikokan structure could be a significant thrust fault that displaced allochthonous metavolcanic rocks onto the Steep Rock Group. Thrusting could be caused by "thin-skinned" imbrication of oceanic crust at early stages of arc-continent accretion. In this case, the Atikokan fault is likely to be conformable with the upper ashrock contact and extend through most of the eastern and central Steep Rock belt.

Mapping however, shows that the Samuel fault is truncated by the Diversion stock immediately north of the Steep Rock belt and leads to the interpretation shown in Section A-A' (Map 1666A) where paraconformable, reverse-displacement structures corresponding to the Samuel and Atikokan faults are rooted in granodiorite (unit 8b) at depth. Reverse displacement, particularly on the Samuel fault, could be caused by intrusion beneath the Steep Rock belt of felsic magma such as occurs in the Diversion stock.

Rawn fault

The Rawn fault separates the Steep Rock belt from the Margaret stock and extends northeast into the Marmion batholith. Fault rocks are schistose, altered, and highly fractured tonalite and metagabbro dykes, comparable to material in faults of the Marmion system. Elongate mineral grains plunge southwesterly (Fig. 65) but the amount of

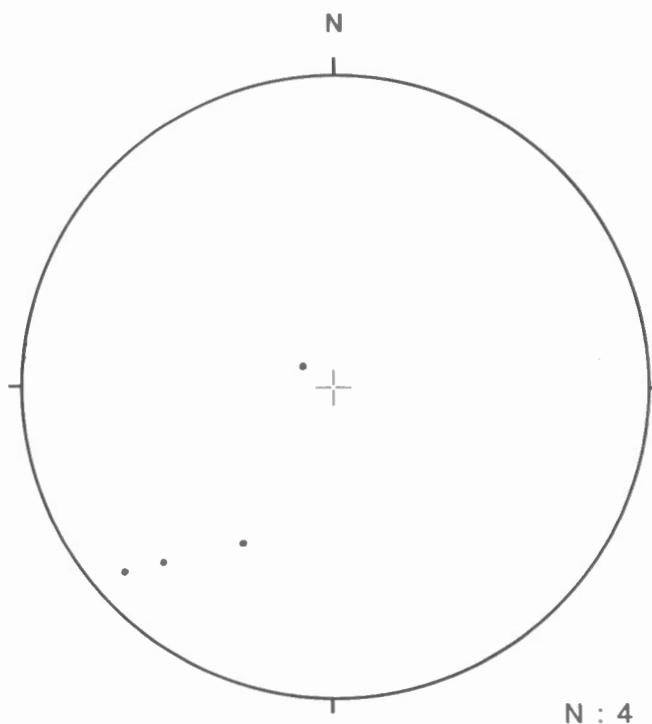


Figure 65. Lineations defined by elongate mineral grains in the Rawn fault. Lower hemisphere equal-area projection.

displacement is not known. Fault rocks show evidence mainly of brittle deformation suggesting that faulting occurred near surface at a temperature below 300°C (Sibson, 1977).

Faults in Quetico metasediments

Several northeast- and northwest-trending minor faults occur within clastic metasediments of the Quetico Subprovince. They are 1 to 10 m wide zones where the strata are disrupted and brecciated. Quartz veins and angular fragments of wall rocks occur within a finely brecciated matrix of chlorite, quartz, and lithic fragments. Slickenlines are subhorizontal and narrow dimensions of the zones suggest that displacements do not exceed a few hundred metres. These structures were probably active during late stages of folding and transpression of Quetico metasediments.

Quetico fault

Many authors (e.g. Shklanka, 1972; Fumerton, 1986) have inferred that a major fault zone (Quetico fault zone) occurs at the Quetico-Wabigoon boundary. The existence of a large fault at this boundary was first proposed by Hawley (1930), and although Moore (1939) found no evidence for it, most recent authors acknowledge the fault. Parkinson (1962) interpreted airphoto lineaments as evidence for faulting. Mackasey et al. (1974) proposed a large dextral displacement on the order of 100 km to account for a possible lithological offset in the Mine Centre-Rainy Lake area. Shklanka (1972)

showed several faults within the Steep Rock belt (Fig. 8) as splays of the Quetico fault. Pirie (1978), Pirie and Mackasey (1978), Borradaile (1982), and Percival and Stern (1984) produced maps that show the Quetico fault separating northern volcano-plutonic terrane from metasediments to the south.

Borradaile et al. (1988), Devaney and Williams (1989), and Percival and Williams (1989) showed evidence for dextral transpression of Quetico metasediments after accretion of the Quetico prism. Shear strain was thought to have been initially taken up along discrete "panels" or "slides" within the metasediments and subsequently became concentrated on transcurrent boundary faults.

The Quetico boundary fault is prominent in the Rainy Lake area (Poulsen, 1986) and is described at other localities (Pirie, 1978; Bau, 1979; Kennedy, 1984) but does not appear to be well developed at Atikokan. Although the present survey confirms evidence for dextral transpression, mainly in the form of widespread asymmetrical Z-style folds, it fails to identify a major transcurrent fault. In particular, the mapping could not show a straight and continuous zone of fault rocks, an associated lineament, or a straight zone of subhorizontal mineral lineations. Results of the mapping are puzzling and may indicate that the effects of faulting are somehow masked or that the structure is discontinuous or transitional to broad zones of transpression. In the latter cases caution may be advisable in application of tectonic models that require a large-displacement transcurrent fault everywhere at the Quetico-Wabigoon boundary.

Fractures in the Eye-Dashwa pluton

Fracture characteristics of the Eye-Dashwa pluton were the subject of research by Atomic Energy of Canada Limited between 1979 and 1985. Work included geophysical surveys, regional mapping, detailed surface mapping, drilling, and core logging.

Detailed surface fracture mapping and drilling were concentrated on the Forsberg Lake grid area at the eastern edge of the pluton (see Fig. 1). Overburden was removed from 15 000 m² of outcrop using excavators and water pumps to allow measurement of fracture length and spacing distributions using the linescan method (Fig. 66). Fractures in outcrop are relatively short (median length: 4 m) and closely spaced (median spacing: 0.3 m) in the Eye-Dashwa pluton compared to the White Otter batholith and Lac du Bonnet batholith of southeastern Manitoba (unpublished data by the authors and Stone et al., 1989).

Five boreholes were drilled to depths ranging from 200 m to 1100 m at the Forsberg Lake grid area. Borehole television cameras, borehole viewers, and oriented core were used to determine the orientation, spacing, and depth distribution of fractures. In general, fractures have highly variable but dominantly subhorizontal and subvertical orientations (Fig. 67). Three other boreholes, located west-centrally in the Eye-Dashwa pluton (Fig. 68) intersected abundant closely spaced and variably oriented fractures comparable to those at the Forsberg Lake grid area. Borehole ATK-8 intersected a

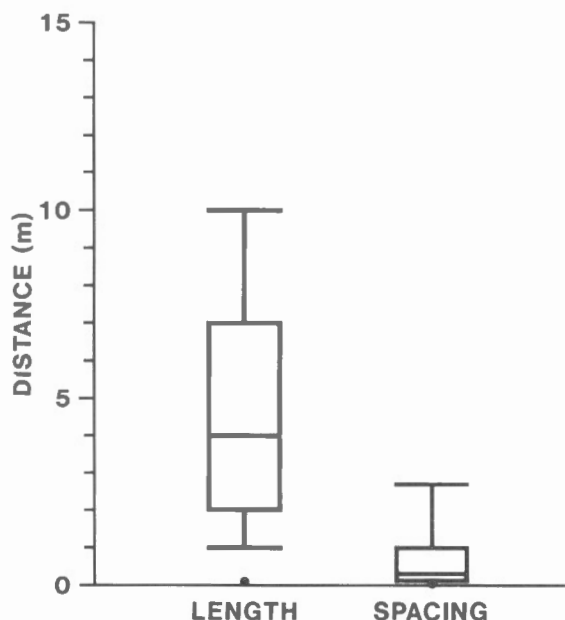


Figure 66. Length and spacing distributions of fractures at the grid area as shown by "box whisker" symbols. Dots represent extreme values of the distribution; horizontal bars are 10% and 90% values; ends of the "boxes" are 25% and 75% values; and the horizontal bars within the boxes are median values.

major fracture zone that underlies a prominent airphoto lineament extending through Eye Lake and Dashwa Lake (compare Fig. 61 and 68).

The majority of fractures in the Eye-Dashwa pluton are tightly sealed with minerals such as epidote and chlorite and are pervasively distributed. Figure 69 illustrates the distribution of fractures from surface to 1200 m depth in borehole ATK-6. Fractures have a more-or-less uniform abundance along the borehole with the exception of a major fault zone at 1140 m depth. Transcurrent faults such as in borehole ATK-6 appear to be the longest and most significant elements of the fracture network. At the Forsberg Lake grid area, many faults have a sigmoidal shape with splayed ends

that curve toward the receding side (Fig. 70). Stone and Kamineni (1982) noted a conjugate set of dextral and sinistral transcurrent faults at this locality and concluded that faulting occurred in response to northwesterly compression.

The mineral infilling in some fractures is itself fractured, resulting in discontinuities that presently contain groundwater. These open fractures have the largest apertures within about 200 m of surface (Fig. 71) and contribute to significantly higher permeability near surface than at depth (Lee et al., 1983). The concentration of dissolved solids in groundwater increases downward (Fig. 72), which may reflect restricted groundwater circulation at depth.

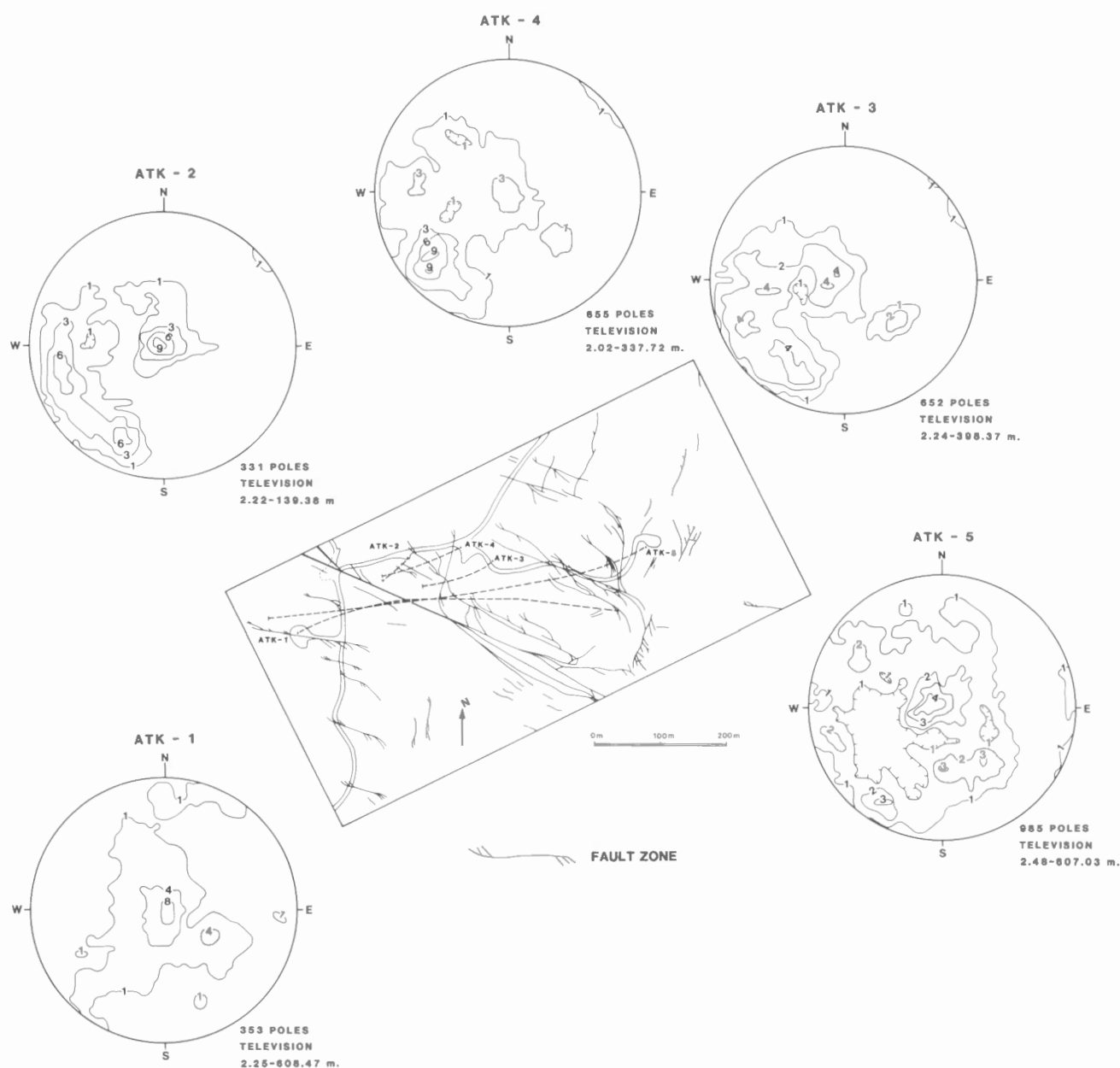


Figure 67. Location of boreholes ATK-1 to ATK-5 at the grid area (see Fig. 1) showing contoured diagrams (equal-area net, lower hemisphere projection) of poles to fractures.

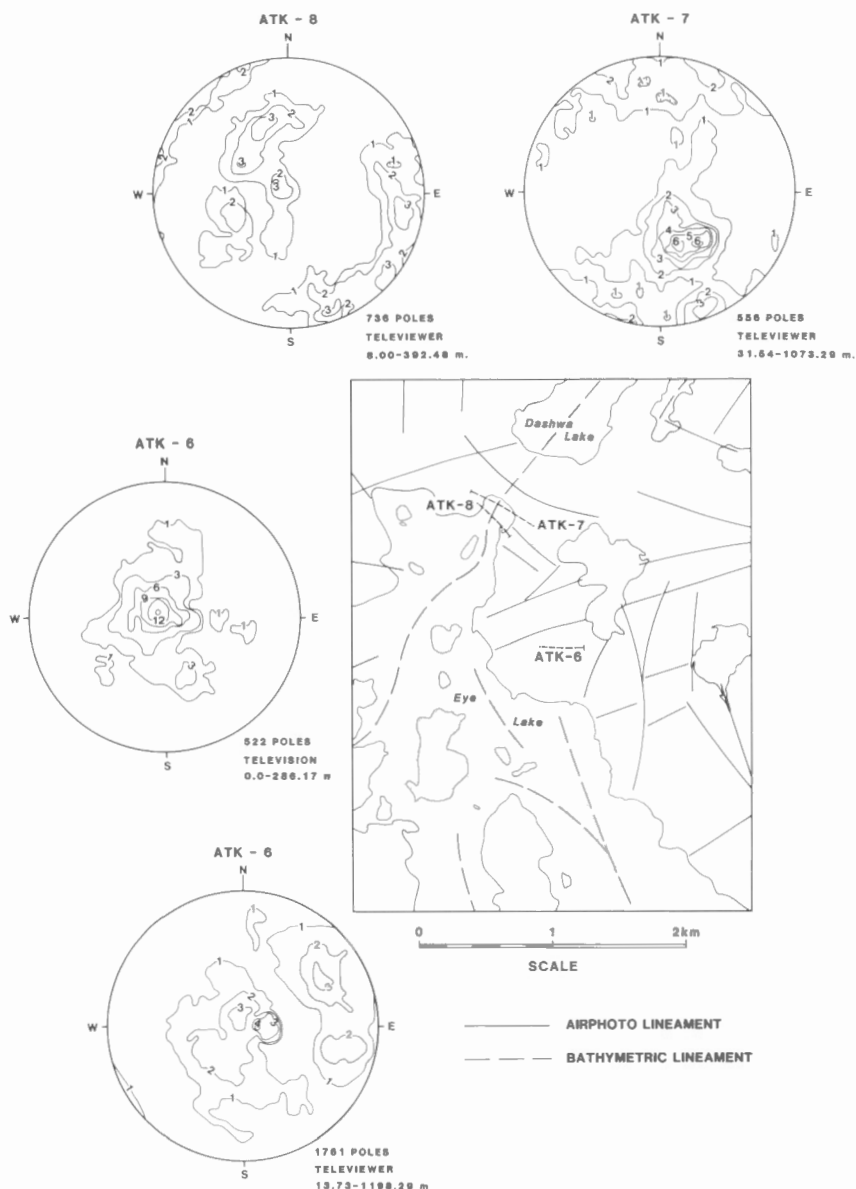
Fractures of the Eye-Dashwa pluton are classified according to their filling materials and crosscutting relations. Isotopic and fluid inclusion studies of the filling materials provide estimates for the age and temperature conditions during fracturing (Table 8). The oldest fractures were filled with magmatic material, including pegmatite, aplite, and hornblende-porphyry, at high temperatures shortly after emplacement of the granite. The Eye-Dashwa pluton was extensively fractured in the Early Proterozoic. Crosscutting and textural evidence discussed by Stone and Kamineni (1982) showed that these fractures were filled with epidote- and chlorite-dominated mineral assemblages at the time of fracturing. Rb-Sr dating of epidote indicates that the brittle deformation occurred at about 2300 Ma (Table 8). Epidote- and chlorite-filled fractures are pervasively distributed, both on surface and to depth (e.g. Fig. 69) and are the main elements of the present fracture network. Kamineni et al. (1990) proposed that these Early Proterozoic discontinuities

that are observed in outcrop and probably underlie most airphoto lineaments, are the product of a major brittle deformation event in the western Superior Province.

Renewed fracturing occurred at about 1100 Ma as indicated by diabase, adularia, and possibly gypsum fillings. These materials are relatively rare and imply mild deformation of the Eye-Dashwa pluton contemporaneous with rifting, volcanism, and mafic plutonism in the Lake Superior area (Stone et al., 1989).

Within about 200 m of surface and sporadically at deeper levels, epidote- and chlorite-filled fractures are rejuvenated, resulting in young discontinuities that contain either no filling (Fig. 71) or soft materials such as carbonate, iron oxides-hydroxides, and clay. The soft materials are stable only at low-temperature conditions such as have existed in the Eye-Dashwa pluton after the Early Proterozoic. They imply existence of a mechanism that has caused ancient sealed fractures to be broken open near surface.

Figure 68. Location of boreholes ATK-6 to ATK-8 showing contoured diagrams (equal-area net, lower hemisphere projection) of poles to fractures.



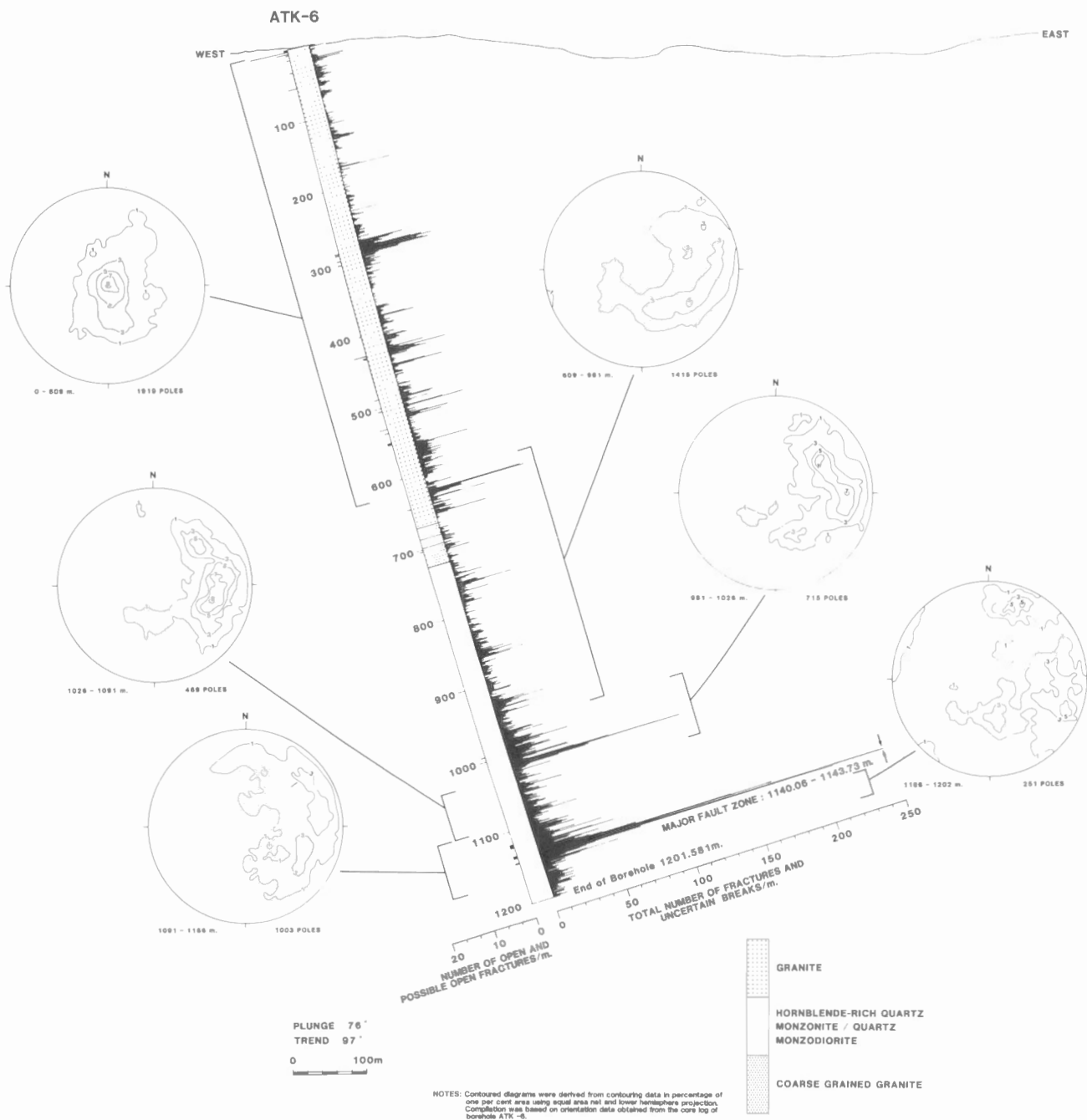


Figure 69. Total fractures, open and possibly open fractures, lithology, and fracture orientations in borehole ATK-6.

The rejuvenations could have occurred more-or-less continuously or in an unknown number of episodes since the Early Proterozoic. Although there are several varieties of carbonates, some of which are associated with early epidote, ^{14}C analyses (Table 8) show that other carbonates are only a few thousand years old. Kamineni and Stone (1983) noted that the young carbonate is coeval with retreat of the Laurentide ice sheet from the Atikokan area and may indicate that some low-temperature fractures originated during a supergene fracturing event associated with glacial loading/unloading.

METAMORPHISM

Mineral assemblages in rocks of the Atikokan area record metamorphic conditions ranging from subgreenschist to amphibolite facies. These data are described in terms of three major lithological subdivisions – metavolcanic rocks and tonalites and gneisses of the Wabigoon Subprovince and the Quetico metasediments.

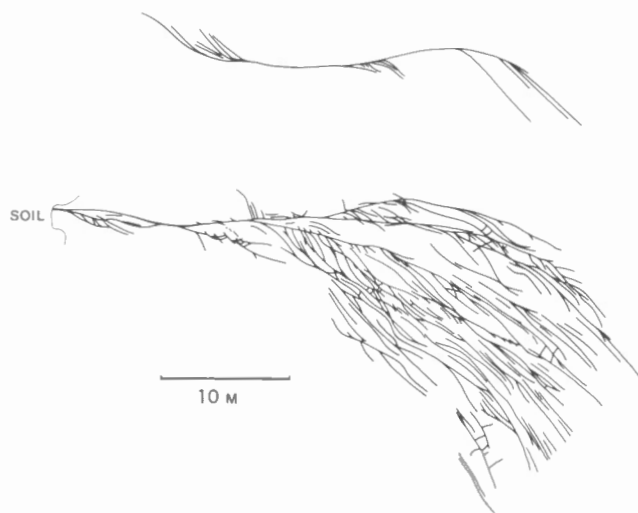


Figure 70. Surface traces of dextral faults with curved and splayed ends at the grid area (see Fig. 1).

Metavolcanic rocks (units 3a, 3b, 3c)

The metavolcanic units, including the Dismal Ashrock Formation (unit 3a) are folded, variably metamorphosed, and faulted. Chlorite-calcite-iron oxide assemblages are common in the Dismal Ashrock Formation, and actinolite and talc are present more commonly within the shear zones. The assemblages indicate greenschist facies conditions (Winkler, 1976).

The metavolcanic rocks within the core of the Steep Rock belt are characterized by epidote- and chlorite-bearing assemblages (epidote-chlorite-calcite-plagioclase of $An_{15-30} \pm$ actinolite). The sporadic occurrence of Ca-amphibole in this belt indicates that the metamorphic conditions vary from greenschist to epidote-amphibolite facies, but no meaningful pressure-temperature (P-T) gradients can be established with the available data. The margins of the metavolcanic belts, however, show a P-T gradient as evidenced by consistent occurrence of hornblende; hornblende replaces chlorite and actinolite that are present at a lower grade, i.e. in the central part of the belts. Such metamorphic gradients are well developed in the Finlayson metavolcanic belt where the grade increases from

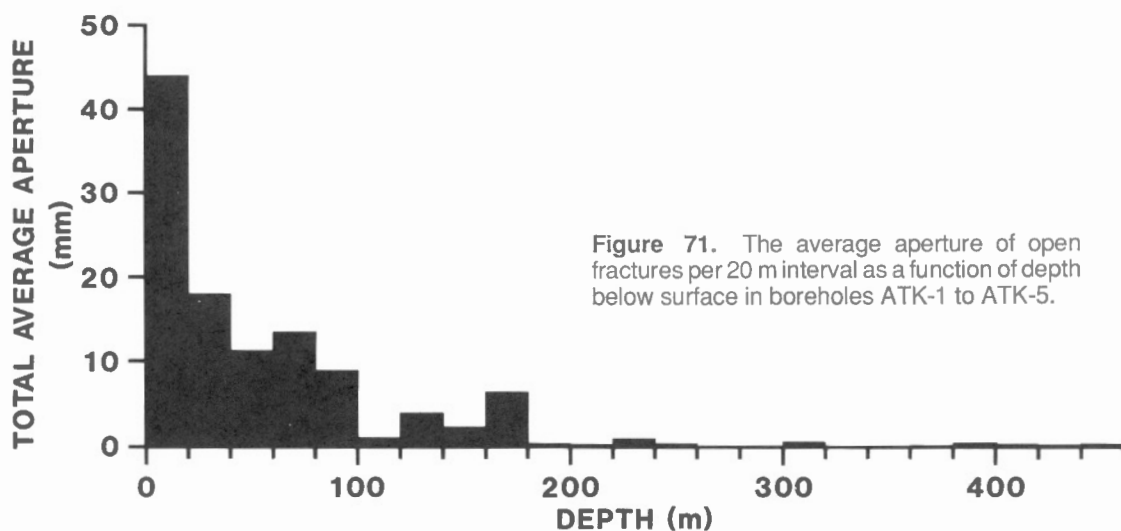


Figure 71. The average aperture of open fractures per 20 m interval as a function of depth below surface in boreholes ATK-1 to ATK-5.

Figure 72. Variation in composition of groundwater with depth in the Eye-Dashwa pluton.

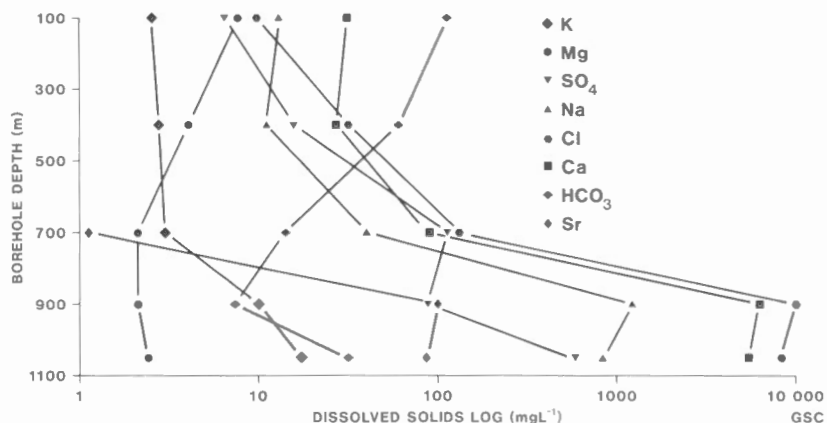


Table 8. Fracture groups in the Eye-Dashwa pluton

Fracture Filling Group	Fracture Filling (Age (Ma))	Temperature during emplacement (°C)	References
Pegmatite	2665.-2655.	650.-600.	Zartman and Kwak (1990)
Aplite	2655. \pm 31. (K-Ar, muscovite)	650.-600.	Kamineni and Stone (1983), Stone and Kamineni (1982)
Hornblende-porphry	2487. \pm 72. (K-Ar, hornblende)	650.-600.	Kamineni and Stone (1983)
Epidote	2308. \pm 155. (Rb-Sr)	330.-260.	Peterman et al. (1985), Kerrick and Kamineni (1985)
Chlorite-Prehnite	2308.-0.	320.-250.	Kerrick (1984)
Carbonate	2308.-.01 (Lower Limit by ^{14}C)	270.-240.*	Kamineni and Stone (1983), Kerrick (1984)
Iron Oxides	2308.-0.	230.-140. (hematite)	Kerrick (1984)
Diabase	1138. \pm 27. (K-Ar, whole rock)	—	Kamineni and Stone (1983)
Adularia	1100. \pm 3. (Ar-Ar)	210.-140.	D. York, University of Toronto, pers. comm., Kerrich (1984)
Gypsum	Precambrian (sulphur isotope)	50.	Kamineni (1983), Kerrick (1984)
Clay	<2. (oxygen isotope)	<100.	Kerrick (1984), Kerrick and Kamineni (1985)
* The temperature range is for vein-filling calcite as determined by fluid inclusion and oxygen isotope techniques (Kerrick, 1984) but other carbonate, such as occurs in glacial induced chattermarks, must have formed at temperatures below 100°C.			

lower greenschist facies at the long axis to epidote-amphibolite facies at the northwestern and southeastern margins. The former margin merges with the Hardtack pluton while the latter is juxtaposed with the Diversion stock (Fig. 9; Map 1666A).

The thin metavolcanic units in the gneisses contain the assemblage hornblende-plagioclase (An_{35-40})- biotite-ilmenite±sphen indicating metamorphism of the gneissic areas under amphibolite conditions.

Some postmetamorphic alteration is present in the metavolcanic rocks. For example, Smith (1942) noted limonite and goethite in the Jolliffe Ore Zone Formation and considered these minerals to be low-temperature alteration products. This view was supported by Shklanka (1972), Kimberly and Sorbara (1976), and Wilks (1986). Accordingly, metamorphic grade varies considerably within the metavolcanic areas. Amphibolite facies adjacent to the gneisses and felsic intrusions gives way to greenschist facies throughout interiors of the metavolcanic belts, which are locally altered to subgreenschist facies.

Tonalites and gneisses (units 1a, 1b, 1c, 1d, 6)

The tonalites and gneisses are well foliated by an alignment of platy and prismatic minerals. Quartz and feldspar, in some instances, show strong dimensional orientation and suggest that the tonalites and gneisses have undergone varying degrees of deformation.

The most common assemblage is quartz- plagioclase-potassium feldspar-biotite-hornblende- sphen- apatite-opaques (ilmenite and magnetite). Muscovite, chlorite, and epidote are locally present as retrograde phases after feldspars, biotite, and hornblende. Garnet is noted in a few outcrops of mafic tonalite gneiss.

Temperatures and pressures of metamorphism are estimated using the two-feldspar geothermometers of Whitney and Stormer (1977) and the total Al in the hornblende geobarometer of Hammarstrom and Zen (1986). The compositions of coexisting potassium-feldspar and plagioclase in "old" tonalite, mafic tonalite, tonalite gneiss, and "young" tonalite were determined by microprobe

Table 9. Microprobe analyses of feldspars

"Old" Tonalite 3-208-1			Mafic Tonalite 06-04-1		Tonalite Gneiss 06-160-1		"Young" Tonalite 58-98-2A	
	K-spar	plag.	K-spar	plag.	K-spar	plag.	K-spar	plag.
SiO ₂	65.19	59.80	64.95	59.63	64.75	61.21	65.11	61.00
Al ₂ O ₃	19.02	26.07	19.05	26.22	19.25	24.62	19.12	25.07
Na ₂ O	2.66	7.13	2.92	6.68	3.15	7.89	3.08	7.51
CaO	0.27	7.48	0.56	7.84	0.75	5.96	0.78	6.22
K ₂ O	12.93	0.19	12.78	0.07	12.33	0.13	12.50	0.12
Total	100.07	100.67	100.26	100.44	100.23	99.81	100.59	99.92
Formulae (Based on 32 Oxygens)								
Si	11.912	10.581	11.861	10.542	11.842	10.882	11.858	10.779
Al	4.097	5.438	4.100	5.504	4.145	5.142	4.116	5.221
	16.009	16.019	15.961	16.046	15.987	16.024	15.974	16.000
Na	0.942	2.446	1.090	2.289	1.084	2.721	1.033	2.712
Ca	0.053	1.419	0.102	1.486	0.130	0.136	0.146	1.197
K	3.013	0.042	2.943	0.017	2.865	0.030	2.900	0.028
	4.008	3.907	4.135	3.792	4.079	3.887	4.079	3.937
Ab	23.50	62.61	26.36	60.36	26.56	70.00	25.35	68.88
An	1.32	36.32	2.46	39.19	3.80	29.23	3.55	30.40
Or	75.18	1.07	71.18	0.45	70.24	0.77	71.10	0.71
T°C	728		712		658		672	

analysis (Table 9). Temperature estimates calculated from the two-feldspar geothermometers range from 658 to 728°C. The compositions of calcic amphiboles are listed in Table 10 together with the estimated pressures that range from 505 to 641 MPa. Samples having the highest temperature estimates also yielded the highest pressures, indicating amphibolite facies conditions.

Quetico metasediments (unit 4a)

The Quetico metasediments are characterized by a southward increasing metamorphic grade (Pirie and Mackasey, 1978; Percival and Stern, 1984). The lowest metamorphic grade occurs adjacent to the Wabigoon-Quetico subprovince boundary and is characterized by an assemblage of chlorite-sericite±biotite±carbonate±epidote. Biotite is identified mostly in thin sections (Johnson, 1987), and

calcium-rich layers in the metasediments contain actinolite, hornblende, and epidote. Mineral isograds, defining the first appearance of biotite visible in hand specimens followed by amphibole and garnet, trend approximately east (see Map 1666A).

The appearance of biotite is accompanied by a decrease in chlorite, suggesting that the biotite formed from the breakdown of chlorite. Similar inverse relations between chlorite and biotite were noted by Pirie and Mackasey (1978) in other parts of the Quetico Subprovince, and by Ramsay and Kamineneni (1977) in metasediments of the Slave Province.

Calcium-rich amphibole, showing the optical characteristics of hornblende, appears about 4.5 km south of the Quetico boundary. The randomly oriented amphibole needles are restricted to certain sedimentary layers possibly reflecting a compositional control on their growth.

The garnet zone represents the highest grade within metasediments of the area and contains the following assemblages:

biotite-garnet,
biotite-garnet-staurolite,
biotite-garnet-andalusite-staurolite, and
biotite-garnet-Ca amphibole.

Quartz and plagioclase are ubiquitous in all assemblages. Muscovite is noted in most thin sections. Ilmenite, rutile, and apatite are present as accessory minerals.

Garnet-biotite pairs were analyzed using an electron microprobe and their formulae recalculated (Table 11). The formulae cations were used to calculate the following ratios for garnet (Ga) and biotite (Bi):

$$\begin{array}{cc} \text{Garnet} & \text{Biotite} \\ X_{Fe}^{Ga} = Fe / (Fe + Mg) & X_{Fe}^{Bi} = Fe / (Fe + Mg) \\ X_{Mg}^{Ga} = Mg / (Fe + Mg) & X_{Mg}^{Bi} = Mg / (Fe + Mg) \end{array}$$

The ratios for garnet and biotite were used to determine K_D values where

$$K_D = \frac{(X_{Mg}^{Ga})}{(X_{Fe}^{Ga})} \frac{(X_{Fe}^{Bi})}{(X_{Mg}^{Bi})}$$

is derived from the exchange reaction:



The above exchange reaction has been calibrated empirically, based on field data (Thompson, 1976; Goldman and Albee, 1977; Perchuk, 1977; Indares and Martignole, 1985), and by experimental studies (Ferry and Spear, 1978; Perchuk and Lavrent'eva, 1983).

The chemical analyses (Table 11) indicate significant concentrations of Mn in garnet. Garnets show normal zoning with Mn concentrated in the cores and depleted at the rims. Sample Q10 has the opposite, reversely zoned trend. Hollister (1966) and Harte and Henley (1966) attributed such reverse zonation as in Q10, to slow growth of garnet coupled with a steady state diffusion of Mn toward the rim. Birk (1973) interpreted reversely zoned garnets in metasediments at Kashabowie (135 km east of Atikokan) as a consequence of retrograde metamorphism, which caused resorption of the original garnet rims and inward migration of Mn. The interpretation of Birk (1973) is favoured here, since sample Q10 shows the following evidence of retrograde metamorphism: (1) the garnet appears annealed due to embayment of quartz grains; (2) some garnet grains have reaction rims with chlorite; and (3) chlorite locally overgrows biotite. Accordingly, sample Q10 may represent a nonequilibrium assemblage. For the remaining garnets that

are normally zoned, rim analyses are used for temperature calculations because they contain less Mn, which has minimal effect on Mg-Fe solution.

Table 10. Microprobe analyses of calcic amphiboles

	"Old" Tonalite 3-208-1	Mafic Tonalite 06-04-1	Tonalite Gneiss 06-160-1	"Young" Tonalite 58-98-2A
SiO ₂	42.88	42.93	43.19	42.80
Al ₂ O ₃	12.19	10.58	9.91	10.06
TiO ₂	0.72	1.18	0.86	1.01
Fe ₂ O ₃ *	4.34	4.63	4.31	4.81
FeO	13.48	11.18	15.18	14.89
MnO	0.40	0.18	0.19	0.32
MgO	9.54	12.15	9.95	9.51
CaO	12.00	11.80	12.36	11.82
Na ₂ O	1.47	1.90	1.13	1.52
K ₂ O	0.68	1.11	1.15	1.33
Total	97.70	97.64	98.23	98.07
Formulae (Based on 23 Oxygens)				
Si	6.466	6.392	6.452	6.456
Al	1.533	1.608	1.548	1.544
	8.000	8.000	8.000	8.000
Al	0.521	0.249	0.237	0.305
Ti	0.080	0.132	0.097	0.113
Fe ³⁺	0.495	0.518	0.499	0.550
Fe ²⁺	1.755	1.391	1.926	1.876
Mn	0.052	0.023	0.025	0.041
Mg	2.108	2.697	2.216	2.121
	5.001	5.011	5.000	5.006
Ca	1.897	1.883	1.979	1.896
Na	0.103	0.117	0.021	0.104
	2.000	2.000	2.000	2.000
Na	0.318	0.433	0.306	0.337
K	0.128	0.210	0.220	0.262
	0.446	0.643	0.526	0.599
Pressure (MPa)	641.	540.	505.	538.
* Fe ₂ O ₃ is calculated from FeO (total) by adjustment of total cations (excluding Ca, Na, and K) in the T and C sites to 5 and 8 respectively, using the method of Leake (1978).				

Table 11. Recalculated formulae for garnet and biotite

Sample number	Q6-1	Q9	Q9	Q9	Q10	Q10	40-115	40-115
Garnet (atomic proportions)								
	average	centre	half	rim	core	rim	rim	core
Si	5.883	5.926	6.001	5.980	5.923	5.927	5.926	5.9411
Ti	0.023	0.010	0.010	0.018	0.005	0.010	0.000	0.0097
Al	3.884	3.966	3.900	3.910	4.018	3.905	3.994	3.9274
Cr	0.012				0.000	0.000	0.000	0.0000
Fe	2.614	3.241	3.343	3.451	4.001	4.073	4.484	4.2840
Mn	2.088	1.604	1.524	1.396	0.909	1.141	0.743	0.8366
Mg	0.275	0.350	0.304	0.315	0.429	0.476	0.619	0.6301
Ca	1.367	0.983	0.957	0.975	0.778	0.579	0.239	0.3831
Na	0.000	0.000	0.000	0.000	0.000	0.000	0.141	0.1366
K	0.000	0.000	0.000	0.000	0.000	0.000	0.003	0.0102
$X_{\text{Ga}}^{\text{Mg}}$	0.095	0.097	0.083	0.084	0.097	0.105	0.120	0.128
Biotite (atomic proportions)								
Si	5.483	5.571	5.571	5.571	5.411	5.411	5.448	5.4478
Ti	0.280	0.271	0.271	0.271	0.242	0.242	0.200	0.2003
Al	2.915	3.021	3.021	3.021	3.185	3.185	3.211	3.2107
Fe	2.716	2.539	2.539	2.539	2.590	2.590	2.540	2.5401
Mn	0.053	0.018	0.018	0.018	0.035	0.035	0.006	0.0059
Mg	2.309	2.257	2.257	2.257	2.312	2.312	2.367	2.3667
Ca	0.046	0.018	0.018	0.018	0.038	0.038	0.006	0.0064
Na	0.104	0.100	0.100	0.100	0.101	0.101	0.099	0.0987
K	1.817	1.805	1.805	1.805	1.786	1.786	1.838	1.8382
$X_{\text{Bi}}^{\text{Mg}}$	0.459	0.471	0.471	0.471	0.472	0.472	0.482	0.4817

The temperatures calculated from various geothermometers range between 419 and 577°C (see Table 12). Samples Q6-1, Q9, Q10, and 40-115 represent a prograde sequence located progressively farther from the garnet isograd. With the exception of sample Q6-1, the estimated temperatures increase progressively through the sequence. Sample Q6-1 probably deviates from the normal prograde sequence because it is amphibole-bearing and the

garnet is unusually rich in MnO (~15%) and CaO (~5%). From this it appears that none of the calibrated garnet-biotite geothermometers can correct adequately for these components, especially when they are present in extremely high concentrations as in sample Q6-1.

High Mn in garnet has the effect of reducing the K_D value, resulting in low temperatures (Kretz, 1959; Saxena, 1968; Goldman and Albee, 1977). The geothermometer of Ferry

Sample	Q6-1	Q9 centre	Q9 half	Q9 rim	Q10 core	Q10 rim	40-115 rim	40-115 core
1	428	419	420	422	457	451	509	503
2	506	472	473	474	504	500	525	529
3	550	519	517	518	537	532	564	566
4	572	485	481	476	466	460	461	476
5	577	544	544	545	556	550	546	554
6	526	500	501	502	536	531	541	553

1. Ferry and Spear (1978)
2. Hodges and Spear (1982)
3. Ganguly and Saxena (1985)

4. Indares and Martignole (1985)
5. Perchuk et al. (1985)
6. Hoinkes (1986)

Six garnet-biotite geothermometers – (1) Ferry and Spear (1978), (2) Hodges and Spear (1982), (3) Ganguly and Saxena (1985), (4) Indares and Martignole (1985), (5) Perchuk et al. (1985) and (6) Hoinkes (1986) – are utilized here. The geothermometers indicate upper greenschist facies conditions of metamorphism of the Quetico metasedimentary rocks with temperature estimates in the order of 450 to 550°C (Table 12).

$$3CaAl_2Si_2O_8 = Ca_3Al_2Si_3O_{17} + 2Al_2SiO_5 + SiO_2.$$

respectively (Table 13). These data indicate either that uplift occurred during garnet growth or that the garnet rim pressure determination is lower than the actual pressure of equilibrium, and the pressure for the garnet core is an overestimate. In either case, the garnet zone of the Quetico metasediments was probably formed at a median pressure of about 3.5 kb (350 MPa).

The lithological units of the Atikokan area contain mineral assemblages characteristic of their bulk chemical composition and the P-T conditions of metamorphism. All rocks, with the exception of late synkinematic granite plutons and the gabbro dykes (units 8c, 9), show evidence of metamorphism.

Lowest metamorphic grade occurs in the cores of large supracrustal belts, which include metavolcanic belts and clastic metasediments of the northern Quetico Subprovince. These belts are metamorphically zoned and show increased metamorphic grade toward intrusive gneisses and plutons at belt margins. A notable exception is the eastern Steep Rock belt, which contains greenschist assemblages at the unconformable contact with the Marmion batholith.

A pattern of metamorphic zonation was documented by Ayres (1978) in the Setting Net Lake and Muskrat Dam Lake metavolcanic belts of the Sachigo Subprovince. The greenschist facies cores of metavolcanic belts at these localities were interpreted to grade laterally and vertically downward into amphibolite facies. Ayres (1978) noted that the metamorphic zonation transects both stratigraphic and structural trends and must be a relatively late feature, which he attributed to the effects of contact metamorphism by granite batholiths (amphibolite-facies rims of belts) superimposed on regional burial metamorphic assemblages.

Table 13. Geobarometer data for section 40-115-1

	plagioclase				garnet	
weight percent	garnet contact	garnet contact	matrix	average	rim	core
SiO ₂	62.30	60.47	61.20	61.32	36.63	37.02
TiO ₂	0.00	0.00	0.00	0.00	0.00	0.08
Al ₂ O ₃	24.33	25.15	24.22	24.57	20.94	20.76
Cr ₂ O ₃				0.00	0.00	0.00
FeO	0.14	0.28	0.14	0.19	33.14	31.91
MnO	0.00	0.00	0.00	0.00	5.42	6.16
MgO	0.00	0.00	0.00	0.00	2.57	2.64
CaO	4.98	6.43	5.27	5.56	1.38	2.23
Na ₂ O	7.88	7.20	8.38	7.82	0.45	0.45
K ₂ O	0.05	0.10	0.10	0.08	0.02	0.05
Formula Cations						
Si	11.03	10.78	10.93	10.91	5.93	5.94
Ti	0.00	0.00	0.00	0.00	0.00	0.01
Al	5.08	5.28	5.10	5.15	3.99	3.93
Cr	0.00	0.00	0.00	0.00	0.00	0.00
Fe	0.03	0.04	0.03	0.03	4.48	4.28
Mn	0.00	0.00	0.00	0.00	0.74	0.84
Mg	0.00	0.00	0.00	0.00	0.62	0.63
Ca	0.94	1.23	1.01	1.06	0.24	0.38
Na	2.71	2.49	2.90	2.70	0.14	0.14
K	0.01	0.02	0.02	0.02	0.00	0.01
X _{Ca}	0.26	0.33	0.26	0.28	0.03924	0.06246
K _D (rim)	0.14					
Ln K _D (rim)	-5.92					
K _D (core)	0.01					
Ln K _D (core)	-4.52					
P (rim) (bars)	2290	(229. MPa)				
P (rim) (bars)	4276	(427.6 MPa)				
formula cations based on 24 oxygens/unit cell for garnet and 22 oxygens/unit cell of biotite, recalculated following the method of Deer et al. (1966).						

(greenschist-facies cores of belts). Percival (1989) offered a comparable model for metamorphic effects at the central axis of the Quetico Subprovince. A postsubduction heating event produced granites that were emplaced into metasediments at higher structural levels and caused widespread low-pressure, high-temperature metamorphism. This may explain the trend of southward increasing metamorphic grade in the present area that lies on the northern flank of the central plutonic segment of the Quetico.

CONCLUSIONS

Supracrustal rocks

Broad subdivisions of supracrustal rocks at Atikokan include early platformal sediments, volcanic extrusions, and syn- to postvolcanic sediments. The early clastic-, carbonate-, and iron-bearing lithologies were laid down in a restricted, shallow-water environment on sialic rocks. Volcanic detritus is not recognized in the early clastic sediments and geochemical evidence suggests a dominantly tonalitic provenance.

Three lithologically and chemically distinct volcanic units include ultramafic (komatiitic) pyroclastics succeeded by mafic pillow lavas and flows, tuffs, and breccias of intermediate to felsic mineralogy. The early komatiites have unusual chemical characteristics for ultramafic rocks (e.g. LREE enrichment) and an unusual mode of occurrence (tuffaceous). The latter may be due to phreatomagmatic eruption.

Mafic volcanism was dominantly submarine and may have initiated as fissure eruptions that subsequently became concentrated in central vents such as in the western Steep Rock belt. The flat REE patterns are consistent with an origin by fractional crystallization of a more primitive high magnesium number basalt. LREE enrichment and certain trace element abundances argue against an origin of the intermediate to felsic metavolcanics by single-stage fractionation of the tholeiites. Magma mixing or assimilation/contamination processes are preferred.

Syn- to postvolcanic sediments include sporadic avalanche and alluvial fan-fluvial facies deposits that appear to be derived mainly by erosion of nearby volcanic edifices and elevated felsic plutonic sources. Distal resedimented (turbidite) facies assemblages occur in small units within the metavolcanic belts and extensively in the Quetico Subprovince. Clast lithologies and chemical characteristics show a source of mainly intermediate to felsic volcanic material and tonalite and a lesser component of mafic volcanic detritus.

Felsic intrusive rocks

Complex evolution in the composition and origin of felsic magmas took place during the 300 Ma period of active plutonism at Atikokan. The pre- to synvolcanic tonalites are depleted in K_2O and have REE geochemistry consistent with

melting of a pyroxene granulite of tholeiitic composition (possibly ancient supracrustal rocks) leaving an eclogite residue.

Syn- to postvolcanic intrusions are marked by enrichment in K_2O and compositions that range from tonalite through granodiorite to granite. Several late plutons are zoned with quartz monzodiorite rims and granodiorite/granite cores.

REE patterns with slight negative Eu anomalies in intermediate age tonalites such as the Righteye pluton imply a component of recycled crust in the source. Late, zoned plutons, such as the Eye-Dashwa pluton, lack Eu anomalies and are enriched in LREE and Sr. This implies a two-stage evolution: (1) formation of quartz monzodiorite from an LREE-enriched mantle; and (2) subsequent melting of the quartz monzodiorite and extraction of a mafic residue to give the granodiorite/granite phases.

Stratigraphy

The Steep Rock belt hosts a rare example of Archean supracrustal sequences unconformably overlying sialic basement of 3000 Ma age. The Steep Rock Group consists of discontinuous conglomerate and sandstone (Wagita Formation) at the unconformity overlain, in turn, by limestone beds (Mosher Carbonate Formation), goethite-bearing ironstones (Jolliffe Ore Zone Formation), and komatiitic pyroclastic rocks (Dismal Ashrock Formation). Total thickness of the Steep Rock Group is about 1000 m.

Most of the Steep Rock and neighbouring belts are composed of pillowed mafic flows with a lesser component of intermediate to felsic, commonly tuffaceous metavolcanic rocks and metasediments. The stratigraphic relationship of the Steep Rock Group to these contiguous rocks is unclear due to the tectonized and poorly exposed nature of their mutual contacts.

The available structural data suggest that the mafic flows are succeeded by intermediate to felsic extrusions; however, stratigraphy of the belts may be complicated by conformable faults and depositional time gaps of up to 300 Ma. Quetico sediments were deposited at about 2695 Ma and appear to postdate known volcanism at other localities along the southern margin of the Wabigoon Subprovince by about 20 Ma.

Structure

The east-trending Quetico-Wabigoon boundary separates turbidites on the south from mainly volcanic rocks to the north and is a first order lithostructural feature in the map area. Regional juxtaposition of the contrasting lithologies has been attributed to subduction-related accretion of the Quetico sedimentary prism against the Wabigoon volcanic arc about 2695 Ma ago.

Quetico metasediments have pervasive easterly structural trends and isoclinal, mainly east-facing folds possibly generated by strong dextral transpression after accretion.

In contrast, the Wabigoon Subprovince shows megascopic oval structures defined by concentrically zoned structural trends in gneisses and supracrustal rocks that envelope felsic plutons. Metavolcanic belts are situated between some oval structures. This structural pattern may have originated due to rise of granites and gneisses in central parts of oval structures attendant with slumping of dense overlying supracrustal rocks into marginal troughs (metavolcanic belts).

The axes of six major folds extend along the central Finlayson belt whereas the Steep Rock belt shows fewer folds and a thick east-younging sequence of pillow lavas that may be a deformed lava cone. The Perch belt shows severe, fold-dominated deformation.

A complex system of oblique-slip and normal faults and metagabbro dykes transect the Marmion batholith. The dip-slip, probably reverse displacement Samuel fault appears to have uplifted a segment of the batholith into the central Steep Rock belt. Displacements of reverse sense are also likely to have occurred on the Atikokan fault, which is conformable with the upper ashrock contact in the Steep Rock Mine area. Mapping failed to identify clear evidence of a major transcurrent fault in the vicinity of the Quetico-Wabigoon boundary.

The Eye-Dashwa pluton was subjected to northwesterly horizontal compression that generated extensive fractures dominated by a conjugate set of transcurrent faults in the Early Proterozoic. A regional network of lineaments probably formed at the same time. The top section (down to 200 m depth) of the Proterozoic fracture network was the locus of an unknown number of subsequent rejuvenations. These rejuvenations caused existing discontinuities to be reopened and significantly affect the strength and permeability of the rock.

Metamorphism

Supracrustal belts of the Atikokan area are metamorphically zoned. Metavolcanic belts have greenschist assemblages at their cores (chlorite-epidote-plagioclase-calcite±actinolite) and amphibolite assemblages at the margins (hornblende-plagioclase-biotite-ilmenite-sphene). Metamorphic grade does not change abruptly at the Quetico-Wabigoon boundary but increases steadily southward as defined by biotite, Ca-amphibole, garnet, and staurolite isograds. Pressure-temperature conditions in the garnet zone of Quetico metasediments fall in the upper greenschist facies ($P \approx 230\text{--}430$ MPa, $T \approx 419\text{--}577^\circ\text{C}$).

Except for greenschist assemblages in the Marmion batholith adjacent to the Steep Rock belt, tonalites and gneisses show amphibolite conditions ($P=560$ MPa, $T=700^\circ\text{C}$).

The high metamorphic grade of gneisses within oval structures is attributed to their having risen from deeper crustal levels, as well as proximity to felsic plutons. Thermal anomalies associated with oval structures and plutons, superimposed on regional burial metamorphism, may be responsible for the metamorphic zonation of supracrustal belts.

ACKNOWLEDGMENTS

The authors would like to acknowledge the assistance provided by many people during four seasons of field work. These include R.H. Thivierge, J. Pseutka, J. Misiura, G.F.D. McCrank, P.A. Brown, N. Rey, G. Vincent, B. Zayachivsky, W. Neely, M. Carter, J. Schnessl, B. Shanks, M. Forrester, M. Beckett, S. Dawson, G. Butler, J. Coderre, and P. Johnson. M. Wilks also assisted with geological mapping on the Steep Rock Group as part of M.Sc. research at the University of Saskatchewan. G. Carmichael, R. Buchanan, and C. Gougeon provided cartographic services.

Ray Bernatchez, consulting geologist, and staff of the Atikokan Museum provided maps, reports, and photographs related to iron mining at Steep Rock Lake. R.A. Gibb, Geophysics Division of the Geological Survey of Canada, provided unpublished gravity data for construction of Section B-B'-B'' (Map 1666A). Staff of Cartographic Services, the Analytical Chemistry Section, and the Word Processing Centre of the Geological Survey of Canada are thanked for their assistance. Don Davis of the Royal Ontario Museum kindly provided unpublished geochronological data. Reviews by S. Tella, H. Williams, and K. Card and editing by C. Davison, and staff of A.E.C.L. Technical Information Services considerably improved the text.

REFERENCES

- Adams, F.D., Bell, R., Lane, A.C., Leith, C.K., Miller, W.G., and Van Hise, C.R.
1905: Report of the special committee for the Lake Superior Region; *Journal of Geology*, v. 13, p. 89-104.
- Anetevs, E.
1951: Glacial clays in Steep Rock Lake, Ontario, Canada; *Geological Society of America Bulletin*, v. 62, no. 10, p. 1223-1262.
- Arndt, N.T. and Nisbet, E.G.
1982: What is a komatiite? in *Komatiites*, edited by N.T. Arndt and E.G. Nisbet, George Allen and Unwin, London, p. 19-27.
- Arndt, N.T., Naldrett, A.J., and Pyke, D.R.
1977: Komatiitic and iron-rich tholeiitic lavas of Munro Township, northeast Ontario; *Journal of Petrology*, v. 18, p. 319-369.
- Arth, J.G.
1976: Behaviour of trace elements during magmatic processes — a summary of theoretical models and their applications; *Journal of the United States Geological Survey*, v. 4, p. 41-47.
- Arth, J.G. and Hanson, G.N.
1972: Quartz diorites derived by partial melting of eclogite or amphibolite at upper mantle depths; *Contributions to Mineralogy and Petrology*, v. 37, p. 161-174.
- 1975: Geochemistry and origin of the early Precambrian crust of northeastern Minnesota; *Geochimica et Cosmochimica Acta*, v. 39, p. 325-362.
- Ayres, L.D.
1978: Metamorphism in the Superior Province of northwestern Ontario and its relationship to crustal development; in *Metamorphism in the Canadian Shield*, edited by J.A. Fraser and W.W. Heywood; Geological Survey of Canada, Paper 78-10, p. 25-36.
- Bau, A.
1979: History of regional deformation of Archean rocks in the Keshabowic Lake — Lac des Mille Lac area, northwestern Ontario; Ph.D. thesis, University of Toronto, Toronto, Ontario.
- Bell, R.
1873: Report on the country between Lake Superior and Lake Winnipeg; Geological Survey of Canada, Report of Progress, p. 87-111.
1882: Report on the geology of the Lake of the Woods and adjacent country; Geological Survey of Canada, Report of Progress, pt. C, p. 11-15.

- Birk, D.**
1973: Chemical zoning in garnets of the Kashabowie Group, Shebandowan, Ontario; *Canadian Mineralogist*, v. 12, p. 124-128.
- Birk, D. and McNutt, R.H.**
1981: Geochronology of Wabigoon belt granitoids, northwestern Ontario. Rb/Sr isochrons for seven late-tectonic plutons; *Canadian Journal of Earth Sciences*, v. 18, p. 157-175.
- Blackburn, C.E., Bond, W.D., Breaks, F.W., Davis, D.W., Edwards, G.R., Poulsen, K.H., Trowell, N.F., and Wood, J.**
1985: Evolution of Archean volcanic-sedimentary sequences of the western Wabigoon Subprovince and its margins: a review; in *Evolution of Archean Supracrustal Sequences*, edited by L.D. Ayres, P.C. Thurston, K.D. Card, and W. Weber, Geological Association of Canada, Special Paper 28, p. 89-116.
- Borradaile, G.J.**
1982: Comparison of Archean structural styles in two belts of the Canadian Superior Province; *Precambrian Research*, v. 19, p. 179-189.
- Borradaile, G., Sarvas, P., Dutka, R., Stewart, R., and Stuble, M.**
1988: Transpression in slates along the margin of an Archean gneiss belt, northern Ontario – magnetic fabrics and petrofabrics; *Canadian Journal of Earth Sciences*, v. 25, p. 1069-1077.
- Brant, A.**
1939: Geophysical work at Steeprock Lake, 1938-39; *Canadian Mining Journal*, v. 61, p. 573-574.
- Brooks, C. and Hart, S.R.**
1974: On the significance of komatiite; *Geology*, v. 2, p. 107-110.
- Brown, G.C. and Fyfe, W.S.**
1970: Production of granitic melts during ultrametamorphism; *Contributions to Mineralogy and Petrology*, v. 28, p. 310-318.
- Brown, P.A., Kaminen, D.C., Stone, D., and Thivierge, R.H.**
1980: General geology of the Eye-Dashwa Lakes pluton, Atikokan, northwestern Ontario; in *Current Research, Part A*, Geological Survey of Canada, Paper 80-1A, p. 379-384.
- Bursnall, J.T., Nisbet, E.G., and Shrad, C.H.**
1988: Structural relationship between Steep Rock Group and contiguous mafic metavolcanics, NW Ontario; *Geological Association of Canada, Program with Abstracts*, v. 13, p. A15.
- Card, K.D. and Ciesielski, A.**
1986: DNAG No. 1. Subdivisions of the Superior Province of the Canadian Shield; *Geoscience Canada*, v. 13, p. 5-13.
- Carmichael, D.M.**
1978: Metamorphic bathozones and bathograds: a measure of depth of post-metamorphic uplift and erosion on the regional scale; *American Journal of Science*, v. 278, p. 769-797.
- Cerny, P., Fryer, B.J., Longstaffe, F.J., and Tammemagi, H.Y.**
1987: The Archean Lac du Bonnet batholith, Manitoba: igneous history, metamorphic effects, and fluid overprinting; *Geochimica et Cosmochimica Acta*, v. 51, p. 421-438.
- Coleman, A.P.**
1988: Clastic Huronian rocks of western Ontario; *Geological Society of America Bulletin*, v. 9, p. 223-238.
- Compston, P.**
1978: Rare earth evidence for the origin of the Nuk gneisses Buksefjorden region, southern West Greenland; *Contributions to Mineralogy and Petrology*, v. 66, p. 283-293.
- Corfu, F. and Andrew, A.J.**
1987: Geochronological constraints on the timing of magmatism, deformation, and gold mineralization in the Red Lake greenstone belt, northwestern Ontario; *Canadian Journal of Earth Sciences*, v. 24, p. 1302-1320.
- Cowan, W.R. and Sharpe, D.R.**
1988: Character and origin of the Hartman, Eagle Finlayson and Lac Seul moraines, Dryden area, northwestern Ontario, Canada; *Geological Association of Canada, Program with Abstracts*, v. 13, p. A27.
- Cullers, R.L. and Garf, J.L.**
1984: Rare earth elements in igneous rocks of the continental crust: predominantly basic and ultrabasic rocks; in *Rare Earth Element Geochemistry, Developments in Geochemistry 2*, edited by P. Henderson, Elsevier, Amsterdam, p. 237-274.
- Davis, D.W.**
1988: Are Archean greenstone belts the product of rifting or subduction? New evidence from geochronology in the Wabigoon Subprovince, N.W. Ontario; *Geological Association of Canada, Program with Abstracts*, v. 13, p. A30.
- Davis, D.W. and Edwards, G.R.**
1986: Crustal evolution of Archean rocks in the Kakagi Lake area, Wabigoon Subprovince, Ontario, as interpreted from high precision U-Pb geochronology; *Canadian Journal of Earth Sciences*, v. 23, p. 182-192.
- Davis, D.W. and Jackson, M.C.**
1985: Preliminary U-Pb zircon ages from the Lumby Lake-Marmion Lake area, Districts of Kenora and Rainy River; in *Summary of Field Work and Other Activities 1985*, edited by J. Wood, O.L. White, R.B. Barlow, and A.C. Colvine, Ontario Geological Survey, MP 126, p. 135-137.
- 1988: Geochronology of the Lumby Lake greenstone belt: a 3 Ga complex within the Wabigoon Subprovince, northwest Ontario; *Geological Society of America Bulletin*, v. 100, p. 818-824.
- Davis, D.W., Corfu, F., and Krogh, T.E.**
1986: High precision U-Pb geochronology and implications for the tectonic evolution of the Superior Province; in *Workshop on the Tectonic Evolution of Greenstone Belts*, edited by M.J. de Wit and L.D. Ashwal, Lunar and Planetary Institute, L.P.I. Technical Report 86-10, Houston, p. 77-79.
- Davis, D.W., Pezzutto, F., and Ojakangas, R.W.**
1990: The age and provenance of metasedimentary rocks in the Quetico Subprovince, Ontario, from single zircon analyses: implications for Archean sedimentation and tectonics in the Superior Province; *Earth and Planetary Science Letters*, v. 99, p. 195-205.
- Davis, D.W., Poulsen, K.H., and Kamo, L.**
1989: New insight into Archean crustal development from geochronology in the Rainy Lake area, Superior Province, Canada; *The Journal of Geology*, v. 97, p. 379-398.
- Deer, W.A., Howie, R.A., and Zussman, J.**
1966: *An Introduction to the Rock-Forming Minerals*; Longman, London, 528 p.
- Devaney, J.R. and Williams, H.R.**
1989: Evolution of an Archean subprovince boundary: a sedimentological and structural study of part of the Wabigoon-Quetico boundary in northern Ontario; *Canadian Journal of Earth Sciences*, v. 26, p. 1013-1026.
- Dixon, J.M.**
1975: Finite strain and progressive deformation in models of diapiric structures; *Tectonophysics*, v. 28, p. 89-124.
- Dormuth, K.W. and Nuttall, K.**
1987: The Canadian Nuclear Fuel Waste Management Program; *Radioactive Waste Management and the Nuclear Fuel Cycle*, v. 8, p. 93-104.
- Dreimanis, A.**
1956: Steep Rock iron ore boulder train; *Geological Society of Canada, Proceedings*, v. 8, pt. 1, p. 27-70.
- Drury, S.A.**
1978: REE distributions in a high-grade Archean gneiss complex in Scotland: implications for the genesis of ancient sialic crust; *Precambrian Research*, v. 7, p. 237-257.
- Dutka, A.J.A.**
1982: The structure and lithology of the Quetico metasediments in the Atikokan area; B.Sc. thesis, Lakehead University, Thunder Bay, Ontario.
- Eden, W.J.**
1955: A laboratory study of varved clay from Steep Rock Lake, Ontario; *American Journal of Science*, v. 253, p. 659-674.
- Ernst, W.G.**
1987: Mafic meta-igneous arc rocks of apparent komatiitic affinities, Sawyers Bar area, central Klamath Mountains, northern California; in *Magmatic Processes: Physicochemical Principles*, edited by B.C. Mysen, Geochemical Society Special Publication 1, p. 191-208.
- Faure, G. and Powell, J.L.**
1972: *Strontium Isotope Geology*; Berlin, Springer Verlag, 1188 p.
- Fenwick, K.G.**
1976: Geology of the Finlayson Lake area, District of Rainy River; Ontario Division of Mines, *Geoscience Report* 145, 86 p.
- Ferry, J.M. and Spear, F.S.**
1978: Experimental calibration of the partitioning of Fe and Mg between biotite and garnet; *Contributions to Mineralogy and Petrology*, v. 66, p. 113-117.
- Fumerton, S.L.**
1986: Geology of the Righteye Lake area, District of Rainy River; Ontario Geological Survey, Report 239, 57 p.

- Ganguly, J. and Saxena, S.K.**
1984: Mixing properties of aluminosilicate garnets: constraints from natural and experimental data, and applications to geothermo-barometry; *American Mineralogist*, v. 69, p. 88-97.
1985: Mixing properties of aluminosilicate garnets: constraints from natural and experimental data, and applications to geothermo-barometry clarifications; *American Mineralogist*, v. 70, p. 1320.
- Gelinas, L., Lajoie, J., and Brooks, B.**
1977: The origin and significance of Archean ultramafic volcanics from Spinifex Ridge, Lomotte Township, Quebec; in *Volcanic Regimes in Canada*, edited by W.R.A. Baragar, Geological Association of Canada, Special Paper 16, p. 297-309.
- Ghent, E.D.**
1976: Plagioclase-garnet- Al_2SiO_5 -Quartz: a potential geobarometer-geothermometer; *American Mineralogist*, v. 61, p. 710-714.
- Gibb, R.A., Nagy, O., Coderre, J., Fogarasi, S., and Thomas, M.D.**
1988: Gravity surveys and interpretations, Eye-Dashwa Lakes pluton, Atikokan (RA-4), Ontario; Atomic Energy of Canada Limited, Technical Record TR 438, 20 p.
- Gill, J.E.**
1931: "Seine" or "Coutchiching" by J.E. Hawley: a discussion; *Journal of Geology*, v. 39, no. 7, p. 655-669.
- Goldich, S.**
1938: A study of rock weathering; *Journal of Geology*, v. 46, p. 17-58.
- Goldman, D.S. and Albee, A.L.**
1977: Correlation of Mg/Fe partitioning between garnet and biotite with $^{18}\text{O}/^{16}\text{O}$ partitioning between quartz and magnetite; *American Journal of Science*, v. 277, p. 750-767.
- Gower, C.F., Paul, O.K., and Crockett, J.H.**
1982: Protoliths and petrogenesis of Archean gneisses from the Kenora area, English River Subprovince, northwest Ontario; *Precambrian Research*, v. 17, p. 245-274.
- Grout, F.F.**
1925: Coutchiching problem; *Geological Society of America Bulletin*, v. 36, no. 2, p. 351-364.
- Hamilton, W. and Myers, W.B.**
1962: Menan buttes, cones of glassy basalt tuff in the Snake River Plain, Idaho; United States Geological Survey, Professional Paper 450-E, p. E114-E118.
- Hammarstrom, J.M. and Zen, E.**
1986: Aluminum in hornblende: an empirical igneous geobarometer; *American Mineralogist*, v. 71, p. 1297-1313.
- Hanson, G.N.**
1980: Rare earth elements in petrogenetic studies of igneous systems; *Annual Reviews of Earth and Planetary Science*, v. 8, p. 371-405.
- Hanson, G.N. and Goldich, S.S.**
1972: Early Precambrian rocks in the Saganaga Lake – Northern Light Lake Area, Minnesota – Ontario, II. Petrogenesis; *Geological Society of America, Memoir 135*, p. 179-192.
- Hardy, R.M. and Legget, R.F.**
1960: Boulder in varved clay at Steep Rock Lake, Ontario, Canada; *Geological Society of America Bulletin*, v. 71, no. 1, p. 93-94.
- Harte, B. and Henley, K.J.**
1966: Occurrence of compositionally zoned almanditic garnets in regionally metamorphosed rocks; *Nature*, v. 210, p. 689-692.
- Haskin, L.A., Haskin, M.A., Frey, F.A., and Wildeman, T.R.**
1968: Relative and absolute terrestrial abundances of the rare earths; in *Origin and Distribution of the Elements*, edited by L.H. Ahrens, Pergamon, Oxford, p. 889-911.
- Hawley, J.E.**
1930: "Seine" or "Coutchiching"?; *Journal of Geology*, v. 38, p. 521-547.
- Hicks, H.S.**
1950: Geology of the iron deposits of Steep Rock Iron Mines Limited; *The Precambrian*, v. 23, p. 8-10.
- Hodges, K.V. and Spear, F.S.**
1982: Geothermometry, geobarometry and the Al_2SiO_5 triple point at Mt. Moosilauke, New Hampshire; *American Mineralogist*, v. 67, p. 1118-1134.
- Hoffman, P.F.**
1989: Precambrian geology and tectonic history of North America; in *The Geology of North America – An Overview*, edited by A.W. Bally and A.R. Palmer, Geological Society of America, The Geology of North America, v. A, p. 447-512.
- Hofmann, H.J.**
1971: Precambrian fossils, pseudofossils, and problematica in Canada; *Geological Survey of Canada, Bulletin 189*, 146 p.
- Hoinkes, G.**
1986: Effect of grossular-content in garnet on the partitioning of Fe and Mg between garnet and biotite; *Contributions to Mineralogy and Petrology*, v. 92, p. 393-399.
- Hollister, L.S.**
1966: Garnet zoning: an interpretation based on the Rayleigh fractionation model; *Science*, v. 154, p. 1647-1651.
- Holloway, A.L.**
1985: Sonar profiling in lakes near the Atikokan Research Area, Ontario; in *The Geoscience Program – Proceedings of the Seventeenth Information Meeting of the Nuclear Fuel Waste Management Program*, Atomic Energy of Canada Limited, Technical Record TR 299, p. 622-633.
- Huston, W.J.**
1956: The Steeprock Manganiferous Foot-wall Paint; M.Sc. thesis, Queen's University, Kingston, Ontario.
- Indares, A. and Martignole, J.**
1985: Biotite-garnet geothermometry in the granulite facies: the influence of Ti and Al in biotite; *American Mineralogist*, v. 70, p. 272-278.
- Irvine, T.N. and Baragar, W.R.A.**
1971: A guide to the chemical classification of the common volcanic rocks; *Canadian Journal of Earth Sciences*, v. 8, p. 523-548.
- Jackson, M.C.**
1985: Geology of the Lumby Lake area, western part, Districts of Kenora and Rainy River; Ontario Geological Survey, Open File Report 5534, 151 p.
- Jahn, B., Shih, C., and Murthy, V.R.**
1974: Trace element geochemistry of Archean volcanic rocks; *Geochimica et Cosmochimica Acta*, v. 38, p. 611-627.
- Johnson, P.J.**
1987: Metamorphism of the Quetico metasediments near Atikokan, Ontario; B.Sc. thesis, Carleton University, Ottawa, Ontario, 52 p.
- Jolliffe, A.W.**
1955: Geology and iron ores of Steep Rock Lake; *Economic Geology*, v. 50, no. 4, p. 373-398.
1966: Stratigraphy of the Steep Rock Group, Steep Rock Lake, Ontario; in *The relationship of mineralization to Precambrian stratigraphy in certain mining areas of Ontario and Quebec*, Precambrian Symposium, edited by A.M. Goodwin, Geological Association of Canada, Special Paper No. 3, p. 75-98.
- Kamineni, D.C.**
1983: Sulphur-isotope geochemistry of fracture-filling gypsum in an Archean granite near Atikokan, Ontario, Canada; *Chemical Geology*, v. 39, p. 263-272.
- Kamineni, D.C. and Brown, P.A.**
1981: A preliminary report on the petrology and fracture filling of the Eye-Dashwa Lakes pluton, Atikokan, northwestern Ontario; Atomic Energy of Canada Limited, Technical Record TR 123, 37 p.
- Kamineni, D.C. and Dugal, J.J.B.**
1982: A study of rock alteration in the Eye-Dashwa Lakes pluton, Atikokan, northwestern Ontario, Canada; *Chemical Geology*, v. 36, p. 35-57.
- Kamineni, D.C. and Stone, D.**
1983: The ages of fractures in the Eye-Dashwa Lakes pluton, Atikokan, Canada; *Contributions to Mineralogy and Petrology*, v. 83, p. 237-246.
- Kamineni, D.C., Thivierge, R.H., and Stone, D.**
1988: Development of a cataclastic fault zone in an Archean granitic pluton of the Superior Province: structural, geochemical and geophysical characteristics; *American Journal of Science*, v. 288, p. 458-494.
- Kamineni, D.C., Stone, D., and Peterman, Z.E.**
1990: Early Proterozoic deformation in the western Superior province, Canadian Shield; *Geological Society of America Bulletin*, v. 102, p. 1623-1634.
- Kehlenbeck, M.M.**
1984: Use of stratigraphic and structural-facing directions to delineate the geometry of refolded folds near Thunder Bay, Ontario; *Geoscience Canada*, v. 11, p. 23-32.
1986: Folds and folding in the Beardmore-Geraldton fold belt; *Canadian Journal of Earth Sciences*, v. 23, p. 158-171.
- Kennedy, M.**
1984: The Quetico fault in the Superior Province of the southern Canadian Shield; M.Sc. thesis, Lakehead University, Thunder Bay, Ontario.

- Kerrick, R.**
1984: Chronology and ambient temperature/pressure conditions of fluid flow through the Eye-Dashwa Lakes pluton based on the $^{18}\text{O}/^{16}\text{O}$ ratio and fluid inclusions; Atomic Energy of Canada Limited, Technical Record TR 267, 17 p.
- Kerrick, R. and Kaminen, D.C.**
1985: Oxygen and hydrogen isotope study of fracture-related fluid flow in the Eye-Dashwa Lakes pluton, Atikokan, northwestern Ontario; Atomic Energy of Canada Limited, Technical Record TR 361, 20 p.
- Kimberley, M.M. and Sorbara, J.P.**
1976: Post-Archean weathering of Steep Rock Group Iron Formation; Proceedings of the 1976 Geotraverse Conference, University of Toronto, Toronto, Ontario, p. 128-136.
- Kretz, R.**
1959: Chemical study of garnet, biotite, and hornblende from gneisses of southwestern Quebec, with emphasis on distribution of elements in coexisting minerals; *Journal of Geology*, v. 67, p. 371-402.
- Lambert, R.St.J. and Holland, J.G.**
1976: Amitsoq gneiss geochemistry: preliminary observations; in *Early History of the Earth*, edited by B.F. Windley, Wiley, New York, p. 191-201.
- Larsen, E.S.**
1938: Some new variation diagrams for groups of igneous rocks; *Journal of Geology*, v. 46, p. 505-520.
- Lawson, A.C.**
1885: Report on the geology of the Lake of the Woods region with special emphasis on the Keewatin (Huronian) belt of Archean rocks; Geological Survey of Canada, Annual Report, pt. CC, p. 5-151.
1888: Report on the geology of the Rainy Lake region; Geological Survey of Canada, Annual Report, pt. F, p. 1-182.
1912: The Geology of Steeprock Lake, Ontario; Geological Survey of Canada, Memoir 28, p. 7-15.
1913: The Archean geology of Rainy Lake re-studied; Geological Survey of Canada, Memoir 40, 115 p. Accompanied by Map 98A (issued 1914), scale 1 inch to 1 mile.
- Leake, B.D.**
1978: Nomenclature of amphiboles; *Journal of the Mineralogical Society of Canada*, v. 16, p. 501-520.
- Lee, P.K., Pearson, R., Leech, R.E.J., and Dickin, R.**
1983: Hydraulic testing of deep fractures in the Canadian Shield; *Bulletin of the International Association of Engineering Geology*, no. 26-27, p. 461-465.
- Legget, R.F. and Bartley, M.W.**
1953: An engineering study of glacial deposits at Steep Rock Lake, Ontario, Canada; *Economic Geology*, v. 48, p. 513-540.
- Logan, W.E., Murray, A., Hunt, T.S., and Billings, E.**
1863: Geological Survey of Canada, report of progress from its commencement to 1863; Geological Survey of Canada, Report of Progress, 983 p.
- Mackasey, W.O., Blackburn, C.E., and Trowell, N.F.**
1974: A regional approach to the Wabigoon-Quetico Belts and its bearing on exploration in northwestern Ontario; Ontario Division of Mines, Miscellaneous Paper 58, 30 p.
- Martin, H.**
1987: Evolution in composition of granitic rocks controlled by time-dependent changes in petrogenetic processes: examples from the Archean of Eastern Finland; *Precambrian Research*, v. 35, p. 257-276.
- Masuda, A., Nakamura, N., and Tanaka, T.**
1973: Fine structures of mutually normalized rare-earth patterns of chondrites; *Geochimica et Cosmochimica Acta*, v. 37, p. 239-248.
- McInnes, W.**
1897: Report on the geology of the area covered by the Seine River and Lake Shebandowan map sheets, comprising portions of Rainy River and Thunder Bay districts, Ontario; Geological Survey of Canada, Annual Report, 1897, v. 10, pt. H, p. 1-65.
- McIntosh, J.R.**
1972: The Caland Ore Company Limited Deposit – a geological description; Ontario Department of Mines and Northern Affairs, Geological Report 93, p. 83-105.
- Merritt, P.L.**
1934: Seine-Coutchiching problem; *Geological Society of America Bulletin*, v. 45, p. 333-374.
- Miller, W.G.**
1903: Iron ranges of northern Ontario; Ontario Bureau of Mines, v. 12, p. 304-317.
- Moore, E.S.**
1938: The Steeprock Series; Royal Society of Canada, Transaction Section 4, 3rd series, v. 32, p. 11-23.
1939: Geology and ore deposits of the Atikokan area; Ontario Department of Mines, v. 48, pt. 2, p. 1-34 (published 1940). Accompanied by Map 48a, scale 1 inch to 1 mile.
- Morgan, J.**
1987: Three dimensional strain in centrifuge models and an Archean greenstone belt; Ph.D. thesis, University of Toronto, Toronto, Ontario.
- Morris, M.V.**
1986: Geochemistry and tectonic setting of the Steep Rock greenstone belt, Atikokan, Canada; B.Sc. thesis, Carleton University, Ottawa, Ontario, 162 p.
- Newton, R.C. and Haselton, H.T.**
1981: Thermodynamics of the garnet-plagioclase- Al_2SiO_5 -quartz geobarometer; in *Thermodynamics of Minerals and Melts*, edited by R.C. Newton, A. Navrotsky, and B.J. Wood, Springer, p. 131-148.
- Nisbet, E.G.**
1982: The tectonic setting and petrogenesis of komatiites; in *Komatiites*, edited by N.T. Arndt and E.G. Nisbet, George Allen and Unwin, p. 501-530.
- Northern Miner Press**
1981: Canadian Mines Handbook 1980-81; Northern Miner Press Ltd., Toronto, 368 p.
- Nunes, P.D. and Thurston, P.C.**
1980: Two hundred and twenty million years of Archean evolution: a zircon U-Pb age stratigraphic study of the Uchi-Confederation Lakes greenstone belt, northwestern Ontario; *Canadian Journal of Earth Sciences*, v. 17, p. 710-721.
- Nur, A.**
1983: The origin of tensile fracture lineaments; *Journal of Structural Geology*, v. 4, p. 31-40.
- Ojakangas, R.W.**
1985: Review of Archean clastic sedimentation, Canadian Shield: major felsic volcanic contributions to turbidite and alluvial fan-fluvial facies association; in *Evolution of Archean Supracrustal Sequences*, edited by L.D. Ayres, P.C. Thurston, K.D. Card, and W. Weber, Geological Association of Canada, Special Paper 28, p. 23-48.
- Ontario Geological Survey**
1980: Airborne electromagnetic and total intensity magnetic survey, Atikokan-Mine Centre area, eastern parts District of Rainy River; by Questor Surveys Limited for the Ontario Geological Survey, Geophysical/Geochemical Series Map 80514, scale 1:20 000.
- Parkinson, R.N.**
1962: Operation Overthrust; in *The Tectonics of the Canadian Shield*, Royal Society of Canada, Special Publication No. 4, p. 90-101.
- Pearce, J.A. and Cann, J.R.**
1973: Tectonic setting of basic volcanic rocks determined using trace element analysis; *Earth and Planetary Science Letters*, v. 19, p. 290-300.
- Perchuk, L.L.**
1977: Thermodynamic control of metamorphic processes; in *Energetics of Geological Processes*, edited by S.K. Saxena and S. Bhattacharji, Springer-Verlag, Berlin, p. 286-352.
- Perchuk, L.L. and Lavrent'eva, I.V.**
1983: Experimental investigation of exchange equilibria in the system cordierite-garnet-biotite; in *Kinetics and Equilibrium in Mineral Reactions*, edited by S.K. Saxena, Springer Verlag, Berlin, p. 199-239.
- Perchuk, L.L., Aranovich, L.Ya., Podlesskii, K.K., Lavrent'eva, I.V., Gerasimov, V.Yu., Fed'kin, V.V., Kitsul, V.I., Karsakov, L.P., and Berdnikov, N.V.**
1985: Precambrian granulites of the Aldan shield, eastern Siberia, USSR; *Journal of Metamorphic Geology*, v. 3, no. 3, p. 265-310.
- Percival, J.**
1989: A regional perspective of the Quetico metasedimentary belt, Superior Province, Canada; *Canadian Journal of Earth Sciences*, v. 26, p. 677-693.
- Percival, J.A. and Stern, R.A.**
1984: Geological synthesis in the western Superior Province, Ontario; in *Current Research, Part A*, Geological Survey of Canada, Paper 84-1A, p. 397-408.
- Percival, J.A. and Williams, H.R.**
1989: The Late Archean Quetico accretionary complex, Superior Province, Canada; *Geology*, v. 17, p. 23-25.

- Peterman, Z.E., Goldich, S.S., Doe, B.R., Naeser, C.W., Rosholt, J.N., Zartman, R.E., and Kamineni, D.C.**
1985: Isotopic studies of core samples from the Eye-Dashwa Lakes pluton, Atikokan, Ontario; in *The Geoscience Program – Proceedings of the Seventeenth Information Meeting of the Nuclear Fuel Waste Management Program*, Atomic Energy of Canada Limited, Technical Record TR-299, p. 642-643.
- Pirie, J.**
1978: Geology of the Crooked Pine Lake area, District of Rainy River; Ontario Geological Survey, Report 179, 73 p.
- Pirie, J. and Mackasey, W.O.**
1978: Preliminary examination of regional metamorphism in parts of Quetico metasedimentary belt, Superior Province, Ontario; in *Metamorphism in the Canadian Shield*, edited by J.A. Fraser and W.W. Heywood, Geological Survey of Canada, Paper 78-10, p. 37-48.
- Poulsen, K.H.**
1986: Rainy Lake wrench zone: an example of an Archean subprovince boundary in northwestern Ontario; in *Workshop on Tectonic Evolution of Greenstone Belts*, edited by M.J. deWit and L.D. Ashwal, LPI Technical Report 86-10, Lunar and Planetary Institute, Houston, p. 177-179.
- Poulsen, K.H., Borradaile, G.J., and Kehlenbeck, M.M.**
1980: An inverted Archean succession at Rainy Lake, Ontario; *Canadian Journal of Earth Sciences*, v. 18, p. 1358-1369.
- Rajamani, V., Shivkumar, K., Hanson, G.N., and Shirey, S.B.**
1985: Geochemistry and petrogenesis of amphibolites, Kolar Schist belt, South India: evidence for komatiitic magma derived by low percentage melting of the mantle; *Journal of Petrology*, v. 26, p. 92-123.
- Ramsay, C.R. and Kamineni, D.C.**
1977: Petrology and evolution of an Archean metamorphic aureole in the Slave Craton, Canada; *Journal of Petrology*, v. 18, p. 460-486.
- Ramsay, J.G.**
1980: Shear zone geometry: a review; *Journal of Structural Geology*, v. 2, p. 83-100.
- Ramsay, J.G. and Huber, M.I.**
1987: *The Techniques of Modern Structural Geology, Volume 2: Folds and Fractures*; Academic Press, London, 700 p.
- Roberts, T.L. and Bartley, M.V.**
1943: Hydrothermal replacement in deep seated iron ore deposits of the Lake Superior region; *Economic Geology*, v. 38, p. 1-24.
- Saxena, S.K.**
1968: Distribution of elements between coexisting minerals and the nature of the solid solution in garnet; *American Mineralogist*, v. 53, p. 994-1014.
- Schaefer, S.J.**
1989: A comparison of two ultramafic pyroclastic rock units, northwestern Ontario; *Institute of Lake Superior Geology Proceedings*, v. 35, p. 77.
- Schau, M. and Henderson, J.B.**
1983: Archean chemical weathering at three localities on the Canadian shield; *Precambrian Research*, v. 20, p. 189-224.
- Schwerdtner, W.M.**
1988: Recognition of pervasive prestrain in total-strain pattern of large folds; *Journal of Structural Geology*, v. 10, p. 33-40.
1989: Structural tests of diapir hypotheses in the Archean crust of northwestern Ontario; *Geological Association of Canada, Program with Abstracts*, v. 14, p. A55.
- Schwerdtner, W.M., Morgan, J., and Stott, G.M.**
1985: Contacts between greenstone belts and gneiss complexes within the Wabigoon Subprovince, northwestern Ontario; in *Evolution of Supracrustal Sequences*, edited by L.D. Ayres, P.C. Thurston, K.D. Card, and W. Weber, Geological Association of Canada, Special Paper 28, p. 117-123.
- Schwerdtner, W.M., Stone, D., Osadetz, K., Morgan, J., and Stott, G.M.**
1979: Granitoid complexes and the Archean tectonic record in the southern part of northwestern Ontario; *Canadian Journal of Earth Sciences*, v. 16, p. 1965-1977.
- Shaw, D.M.**
1956: Geochemistry of pelitic rocks. Part III. Major elements and general geochemistry; *Geological Society of America Bulletin*, v. 67, p. 919-934.
1972: Origin of the Apsley gneiss, Ontario; *Canadian Journal of Earth Sciences*, v. 9, p. 18-35.
- Shaw, D.M., Reilly, G.A., Muysson, J.R., Pattenden, G.E., and Campbell, F.E.**
1967: An estimate of the chemical composition of the Canadian Shield; *Canadian Journal of Earth Sciences*, v. 4, p. 829-853.
- Shirey, S.B. and Hanson, G.N.**
1984: Mantle-derived Archean monzodiorites and trachyandesites; *Nature*, v. 310, p. 222-224.
1986: Mantle heterogeneity and crustal recycling in Archean granite-greenstone belts: evidence from Nd isotopes and trace elements in the Rainy Lake area, Superior Province, Ontario, Canada; *Geochimica et Cosmochimica Acta*, v. 50, p. 2631-2651.
- Shklanka, R.**
1972: Geology of the Steep Rock Lake area, District of Rainy River; Ontario Department of Mines and Northern Affairs, Geological Report 93, 114 p.
- Sibson, R.H.**
1977: Fault rocks and fault mechanisms; *Journal of the Geological Society of London*, v. 133, p. 191-213.
- Smaglik, S.M.**
1987: Petrogenetic and tectonic implications for Archean mafic and ultramafic magmas in the Elmer's Rock greenstone belt, Laramie Range, Wyoming; M.Sc. thesis, Colorado School of Mines, Colorado, 126 p.
1988: Petrology of Archean mafic and ultramafic magmas from the Elmer's Rock Greenstone belt, Laramie Range, Wyoming; Abstract, American Geophysical Union, Fall Meeting, San Francisco.
- Smith, F.G.**
1942: Notes on the iron ores of Steeprock Lake, Ontario; University of Toronto Studies, Geological Series, No. 47, Contributions to Canadian Mineralogy, p. 71-75.
- Smith, W.H.C.**
1893: The Archean rocks west of Lake Superior; *Geological Society of America Bulletin*, v. 4, p. 333-348.
- Smith, W.H.C. and McInnes, W.**
1897: Seine River Sheet. Geological Survey of Canada, scale 1:253 440.
- Smyth, H.L.**
1891: Structural geology of Steep Rock Lake, Ontario; *American Journal of Science*, v. 42, p. 317-331.
- Stern, R.A., Hanson, G.H., and Shirey, S.B.**
1989: Petrogenesis of mantle-derived, LILE-enriched Archean monzodiorites and trachyandesites (sanukitoids) in southwestern Superior Province; *Canadian Journal of Earth Sciences*, v. 26, p. 1688-1712.
- Stone, D.**
1984: Summary of geoscience work at the AECL research site near Atikokan, Ontario; Atomic Energy of Canada Limited Report AECL 7815, 50 p.
- Stone, D. and Kamineni, D.C.**
1982: Fractures and fracture in fillings of the Eye-Dashwa Lakes pluton, Atikokan, Ontario; *Canadian Journal of Earth Sciences*, v. 19, p. 789-803.
- Stone, D., Kamineni, D.C., Brown, A., and Everitt, R.A.**
1989: A comparison of fracture styles in two granitic bodies of the Superior Province; *Canadian Journal of Earth Sciences*, v. 26, p. 387-403.
- Streckeisen, A.**
1976: To each plutonic rock its proper name; *Earth Science Reviews*, v. 12, p. 1-33.
- Sun, S.S. and Nesbitt, R.W.**
1978: Petrogenesis of Archean ultra basic and basic volcanics: evidence from rare earth elements; *Contributions to Mineralogy and Petrology*, v. 65, p. 301-325.
- Tanton, T.L.**
1926: Recognition of the Couthiching near Steep Rock Lake, Ontario; *Royal Society of Canada, Transactions, Section 4*, v. 20, p. 39-49.
1927: Mineral deposits of Steep Rock Lake map-area, Ontario; *Geological Survey of Canada, Summary Report*, 1925, pt. C, p. 1C-11C.
1937: Quetico (west half) Rainy River District, Ontario; Canada Department of Mines and Resources, Map 534A, scale 1:253 440.
1941: Origin of the hematite deposits at Steep Rock Lake, Ontario; *Royal Society of Canada, Transactions*, v. 35, p. 131-141.
1946: The iron ore at Steep Rock Lake; *Royal Society of Canada, Transactions*, v. 40, p. 103-112.

- Taylor, S.R. and Hallberg, J.A.**
1977: Rare earth elements in the Narda calc-alkaline suite: an Archean geochemical analogue of Andean-type volcanism; *Geochimica et Cosmochimica Acta*, v. 41, p. 1125-1136.
- Taylor, S.R. and McLennan, S.M.**
1985: The continental crust: its composition and evolution; Blackwell Scientific Publications, Oxford, 312 p.
- Thompson, A.B.**
1976: Mineral reactions in pelitic rocks: II. Calculation of some P-T-X (Fe-Mg) phase relations; *American Journal of Science*, v. 276, p. 425-454.
- Thurston, P.C. and Chivers, K.M.**
1990: Secular variation in greenstone sequence development emphasizing Superior Province, Canada; *Precambrian Research*, v. 46, p. 21-58.
- Uglow, W.L.**
1913: Geology of the vicinity of Steep Rock Lake; in Guide Book No. 8, pt. 1, 12th International Geological Congress, issued by the Geological Survey of Canada, p. 46-53.
- van Hise, C.R. and Leith, C.K.**
1911: The geology of the Lake Superior region; United States Geological Survey, Monograph, v. 52, 641 p.
- Viljoen, R.P. and Viljoen, M.J.**
1969: The geology and geochemistry of the lower ultramafic unit of the Onverwacht Group and a proposed new classification of igneous rocks; Geological Society of South Africa, Special Publication, v. 2, p. 55-86.
- Walcott, C.D.**
1912: Notes on fossils from limestone of Steeprock Series, Ontario, Canada; Geological Survey of Canada, Memoir 28, p. 16-23.
- Whitney, J.A. and Stormer, J.C., Jr.**
1977: Two-feldspar geothermometry, geobarometry in mesozonal intrusions: three examples from the piedmont of Georgia; *Contributions to Mineralogy and Petrology*, v. 63, p. 51-64.
- Wilks, M.E.**
1986: The geology of the Steep Rock Group, northwestern Ontario: a major Archean unconformity and Archean stromatolites; M.Sc. thesis, University of Saskatchewan, Saskatoon, Saskatchewan, 206 p.
- Wilks, M.E. and Nisbet, E.G.**
1985: Archean stromatolites from the Steep Rock Group, northwestern Ontario, Canada; *Canadian Journal of Earth Sciences*, v. 22, p. 792-799.
1988: Stratigraphy of the Steep Rock Group, northwestern Ontario: a major Archean unconformity and Archean stromatolites; *Canadian Journal of Earth Sciences*, v. 25, p. 370-391.
- Winkler, H.G.F.**
1976: Petrogenesis of Metamorphic Rocks; 4th edition; Springer-Verlag, New York, 254 p.
- Wood, J.**
1980: Epiclastic sedimentation and stratigraphy in the North Spirit Lake and Rainy Lake areas: a comparison; *Precambrian Research*, v. 12, p. 227-255.
- Wright, C.M.**
1959: Pyrite zones in the hangingwall of the Steeprock Ore Zone; M.Sc. thesis, Queen's University, Kingston, Ontario.
- Zartman, R.E. and Kwak, L.M.**
1990: U-Th-Pb systematics in zircon and titanite; in *Isotopic Studies of the Eye-Dashwa Lakes Pluton and the Long-term Integrity of Whole-rock and Mineral Systems*, edited by Z.E. Peterman and D.C. Kameneni, Atomic Energy of Canada Limited, Report 10120, p. 25-36.
- Zoltai, S.C.**
1961: Glacial history of part of northwestern Ontario; *Proceedings of the Geological Association of Canada*, v. 13, p. 61-83.
1965a: Glacial features of the Quetico-Nipigon area, Ontario; *Canadian Journal of Earth Sciences*, v. 2, p. 247-269.
1965b: Surficial Geology, Kenora-Rainy River; Ontario Department of Lands and Forests, Map S165, scale 1:506 880.

APPENDIX 1

Table A1. Modal analyses of crystalline rocks

Rock type	Sample No.	quartz	microcline	plagioclase	biotite	hornblende	muscovite	chlorite	epidote	titania	calcite	apatite	opaques	others
Granite, Eye-Dashwa pluton core (8c)		26	28	34	7	1	<1	<1	1	1	—	—	1	—
Granite, White Otter batholith (8c)	135	19	34	30	6	—	4	2	1	—	—	1	2	1
Granodiorite, Margaret stock (8b)	120	18	23	34*	<1	14	—	2	3	2	—	1	1	1
Quartz monzodiorite, Eye-Dashwa pluton rim (8a)		8	16	46	2	23	—	1	2	1	—	—	1	—
Hornblende (7)	115	1	—	2	13	75	—	—	1	—	4	2	1	1
"Young" tonalite (6)	121	18	5	42	14	12	—	—	3	2	—	2	1	1
	124	29	—	37	19	—	3	—	6	2.5	—	1.5	1	1
	129	26	21	27	8	—	5	1	8	1	—	—	2	1
	101	29	18	28	8	—	5	1	7	1	—	—	2	1
	126	18	—	30	—	—	20	15	6	3	5	—	2	1
	104	27	10	41	12	—	—	3	1	2	—	2	1	1
	105	22	13	44	13	11	—	—	4	2	—	1	2	1
	131	28	10	40	11	—	—	1	5	1	—	1	2	1
	107	22	5	44	14	6	—	3	2	1	—	1	1	1
	111	17	<1	31	11	36	—	—	1	<1	—	1	<1	—
Mafic tonalite gneiss (1d)	117	22	18	32	10	12	—	—	2	1	—	1	1	1
	133	22	2	27	4	39	—	—	2	1	tr	—	1	1
	134	26	15	36	10	1	—	—	7	2	—	—	2	1
Tonalite gneiss (1c)	110	24	20	38	8	—	5	—	2	<1	—	—	1	1
	106	25	15	31	13	8	—	—	2.5	2	—	1.5	1	1
	119	20	—	38	18	8	—	—	7	3	2	1	2	1
	122	32	15	34	11	—	—	—	3	<1	—	1	2	1
	116	25	15	37	14	tr	3	—	2	1	—	<1	1	1
	127	21	—	36	—	—	18	10	7	—	4	—	3	1
"Old" tonalite (1b)	128	25	—	46	—	—	11	12	3	—	—	—	2	1
	103	25	—	40	18	7	—	—	5	1	—	—	2	1
	130	24	—	46	17	—	—	2	5	2	—	1	2	1
	108	25	—	38	20	—	5	3	6	—	—	—	2	1
	138	30	—	36	16	—	6	3	4	1	2	—	1	1
	112	18	18	27	—	—	11	12	4	—	6	—	3	1
Mafic tonalite (1a)	102	18	—	41	8	22	—	—	2	3	—	2	3	1

* includes 15% sericite as alteration product

tr = trace

APPENDIX 2

Table A2. Major element geochemistry. Where the number of analyses is less than 6, each analysis is listed and the mean is given. Median and mean statistics are given for larger numbers of analyses excluding those of the Eye-Dashwa pluton.

ROCK TYPE: GABBRO DYKES (Map unit 9)					
Oxide (%)	Mean	Number	Data list		
SiO ₂	50.43	3	50.1	51.4	49.8
TiO ₂	1.35	3	1.36	1.34	1.35
Al ₂ O ₃	13.20	3	13.3	13.2	13.1
Fe ₂ O ₃	3.87	3	4.2	3.9	3.5
FeO	8.90	3	8.8	8.6	9.3
MnO	0.23	3	0.23	0.22	0.23
MgO	6.29	3	6.37	6.24	6.26
CaO	10.83	3	10.90	11.50	10.10
Na ₂ O	2.37	3	2.58	2.21	2.32
K ₂ O	0.51	3	0.41	0.28	0.85
H ₂ O	1.67	3	1.6	1.5	1.9
CO ₂	0.33	3	0.3	0.4	0.3
P ₂ O ₅	0.13	3	0.14	0.12	0.14
S	0.07	3	0.04	0.00	0.17

ROCK TYPE: WHITE OTTER BATHOLITH (Map unit 8c)									
Oxide (%)	Most Freq. value	Minimum	10%	Median	90%	Maximum	Mean	Std Dev.	Number
SiO ₂	74.6	70.9	72.7	74.5	76.1	76.4	74.32	1.24	30
TiO ₂	0.11	0.08	0.08	0.12	0.21	0.25	0.14	0.05	30
Al ₂ O ₃	13.3	12.3	13.0	13.7	14.7	14.8	13.72	0.61	30
Fe ₂ O ₃	0.7	0.3	0.6	0.7	1.1	1.3	0.76	0.21	30
FeO	0.5	0.1	0.2	0.5	0.9	0.9	0.49	0.24	30
MnO	0.03	0.01	0.01	0.03	0.04	0.05	0.03	0.01	30
MgO	0.26	0.00	0.12	0.30	0.48	0.62	0.29	0.14	30
CaO	1.14	0.45	0.73	1.04	2.00	2.25	1.15	0.45	30
Na ₂ O	4.02	3.23	3.47	3.84	5.04	5.30	4.00	0.55	30
K ₂ O	4.86	1.89	2.70	4.84	5.42	5.72	4.41	1.08	30
H ₂ O	0.3	0.1	0.2	0.3	0.5	0.8	0.34	0.14	30
CO ₂	0.1	0.0	0.0	0.1	0.2	0.3	0.14	0.08	30
P ₂ O ₅	0.04	0.01	0.03	0.04	0.08	0.09	0.05	0.02	30
S	0.04	0.00	0.00	0.00	0.00	0.04	0.00	0.01	30

ROCK TYPE: BEWAG STOCK (Map unit 8c)				
Oxide (%)	Mean	Number	Data list	
SiO ₂	68.95	2	69.1	68.8
TiO ₂	0.26	2	0.24	0.27
Al ₂ O ₃	15.95	2	15.9	16.0
Fe ₂ O ₃	0.90	2	0.9	0.9
FeO	1.25	2	1.2	1.3
MnO	0.05	2	0.04	0.05
MgO	0.80	2	0.76	0.83
CaO	1.61	2	1.53	1.69
Na ₂ O	5.03	2	5.08	4.98
K ₂ O	4.56	2	4.53	4.58
H ₂ O	0.60	2	0.6	0.6
CO ₂	0.05	2	0.0	0.1
P ₂ O ₅	0.16	2	0.15	0.16
S	0.02	2	0.0	0.04

Appendix 2 (cont'd)

ROCK TYPE: EYE-DASHWA PLUTON CORE (Map unit 8c)

Oxide (%)	Mean	Number
SiO ₂	71.28	14
TiO ₂	0.24	14
Al ₂ O ₃	15.16	14
Fe ₂ O ₃	1.08	14
FeO	0.65	14
MnO	0.03	14
MgO	0.61	14
CaO	1.79	14
Na ₂ O	4.25	14
K ₂ O	3.80	14
H ₂ O	0.55	14
CO ₂	0.06	14
P ₂ O ₅	0.12	14
S	0.05	14

ROCK TYPE: EYE-DASHWA PLUTON RIM (Map units 8a, c)

Oxide (%)	Mean	Number
SiO ₂	67.53	19
TiO ₂	0.43	19
Al ₂ O ₃	15.40	19
Fe ₂ O ₃	1.74	19
FeO	1.18	19
MnO	0.04	19
MgO	1.29	19
CaO	2.79	19
Na ₂ O	4.60	19
K ₂ O	3.42	19
H ₂ O	0.58	19
CO ₂	0.05	19
P ₂ O ₅	0.24	19
S	0.05	19

ROCK TYPE: EYE-DASHWA PLUTON OUTERMOST RIM (Map unit 8a)

Oxide (%)	Mean	Number
SiO ₂	59.16	8
TiO ₂	0.71	8
Al ₂ O ₃	15.10	8
Fe ₂ O ₃	2.73	8
FeO	3.37	8
MnO	0.10	8
MgO	3.84	8
CaO	5.24	8
Na ₂ O	3.97	8
K ₂ O	3.73	8
H ₂ O	0.90	8
CO ₂	0.10	8
P ₂ O ₅	0.55	8
S	0.05	8

Appendix 2 (cont'd.)

ROCK TYPE: DIVERSION STOCK (Map unit 8b)

Oxide (%)	Most freq. value	Minimum	10%	Median	90%	Maximum	Mean	Std dev.	Number
SiO ₂	75.4	70.9	71.9	73.4	76.0	76.3	73.81	1.77	11
TiO ₂	0.22	0.07	0.09	0.22	0.31	0.36	0.23	0.09	11
Al ₂ O ₃	12.0	10.8	12.0	12.8	13.5	14.5	12.70	0.96	11
Fe ₂ O ₃	1.6	0.0	0.3	0.8	1.6	1.6	0.85	0.53	11
FeO	1.5	0.2	0.5	1.2	1.5	1.7	1.06	0.49	11
MnO	0.05	0.03	0.03	0.05	0.06	0.06	0.05	0.01	11
MgO	1.09	0.25	0.29	0.88	1.07	1.09	0.80	0.29	11
CaO	2.72	0.64	0.77	1.73	2.56	2.72	1.65	0.73	11
Na ₂ O	3.87	3.02	3.47	3.87	4.4	5.05	3.89	0.53	11
K ₂ O	3.64	1.64	1.97	2.41	3.45	3.64	2.49	0.60	11
H ₂ O	0.9	0.3	0.4	0.8	1.1	1.3	0.77	0.31	11
CO ₂	1.0	0.3	0.4	0.9	1.3	1.4	0.80	0.36	11
P ₂ O ₅	0.07	0.04	0.06	0.07	0.09	0.11	0.07	0.02	11
S	0.0	0.0	0.0	0.0	0.0	0.0	0.0	0.0	11

ROCK TYPE: MARGARET STOCK (Map unit 8b)

Oxide (%)	Mean	Number	Data list	
			Rim	Core
SiO ₂	67.55	2	65.6	69.5
TiO ₂	0.44	2	0.54	0.34
Al ₂ O ₃	15.10	2	15.5	14.7
Fe ₂ O ₃	1.70	2	2.5	1.1
FeO	1.80	2	2.5	1.1
MnO	0.06	2	0.06	0.05
MgO	1.40	2	1.8	1.0
CaO	3.08	2	3.66	2.49
Na ₂ O	4.00	2	4.5	3.5
K ₂ O	2.23	2	1.12	3.34
H ₂ O	1.80	2	2.0	1.6
CO ₂	0.55	2	0.7	0.4
P ₂ O ₅	0.16	2	0.17	0.14
S	0.05	2	0.05	0.04

ROCK TYPE: LITTLE EYE STOCK (Map unit 7)

Oxide (%)	Mean	Number	Data list	
			Rim	Core
SiO ₂	45.80	2	51.8	39.8
TiO ₂	0.92	2	0.65	1.19
Al ₂ O ₃	16.20	2	21.9	10.5
Fe ₂ O ₃	3.75	2	2.3	5.2
FeO	6.30	2	3.6	9.0
MnO	0.13	2	0.05	0.20
MgO	7.70	2	3.90	11.50
CaO	11.32	2	8.708	13.85
Na ₂ O	2.90	2	4.70	1.10
K ₂ O	1.28	2	0.55	2.01
H ₂ O	1.90	2	1.7	2.1
CO ₂	0.10	2	0.0	0.2
P ₂ O ₅	1.58	2	0.33	2.83
S	0.02	2	0.00	0.04

Appendix 2 (cont'd.)

ROCK TYPE: "YOUNG" TONALITE (Map unit 6)

Oxide (%)	Most freq.		10%	Median	90%	Maximum	Mean	Std dev.	Number
	value	Minimum							
SiO ₂	73.0	67.9	68.3	69.4	73.0	73.0	69.65	1.94	6
TiO ₂	0.51	0.20	0.24	0.42	0.51	0.51	0.35	0.12	6
Al ₂ O ₃	16.5	15.6	15.6	16.3	16.5	16.50	16.03	0.41	6
Fe ₂ O ₃	0.7	0.6	0.6	0.7	1.6	1.6	0.82	0.39	6
FeO	2.3	0.9	1.1	2.3	2.6	2.6	1.85	0.70	6
MnO	0.03	0.02	0.02	0.03	0.06	0.06	0.03	0.02	6
MgO	1.00	0.40	0.60	1.00	1.30	1.30	0.88	0.33	6
CaO	4.19	2.62	2.98	3.76	4.19	4.19	3.46	0.58	6
Na ₂ O	5.60	4.30	4.60	5.20	5.60	5.60	4.95	0.49	6
K ₂ O	1.56	1.08	1.10	1.23	1.56	1.56	1.25	0.18	6
H ₂ O	0.7	0.5	0.5	0.7	0.9	0.9	0.68	0.16	6
CO ₂	0.1	0.0	0.0	0.1	0.1	0.1	0.07	0.05	6
P ₂ O ₅	0.08	0.04	0.06	0.08	0.12	0.12	0.08	0.03	6
S	Below detection limit								

ROCK TYPE: RIGHTEYE PLUTON (Map unit 6)

Oxide (%)	Most freq.		10%	Median	90%	Maximum	Mean	Std dev.	Number
	value	Minimum							
SiO ₂	77.0	66.2	70.6	71.9	77.0	77.0	71.86	3.05	8
TiO ₂	0.61	0.14	0.15	0.27	0.61	0.61	0.30	0.15	8
Al ₂ O ₃	15.5	11.5	12.6	14.5	15.5	15.5	13.99	1.34	8
Fe ₂ O ₃	1.2	0.4	0.5	0.8	1.2	1.2	0.81	0.34	8
FeO	4.4	0.8	1.1	1.6	4.4	4.4	1.89	1.13	8
MnO	0.05	0.04	0.04	0.05	0.11	0.11	0.06	0.02	8
MgO	0.60	0.30	0.30	0.60	3.14	3.14	0.88	0.93	8
CaO	3.90	1.95	2.03	2.83	3.90	3.90	2.76	0.64	8
Na ₂ O	5.30	3.00	3.10	4.30	5.30	5.30	4.03	0.79	8
K ₂ O	3.05	0.99	1.26	1.55	3.05	3.05	1.78	0.78	8
H ₂ O	0.8	0.6	0.6	0.8	1.3	1.3	0.79	0.24	8
CO ₂	1.3	0.0	0.0	0.0	1.3	1.3	0.21	0.45	8
P ₂ O ₅	0.07	0.04	0.04	0.07	0.13	0.13	0.07	0.04	8
S	0.23	0.00	0.00	0.00	0.23	0.23	0.04	0.08	8

ROCK TYPE: METAGABBRO (Map unit 5)

Oxide (%)	Most freq.		10%	Median	90%	Maximum	Mean	Std dev.	Number
	value	Minimum							
SiO ₂	62.6	42.6	46.5	49.5	62.6	62.6	49.93	5.57	9
TiO ₂	2.34	0.63	0.64	1.03	2.34	2.34	1.22	0.57	9
Al ₂ O ₃	15.9	11.0	11.5	13.8	15.9	15.9	13.63	1.58	9
Fe ₂ O ₃	13.7	0.0	1.5	3.1	13.7	13.7	4.01	3.95	9
FeO	11.5	5.5	6.1	8.3	12.6	12.6	9.09	2.61	9
MnO	0.27	0.12	0.17	0.20	0.33	0.33	0.21	0.06	9
MgO	14.00	3.08	4.03	6.47	14.00	14.00	7.39	3.73	9
CaO	12.80	1.26	2.11	9.22	12.80	12.80	7.88	3.83	9
Na ₂ O	2.69	0.50	0.70	2.10	2.69	2.69	1.73	0.78	9
K ₂ O	2.36	0.00	0.09	0.19	2.36	2.36	0.45	0.73	9
H ₂ O	6.1	2.4	2.8	3.6	6.1	6.1	3.72	1.13	9
CO ₂	0.2	0.0	0.0	0.2	4.9	4.9	0.69	1.59	9
P ₂ O ₅	0.16	0.05	0.06	0.15	0.38	0.38	0.15	0.10	9
S	0.18	0.00	0.00	0.00	0.18	0.18	0.05	0.07	9

Appendix 2 (cont'd.)

ROCK TYPE: QUETICO METASEDIMENTS (Map unit 4a)

Oxide (%)	Most freq. value	Minimum	10%	Median	90%	Maximum	Mean	Std dev.	Number
SiO ₂	65.2	56.0	58.7	65.0	74.8	74.8	64.07	4.73	14
TiO ₂	0.46	0.17	0.22	0.52	0.68	0.68	0.50	0.15	14
Al ₂ O ₃	16.2	11.3	11.8	15.6	17.6	17.6	15.06	1.84	14
Fe ₂ O ₃	0.8	0.3	0.4	0.9	1.7	1.7	0.89	0.42	14
FeO	4.4	1.2	3.2	4.4	6.0	6.0	4.18	1.19	14
MnO	0.19	0.05	0.06	0.13	0.19	0.19	0.12	0.05	14
MgO	2.63	0.50	1.21	2.70	4.38	4.38	2.51	0.92	14
CaO	9.10	1.34	1.83	3.52	9.10	9.10	3.80	2.04	14
Na ₂ O	4.26	2.04	2.08	3.43	4.26	4.26	3.32	0.74	14
K ₂ O	5.74	0.80	1.46	1.90	5.74	5.74	2.16	1.16	14
H ₂ O	2.2	0.2	1.0	1.9	2.5	2.5	1.71	0.64	14
CO ₂	1.0	0.0	0.0	0.3	8.2	8.2	1.29	2.21	14
P ₂ O ₅	0.14	0.06	0.07	0.14	0.28	0.28	0.14	0.05	14
S	0.12	0.00	0.00	0.06	0.37	0.37	0.10	0.11	14

ROCK TYPE: STEEP ROCK UPPER FELSIC UNIT (Map unit 3c)

Oxide (%)	Most freq. value	Minimum	10%	Median	90%	Maximum	Mean	Std dev.	Number
SiO ₂	71.2	47.4	56.5	60.8	66.9	71.2	60.29	5.20	15
TiO ₂	0.89	0.65	0.68	0.78	1.20	1.59	0.88	0.25	15
Al ₂ O ₃	14.9	13.0	14.1	14.9	15.9	16.0	14.88	0.85	15
Fe ₂ O ₃	1.3	0.0	1.1	2.0	3.1	3.7	1.91	0.98	15
FeO	4.5	0.0	3.6	4.4	6.4	10.9	4.53	2.50	15
MnO	0.14	0.04	0.10	0.14	0.22	0.27	0.14	0.06	15
MgO	7.59	0.38	2.27	3.37	4.73	7.59	3.48	1.59	15
CaO	10.00	2.65	3.45	6.05	8.71	10.00	5.71	2.00	15
Na ₂ O	5.54	0.29	2.87	3.49	4.83	5.54	3.51	1.27	15
K ₂ O	1.71	0.12	0.50	0.87	1.48	1.71	0.91	0.46	15
H ₂ O	2.4	0.7	1.6	2.4	4.1	4.5	2.39	0.96	15
CO ₂	4.6	0.0	0.0	0.4	3.2	4.6	1.01	1.36	15
P ₂ O ₅	0.17	0.14	0.16	0.23	0.33	0.55	0.24	0.10	15
S	0.03	0.00	0.00	0.00	0.02	0.03	0.00	0.01	15

ROCK TYPE: FINLAYSON UPPER FELSIC UNIT (Map unit 3c)

Oxide (%)	Mean	Number	Data list			
SiO ₂	70.50	4	68.4	76.7	69.4	67.5
TiO ₂	0.32	4	0.32	0.22	0.47	0.28
Al ₂ O ₃	14.85	4	16.4	12.8	15.7	14.5
Fe ₂ O ₃	0.38	4	0.2	0.4	0.4	0.5
FeO	1.18	4	1.1	0.5	1.6	1.5
MnO	0.04	4	0.03	0.03	0.04	0.04
MgO	0.98	4	0.68	0.38	2.07	0.80
CaO	2.92	4	4.57	2.20	1.20	3.71
Na ₂ O	2.95	4	2.50	3.20	5.90	0.20
K ₂ O	3.10	4	2.22	2.00	0.62	7.57
H ₂ O	1.13	4	1.3	0.7	1.2	1.3
CO ₂	1.75	4	1.7	1.7	0.8	2.8
P ₂ O ₅	0.10	4	0.09	0.08	0.14	0.09
S	0.02	4	0.02	0.00	0.06	0.00

Appendix 2 (cont'd.)

ROCK TYPE: PERCH UPPER FELSIC UNIT (Map unit 3c)

Oxide (%)	Mean	Number	Data list	
SiO ₂	70.6	2	76.3	64.9
TiO ₂	0.42	2	0.04	0.80
Al ₂ O ₃	15.1	2	14.0	16.1
Fe ₂ O ₃	1.0	2	0.3	1.8
FeO	2.1	2	0.4	3.8
MnO	0.06	2	0.02	0.09
MgO	2.49	2	0.57	4.41
CaO	3.54	2	4.00	3.08
Na ₂ O	2.18	2	2.66	1.70
K ₂ O	1.60	2	1.0	2.2
H ₂ O	1.60	2	1.0	2.2
CO ₂	0.2	2	0.4	0.0
P ₂ O ₅	0.09	2	0.00	0.18
S	0.03	2	0.05	0.00

ROCK TYPE: STEEP ROCK LOWER MAFIC UNIT (Map unit 3b)

Oxide (%)	Most freq. value	Minimum	10%	Median	90%	Maximum	Mean	Std dev.	Number
SiO ₂	48.4	42.1	46.0	49.1	55.3	61.3	49.90	3.89	29
TiO ₂	0.87	0.51	0.60	0.79	1.21	1.67	0.85	0.26	29
Al ₂ O ₃	15.7	12.1	12.9	14.7	15.8	18.4	14.52	1.33	29
Fe ₂ O ₃	2.4	0.8	1.4	2.4	4.4	4.7	2.52	1.05	29
FeO	7.1	1.6	5.6	7.1	9.3	11.2	7.05	1.78	29
MnO	0.21	0.11	0.16	0.21	0.26	0.29	0.21	0.04	29
MgO	7.21	2.98	4.04	6.11	8.38	12.10	6.32	2.13	29
CaO	13.20	3.51	7.78	10.40	14.20	16.60	10.72	2.74	29
Na ₂ O	1.30	0.00	0.80	2.00	3.87	4.41	2.04	1.17	29
K ₂ O	0.05	0.00	0.00	0.05	0.72	1.14	0.18	0.30	29
H ₂ O	3.6	1.5	2.0	3.3	4.0	5.0	3.23	0.78	29
CO ₂	0.2	0.0	0.2	1.8	6.5	7.8	2.64	2.56	29
P ₂ O ₅	0.07	0.03	0.04	0.07	0.11	0.53	0.09	0.09	29
S	0.04	0.00	0.00	0.04	0.21	0.33	0.07	0.09	29

ROCK TYPE: FINLAYSON LOWER MAFIC UNIT (Map unit 3b)

Oxide (%)	Most freq. value	Minimum	10%	Median	90%	Maximum	Mean	Std dev.	Number
SiO ₂	55.2	46.3	46.8	50.1	53.5	55.2	50.22	2.45	17
TiO ₂	2.26	0.49	0.65	0.82	1.24	2.26	0.91	0.40	17
Al ₂ O ₃	13.4	10.6	12.4	14.1	16.9	17.6	14.06	1.87	17
Fe ₂ O ₃	3.2	0.9	1.8	2.3	3.4	3.9	2.43	0.82	17
FeO	7.4	4.4	5.4	7.7	10.5	10.8	7.56	1.75	17
MnO	0.21	0.17	0.19	0.22	0.29	0.29	0.23	0.04	17
MgO	9.40	3.02	4.68	5.50	8.55	9.40	6.13	1.75	17
CaO	14.50	4.73	7.92	11.50	13.90	14.50	10.72	2.69	17
Na ₂ O	2.00	0.00	0.90	1.60	2.10	2.50	1.51	0.63	17
K ₂ O	0.15	0.00	0.00	0.12	0.97	1.04	0.23	0.35	17
H ₂ O	4.3	1.3	1.7	2.7	4.3	4.6	2.76	1.00	17
CO ₂	0.9	0.0	0.1	2.3	7.9	11.7	3.29	3.23	17
P ₂ O ₅	0.11	0.05	0.06	0.08	0.11	0.27	0.09	0.05	17
S	0.05	0.00	0.00	0.07	0.25	0.29	0.10	0.11	17

Appendix 2 (cont'd.)

ROCK TYPE: FINALYSON AMPHIBOLITE GRADE MAFIC METAVOLCANIC ROCKS (Map unit 3b)

Oxide (%)	Most freq. value	Minimum	10%	Median	90%	Maximum	Mean	Std dev.	Number
SiO ₂	63.4	40.9	48.9	56.7	63.4	63.4	53.38	7.74	6
TiO ₂	1.05	0.39	0.66	0.90	1.05	1.05	0.79	0.25	6
Al ₂ O ₃	16.5	15.2	15.8	16.1	16.5	16.5	15.95	0.44	6
Fe ₂ O ₃	2.1	1.1	1.8	2.1	4.1	4.1	2.50	1.18	6
FeO	9.0	1.6	2.5	5.0	9.0	9.0	4.78	2.66	6
MnO	0.16	0.12	0.16	0.18	0.26	0.26	0.18	0.05	6
MgO	9.51	2.13	2.59	3.60	9.51	9.51	4.22	2.68	6
CaO	22.90	4.84	10.10	11.40	22.90	22.90	12.31	5.99	6
Na ₂ O	1.50	0.00	0.70	1.50	5.10	5.10	1.63	1.79	6
K ₂ O	1.10	0.02	0.02	0.17	1.10	1.10	0.28	0.42	6
H ₂ O	2.6	0.8	1.5	2.3	2.6	2.6	1.90	0.70	6
CO ₂	5.9	0.0	0.2	2.4	5.9	5.9	2.18	2.24	6
P ₂ O ₅	0.10	0.07	0.09	0.10	0.26	0.26	0.12	0.07	6
S	0.02	0.00	0.00	0.02	0.16	0.16	0.04	0.06	6

ROCK TYPE: PERCH LOWER MAFIC UNIT (Map unit 3b)

Oxide (%)	Mean	Number	Data list	
SiO ₂	50.0	2	47.7	52.3
TiO ₂	0.95	2	1.01	0.88
Al ₂ O ₃	15.0	2	16.0	13.9
Fe ₂ O ₃	4.0	2	3.8	4.2
FeO	7.5	2	8.0	6.9
MnO	0.20	2	0.21	0.19
MgO	6.18	2	6.48	5.87
CaO	11.80	2	11.90	11.70
Na ₂ O	1.43	2	1.61	1.24
K ₂ O	0.05	2	0.04	0.05
H ₂ O	3.7	2	4.0	3.3
CO ₂	0.3	2	4.0	3.3
P ₂ O ₅	0.07	2	0.07	0.07
S	0.07	2	0.03	0.10

ROCK TYPE: DISMAL ASHROCK FORMATION (Map unit 3a)

Oxide (%)	Mean	Number	Data list				
SiO ₂	40.16	5	42.0	42.6	38.8	37.4	40.00
TiO ₂	1.52	5	1.83	1.69	1.38	1.36	1.36
Al ₂ O ₃	4.81	5	5.5	5.3	4.7	4.28	4.28
Fe ₂ O ₃	5.40	5	5.1	5.2	3.9	6.5	6.3
FeO	11.34	5	12.8	12.9	11.4	9.4	10.2
MnO	0.32	5	0.25	0.27	0.31	0.41	0.38
MgO	19.26	5	20.40	20.30	16.70	19.10	19.80
CaO	7.55	5	3.35	3.85	12.20	9.80	8.53
Na ₂ O	0.11	5	0.20	0.10	0.00	0.13	0.13
K ₂ O	0.10	5	0.17	0.01	0.16	0.06	0.12
H ₂ O	5.18	5	6.6	5.6	5.0	3.5	5.2
CO ₂	3.60	5	0.6	2.5	6.0	5.4	3.5
P ₂ O ₅	0.11	5	0.12	0.11	0.12	0.10	0.11
S	0.06	5	0.29	0.00	0.00	0.00	0.00

Appendix 2 (cont'd.)

ROCK TYPE: MOSHER CARBONATE FORMATION (Map unit 2b)

Oxide (%)	Mean	Number	Data list	
SiO ₂	0.55	2	0.8	0.3
TiO ₂	0.01	2	0.02	0.00
Al ₂ O ₃	0.11	2	0.1	0.1
Fe ₂ O ₃	0.15	2	0.2	0.1
FeO	0.35	2	0.0	0.7
MnO	1.18	2	1.47	0.88
MgO	0.76	2	0.80	0.71
CaO	53.46	2	52.91	54.00
Na ₂ O	Below detection limit			
K ₂ O	0.03	2	0.03	0.02
H ₂ O	0.15	2	0.3	0.0
CO ₂	43.90	2	44.2	43.6
P ₂ O ₅	Below detection limit			
S	0.06	2	0.11	0.00

ROCK TYPE: WAGITA FORMATION (Map unit 2a)

Oxide (%)	Mean	Number	Data list
SiO ₂	74.60	1	74.6
TiO ₂	0.85	1	0.85
Al ₂ O ₃	14.70	1	14.7
Fe ₂ O ₃	Below detection limit		
FeO	1.10	1	1.1
MnO	0.03	1	0.03
MgO	0.43	1	0.43
CaO	1.31	1	1.31
Na ₂ O	1.60	1	1.60
K ₂ O	3.57	1	3.57
H ₂ O	1.40	1	1.4
CO ₂	1.10	1	1.1
P ₂ O ₅	0.06	1	0.06
S	Below detection limit		

ROCK TYPE: MAFIC TONALITE GNEISS (Map unit 1d)

Oxide (%)	Mean	Number	Data list		
SiO ₂	65.70	3	62.3	71.4	63.4
TiO ₂	0.48	3	0.66	0.23	0.55
Al ₂ O ₃	14.13	3	14.5	14.9	13.0
Fe ₂ O ₃	1.77	3	1.9	0.7	2.7
FeO	4.00	3	5.3	1.6	5.1
MnO	0.09	3	0.11	0.04	0.12
MgO	3.07	3	4.40	0.80	4.00
CaO	4.51	3	4.39	2.86	6.27
Na ₂ O	3.17	3	2.60	3.90	3.00
K ₂ O	2.05	3	2.32	2.79	1.05
H ₂ O	1.23	3	1.8	0.7	1.2
CO ₂	0.03	3	0.0	0.1	0.0
P ₂ O ₅	0.05	3	0.03	0.05	0.07
S	0.03	3	0.04	0.04	0.00

Appendix 2 (cont'd.)

ROCK TYPE: TONALITE GNEISS (Map unit 1c)

Oxide (%)	Mean	Number	Data list				
SiO ₂	72.16	5	69.0	72.1	71.6	72.7	75.4
TiO ₂	0.24	5	0.29	0.22	0.21	0.21	0.26
Al ₂ O ₃	14.68	5	14.9	15.2	15.9	14.4	13.0
Fe ₂ O ₃	0.62	5	1.0	0.6	0.0	0.7	0.8
FeO	1.42	5	1.7	1.1	1.6	1.0	1.7
MnO	0.03	5	0.05	0.03	0.02	0.02	0.05
MgO	0.64	5	0.90	0.50	0.50	0.40	0.90
CaO	2.71	5	3.03	2.64	2.82	2.72	2.32
Na ₂ O	4.52	5	4.30	4.90	5.20	4.50	3.70
K ₂ O	1.65	5	1.93	1.68	1.50	1.32	1.82
H ₂ O	0.74	5	0.9	0.9	0.60	0.6	0.7
CO ₂	0.06	5	0.1	0.1	0.0	0.1	0.0
P ₂ O ₅	0.05	5	0.07	0.05	0.06	0.06	0.00
S	0.01	5	0.00	0.00	0.00	0.03	0.00

ROCK TYPE: "OLD" TONALITE (Map unit 1b)

Oxide (%)	Most freq.			Median	90%	Maximum	Mean	Std dev.	Number
	value	Minimum	10%						
SiO ₂	72.3	57.3	58.8	71.4	73.4	73.4	68.42	5.78	12
TiO ₂	0.20	0.14	0.18	0.26	0.88	0.88	0.34	0.22	12
Al ₂ O ₃	15.0	12.8	13.5	15.0	17.1	17.1	14.96	1.35	12
Fe ₂ O ₃	0.5	0.3	0.4	0.5	4.1	4.1	1.05	1.12	12
FeO	1.7	0.0	1.1	1.7	4.2	4.2	2.08	1.31	12
MnO	0.03	0.02	0.03	0.05	0.11	0.11	0.06	0.03	12
MgO	4.03	0.40	0.50	0.85	4.03	4.03	1.47	1.31	12
CaO	3.30	0.37	2.00	2.63	7.46	7.46	3.17	2.03	12
Na ₂ O	5.90	1.59	3.20	4.50	5.90	5.90	4.33	1.16	12
K ₂ O	1.27	0.26	0.36	1.27	3.56	3.56	1.29	0.88	12
H ₂ O	1.1	0.6	0.6	1.1	2.4	2.4	1.22	0.64	12
CO ₂	4.5	0.0	0.0	0.4	4.5	4.5	0.86	1.33	12
P ₂ O ₅	0.12	0.04	0.05	0.08	0.28	0.28	0.11	0.08	12
S	0.03	0.00	0.00	0.00	0.03	0.03	0.00	0.01	12

ROCK TYPE: MAFIC TONALITE (Map unit 1a)

Oxide (%)	Mean	Number	Data list				
SiO ₂	64.15	4	62.1	66.3	67.0	61.2	
TiO ₂	0.67	4	0.73	0.72	0.56	0.65	
Al ₂ O ₃	15.10	4	16.4	14.7	15.3	14.0	
Fe ₂ O ₃	2.00	4	2.1	1.7	1.3	2.9	
FeO	3.73	4	4.0	3.0	3.3	4.6	
MnO	0.09	4	0.09	0.06	0.08	0.12	
MgO	2.30	4	2.50	1.40	1.30	3.98	
CaO	4.81	4	5.76	2.21	4.09	7.16	
Na ₂ O	3.77	4	4.30	3.90	3.90	2.97	
K ₂ O	1.35	4	0.84	2.14	1.73	0.69	
H ₂ O	1.50	4	1.1	2.1	0.9	1.9	
CO ₂	0.45	4	0.0	1.5	0.2	0.1	
P ₂ O ₅	0.22	4	0.17	0.22	0.14	0.33	
S	0.03	4	0.04	0.04	0.00	0.04	

APPENDIX 3

Table A3. Trace element geochemistry. Where the number of analyses is less than 6, each analysis is listed and the mean given. Mean, minimum, and maximum values are given for larger numbers of analyses.

ROCK TYPE: GABBRO DYKES (Map unit 9)					
Element (ppm)	Mean value	Number	Data list		
Ba	283.33	3	290.	240.	320.
Be	1.23	3	1.2	1.2	1.3
Co	47.67	3	47.	48.	48.
Cr	53.67	3	47.	54.	60.
Cu	103.33	3	100.	110.	100.
La	20.67	3	20.	21.	21.
Ni	59.33	3	59.	59.	60.
Pb	7.67	3	7.	10.	6.
V	283.33	3	280.	280.	290.
Yb	2.37	3	2.3	2.3	2.5
Zn	105.00	3	100.	95.	120.
Li					
As	10.00	3	0.	4.	26
Br					
Mo	3.67	3	5.	2.	4.
Nb	16.00	3	16.	15.	17.
Rb	31.67	3	22.	10.	63.
Sr	216.67	3	200.	250.	200.
Th	0.67	3	0.	0.	2.
U					
Y	29.33	3	30.	29.	29.
Zr	120.00	3	120.	120.	120.
ROCK TYPE: WHITE OTTER BATHOLITH (Map unit 8c)					
Element (ppm)	Mean value	Minimum	Maximum	Number	
Ba	814.00	470.	1300.	30	
Be	1.31	1.0	1.8	30	
Co	4.07	1.	6	30	
Cr	6.10	4.	10.	30	
Cu	7.03	4.	14.	30	
La	31.83	13.	75.	30	
Ni	24.20	16.	33.	30	
Pb	23.14	15.	34.	28	
V	7.40	3.	13.	30	
Yb	0.45	0.1	1.8	30	
Zn	36.10	8.	56.	30	
Li					
As	6.46	0.	28.	28	
Br	0.71	0.	6.	28	
Mo	0.39	0.	6.	28	
Nb	3.93	0.00	15.	30	
Rb	178.93	72.	260.	30	
Sr	314.80	168.	620.	30	
Th	15.82	0.00	55.	28	

Appendix 3 (cont'd.)

ROCK TYPE: WHITE OTTER BATHOLITH (Map unit 8c) (cont'd.)

Element (ppm)	Mean value	Minimum	Maximum	Number
U	1.29	0.00	36.	28
Y	4.83	0.	18.	30
Zr	124.70	54.	230.	30

ROCK TYPE: BEWAG STOCK (Map unit 8c)

Element (ppm)	Mean value	Number	Data list	
Ba	800.00	2	770.	830.
Be	4.05	2	4.4	3.5
Co	7.50	2	8.	7.
Cr	14.50	2	14.	15.
Cu	13.00	2	12.	14.
La	41.50	2	34.	49.
Ni	31.50	2	31.	32.
Pb	37.50	2	42.	33.
V	23.00	2	23.	23.
Yb	0.90	2	0.9	0.9
Zn	47.50	2	49.	46.
Li				
As				
Br				
Mo				
Nb				
Rb				
Sr				
Th				
U				
Y				
Zr	9.50	2	9.	10.

ROCK TYPE: MARGARET STOCK (Map unit 8b)

Element (ppm)	Mean value	Number	Data list	
Ba	749.50	2	518.	981.
Be	0.75	2	0.7	0.8
Co	10.50	2	13.	8.
Cr	19.50	2	20.	19.
Cu	29.50	2	41.	18.
La	43.00	2	47.	39.
Ni	36.00	2	32.	40.
Pb				
V	47.50	2	55.	40.
Yb	0.70	2	0.6	0.8
Zn	50.00	2	62.	38.
Li				
As				
Br				
Mo				
Nb	0.00	2	0.	0.
Rb	54.00	2	54.	54.

Appendix 3 (cont'd.)

ROCK TYPE: MARGARET STOCK (Map unit 8b) (cont'd)

Element (ppm)	Mean value	Number	Data list	
Sr	300.00	2	221.	379.
Th				
U				
Y	.00	2	0.	0.
Zr	147.50	2	155.	140.

ROCK TYPE: DIVERSION STOCK (Map unit 8b)

Element (ppm)	Mean value	Minimum	Maximum	Number
Ba	566.09	300.	900.	11
Be	0.93	0.7	1.2	11
Co	9.09	5.	15.	11
Cr	12.18	8.	19.	11
Cu	27.00	0.	48.	11
La	30.18	11.	43.	11
Ni	33.18	18.	46.	11
Pb	8.10	4.	10.	10
V	35.70	12.	56.	11
Yb	1.39	0.3	2.2	11
Zn	47.91	20.	69.	11
Li	8.20	1.	13.	10
As	23.40	0.	67.	10
Br	2.40	0.	6.	10
Mo	2.20	0.	7.	10
Nb	7.45	0.	13.	11
Rb	68.64	35.	99.	11
Sr	198.45	97.	330.	11
Th	9.40	0.	11.	10
U	1.00	0.	10.	10
Y	5.00	0.	10.	10
Zr	106.36	67.	130.	11

ROCK TYPE: LITTLE EYE STOCK (Map unit 7)

Element (ppm)	Mean value	Number	Data list	
			Rim	Core
Ba	854.50	2	331.	1378.
Be	1.00	2	0.7	1.30
Co	41.50	2	21.	62.
Cr	50.00	2	59.	41.
Cu	114.50	2	39.	190.
La	57.50	2	15.	100.
Ni	84.00	2	58.	110.
Pb				
V	213.50	2	97.	330.
Yb	1.35	2	0.9	1.8
Zn	84.50	2	49.	120.
Li				
As				
Br				
Mo				
Nb				
Rb	36.00	2	9.	63.

Appendix 3 (cont'd.)

ROCK TYPE: LITTLE EYE STOCK (Map unit 7) (cont'd.)				
Element (ppm)	Mean value	Number	Data list	
			Rim	Core
Sr	944.50	2	1386.	503.
Th				
U				
Y	27.50	2	0.	55.
Zr	125.5	2	152.	99.
ROCK TYPE: "YOUNG" TONALITE (Map unit 6)				
Element (ppm)	Mean value	Minimum	Maximum	Number
Ba	335.50	245.	503.	6
Be	0.70	0.5	0.8	6
Co	7.67	4.	10.	6
Cr	11.67	7.	16.	6
Cu	23.33	8.	81.	6
La	15.17	7.	27.	6
Ni	21.17	13.	29.	6
Pb				
V	31.00	11.	49.	6
Yb	0.35	0.1	0.9	6
Zn	44.50	30.	61.	6
Li				
As				
Br				
Mo				
Nb				
Rb	46.17	31.	80.	6
Sr	420.50	265.	582.	6
Th				
U				
Y				
Zr	134.83	93.	182.	6
ROCK TYPE: RIGHT EYE PLUTON (Map unit 6)				
Element (ppm)	Mean value	Minimum	Maximum	Number
Ba	446.25	146.	838.	8
Be	0.99	0.6	1.3	8
Co	9.00	4.	26.	8
Cr	20.50	8.	94.	8
Cu	24.38	5.	64.	8
La	24.13	11.	56.	8
Ni	32.50	12.	97.	8
Pb	7.33	5.	9.	3
V	33.63	10.	120.	8
Yb	1.39	0.4	2.4	8
Zn	54.00	27.	96.	8
Li	35.33	30.	43.	3
As	13.33	0.	34.	3
Br	2.67	0.	7.	3
Mo	1.00	0.	3.	3
Nb	2.50	0.	5.	8
Rb	71.50	37.	161.	8
Sr	267.88	160.	640.	8
Th	6.33	2.	17.	3
U	0.00	0.	0.	3
Y	5.25	0.	16.	8
Zr	175.25	96.	430.	8

Appendix 3 (cont'd.)

ROCK TYPE: METAGABBRO (Map unit 5)

Element (ppm)	Mean value	Minimum	Maximum	Number
Ba	142.22	30.	710.	9
Be	0.71	0.3	1.1	9
Co	44.00	23.	53.	9
Cr	123.22	0.	720.	9
Cu	77.44	0.	190.	9
La	19.00	0.	52.	9
Ni	106.33	23.	380.	9
Pb	2.78	0.	14.	9
V	247.78	120.	390.	9
Yb	2.39	1.0	4.5	9
Zn	107.56	77.	150.	9
Li	25.00	3.	80.	7
As	4.75	0.	12.	4
Br	.50	0.	2.	4
Mo	4.00	2.	6.	4
Nb	7.50	3.	12.	4
Rb	13.00	0.	42.	4
Sr	127.50	20.	200.	4
Th	0.00	0.	0.	4
U	0.00	0.	0.	4
Y	17.50	11.	25.	4
Zr	98.75	32.	200.	4

ROCK TYPE: QUETICO METASEDIMENTS (Map unit 4a)

Element (ppm)	Mean value	Minimum	Maximum	Number
Ba	617.57	100.	1800.	14
Be	1.23	0.5	2.0	14
Co	21.00	8.	32.	14
Cr	119.43	10.	290.	14
Cu	49.57	18.	74.	14
La	27.57	11.	50.	14
Ni	75.93	36.	150.	14
Pb	26.15	1.	91.	13
V	93.50	23.	140.	14
Yb	1.66	1.0	3.1	14
Zn	77.57	45.	120.	14
Li	28.00	9.	35.	4
As	16.50	0.	51.	4
Br	1.50	0.	6.	4
Mo	3.25	2.	5.	4
Nb	6.00	0.	10.	5
Rb	56.60	11.	130.	5
Sr	301.60	210.	490.	5
Th	0.25	0.	1.	4
U	0.00	0.	0.	4
Y	12.79	1.	34.	14
Zr	127.20	96.	160.	5

Appendix 3 (cont'd.)

ROCK TYPE: STEEP ROCK UPPER FELSIC UNIT (Map unit 3c)

Element (ppm)	Mean value	Minimum	Maximum	Number
Ba	318.67	20.	620.	15
Be	0.93	0.8	1.2	15
Co	22.33	15.	35.	15
Cr	77.87	33.	120.	15
Cu	35.07	0.	58.	15
La	30.87	22.	50.	15
Ni	62.33	32.	93.	15
Pb	8.80	0.	22.	15
V	128.53	68.	190.	15
Yb	2.34	1.4	4.	15
Zn	91.47	50.	150.	15
Li	14.37	6.	37.	8
As	4.86	0.	35.	14
Br	0.47	0.	6.	14
Mo	1.80	0.	5.	14
Nb	10.92	8.	15.	14
Rb	13.20	0.	36.	14
Sr	302.14	140.	510.	14
Th	0.07	0.	1.	14
U	0.00	0.	0.	14
Y	24.00	19.	31.	14
Zr	202.15	170.	260.	14

ROCK TYPE: FINALYSON UPPER FELSIC UNIT (Map unit 3c)

Element (ppm)	Mean value	Number	Data list			
Ba	527.50	4	670.	400.	160.	880.
Be	0.70	4	1.	0.7	0.4	0.7
Co	6.75	4	8.	4.	9.	6.
Cr	21.00	4	17.	10.	41.	16.
Cu	15.50	4	19.	7.	16.	20.
La	16.75	4	22.	14.	16.	15.
Ni	30.50	4	39.	19.	28.	36.
Pb	2.25	4	3.	1.	0.	5.
V	44.75	4	42.	26.	75.	36.
Yb	0.65	4	0.6	0.5	0.9	0.6
Zn	30.00	4	17.	27.	46.	30.
Li	6.75	4	6.	6.	6.	9.
As						
Br						
Mo						
Nb						
Rb						
Sr						
Th						
U						
Y						
Zr						

Appendix 3 (cont'd.)

ROCK TYPE: PERCH UPPER FELSIC UNIT (Map unit 3c)

Element (ppm)	Mean value	Number	Data list	
Ba	285.50	2	221.	350.
Be	0.95	2	1.	0.9
Co	9.50	2	1.	18.
Cr	20.50	2	4.	37.
Cu	11.50	2	6.	17.
La	13.00	2	10.	16.
Ni	24.00	2	8.	40.
Pb	7.00	2	0.	14.
V	70.00	2	0.	140.
Yb	1.70	2	1.9	1.5
Zn	48.00	2	39.	57.
Li				
As	0.00	2	0.	0.
Br	0.00	2	0.	0.
Mo	2.00	2	0.	4.
Nb	5.00	2	3.	7.
Rb	76.00	2	96.	56.
Sr	159.50	2	69.	250.
Th	0.00	2	0.	0.
U	0.00	2	0.	0.
Y	13.00	2	12.	14.
Zr	106.00	2	62.	150.

ROCK TYPE: STEEP ROCK LOWER MAFIC UNIT (Map unit 3b)

Element (ppm)	Mean value	Minimum	Maximum	Number
Ba	55.86	0.	400.	29
Be	0.52	0.2	1.1	29
Co	48.76	33.	76.	29
Cr	306.93	0.	920.	29
Cu	122.10	21.	180.	29
La	9.62	1.	60.	29
Ni	130.17	17.	320.	29
Pb	7.03	0.	24.	29
V	252.41	200.	370.	29
Yb	1.57	0.8	3.6	29
Zn	91.21	66.	130.	29
Li	11.35	3.	35.	17
As	5.67	0.	19.	15
Br	0.07	0.	1.	15
Mo	4.60	1.	8.	15
Nb	5.93	4.	16.	15
Rb	3.73	0.	29.	15
Sr	125.00	30.	420.	15
Th	0.00	0.	0.	15
U	0.00	0.	0.	15
Y	14.40	9.	28.	15
Zr	50.93	25.	230.	15

Appendix 3 (cont'd.)

ROCK TYPE: FINLAYSON LOWER MAFIC UNIT (Map unit 3b)

Element (ppm)	Mean value	Minimum	Maximum	Number
Ba	98.82	10.	350.	17
Be	0.62	0.4	1.3	17
Co	45.65	38.	58.	17
Cr	284.65	21.	850.	17
Cu	86.00	11.	170.	17
La	13.47	7.	42.	17
Ni	120.94	38.	230.	17
Pb	0.00	0.	0.	17
V	271.18	190.	390.	17
Yb	1.68	1.0	3.7	17
Zn	83.24	57.	120.	17
Li	9.35	1.	21.	17
As				
Br				
Mo				
Nb				
Rb				
Sr				
Th				
U				
Y				
Zr				

ROCK TYPE: FINLAYSON LAKE AMPHIBOLITE GRADE MAFIC METAVOLCANIC ROCKS (Map unit 3b)

Element (ppm)	Mean value	Minimum	Maximum	Number
Ba	88.33	30.	190.	6
Be	0.67	0.6	0.9	6
Co	34.33	14.	47.	6
Cr	140.17	22.	240.	6
Cu	82.00	30.	30.	6
La	17.00	12.	30.	6
Ni	89.00	33.	160.	6
Pb	0.50	0.	3.	6
V	219.83	69.	300.	6
Yb	1.57	0.9	2.1	6
Zn	71.33	46.	84.	6
Li	9.00	3.	14.	6
As				
Br				
Mo				
Nb				
Rb				
Sr				
Th				
U				
Y				
Zr				

Appendix 3 (cont'd.)

ROCK TYPE: PERCH LOWER MAFIC UNIT (Map unit 3b)

Element (ppm)	Mean value	Number	Data list	
Ba	5.	2	10.	0.
Be	0.6	2	0.7	0.4
Co	44.	2	45.	43.
Cr	195.	2	260.	130.
Cu	130.	2	120.	140.
La	4.	2	5.	3.
Ni	107.	2	130.	84.
Pb	3.	2	12.	6.
V	280.	2	290.	270.
Yb	1.9	2	2.1	1.6
Zn	86.	2	94.	77.
Li				
As	7.	2	13.	0.
Br	0.	2	0.	0.
Mo	5.	2	5.	4.
Nb	6.	2	6.	5.
Rb	0.	2	0.	0.
Sr	240.	2	280.	200.
Th	0.	2	0.	0.
U	0.	2	0.	0.
Y	18.	2	18.	17.
Zr	51.	2	55.	47.

ROCK TYPE: DISMAL ASHROCK FORMATION (Map unit 3a)

Element (ppm)	Mean value	Number	Data list				
Ba	34.00	5	60.	30.	50.	10.	20.
Be	1.10	5	1.1	1.0	1.4	0.9	1.1
Co	107.40	5	120.	110.	97.	110.	100.
Cr	1540.00	5	1900.	1700.	1400.	1300.	1400.
Cu	260.00	5	300.	280.	220.	250.	250.
La	24.80	5	26.	33.	25.	20.	20.
Ni	1032.00	5	1200.	1100.	870.	1000.	990.
Pb	1.00	5	0.	0.	0.	4.	1.
V	214.00	5	240.	230.	200.	200.	200.
Yb	1.96	5	2.0	2.0	1.7	2.0	2.1
Zn	109.80	5	110.	120.	99.	110.	110.
Li	32.20	5	43.	30.	23.	35.	30.
As	20.00	2				0.	40.
Br	0.00	2				0.	0.
Mo	8.50	2				5.	12.
Nb	15.50	2				18.	13.
Rb	0.00	2				0.	0.
Sr	71.50	2				110.	33.
Th	0.00	2				0.	0.
U	0.50	2				0.	1.
Y	5.50	2				8.	3.
Zr	55.50	2				82.	29.

Appendix 3 (cont'd.)

ROCK TYPE: MOSHER CARBONATE FORMATION (Map unit 2b)

Element (ppm)	Mean value	Number	Data list	
Ba	29.00	2	58.	0.
Be	0.50	2	0.5	0.5
Co	3.50	2	7.	0.
Cr	32.50	2	37.	28.
Cu	11.50	2	14.	9.
La	3.00	2	6.	0.
Ni	13.00	2	20.	6.
Pb	3.00	2	0.	6.
V	9.50	2	8.	11.
Yb	0.20	2	0.4	0.
Zn	8.00	2	9.	7.
Li	1.00	1		1.
As				
Br				
Mo	9.00	1		9.
Nb	3.50	2	0.	7.
Rb	3.00	2	6.	0.
Sr	55.00	2	74.	36.
Th				
U				
Y	1.00	2	0.	2.
Zr	1.50	2	0.	3.

ROCK TYPE: WAGITA FORMATION (Map unit 2a)

Element (ppm)	Mean value	Number	Data list	
Ba	580.00	1	580.	
Be	1.10	1	1.1	
Co	9.00	1	9.	
Cr	13.00	1	13.	
Cu				
La	88.00	1	88.	
Ni	31.00	1	31.	
Pb				
V	34.00	1	34.	
Yb	3.60	1	3.6	
Zn	82.00	1	82.	
Li				
As				
Br				
Mo				
Nb				
Rb				
Sr				
Th				
U				
Y	36.00	1	36.	
Zr				

Appendix 3 (cont'd.)

ROCK TYPE: MAFIC TONALITE GNEISS (Map unit 1d)							
Element (ppm)	Mean value	Number	Data list				
Ba	430.00	3	571.	520.	199.		
Be	0.83	3	0.8	0.8	0.9		
Co	22.33	3	33.	7.	27.		
Cr	196.00	3	350.	18.	220.		
Cu	34.33	3	53.	15.	35.		
La	13.67	3	24.	8.	9.		
Ni	94.67	3	160.	28.	96.		
Pb							
V	103.00	3	160.	29.	120.		
Yb	1.40	3	1.5	0.4	2.3		
Zn	70.33	3	100.	40.	71.		
Li							
As							
Br							
Mo							
Nb	0.00	3	0.	0.	0.		
Rb	77.33	3	56.	95.	81.		
Sr	196.67	3	226.	221.	143.		
Th							
U							
Y	14.67	3	4.	0.	40.		
Zr	109.67	3	122.	119.	88.		
ROCK TYPE: TONALITE GNEISS (Map unit 1c)							
Element (ppm)	Mean value	Number	Data list				
Ba	478.00	5	416.	528.	530.	541.	375.
Be	0.86	5	0.9	0.8	1.0	0.7	0.9
Co	5.80	5	8.	6.	5.	5.	5.
Cr	10.60	5	19.	9.	6.	8.	11.
Cu	17.20	5	11.	28.	12.	28.	7.
La	18.80	5	19.	13.	27.	16.	19.
Ni	22.20	5	28.	22.	21.	21.	19.
Pb							
V	19.40	5	32.	20.	18.	13.	14.
Yb	0.44	5	0.7	0.2	0.2	0.2	0.9
Zn	31.00	5	52.	20.	25.	16.	42.
Li							
As							
Br							
Mo							
Nb	0.20	5	0.	0.	0.	0.	1.
Rb	59.80	5	60.	46.	34.	91.	68.
Sr	330.60	5	231.	397.	399.	373.	253.
Th							
U							
Y	0.00	5	0.	0.	0.	0.	0.
Zr	155.80	5	144.	106.	110.	158.	261.

Appendix 3 (cont'd.)

ROCK TYPE: "OLD" TONALITE (Map unit 1b)

Element (ppm)	Mean value	Minimum	Maximum	Number
Ba	342.67	100.	600.	12
Be	0.77	0.4	1.4	12
Co	10.92	3.	31.	12
Cr	17.17	0.	91.	12
Cu	23.25	1.	70.	12
La	19.42	8.	34.	12
Ni	34.83	14.	110.	12
Pb	5.75	2.	9.	8
V	47.08	11.	140.	12
Yb	0.92	0.0	2.3	12
Zn	66.08	30.	120.	12
Li	15.14	3.	37.	7
As	15.28	0.	40.	7
Br	1.28	0.	4.	7
Mo	1.29	0.	4.	7
Nb	3.36	0.	18.	11
Rb	46.37	0.	93.	11
Sr	337.27	81.	760.	11
Th	0.00	0.	0.	7
U	0.00	0.	0.	7
Y	3.67	0.	18.	12
Zr	113.17	0.	260.	12

ROCK TYPE: MAFIC TONALITE (Map unit 1a)

Element (ppm)	Mean value	Number	Data list			
Ba	328.75	4	272.	321.	422.	300.
Be	0.78	4	0.8	0.7	0.9	0.7
Co	17.00	4	20.	9.	12.	27.
Cr	26.50	4	46.	9.	16.	35.
Cu	34.50	4	19.	23.	13.	83.
La	30.50	4	11	61.	27.	23.
Ni	46.50	4	50.	20.	25.	91.
Pb	3.00	1				3.
V	84.50	4	99.	50.	59.	130.
Yb	1.63	4	0.7	1.9	1.9	2.0
Zn	71.00	4	70.	51.	63.	100.
Li	15.00	1				15.
As	5.00	1				5.
Br	0.00	1				0.
Mo	4.00	1				4.
Nb	6.25	4	0.	14.	0.	11.
Rb	32.25	4	21.	39.	61.	8.
Sr	253.00	4	308.	122.	212.	370.
Th	0.00	1				0.
U	0.00	1				0.
Y	18.50	4	0.	35.	21.	18.
Zr	157.50	4	116.	303.	170.	41.

APPENDIX 4

Table A4. Rare earth element geochemistry. Where the number of analyses is less than 6, each analysis is listed and the mean is given. Median and mean statistics are given for larger numbers of analyses.

ROCK TYPE: GABBRO DYKES (Map unit 9)									
Element (ppm)	Mean value	Number	Data list						
La	19.67	3	20.	19.	20.				
Ce	39.33	3	40.	38.	40.				
Nd	23.67	3	22.	27.	22.				
Sm	4.53	3	4.7	4.2	4.7				
Eu	1.67	3	1.6	1.8	1.6				
Gd	5.47	3	5.2	5.9	5.3				
Dy	5.23	3	5.3	5.2	5.2				
Yb	2.67	3	2.6	2.7	2.7				
Y	29.33	3	30.	29.	29.				
ROCK TYPE: WHITE OTTER BATHOLITH (Map unit 8c)									
Element (ppm)	Most freq. value	Minimum	10%	Median	90%	Maximum	Mean	Std dev.	Number
La	23.	12.	14.	26.	62.	67.	30.00	15.14	30
Ce	51.	22.	28.	51.	110.	120.	55.17	26.28	30
Nd	14.	8.3	10.	16.	33.	43.	17.43	7.96	30
Sm	1.4	0.9	1.3	1.8	3.3	5.9	2.17	1.05	30
Eu	0.5	0.3	0.4	0.5	0.6	0.9	0.48	0.12	30
Gd	1.4	0.5	0.8	1.2	2.3	3.6	1.36	0.67	30
Dy	0.6	0.3	0.4	0.7	1.3	2.9	0.83	0.55	30
Yb	0.3	0.2	0.2	0.3	0.6	1.7	0.38	0.31	30
Y	3.2	1.9	2.8	4.1	7.7	18.	4.95	3.36	30
ROCK TYPE: EYE-DASHWA PLUTON (Map unit 8c)									
Element (ppm)	Most freq. value	Minimum	10%	Median	90%	Maximum	Mean	Std dev.	Number
La	64.08	44.97	49.28	56.15	64.08	65.36	56.10	6.03	20
Ce	114.31	82.46	84.86	100.42	113.54	114.31	100.18	9.87	20
Nd	42.82	35.31	38.32	41.35	45.30	47.20	41.15	2.95	20
Sm	5.88	5.15	5.29	5.88	6.39	7.14	5.81	0.45	20
Eu	1.28	1.13	1.20	1.31	1.41	1.85	1.33	0.15	20
Tb	0.46	0.26	0.33	0.47	0.61	0.66	0.46	0.11	20
Ho	0.57	0.19	0.27	0.57	1.15	2.28	0.64	0.45	20
Tm	0.12	0.03	0.05	0.12	0.21	0.27	0.12	0.06	20
Yb	1.05	0.69	0.81	1.04	1.40	1.51	1.04	0.19	20
Lu	0.16	0.10	0.14	0.16	0.20	0.28	0.16	0.04	20
ROCK TYPE: BEWAG STOCK (Map unit 8c)									
Element (ppm)	Mean value	Number	Data list						
La	36.00	2	28.	44.					
Ce	72.50	2	58.	87.					
Nd	29.00	2	24.	34.					
Sm	2.50	2	2.2	2.8					
Eu	0.95	2	0.8	1.1					
Gd	2.95	2	2.7	3.2					
Dy	1.80	2	0.7	0.7					
Yb	0.70	2	0.7	0.7					
Y	9.35	2	8.8	9.9					

Appendix 4 (cont'd.)

ROCK TYPE: DIVERSION STOCK (Map unit 8b)

Element (ppm)	Most freq. value	Minimum	10%	Median	90%	Maximum	mean	Std dev.	Number
La	27.	11.	14.	21.	28.	29.	21.64	6.28	11
Ce	53.	24.	29.	45.	56.	65.	44.82	13.11	11
Nd	25.	12.	12.	20.	25.	34.	20.00	6.83	11
Sm	5.2	1.6	2.0	3.2	4.8	5.2	3.26	1.14	11
Eu	0.4	0.3	0.4	0.5	0.9	0.9	0.56	0.20	11
Gd	1.9	1.0	1.1	1.7	2.5	3.1	1.78	0.63	11
Dy	1.6	0.8	0.8	1.6	2.2	2.3	1.53	0.55	11
Yb	1.1	0.4	0.5	0.9	1.1	1.1	0.76	0.32	11
Y	10.	5.0	5.1	10.	13.	14.	9.55	3.10	11

ROCK TYPE: MARGARET STOCK (Map unit 8b)

Element (ppm)	Mean value	Number	Data list	
			rim	core
La	45.00	2	49.	41.
Ce	89.50	2	95.	84.
Nd	36.00	2	37.	35.
Sm	4.30	2	5.1	3.5
Eu	1.15	2	1.2	1.1
Gd	3.00	2	2.9	3.1
Dy	2.10	2	1.9	2.3
Yb	0.90	2	0.7	1.1
Y	12.00	2	11.	13.

ROCK TYPE: LITTLE EYE STOCK (Map unit 7)

Element (ppm)	Mean value	Number	Data list	
			rim	core
La	63.00	2	16.	110.
Ce	153.00	2	36.	270.
Nd	92.00	2	24.	160.
Sm	14.25	2	3.5	25.0
Eu	4.05	2	1.6	6.5
Gd	11.40	2	3.8	19.0
Dy	6.05	2	2.5	9.6
Yb	1.30	2	0.6	2.0
Y	27.50	2	11.	44.

ROCK TYPE: "YOUNG" TONALITE (map unit 6)

Element (ppm)	Most freq. value	Minimum	10%	Median	90%	Maximum	Mean	Std dev.	Number
La	27.	7.9	8.5	14.	27.	27.	15.57	7.79	6
Ce	52.	14.	15.	25.	52.	52.	28.17	14.96	6
Nd	11.	6.7	10.	11.	22.	22.	12.45	5.23	6
Sm	2.4	0.3	0.5	1.3	2.4	2.4	1.25	0.85	6
Eu	0.9	0.3	0.3	0.6	0.9	0.9	0.55	0.26	6
Gd	3.0	0.6	1.1	1.3	3.0	3.0	1.50	0.83	6
Dy	2.4	0.4	0.6	0.9	2.4	2.4	1.10	0.74	6
Yb	1.1	0.2	0.2	0.4	1.1	1.1	0.47	0.34	6
Y	13.0	2.1	4.0	5.0	13.0	13.0	6.17	3.91	6

ROCK TYPE: RIGHTEYE PLUTON (Map unit 6)

Element (ppm)	Most freq. value	Minimum	10%	Median	90%	Maximum	Mean	Std dev.	Number
La	19.	9.	12.	19.	45.	45.	21.43	12.34	7
Ce	80.	19.	25.	36.	80.	80.	40.71	21.05	7

Appendix 4 (cont'd.)

ROCK TYPE: RIGHTEYE PLUTON (Map unit 6) (cont'd.)

Element (ppm)	Most freq. value	Minimum	10%	Median	90%	Maximum	Mean	Std dev.	Number
Nd	31.	9.5	12.	15.	31.	31.	16.79	7.14	7
Sm	5.1	0.9	1.3	2.3	5.1	5.1	2.83	1.63	7
Eu	0.6	0.3	0.4	0.6	1.1	1.1	0.59	0.25	7
Gd	3.3	1.1	1.4	2.3	3.3	3.3	2.17	0.81	7
Dy	3.4	1.3	1.5	2	3.4	3.4	2.26	0.86	7
Yb	1.1	0.8	1.0	1.1	2.1	2.1	1.36	0.48	7
Y	23.	8.0	9.	12.	23.	23.	14.00	5.48	7

ROCK TYPE: METAGABBRO (Map unit 5)

Element (ppm)	Most freq. value	Minimum	10%	Median	90%	Maximum	Mean	Std dev.	Number
La	3.0	2.0	3.0	4.3	55.	55.	12.80	17.61	9
Ce	120.0	6.0	7.0	16.	120.	120.	29.78	37.46	9
Nd	55.	4.5	5.3	15.	55.	55.	18.12	16.03	9
Sm	6.5	1.5	2.0	3.4	6.5	6.5	3.63	1.75	9
Eu	2.4	0.5	0.6	1.0	2.4	2.4	1.17	0.63	9
Gd	5.0	2.1	2.4	4.7	6.5	6.5	4.16	1.63	9
Dy	6.7	2.7	2.9	3.7	6.7	6.7	4.18	1.43	9
Yb	2.6	0.9	1.1	2.0	4.10	4.10	2.20	1.07	9
Y	41.	13.	15.	23.	41.	41.	23.67	9.58	9

ROCK TYPE: QUETICO METASEDIMENTS (Map unit 4a)

Element (ppm)	Most freq. value	Minimum	10%	Median	90%	Maximum	Mean	Std dev.	Number
La	22.	7.	8.7	22.	46.	46.	22.62	11.41	14
Ce	42.	15.	17.	42.	83.	83.	43.29	20.46	14
Nd	20.	7.9	11.	21.	38.	38.	21.71	8.91	14
Sm	6.4	0.8	1.2	3.2	6.4	6.4	3.25	1.69	14
Eu	1.0	0.3	0.5	1.0	2.0	2.0	1.01	0.49	14
Gd	3.4	1.0	1.5	3.1	6.3	6.3	3.07	1.43	14
Dy	2.7	1.1	1.2	2.5	5.9	5.9	2.66	1.34	14
Yb	1.9	0.5	0.6	1.4	3.1	3.1	1.44	0.72	14
Y	14.	6.	7.	14.	34.	34.	15.23	7.91	14

ROCK TYPE: STEEP ROCK UPPER FELSIC UNIT (Map unit 3c)

Element (ppm)	Most freq. value	Minimum	10%	Median	90%	Maximum	Mean	Std dev.	Number
La	26.	2.0	23.	26.	36.	36.	26.50	3.71	12
Ce	55.	48.	49.	56.	87.	87.	57.58	9.90	12
Nd	32.	23.	24.	28.	47.	47.	29.00	6.44	12
Sm	3.9	3.7	3.9	6.0	11.0	11.0	5.70	1.99	12
Eu	1.1	0.9	1.0	1.1	2.2	2.2	1.23	0.36	12
Gd	4.4	3.3	4.0	4.3	6.7	6.7	4.53	0.88	12
Dy	4.0	2.9	3.8	4.0	6.5	6.5	4.29	0.90	12
Yb	2.1	1.4	1.9	2.1	2.8	2.8	2.13	0.34	12
Y	25.	17.	22.	25.	36.	36.	25.33	4.91	12

ROCK TYPE: FINLAYSON UPPER FELSIC UNIT (Map unit 3c)

Element (ppm)	Mean value	Number	Data list
La	11.75	4	12. 13 11. 11.0
Ce	23.25	4	27. 21. 25. 20.0
Nd	11.35	4	14. 8.6 13. 9.8
Sm	1.73	4	1.9 1.2 2.4 1.4
Eu	0.58	4	0.9 0.3 0.7 0.4
Gd	1.53	4	2.1 1.0 1.8 1.2
Dy	1.13	4	1.3 0.7 1.7 0.8
Yb	0.55	4	0.5 0.4 0.9 0.4
Y	6.75	4	7.0 5.0 10.0 5.0

Appendix 4 (cont'd.)

ROCK TYPE: PERCH UPPER FELSIC UNIT (Map unit 3c)

Element (ppm)	Mean value	Number	Data list	
La	13.50	2	11.	16.
Ce	27.50	2	23.	32.
Nd	13.00	2	11.	15.
Sm	2.55	2	11.	15.
Eu	0.55	2	0.2	0.9
Gd	3.00	2	2.8	3.2
Dy	3.20	2	3.2	3.2
Yb	1.80	2	1.9	1.7
Y	19.00	2	20.	18.

ROCK TYPE: STEEP ROCK LOWER MAFIC UNIT (Map unit 3b)

Element (ppm)	Most freq. value	Minimum	10%	Median	90%	Maximum	Mean	Std dev.	Number
La	2.0	1.5	2.0	3.0	4.3	5.0	3.01	.93	27
Ce	11.	3.9	4.9	8.0	11.	13.	8.01	2.64	27
Nd	8.0	2.9	3.7	5.9	8.5	9.2	5.93	1.77	27
Sm	2.0	0.9	1.2	1.5	2.4	2.5	1.63	0.46	27
Eu	0.6	0.4	0.5	0.7	0.9	0.9	0.66	0.15	27
Gd	2.6	1.7	1.8	2.6	3.2	3.6	2.57	0.51	27
Dy	3.4	2.2	2.5	3.2	4.0	4.4	3.19	0.59	27
Yb	1.8	1.0	1.3	1.7	2.2	2.4	1.72	0.36	27
Y	18.	12.	14.	18.	22.	24.	17.44	3.37	27

ROCK TYPE: FINLAYSON LOWER MAFIC UNIT (Map unit 3b)

Element (ppm)	Most freq. value	Minimum	10%	Median	90%	Maximum	Mean	Std dev.	Number
La	2.0	0.9	2.0	3.0	6.0	6.0	2.92	1.40	14
Ce	8.0	4.0	5.0	8.0	15.	15.	8.29	2.97	14
Nd	12.	5.3	5.6	9.5	13.	13	9.19	2.62	14
Sm	1.7	0.8	1.0	1.7	2.6	2.6	1.72	0.53	14
Eu	0.7	0.4	0.4	0.7	1.0	1.0	0.69	0.17	14
Gd	2.5	1.8	2.5	3.0	4.3	4.3	3.13	0.74	14
Dy	3.6	2.1	2.1	3.1	4.4	4.4	3.11	0.71	14
Yb	2.1	1.3	1.3	1.8	2.6	2.6	1.89	0.41	14
Y	17.	12.	12.	18.	26.	26.	18.14	4.28	14

ROCK TYPE: FINLAYSON AMPHIBOLITE GRADE MAFIC METAVOLCANIC ROCKS (Map unit 3b)

Element (ppm)	Most freq. value	Minimum	10%	Median	90%	Maximum	Mean	Std dev.	Number
La	22.	3.0	3.0	14.	22.	22.	10.50	8.60	6
Ce	44.	7.0	7.0	23.	44.	44.	20.50	15.57	6
Nd	12.	6.7	7.3	12.	21.	21.	13.17	6.12	6
Sm	3.1	1.5	1.8	2.6	3.1	3.1	2.33	0.63	6
Eu	0.8	0.7	0.8	0.8	1.0	1.0	0.83	0.10	6
Gd	3.8	2.6	2.9	3.2	3.8	3.8	3.15	0.40	6
Dy	4.0	2.1	2.8	3.0	4.0	4.0	3.00	0.62	6
Yb	2.5	1.1	1.6	1.9	2.5	2.5	1.82	0.46	6
Y	17.	13.	17.	18.	24.	24.	18.00	3.58	6

ROCK TYPE: PERCH LOWER MAFIC UNIT (Map unit 3b)

Element (ppm)	Mean value	Number	Data list	
La	2.90	2	3.5	2.3
Ce	7.95	2	9.5	6.4

Appendix 4 (cont'd.)

ROCK TYPE: PERCH LOWER MAFIC UNIT (Map unit 3b) (cont'd.)

Element (ppm)	Mean value	Number	Data list	
Nd	7.95	2	8.4	7.5
Sm	1.95	2	2.5	1.4
Eu	0.75	2	0.8	0.7
Gd	3.20	2	3.5	2.9
Dy	3.70	2	4.0	3.4
Yb	2.15	2	1.9	2.2
Y	21.00	2	21.	21.

ROCK TYPE: DISMAL ASHROCK FORMATION (Map unit 3a)

Element (ppm)	Mean value	Number	Data list				
La	10.80	5	7.0	16.	11.	10.	10.
Ce	26.20	5	19.	38.	27.	23.	24.
Nd	16.80	5	16.	21.	17.	14.	16.
Sm	4.38	5	4.2	4.5	4.2	4.1	4.9
Eu	1.04	5	0.9	0.9	1.2	0.9	1.3
Gd	3.14	5	3.3	3.1	3.2	2.7	3.4
Dy	2.72	5	2.8	2.7	2.8	2.4	2.9
Yb	0.96	5	1.1	1.0	0.9	0.9	0.9
Y	12.40	5	13.	13.	13.	11.	12.

ROCK TYPE: MOSHER CARBONATE FORMATION (Map unit 2b)

Element (ppm)	Mean value	Number	Data list	
La	1.15	2	1.3	1.0
Ce	1.05	2	1.1	1.0
Nd	2.05	2	2.8	1.3
Sm	0.10	2	0.1	0.1
Eu	0.10	2	0.1	0.1
Gd	0.25	2	0.3	0.2
Dy	0.15	2	0.2	0.1
Yb	0.15	2	0.2	0.1
Y	5.70	2	9.4	2.0

ROCK TYPE: WAGITA FORMATION (Map unit 2a)

Element (ppm)	Mean value	Number	Data list
La	85.00	1	85.
Ce	180.00	1	180.
Nd	82.00	1	82.
Sm	9.30	1	9.3
Eu	3.00	1	3.0
Gd	9.20	1	9.2
Dy	8.10	1	8.1
Yb	3.70	1	3.7
Y	36.00	1	36.

ROCK TYPE: MAFIC TONALITE GNEISS (Map unit 1d)

Element (ppm)	Mean value	Number	Data list	
La	15.20	2	22.	8.4
Ce	27.00	2	39.	15.
Nd	11.90	2	18.	5.8
Sm	1.50	2	2.2	0.8
Eu	0.60	2	0.9	0.3
Gd	1.90	2	2.9	0.9
Dy	1.95	2	3.0	0.9
Yb	1.10	2	1.7	0.5
Y	11.65	2	18.	5.3

Appendix 4 (cont'd.)

ROCK TYPE: TONALITE GNEISS (Map unit 1c)

Element (ppm)	Mean value	Number	Data list				
La	19.20	5	19.	12.	29.	16.	20.
Ce	33.20	5	36.	23.	42.	28.	37.
Nd	14.38	5	15.	9.9	19.	11.	17.
Sm	1.64	5	1.7	0.9	2.4	0.9	2.3
Eu	0.54	5	0.6	0.5	0.6	0.5	0.5
Gd	1.86	5	2.4	1.1	2.0	1.3	2.5
Dy	1.32	5	2.1	0.7	1.0	0.7	2.1
Yb	0.54	5	0.8	0.2	0.2	0.3	1.2
Y	7.22	5	11.	3.9	4.5	3.7	13.

ROCK TYPE: "OLD" TONALITE (Map unit 1b)

Element (ppm)	Most freq. value	Minimum	10%	Median	90%	Maximum	Mean	Std dev.	Number
La	28.	12.	12.	18.	28.	28.	19.28	5.41	7
Ce	55.	24.	24.	37.	55.	55.	36.29	10.77	7
Nd	11.	9.4	9.4	13.	22.	22.	13.91	4.49	7
Sm	3.8	1.1	1.1	2.3	3.8	3.8	2.46	0.90	7
Eu	0.5	0.4	0.4	0.6	0.7	0.7	0.63	0.20	7
Gd	1.4	1.0	1.0	1.3	2.0	2.0	1.33	0.34	7
Dy	1.4	0.7	0.7	1.1	1.8	1.8	1.17	0.38	7
Yb	0.4	0.3	0.3	0.4	0.5	0.5	0.47	0.24	7
Y	5.0	3.8	3.8	7.	11.	11.	6.21	2.42	7

ROCK TYPE: MAFIC TONALITE (Map unit 1a)

Element (ppm)	Mean value	Number	Data list				
La	30.25	4	12.	62.	28.	19.	
Ce	61.00	4	23.	120.	55.	46.	
Nd	31.25	4	15.	56.	26.	28.	
Sm	4.75	4	1.9	7.	4.3	5.8	
Eu	1.38	4	1.0	2.3	1.0	1.2	
Gd	4.63	4	2.5	6.9	5.3	3.8	
Dy	3.90	4	2.0	5.2	5.0	3.4	
Yb	1.65	4	0.9	1.9	2.1	1.7	
Y	21.75	4	11.	27.	29.	20.	

APPENDIX 5

Table A5. Selected, least-altered analyses of metavolcanic rocks

Steep Rock lower mafic unit										
Sample no.	5	9	51	80	83	86	88			
	(weight %)	(weight %)	(weight)	(weight %)	(weight %)	(weight %)	(weight %)			
SiO ₂	47.9	49.5	52.2	47.1	51.8	48.6	52.9			
TiO ₂	0.80	0.87	0.73	0.77	0.91	0.79	0.90			
Al ₂ O ₃	15.6	15.4	13.5	15.2	15.7	14.0	15.2			
Fe ₂ O ₃	3.5	3.1	2.4	4.4	2.1	3.2	2.4			
FeO	7.1	6.4	7.6	8.3	7.5	8.3	5.8			
MnO	0.20	0.21	0.18	0.26	0.21	0.15	0.21			
MgO	8.38	7.72	8.02	7.56	7.36	8.10	7.18			
CaO	13.2	12.1	9.93	12.4	7.78	10.2	9.60			
Na ₂ O	0.8	1.3	1.1	1.41	3.87	2.76	2.66			
K ₂ O	0.01	0.02	0.40	0.06	0.05	0.05	0.09			
H ₂ O	3.2	3.4	3.1	3.8	3.5	3.4	3.5			
CO ₂	0.0	0.7	0.2	0.3	0.3	0.0	0.5			
P ₂ O ₅	0.07	0.09	0.04	0.04	0.05	0.03	0.06			
S	0.13	0.04	0.01	0.04	0.00	0.10	0.00			
Total	100.9	100.9	99.5	101.7	101.2	99.8	101.1			
Mg#	63.17	63.80	63.28	56.40	62.18	60.31	65.42			
	(ppm)	(ppm)	(ppm)	(ppm)	(ppm)	(ppm)	(ppm)			
Ba	60.	40.	180.		30.	30.				
Be	0.5	0.6	0.6	0.4	0.5	0.3	0.4			
Co	46.	47.	71.	51.	51.	48.	51.			
Cr	310.	240.	670.	310.	300.	280.	360.			
Cu	140.	120.	120.	150.	100.	150.	120.			
Ni	140.	86.	160.	150.	99.	89.	120.			
V	260.	260.	250.	250.	260.	240.	270.			
Zn	87.	78.	120.	120.	87.	88.	130.			
Zr				39.	57.	47.	52.			
La	2.0	4.0	2.0	2.6	4.2	3.7	3.1			
Ce	8.0	11.	6.0	5.8	11.	8.8	8.0			
Nd	3.9	4.7	7.2	5.7	8.1	6.9	8.5			
Sm	2.4	2.0	1.5	1.4	2.0	1.6	1.5			
Eu	0.7	0.8	0.6	0.6	0.8	0.6	0.7			
Gd	2.6	2.7	2.5	2.6	3.0	2.5	2.9			
Dy	3.5	3.5	2.6	3.4	3.4	2.9	3.2			
Yb	2.0	1.8	1.4	2.2	1.7	1.6	1.8			
Y	19.	18.	15.	21.	18.	16.	18.			
Steep Rock upper felsic unit										
Sample No.	50	61	62	67	72	82	89	90	92	95
	(weight%)	(weight%)	(weight)	(weight%)	(weight%)	(weight%)	(weight%)	(weight%)	(weight%)	(weight%)
SiO ₂	71.2	56.3	62.4	58.0	61.8	59.1	60.9	60.3	62.0	66.9
TiO ₂	0.68	0.92	0.68	0.89	0.94	1.04	0.78	0.76	0.78	0.66
Al ₂ O ₃	15.4	14.6	15.9	14.1	15.5	14.6	15.2	16.0	15.8	14.9
Fe ₂ O ₃	1.1	2.6	1.5	3.1	2.2	2.7	2.4	3.7	2.0	1.7
FeO	0.4	4.5	4.4	4.4	3.6	6.4	4.5	3.9	4.1	4.1
MnO	0.04	0.14	0.12	0.16	0.14	0.22	0.13	0.16	0.10	0.10
MgO	0.38	3.61	2.94	4.45	2.27	4.73	3.37	3.29	2.78	2.50
CaO	4.69	10.0	5.17	6.05	6.11	4.24	6.72	6.60	6.40	2.65
Na ₂ O	3.6	2.15	5.54	3.15	2.87	2.95	2.97	3.32	4.64	4.83
K ₂ O	1.71	1.09	0.80	0.88	1.46	0.12	1.48	0.87	1.22	0.55
H ₂ O	0.7	2.1	1.3	2.4	2.4	4.1	2.3	2.8	1.6	2.2
CO ₂	0.3	2.3	0.0	1.4	0.9	0.4	0.0	0.1	0.0	0.0

Appendix 5 (cont'd.)

Steep Rock upper felsic unit (cont'd.)

Sample No.	50 (weight%)	61 (weight%)	62 (weight)	67 (weight%)	72 (weight%)	82 (weight%)	89 (weight%)	90 (weight%)	92 (weight%)	95 (weight%)
P ₂ O ₅	0.17	0.26	0.18	0.25	0.25	0.29	0.15	0.17	0.14	0.16
S	0.01	0.00	0.00	0.00	0.00	0.00	0.03	0.02	0.00	0.00
Total	100.5	100.6	101.0	99.4	100.5	101.0	101.1	102.0	101.6	101.3
Mg#	36.45	52.54	51.75	56.49	46.04	52.91	51.49	48.84	49.71	48.23
	(ppm)	(ppm)	(ppm)	(ppm)	(ppm)	(ppm)	(ppm)	(ppm)	(ppm)	(ppm)
Ba	400.	300.	300.	400.	420.	20.	430.	360.	620.	270.
Be	0.9	0.8	0.8	0.9	1.2	0.9	0.8	0.9	0.8	0.9
Co	17.	20.	17.	32.	18.	28.	22.	20.	20.	15.
Cr	94.	74.	47.	110.	120.	110.	67.	60.	95.	33.
Cu	42.	15.	0.	57.	58.	31.	33.	41.	10.	38.
Ni	58.	62.	49.	93.	57.	68.	51.	48.	65.	32.
V	110.	140.	120.	140.	130.	140.	130.	120.	120.	68.
Zn	53.	85.	50.	120.	89.	89.	100.	82.	74.	96.
Li	4.	8.	6.	12.						
Zr		180.	190.	180.	210.	220.	170.	180.	190.	240.
La	22.	28.	30.	23.	26.	26.	23.	26.	26.	22.
Ce	49.	58.	56.	55.	59.	59.	48.	55.	53.	44.
Nd	24.	32.	26.	32.	29.	30.	23.	25.	24.	21.
Sm	3.9	6.4	6.0	6.1	5.1	5.5	3.7	3.9	4.0	3.8
Eu	0.9	1.3	1.1	1.2	1.3	1.6	1.0	1.1	1.0	1.1
Gd	3.3	4.4	4.1	4.4	5.0	5.6	4.0	4.3	4.2	4.4
Dy	2.9	4.0	4.0	4.0	4.4	5.5	3.8	4.0	4.0	4.6
Yb	1.4	1.9	2.1	2.0	2.1	2.6	2.1	2.1	2.1	2.7
Y	17.	24.	25.	24.	25.	33.	22.	24.	23.	28.

Finlayson lower mafic unit

Sample No.	23* (weight%)	31 (weight%)	35 (weight)	36 (weight%)	40 (weight%)	44* (weight%)	48* (weight%)
SiO ₂	56.7	53.5	50.0	50.1	51.4	53.5	48.9
TiO ₂	1.05	1.13	1.00	0.79	0.86	1.01	0.90
Al ₂ O ₃	15.9	15.1	14.1	14.2	17.6	15.2	15.8
Fe ₂ O ₃	2.1	2.7	3.2	3.0	3.4	3.8	2.1
FeO	2.5	5.4	8.5	7.7	4.4	6.2	9.0
MnO	0.12	0.18	0.20	0.20	0.22	0.18	0.21
MgO	2.13	3.88	5.07	7.77	4.68	4.00	9.51
CaO	14.0	12.0	12.1	11.9	13.8	11.4	10.6
Na ₂ O	1.5	2.0	2.0	1.1	2.1	1.5	1.0
K ₂ O	0.05	0.46	0.12	0.15	0.14	0.02	0.17
H ₂ O	0.8	1.4	1.3	2.2	1.8	2.6	2.5
CO ₂	2.4	1.6	2.3	0.1	0.0	1.2	0.0
P ₂ O ₅	0.10	0.11	0.10	0.07	0.07	0.09	0.07
S	0.05	0.07	0.25	0.25	0.29	0.16	0.02
Total	99.4	99.7	100.3	99.6	100.7	100.9	100.8
Mg#	50.44	50.97	48.31	61.05	56.82	46.59	64.69
	(ppm)	(ppm)	(ppm)	(ppm)	(ppm)	(ppm)	(ppm)
Ba	70.	90.	50.	70.	70.	50.	80.
Be	0.6	0.7	0.7	0.6	0.7	0.6	0.6
Co	40.	47.	47.	44.	41.	46.	47.
Cr	190.	170.	160.	270.	380.	160.	240.
Cu	59.	98.	150.	110.	130.	120.	79.
Ni	100.	91.	100.	120.	140.	110.	160.
V	300.	340.	290.	260.	280.	300.	270.
Zn	46.	84.	87.	72.	57.	80.	83.

Appendix 5 (cont'd.)

Finlayson lower mafic unit (cont'd.)

Sample No.	23* (weight%)	31 (weight%)	35 (weight)	36 (weight%)	40 (weight%)	44* (weight%)	48* (weight%)
Li	3.	4.	6.	6.	6.	9.	13.
La	18.	4.0	4.0	2.0	2.0	3.0	3.0
Ce	23.	11.	11.	8.0	8.0	9.0	7.0
Nd	12.	13.	12.	8.9	11.	7.3	6.7
Sm	2.1	2.5	2.3	1.7	1.8	2.6	1.8
Eu	0.9	1.0	0.9	0.7	0.7	0.8	0.7
Gd	3.3	4.3	3.7	3.0	3.8	3.2	2.6
Dy	2.9	4.4	3.6	3.0	3.2	4.0	3.2
Yb	1.6	2.6	2.1	1.8	2.1	2.5	2.0
Y	17.	26.	21.	18.	19.	24.	19.

*Amphibolite grade

Finlayson upper felsic unit

Sample No.	24 (weight%)	26 (weight%)	33 (weight)
SiO ₂	68.4	76.7	69.4
TiO ₂	0.32	0.22	0.47
Al ₂ O ₃	16.4	12.8	15.7
Fe ₂ O ₃	0.2	0.4	0.4
FeO	1.1	0.5	1.6
MnO	0.03	0.03	0.04
MgO	0.68	0.38	2.07
CaO	4.57	2.20	1.20
Na ₂ O	2.5	3.2	5.9
K ₂ O	2.22	2.00	0.62
H ₂ O	1.3	0.7	1.2
CO ₂	1.7	1.7	0.8
P ₂ O ₅	0.09	0.08	0.14
S	0.02	0.00	0.06
Total	99.6	100.9	99.7
Mg#	52.70	48.10	68.90
	(ppm)	(ppm)	(ppm)
Ba	670.	400.	160.
Be	1.0	0.7	0.4
Co	8.	4.	9.
Cr	17.	10.	41.
Cu	19.	7.	16.
Ni	39.	19.	28.
V	42.	26.	75.
Zn	17.	27.	46.
Li	6.	6.	6.
La	12.	13.	11
Ce	27.	21.	25.
Nd	14.	8.6	13.
Sm	1.9	1.2	2.4
Eu	0.9	0.3	0.7
Gd	2.1	1.0	1.8
Dy	1.3	0.7	1.7
Yb	0.5	0.4	0.9
Y	7.0	5.0	10.